MITOCHONDRIAL REGULATION OF VASCULAR SMOOTH MUSCLE CELL PROLIFERATION AND MIGRATION IN ATHEROGENESIS AND RE-STENOSIS

A thesis presented by

ZUHAIR SALEH AL-SULTI

In fulfilment of the requirements for the degree of Doctor of Philosophy

March 2017

UNIVERSITY OF STRATHCLYDE, GLASGOW

STRATHCLYDE INSTITUTE OF PHARMACY AND BIOMEDICAL SCIENCES

Acknowledgements

I would like to thank my supervisor Dr. Paul Coats who guided me throughout the course of my PhD. and who provided me with ultimate support to overcome any difficulties. Thank you for spending significant amount of time discussing, providing feedback during my lab work and during writing up my thesis.

I am also extremely grateful to Dr. Robert MacDonald who helped me a lot in running some of the experiment at the University of Glasgow and for the considerable effort in analysing some of the data generated during my time at their lab. I am also extremely grateful to Dr. Rothwelle Tate for his help in the molecular work associated with gene expression and his guidance in overcoming some of the difficulties associated with the technique. I would also like to thank Dr. David Watson for helping in the proteomic analysis presented in this work. I would also like to thank Dr. Mark Macaskill, Dr. Craig Mckittrick and Mr. Graeme Mackenzie for their continuous assistance and advice, and my colleagues in the lab Molly Huq and Hadi Burzangi.

My acknowledgements also go to the Omani ministry of health and ministry of education for funding my PhD. Study abroad. Finally I am very thankful to my wife for her support and patience. This work is dedicated to her, my sons Saleh and Sultan, my mum, dad, brothers and sisters (Thank you all for everything).

Abstract:

Vascular smooth muscle (VSM) cell proliferation and migration are the hallmark of atherosclerosis and re-stenosis. In this study, we have investigated the role of mitochondrial bioactivity in VSM cell proliferation and migration through the regulation of miRNA expression. We also investigated for the first time the role of mitochondrial bioactivity in determining the content of exosomes released by vascular smooth muscle cells and the biological effect these exosomes have on vascular smooth muscle (VSM) cell proliferation and migration.

VSM cells were isolated from 12-week old male Sprague-Dawley rats. Experiments were undertaken using day zero isolated (contractile phenotype), 21-day cultured (synthetic phenotype) and 21-day mitochondrial incompetent (synthetic phenotype- Rho cell). The effect of balloon angioplasty on rat aorta structural remodelling was also studied. VSM cells were also stimulated using 20 ng/ml PDGF and treated with mitochondrial DRP1 inhibitor MDivi-1 (10 μM).

Inhibition of mitochondrial network formation with the DRP1 inhibitor MDivi-1 (10 μM) inhibited angioplasty-dependent remodelling. This observation was confirmed in VSM cell cultures where MDivi-1 significantly reduced proliferation and migration. Total exosomal release was significantly greater in the 21-day cultured cells when compared with quiesced non-proliferating cells and 21-day cultured Rho cells (520 +/- 10 ng, 480 +/- 20 ng and 420 +/- 10 ng per ml respectively) and total exosomal RNA yield was 70.2 +/- 10.2 ng/ul, 118.7 +/- 2.4 ng/ul and 70.8 +/- 4.7 ng/ul respectively.

Mitochondrial function significantly influenced miRNA and mRNA measured in exosomes. When compared with the hyperproliferative synthetic VSM cell miR-21 expression was reduced by 88 +/- 12.1% and miR-145 expression increased by 73 +/- 19.8%. We also measured a 7-fold decrease and 6.6-fold decrease in mTOR, PI3K and 4EBP1 respectively. A significant increase expression of P53, cdkn2a and ROS scavenging proteins including SOD1 and SOD2 were measured in 21-day cultured Rho cells vs. 21-day hyperproliferative VSM cells.

The expression of cellular miRNA was also seen to be influenced by mitochondrial bioactivity. The expression of miR-21 in cells treated with MDivi-1 was 2 ± 0.2 fold lower than the expression level in the PDGF stimulated cells. The expression level of miR-145 in the MDivi-1 treated cells was 0.5 ± 0.1 fold higher than the expression level in the PDGF stimulated cells.

In this study we have further correlated VSM cell hyperproliferative phenotype with mitochondrial function. Moreover, further demonstrated mitochondrial function/ VSM cell phenotype with exosomal release and cargo that potentially drives the hyperproliferative/ migratory phenotype central to atherosclerosis and re-stenosis.

Conferences and Publications

1. Poster communication. "Mitochondrial-Dependent signalling in Vascular Smooth Muscle Cell Proliferation". Presented at the Scottish cardiovascular forum, Scotland, Aberdeen, February 2014.

2. Published abstract, Al-sulti Z, Kingsmore D, Coats P. Mitochondrial-Dependent signalling in Vascular Smooth Muscle Cell Proliferation. *Heart* 2014;**100**:A97 doi:10.1136/heartjnl-2014-306118.170.

3. Poster communication. "Mitochondrial Regulation of micro RNA synthesis in Vascular Smooth Muscle Cell Proliferation". Presented at the British society for cardiovascular research autumn meeting on Cardiovascular Signalling in Health and Disease, University of Reading, September 2014.

4. Poster communication. "Mitochondrial Regulation of micro RNA synthesis in Vascular Smooth Muscle Cell Proliferation". Presented at the Scottish cardiovascular forum, Edinburgh, February 2015.

5. Poster communication. "Mitochondrial dynamics Regulation of ROS and apoptosis". Presented at the British society for cardiovascular research spring meeting on New Frontiers in Cardiovascular Science, Manchester, June 2015.

6. Poster communication. "Mitochondrial Regulation of micro RNA synthesis in Vascular Smooth Muscle Cell Proliferation and Migration". Presented at the British Pharmacological society conference, London, December 2015.

7. Published abstract. Z Al-Sulti, R McDonald, D Kingsmore, A Baker, P Coats. Mitochondrial Regulation of micro RNA synthesis in Vascular Smooth Muscle Cell Proliferation and Migration. E-journal of the British pharmacological society, Proceedings of the British Pharmacological Society at *http://www.pA2online.org/abstracts/Vol13Issue3abst269P.pdf.*(2015).

8. Poster communication. "Mitochondrial regulation of exosomal micro RNA cargo in Vascular Smooth Muscle Cell proliferation". Presented at the keystone symposia on Exosomes/Microvesicles: Novel Mechanisms of Cell-Cell Communication, Colorado, USA, June 2016.

9. Oral presentation. “Mitochondrial Regulation of Exosomal Transported miRNA Play a Central Role in Vascular Smooth Muscle Cell Proliferation and Migration Associated with Atherogenesis and Re-Stenosis”. Presented at the Scottish cardiovascular forum, Glasgow, February 2017.

CONTENTS **Page**

List of Figures **Page**

Chapter 1. Introduction

Chapter 3. Role of mitochondria in VSMC proliferation and migration

Chapter 5. Role of mitochondria in exosomes biogenesis, trafficking and sorting

List of Tables

Chapter 1

General Introduction

1.1 Cardiovascular System:

The cardiovascular system, also known as the circulatory system, consists of the heart functioning as a pump, the arterial system which distributes the oxygenated blood to the tissues, the venous system which collects the deoxygenated blood from the tissues and returns it back to the heart and the capillary system where the exchange of oxygen, nutrients and waste takes place.

The main functions of the cardiovascular system are transporting oxygen and removing carbon dioxide, transporting nutrients and removing wastes, transporting hormones from the endocrine glands to the cells and regulating body temperature.

The circulatory system is divided into two parts; the low pressure pulmonary circulation which links circulation with gas exchange in the lungs and the high pressure systemic circulation which provides oxygen and nutrients to the tissues. The blood flows down the pressure gradient from the high pressure arterial circulation and returning via the low pressure venous circulation (Figure 1.1).

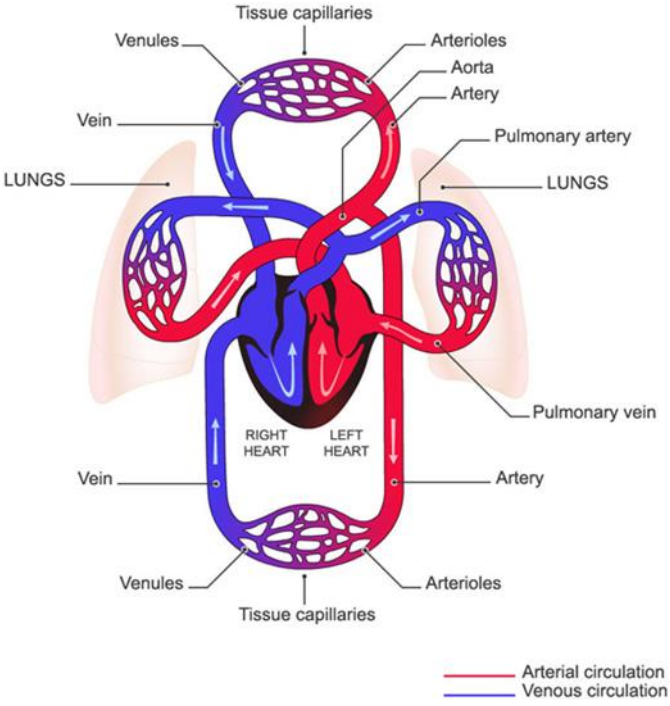

Figure 1.1 *circulatory systems. Diagram shows the pulmonary circulation that transports blood to the lung to be oxygenated and the systemic circulation that transports blood from the lungs to the rest of the body (www.anatomyclass123.com).*

The systemic circulation is responsible for transporting the blood around the body. The oxygenated blood is transported to the body through the aorta which branches into arteries that takes the blood to the upper part of the body first then moves to the lower part through further branches of arteries. The blood is then delivered to different tissues through the smaller capillaries. Once the oxygen is delivered to the tissue, the blood moves back to the capillaries and empties into the veins which then take the blood to the vena cava through which the blood is transported back to the heart (Davies and Hagen, 1994). On the other hand, the pulmonary circulation circulates the blood into and out of the lungs. The deoxygenated blood leaves the heart through pulmonary arteries and enters the lungs where it gets oxygenated and then leaves the lungs through the pulmonary veins and enters the heart.

Blood flow in the circulatory system depends on blood volume that must be sufficient to fill blood vessels and pressure difference across the circulatory system that provides the force to move the blood forward. The arterial system has the highest pressure because of its function as a distribution system (Lee et al., 2004). The capillaries are small vessels linking the arterial system with the venous system and they contain the smallest amount of blood, whereas, the venous system contains the largest volume of blood and lowest pressure as it functions as a reservoir that collects the blood from the tissues. However, the main factors governing blood flow in the cardiovascular system are pressure and resistance. Blood flow through a vessel is determined by the pressure difference between the two ends of the vessel and the resistance that blood must overcome to move through the vessel caused by the friction between the blood and the vessel wall as in the following equation ($F= \Delta P/R$). French physician Poiseuille expanded this equation by relating flow to many determinants of resistance including blood vessel diameter and blood viscosity as in the following equation

$$F = \Delta P \text{ (pressure)} \times \pi \times r \text{ (radius)}^4 \ / \ 8 \times L \text{ (length)} \times \eta \text{ (viscosity)}$$

This shows that because blood flow is directly related to the fourth power of the radius, any small change in vessel radius can produce large change in the blood flow to an organ or tissue (Stary, 1990).

Many diseases affect the cardiovascular system and can have different origins but they share the hallmark of vascular smooth muscle (VSM) cell hyperplasia and migration. Increased cell growth can affect blood vessels which causes change in total peripheral resistance and blood pressure or it can affect cardiac tissues leading to ventricular hypertrophy and heart failure. Some examples of these conditions are atherosclerosis, hypertension and arteriovenous fistula failure (Edgington et al., 1991). Although the triggers are not fully understood, it has been well documented that inflammatory response triggers the progression of these diseases. This inflammatory process can be initiated by focal trauma like in the case of needle injury, general trauma like in the case of atherosclerosis or stress on the blood vessel walls like in the case of hypertension (Mallika et al., 2007). These all lead to the same end point of shifting vascular smooth muscle cells phenotype from quiescence to proliferative, blood vessel remodelling and hence occlusion (Orford et al., 2000). Although all three layers of blood vessel are involved in the progression of cardiovascular disease, the extent of their contribution and the sequence in which each layer comes in the process is not yet conclusive. The inflammatory and proliferative process cascade is not yet fully understood, however, many factors have been identified which help in the stimulation and progression of the diseases such as some inflammatory cytokines and growth factors (McNamara et al., 1996). These factors work through well identified signalling pathways including mitogen activated protein kinase (MAPK), mammalian target of rapamycin (mTOR) and AMP-activated protein kinase (AMPK).

1.2 Blood Vessel Structure:

Blood vessel walls consist of three layers: tunica intima, tunica media and tunica adventitia (Figure 1.2). The tunica intima is a thin inner layer of the blood vessel made of endothelial cells spread on a connective tissue layer known as the internal elastic lamina (IEL). The IEL is made of collagen, laminin and heparin sulfate proteoglycan (Timpl, 1996). The endothelial layer prevents the escape of the plasma, is an anti-thrombotic barrier and releases many vasoactive substances. Tunica media consists of smooth muscle cells arranged in a matrix of elastin and collagen fibres

which gives it strength and contractile power to maintain vessel tone and cardiovascular regulation. The arterial walls are normally thicker than the venous walls because of the presence of more smooth muscle cells and elastic fibres (Davies and Hagen, 1995). The adventitia is made of flexible connective tissue layer made of fibroblasts, nerves and extracellular matrix which helps in tethering the vessel loosely to the surrounding tissue (Thibodeau and Patton, 2003). All three layers contribute differently in regulating vascular response to injury or stress.

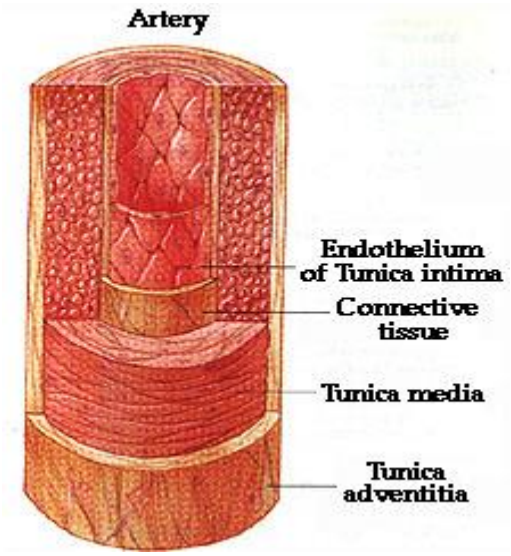

Figure 1.2 *Blood Vessel Structure. Diagram shows the three distinct layers of the blood vessel and the cellular composition of each layer; Adventitial cells, vascular smooth muscle cells and endothelial cells (www.physio-web.org).*

Blood Vessel Structure and Function: Endothelial cells

Endothelial cells cover the inner surface of blood vessels. These cells have several important physiologic functions and are now recognised to be critical for many aspects of vascular homeostasis (Pearson, 2000). Vascular endothelial cells are joined together tightly in a semi-permeable barrier to prevent the efflux of large molecules like low density lipid into the sub-endothelial spaces (Ross, 1993). These

cells also provide the blood vessel with a non thrombogenic surface by inhibiting platelet aggregation. They release platelet inhibitors prostacyclin (PGI_2) and nitric oxide (NO). Another important function of endothelial cells is the secretion of what is known as endothelium-derived relaxing factors (EDRFs; (Furchgott and Vanhoutte, 1989). EDRFs act by relaxing smooth muscle cells causing the blood vessel to relax and the diameter of the lumen to increase. Although many substances are thought to be among the EDRFs, NO is thought to be the best characterised. Some factors that inhibit the migration and proliferation of smooth muscle cells are also secreted by the endothelial cells and this includes heparin sulphate and NO (Consigny, 1995). The endothelial cells are known to be responsible for the primary blood vessel development (vasculogenesis) and the vessel growth after this point (angiogenesis) (Folkman and Shing, 1992).

The active metabolism of endothelial cells is essential for controlling blood pressure through the continuous adjustment of underlying vascular smooth muscle tone. The synthesis and secretion of PGI_2 and NO are very important for vasodilatation in response to elevated blood pressure (Huang et al., 1995). Both NO and PGI_2 synthesis can also be triggered rapidly by many agents that are generated during coagulation or platelet aggregation including bradykinin, thrombin and ATP (Carter and Pearson 1992). Endothelial NO synthesis is also induced by increasing shear stress through the activation of protein kinase B (Fulton et al., 1999). Endothelial cells also secrete some potent vasoconstrictors such as endothelin-1 (ET-1) which can be modulated by physical forces such as shear or stretch (Haynes and Webb, 1998).

Endothelial cells play a role in the control of leukocyte trafficking. Cell activation by thrombin, inflammatory cytokines (such as interlukin-1 and tumour necrosis factor) or endotoxins result in increased expression of adhesive molecules at the endothelial luminal surface which attract the leukocytes to adhere to the endothelium and then emigrate from the blood vessel into the damaged site (Springer, 1995). Vascular cell adhesion molecule (VCAM) and intracellular adhesion molecule (ICAM) are some examples of these adhesive molecules synthesised by the endothelial cells in

response to inflammation, oxidant stress, hyperlipidemia and hyperglycemia which helps in the accumulation of macrophages in the vessel wall (Marui et al., 1993).

Endothelial cells also play an important role in platelet function, coagulation and fibrinolysis. They are responsible for synthesis of von Willebrand factor (vWF) which is a glycoprotein that has mainly two functions; vWF acts as a carrier for coagulation factor VIIII and as a cofactor needed for platelets to bind to the exposed collagen in the damaged vessel wall (Wagner, 1990). Thrombin formation also triggers the release of NO and PGI_2 from the endothelium which are powerful inhibitors of platelet activation (Freedman et al., 1999). Thrombin is also inhibited by anti-thrombin which is synthesised in the liver but binds from the circulation to surface glycosaminoglycans on endothelium (Marcum et al., 1984). The expression of the endothelial transmembrane protein thrombomodulin also targets thrombin and changes its conformation and makes it less efficient at cleaving fibrinogen and more efficient in activating circulating protein C which is an anticoagulant (Esmon, 1995). Fibrinolysis is controlled by two main precursors; tissue plasminogen activator (tPA) and plasminogen activator inhibitor-1 (PAI-1) which are both secreted by endothelial cells (Booth and Bennett, 1994).

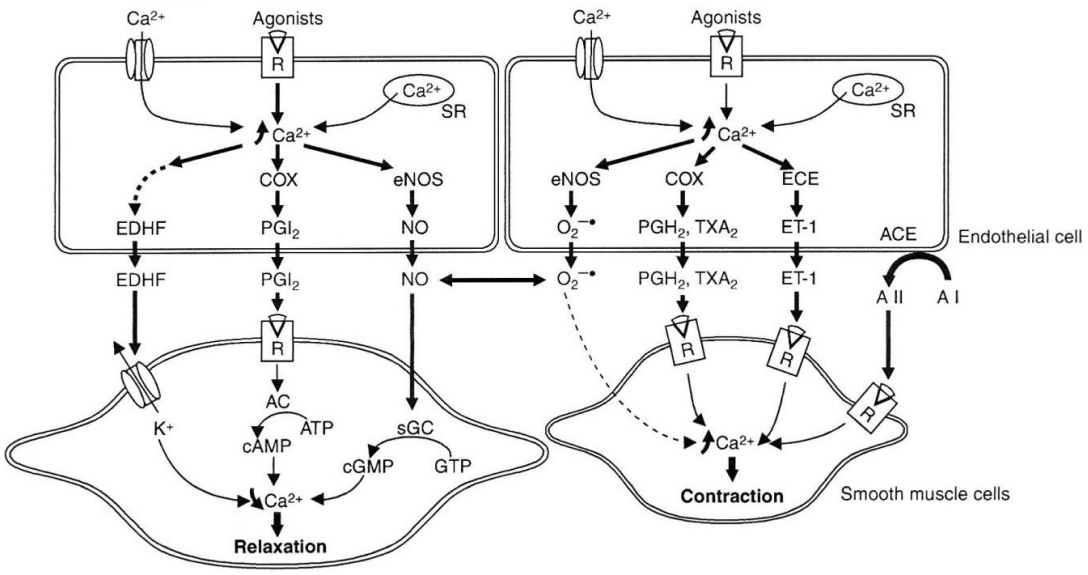

Figure 1.3 *Functions of Endothelial cells. Diagram shows the components of the endothelial cells and the different factors released by endothelial cells on underlying VSM cells (Shiogai et al., 2010).*

Blood Vessel Structure and Function: Vascular smooth muscle cells

Vascular smooth muscle cells which form the medial layer of blood vessels are differentiated cells functioning mainly for contraction. They contain of proteins, ion channels and signalling molecules that help them contract (Owens, 1995). They exhibit extensive plasticity throughout life, during repair of vascular injury caused by balloon angioplasty or stent insertion and disease states such as hypertension. They also have a diverse range of different phenotypes. This diversity occurs in response to different changes in the pathophysiological conditions or under normal conditions depending on the anatomic location of the blood vessel (Cook et al., 1994). The phenotypic difference helps vascular smooth muscle cells carry out different functions in different organs during development such as formation of new blood vessels during embryonic and neonatal phases (Lacolley et al., 2012). It also helps vascular smooth muscle cells repair injury resulting from trauma or inflammation. This can be seen during the early embryonic development when smooth muscle cells have a high rate of proliferation and migration as well as the increase in the production of extracellular matrix (ECM) proteins seen during late embryogenesis (Sasaguri et al., 1994). However, following vascular stress or injury the phenotype changes from contractile to proliferative (Alexander and Owens, 2012). They change in shape from spindle to rhomboid and lose their actin and heavy chain myosin that maintain its contractile state (Figure 1.4). They also gain the ability to migrate and secrete and synthesise extracellular matrix and other biologically mediators that regulate contraction and relaxation, inflammation, proliferation and apoptosis (Inoue et al., 2000). This change in phenotype is not completely understood and although some signalling pathways have been identified, the full picture of the inter-relation between these pathways is not drawn. Some cellular organelles such as mitochondria have been found to play a role in this signalling process but it is still not known how they do that (Leduc et al., 2010).

Vascular smooth muscle cells have different embryological origins which determines the proliferative capacity of these cells once they shift from the quiesced state to the proliferative state following stimulation (Hungerford and Little, 1999). Although most vascular smooth muscle cells are known to be derived from local mesoderm

populations, some smooth muscle cells such as the coronary artery vascular smooth muscle cells are derived from pro-epicardial organ and other evidence suggest that under severe vascular injury or inflammation, circulating stem cells derived from bone-marrow give rise to smooth muscle cells or smooth muscle cell-like cells (Owens et al., 2004).

There are functional differences in smooth muscle cells of different blood vessels including the myogenic tone difference between small and large arteries, difference in signalling pathways which results in variable sensitivities to drugs and difference in calcium regulation between phasic and tonic blood vessel (Somlyo and Somlyo, 2003).

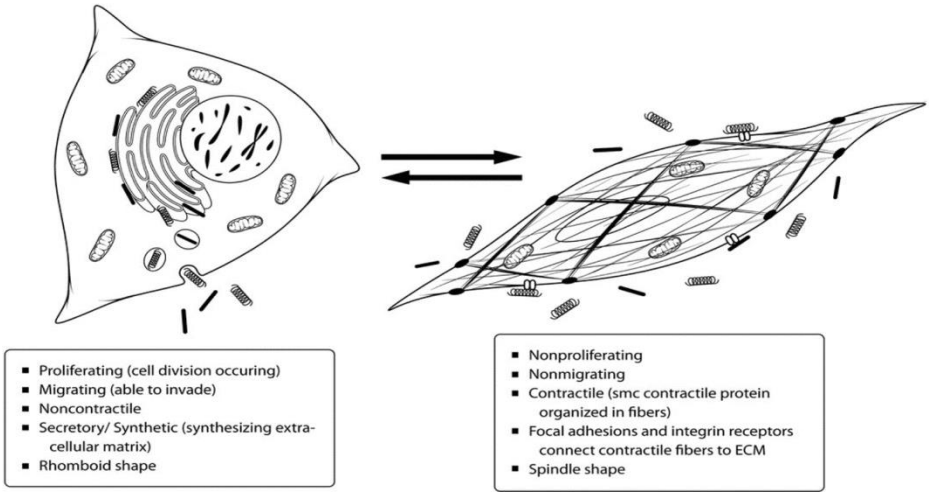

Figure 1.4 *Phenotypic Changes in VSMCs from quiesced contractile to proliferative synthetic phenotype. Diagram shows the morphological changes that occur in the VSMC following stimulation and the functional changes associated with the release of cytokines and growth factors, Dianna M Milewicz et al, 2010.*

Blood Vessel Structure and Function: Adventitia

The vascular adventitia is a very complex compartment in the vessel wall (Figure 1.5). It is composed of fibroblasts, dendritic cells, macrophages, progenitor cells and perivascular nerves embedded in collagen connective tissue matrix (Ishiwata et al., 1997). Adventitial fibroblasts are the first to be activated upon vascular stress or injury leading to alteration in the tone and structure of the vessel wall from the outside in (Rey and Pagano, 2002). They can also sense and direct responses of many stimuli to other adventitial cells in the same tissue as well as the neighbouring tissues. Their activation results in upregulation in expression of extracellular matrix, adhesion proteins and contractile proteins. They also secrete growth factors, cytokines, chemokines and angiogenic factors that are responsible for changing the phenotype of other vascular wall cells and also results in cell proliferation (Henn et al., 1998). High blood pressure also activates the adventitia causing it to lose its elasticity and become stiff (Piek et al., 2000).

Although many cell types are present in the adventitia, adventitial fibroblasts are the most important component as they are the first cells to sense vascular injury and hypertensive state and results in adventitial remodelling which is characterised by adventitial fibroblast proliferation (McEver and Cummings, 1997). In comparison to normal adventitia fibroblasts, hypertensive adventitial fibroblasts have a greater proliferative capacity and produce more chemokines, cytokines and adhesion molecules due to change in their phenotype which correlates with a change in their function and their ability to limit stimulus-induced proliferation (Diacovo et al., 1994). The cross talk between the smooth muscle cells in the medial layer and the adventitia is important in the development of cardiovascular disease. Vascular fibroblasts release large amounts of NADPH oxidase-derived reactive oxygen species which plays a major role in fibroblast proliferation and regulating vascular tone. Adventitial layer has also been seen to act as a barrier to nitric oxide activity which in turn inhibits the function of nitric oxide by stopping it from getting to VSMCs and causing vessel relaxation (Rey and Pagano, 2002). It was reported that adventitial-derived O_2^- diffuses through the vessel layers and interacts with

endothelial derived nitric oxide which inhibits its bioactivity and the NO-dependent relaxation.

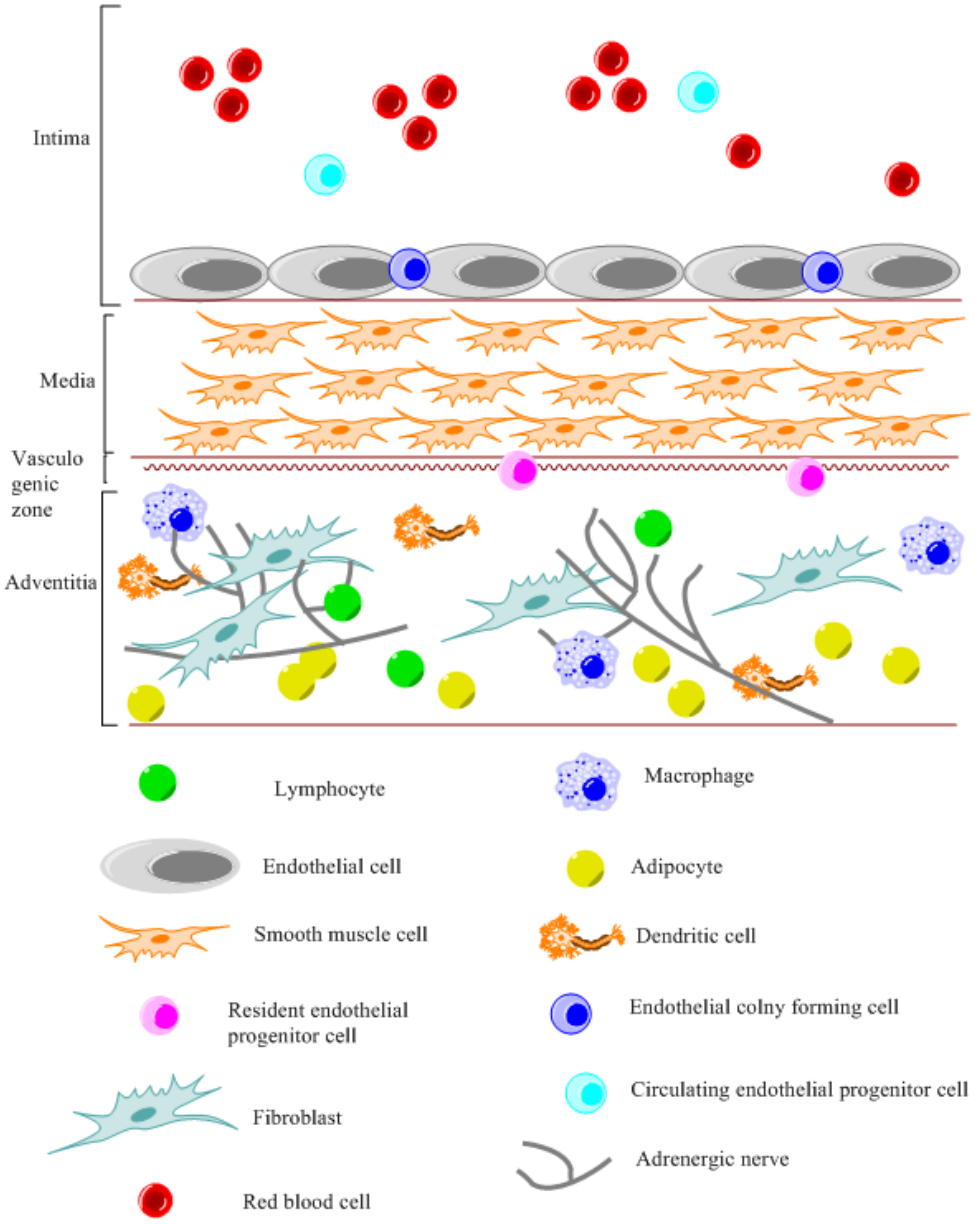

Figure 1.5 *Composition of Tunica adventitia layer of the blood vessel. Diagram shows the different components of the adventitial layer and the factors released by the adventitia.*

1.3 Cardiovascular Disorders:

Many disorders affect the cardiovascular system including hypertension (Hoffman et al., 2011), heart failure and atherosclerosis (Newby and George, 1993). All are in part characterised by vascular smooth muscle cell proliferation and migration. These hyperproliferative diseases can develop normally due to risk factors including diet and life style as in atherosclerosis or iatrogenically after surgical procedures such as percutaneous coronary intervention (PCI) or injury caused by cannulation-dependent injury of the arteriovenous fistula (Chaudhury et al., 2007).

Atherosclerotic occlusion can be treated by stent insertion to the occluded blood vessel or coronary artery bypass grafting (Chen and Fujise, 2005). Both procedures cause injury to the endothelium which is the basis of the formation of intimal hyperplasia which could occur months after the procedure (Stary, 1990). The same problem occurs in the anastomosis site when an arteriovenous fistula is created to gain haemodialysis access for renal failure patients. Many factors are involved in the development and progression of intimal hyperplasia including physical forces, morphologic changes and biochemical events. The sequence in which intimal hyperplasia formation is thought to take place is platelet activation, leucocyte recruitment, activation of coagulation, smooth muscle cell migration and finally smooth muscle cells proliferation (Figure 1.6).

Endothelial damage due to vascular injury results in exposing the sub endothelial matrix causing platelet adhesion and aggregation. The adhered platelets become activated and release thromboxane A_2 which is a potent chemoattractant and a smooth muscle cell mitogen. This is done through the release of ADP and activation of arachidonic acid synthesis pathway (Davies and Hagen, 1994). These activated platelets then release many bioactive substances such as growth factors, platelet-derived growth factor (PDGF), cytokines (IL-1, IL-6, IL-8) and thrombin (Ishiwata et al., 1997). These substances initiate smooth muscle cell proliferation (Lee et al., 2004). Thrombus generation is another consequence for platelet activation which occurs through a trans-membrane protein found on platelets called (CD40L). This protein plays another important role in the expression of many adhesion molecules including P-selectin and E-selectin (Henn et al., 1998).

Following endothelial damage caused by vascular injury or shear stress, the process of leukocyte recruitment and infiltration at the injury site starts. Binding of leukocytes to the adhesion molecules causes inflammation (Piek et al., 2000). The leukocytes bind to the adhered platelets through P-selectin and become activated (McEver and Cummings, 1997) and undergo vessel wall invasion mediated by VCAM and ICAM-2 (Diacovo et al., 1994). Many cytokines are involved in the recruitment of leukocytes including IL-8 in neutrophil recruitment. Others, such as IL-1 and IL-6 play an important role in modulating inflammatory response. The extent of the injury determines the inflammatory response which explains the rich presence of neutrophils and macrophages at the site of stent injury (Inoue et al., 2000).

Damage to the endothelium layer also results in the exposure of tissue factor to the circulating blood (Figure 1.7). Along with monocytes, which release cytokines and growth factors, this triggers coagulation process and results in thrombin formation by binding to factor VII/ VIIa (Edgington et al., 1991). Circulating tissue factor (TF) becomes incorporated into the thrombus between the micro particles and the activated platelet. Thrombin then stimulates smooth muscle cell proliferation by inducing platelet release of platelet-derived growth factor (PDGF; (McNamara et al., 1996).

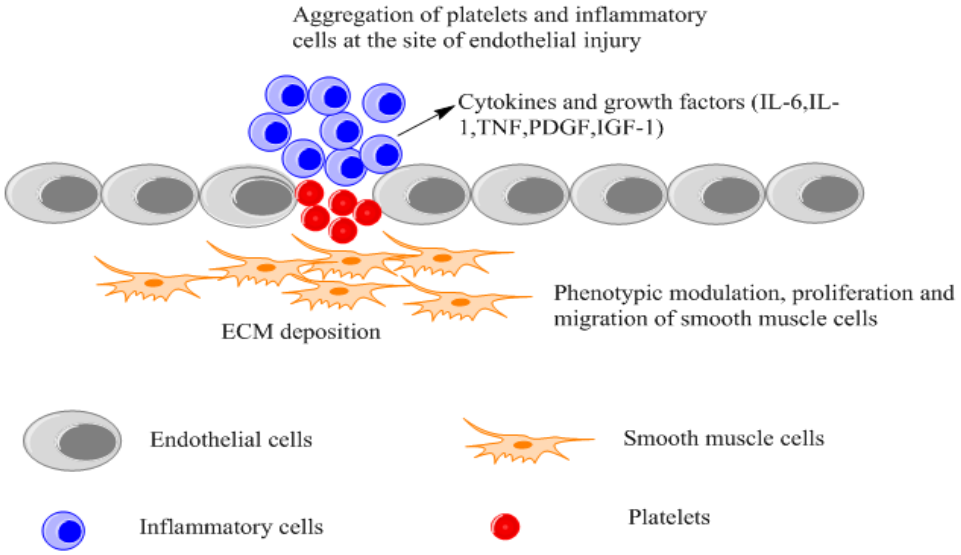

Figure 1.6 *Platelet activation and Leukocyte recruitment. Diagram shows the recruitment of leukocytes and the activation of the platelets following endothelial damage.*

Vascular smooth muscle cells found in the hyperplastic intima has been a subject of intensive studies in an attempt to describe the underlying pathobiology (Michel et al., 2012). Bone marrow-derived somatic progenitor cells have been seen to migrate to the intima and give rise to vascular smooth muscle cells to form the neointima (Religa et al., 2002). Other evidence suggested that vascular injury stimulates the vascular smooth muscle cells in the tunica media and changes them from the quiescent to the proliferative phenotype which then promotes them to migrate from the media into the intima (Chen and Fujise, 2005).

A number of genes have been identified to regulate the migration of the smooth muscle cells whether from the media into the intima or through the blood stream in the case of somatic progenitor cells and one of these is the human tissue inhibitor of metalloproteinease-1 (TIMP-1) which was investigated in an animal model of vascular injury (Dollery et al., 1999).

Once the VSMCs migrate to the intima, they proliferate and secrete extracellular matrix (ECM) which increases in size and eventually causes the narrowing of the

lumen and restenosis. The blood vessel contains a variety of growth factors including platelet-derived growth factors (PDGF), thromboxane A_2, adhesion molecules such as P- and E- selectins and cytokines which then cause VSMC to activate cell-cycle related molecules such as cyclins and cyclin-dependent kinases (Shelat et al., 2001). Some recent evidence also shows that the growth of VSM cells and the production of the ECM is not only positively regulated by growth factors but also negatively controlled by genes within the VSM cell such as tumour suppressor gene p53 which was shown to be significantly increased when the VSM cells were stimulated by growth factors (Mnjoyan et al., 2003). Matsushita (2000) confirmed in a rat carotid artery injury model that an abnormal VSM cell growth was observed when the p53 function was disrupted. Another study showed that when wild type p53 was over expressed by gene transfer, the restenosis was decreased remarkably (Scheinman et al., 1999).

Another protein found to be important in vascular remodelling is Fibulin-5. Fibulin-5 is an elastin-binding protein required for the assembly and organization of the elastic fibres was up regulated in VSM cell within the neointimal hyperplasia in a mouse carotid artery model. Fibulin-5 blocks both neointimal hyperplasia and outward remodelling which was found when fibulin-5 deficient mice had more severe neointimal hyperplasia and larger vascular circumference compared to the wild type (Jeffrey et al., 2005).

Many signalling pathways are involved in the process of vascular proliferative diseases including phosphatidyl-inositol 3-kinase (PI3K), Akt and mitogen-activated protein kinase (MAPK) (Rakesh and Agrawal, 2005). The most important signalling pathway is MAPK which will be discussed in more details in section (1.6).

Activation of PI3K signalling pathway causes it to interact with other signal inducing molecules and activates other pathways (Wymann and Pirola, 1998). PI3K is associated with Ras and MAPK which is involved in cell proliferation, differentiation, motility and cell death (Cobb, 1999). PI3K is also involved in the functioning of Akt signalling pathway which is known to maintain the balance between survival, apoptosis and proliferation (Burgering and Coffer, 1995).

Vascular smooth muscle cells are normally maintained quiescent under normal conditions. When a signalling agent such as a growth factor binds to receptor with intrinsic tyrosine kinase activity, those smooth muscle cells enter the cell cycle again and growth becomes initiated (Cadena and Gill, 1992). Those receptors couple indirectly to many signalling pathways including MAPK and PI3K-Akt (Berra et al., 1993). However, full mechanism and the full picture of the signalling pathways involved is not yet understood which raises the question about the role played by other cellular organelles such as mitochondria in the process of shifting VSM cell phenotype from contractile to synthetic resulting in different vascular hyper proliferative diseases such as atherosclerosis and AVF restenosis.

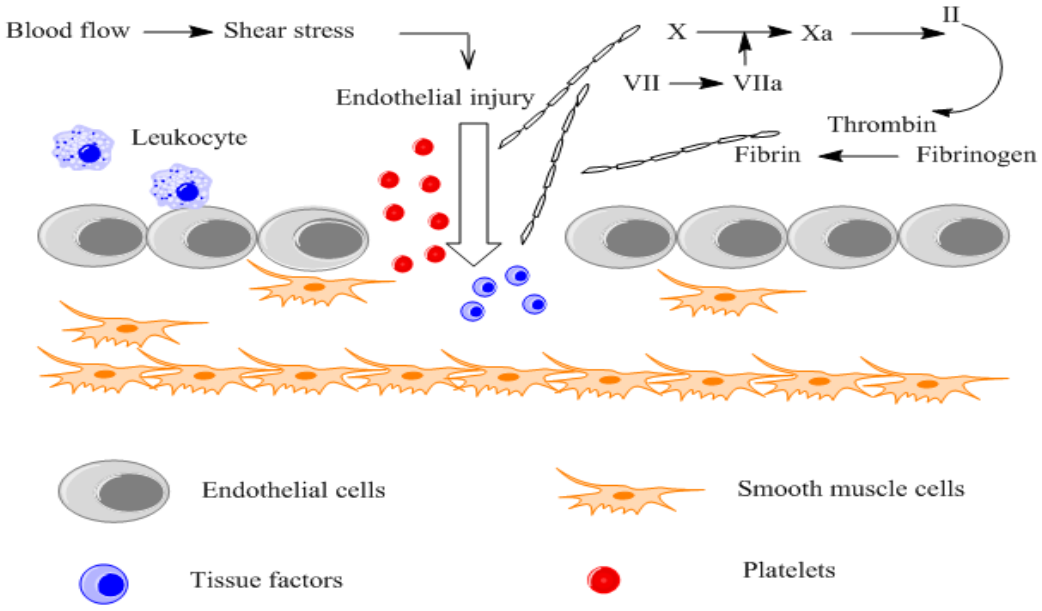

Figure 1.7 *VSMC migration and Proliferation. Diagram shows important factors released following the damage to the endothelium which drives VSMCs to have increased proliferative and migratory capacity.*

Atherosclerosis:

Atherosclerosis is a complicated immuno-inflammatory disease that occurs in medium sized and large arteries (Figure 1.8). The underlying inflammatory event that leads to atherosclerosis occurs long before the disease becomes clinically apparent

(Crowther, 2005). Once atherosclerosis is initiated, it progresses as a result of a series of changes in the constituent cellular make-up of the vessel wall along with cytokine-mediated lesion growth. The atherosclerotic lesion as it develops accumulates lipid laden macrophages (foam cells) and is characterised by fibroblast proliferation (Fleming, 1999). Presently studies revealed that the major players in the development of atherosclerosis are lipids, endothelial cells, leukocytes and more importantly intimal smooth muscle cells (Ross, 1999). Atherosclerosis alone is not always fatal, it is the rupture of the plaque and the circulating debris in the vascular system that causes the devastating consequences when they become trapped and occlude the downstream blood supply resulting in ischemia which can result in stroke or myocardial infarction (Falk, 2006). Atherosclerotic lesions begin to develop under a dysfunctional endothelium which with time becomes de-endothelialised and the endothelial cells become de-endothelialised which leads to the loss of anti-inflammatory and anti-thrombotic properties of the endothelium (Davies et al., 1988). Plasma molecules and lipoproteins leak through the defective endothelium into the sub-endothelial space (Figure 1.8). When the endothelium becomes activated by pro-inflammatory stimuli, the expression of adhesion molecules such as vascular cell adhesion molecule-1 (VCAM-1) become up-regulated which contribute to the recruitment of monocytes and T cells (Libby, 2002). Other adhesion molecules also contribute to the recruitment of blood borne-cells to the atherosclerotic lesion including intracellular adhesion molecule-1 (ICAM-1), E-selectin and P-selectin(Hansson, 2005).In response to atherogenesis, leukocytes are recruited and that is seen in the circulating monocytes and T lymphocytes and neutrophils (Naruko et al., 2002). Some chemokines are required for the adhesion of leukocytes to the endothelium including monocytes chemoattractant protein-1 (MCP-1) which is over-expressed in atherosclerosis. MCP-1 and its receptor on monocyte/macrophages (CCR2) are up-regulated during plaque formation and thought to attract both monocytes and T cells during this process which is then passed into the intima with the help of interlukin-8 (IL-8; (Glass and Witztum, 2001). During disease progression, the immune-inflammatory response is joined by fibro-proliferative response mediated by intimal smooth muscle cells which are responsible for healing and repair after arterial injury (Schwartz et al., 2000). However, these cells undergo

changes in the phenotype that causes the proliferation to be uncontrolled and continue until the lumen size is reduced and blood flow is compromised.

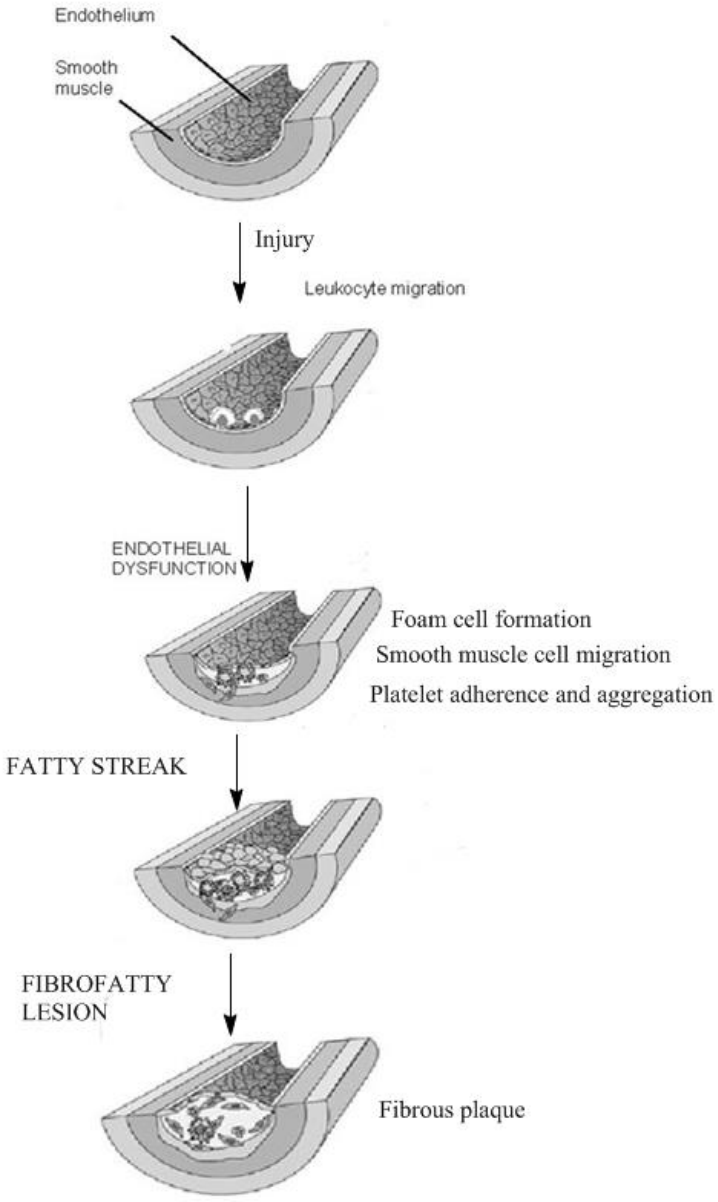

Figure 1.8 *Process of atherosclerosis development. Diagram shows the main steps involved in the initiation and progression of atherosclerosis.*

Arteriovenous Fistula (AVF):

The number of renal failure patients is increasing around the world, in 2001 more than one million patients were reported to receive dialysis worldwide and the numbers are growing at an annual global average rate of 7% (Rakesh and Agrawal, 2005). This brings the need for renal dialysis and arteriovenous fistula creation at the top of the priorities to gain better access to the vein. The technique of Arteriovenous fistula creation was first introduced by Scibner shunt in 1960 (Scribner et al., 1960) and Brescia-Cimino fistula in 1966 (Brescia et al., 1966). This surgery helped in gaining better access to the vein and hence more volume of blood transfused compared to the older method which involved direct insertion of the cannula into a large vein (Figure 1.9). Despite the advantages achieved by this method and the fact that it is the preferred method of renal dialysis, the problem of stenosis and AVF failure remains unresolved (Tordoir et al., 2007). The failure can either be as a result of failure to mature or as a result of neointimal hyperplasia formation which causes vein wall thickening, stenosis and ultimately occlusion. The neointimal hyperplasia is caused by smooth muscle cell proliferation suggesting that there are morphological changes occurring in the vascular smooth cells enhancing the proliferation (Murphy et al., 2002). With a 63% patency rate at one year, more investigations are needed to underline the pathways involved in the proliferation of the smooth muscle cells (Biuckians et al., 2008).

Aneurysm is another cause for AVF failure. It is the rupture and bleeding of the blood vessel wall that occurs in areas of repeated needle puncture sites driven by the loss of elasticity due to destruction of the venous wall and replacement by scar tissue (Mennes et al., 1978). Vascular access site infection leading to sepsis is a very challenging complication and can cause morbidity and mortality among hemodialysis patients. It can also be an important cause for AVF failure after triggering the immune response (Saeed Abdulrahman et al., 2002).

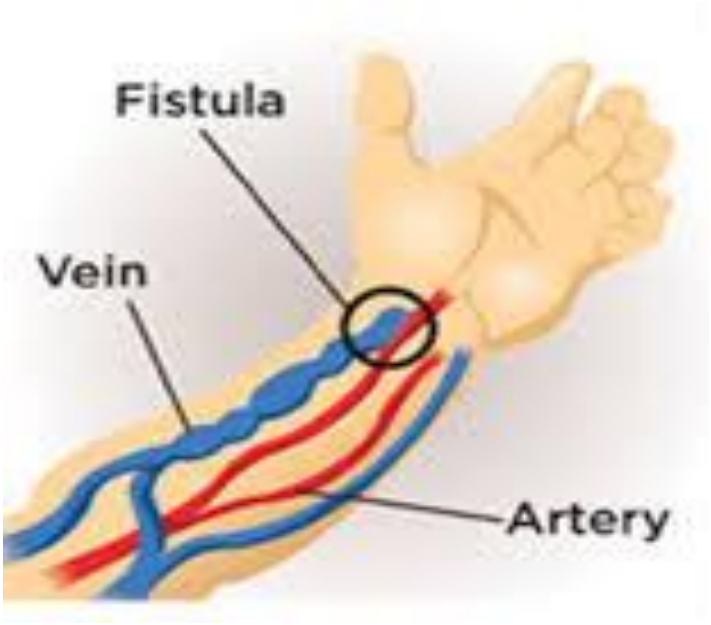

Figure 1.9 *Arteriovenous fistulas. Diagram shows the creation of AV fistula by joining the artery with the vein shown inside the circle.*

AVF Failure to Mature:

Fistula maturation is required to stand the velocity and volume of the blood flowing into the newly created anastomosis. Maturation is achieved when two needles can be cannulated to deliver a minimum blood flow for the total duration of dialysis (Wymann and Pirola, 1998). Almost between 20 and 50% of fistulas fail to mature (Cobb, 1999). Maturation of the fistula depends on having sufficient blood flow to support haemodialysis and prevent thrombosis. This is determined by the pressure gradient and the total resistance in the fistula circuit (Burgering and Coffer, 1995). The capacity of the fistula to dilate is needed to accommodate the increase in blood flow required for the maturation. They need to dilate by nearly 80% to achieve a 10 fold increase in blood flow. Based on clinical studies, the major stimulus for the arterial dilation and remodelling after fistula creation is blood flow velocity and shear stress exerted on blood vessel wall which is sensed by the endothelium. Loss of endothelial cells after fistula creation may contribute to the impairment in dilation and maturation as a result of failing to release the vasodilator nitric oxide which restores the shear stress back to normal (Cadena and Gill, 1992). Formation of

neointimal hyperplasia downstream of the anastomosis has also been implicated with the fistula failure to mature. The overall rate of fistula maturation has been shown to improve following correction of these lesions using inhibitors of pro-hyperplasia signalling pathways. These pathway inhibitors include cell cycle inhibitors, PI3K/Akt/mTOR signalling pathway and MAPK signalling pathway (Mitra; et al., 2005).

AVF Stenosis:

Although the National Kidney Foundation Disease Outcomes Quality Initiative (NKF-DOQI) guidelines recommend that creation of native arteriovenous fistulas is preferable to arteriovenous grafts because of their lower morbidity and higher long-term patency (K/DOQI, 2006), the AVFs are still subject to failure due to stenosis with an estimated failure rate of 23%-46% both in Europe and the United States (Chalmers et al., 2012).

The pathology of stenosis has been the focus of many recent studies which linked the progression of the lesion with the damage caused to the endothelium (Figure 1.10). Many substances have been correlated with endothelial dysfunction as a result of these emerging studies. Plasma levels of asymmetrical dimethylarginine (ADMA), which is an endogenous inhibitor of nitric oxide production, was shown to correlate with endothelial dysfunction and the development of stenosis (Wu et al., 2009). Up to 60% of the patients with high levels of ADMA had target lesion stenosis compared with 25% of those with low levels; suggesting a role for ADMA in the progression of stenoses of AVFs which opens the doors for studying therapeutic targets for ADMA. It was suggested that ADMA competes with L-arginine as the substrate for nitric oxide (NO) synthase, resulting in decreased production of endothelium-dependent NO (Boger et al., 2000). The endothelium plays a crucial role in the maintenance of vascular homeostasis, and NO is the most important mediator of this process. The decrease in NO production affects platelet aggregation and adhesion, leukocyte adhesion, smooth muscle proliferation and extracellular matrix formation, which may contribute to the progression of the stenotic lesion (Sarkar et al., 1996).

The lesion associated with AVF stenosis comprises smooth muscle cells, myofibroblasts and endothelial cells within micro vessels (Roy-Chaudhury P et al., 2006). It was also reported that transforming growth factor β and insulin-like growth factor I were present within the lesion (Stracke et al., 2002). Increase in shear stress (which is the frictional force exerted by blood on the vessel wall) results in endothelial quiescence, orientation of endothelial cells in the direction of flow and the secretion of anti-inflammatory and anticoagulant mediators (Paszkowiak and Dardik, 2003) which then causes dilatation of the blood vessel and reduction in the neointimal hyperplasia (Keren, 1997). On the other hand, a decrease in shear stress results in endothelial cells activation and proliferation and release of inflammatory and procoagulant substances (Meyerson et al., 2001) which causes vascular constriction and increase in neointimal hyperplasia (Honda et al., 2001).

Transmural pressure (the pressure that is generated within the vessel) is another parameter that can cause AV fistula failure with many lines of evidences coming from studies linking the increase in the transmural pressure with smooth muscle cell activation, increased cytokine expression and resulting in thickening in the vessel wall (Lehoux et al., 2006).

Surgical injury to blood vessels by direct needle injury is another risk factor for developing AV fistula stenosis (Konner et al., 2003) and, although angioplasty is a treatment for AV fistula stenosis, the procedure itself can cause significant endothelial and smooth muscle cell injury resulting in a worsening of the restenotic lesion (Chaudhury et al., 2007). This was confirmed by a study which concluded that increased cellular proliferation and shorter time to restenosis was observed in an AV fistula subjected to angioplasty compared with primary stenosis (Chang et al., 2004).

Trauma to blood vessels activates the immune system just like any trauma occurring in any other organ of the body (Gilmore, 2006). The immune system detects the signals and responds with an inflammatory reaction in order to preserve integrity. The release of inflammatory cytokines such as TNF-α and IL-1 triggers the proliferation of the smooth muscle cells. In response to specific signals, the smooth muscle cells alter their phenotype from the contractile to the proliferative type. This has been described by moving from G0 phenotype with very low rate of proliferation

into G1 phenotype with a fast proliferative rate (Charron et al., 2006). The signals transuded mainly through Mitogen Activated Protein Kinase (MAPK) (Johnson and Lapadat, 2002). The inflammatory cytokines mediate the phosphorylation of transcription factor resulting in proliferation which will be discussed in section (1.5).

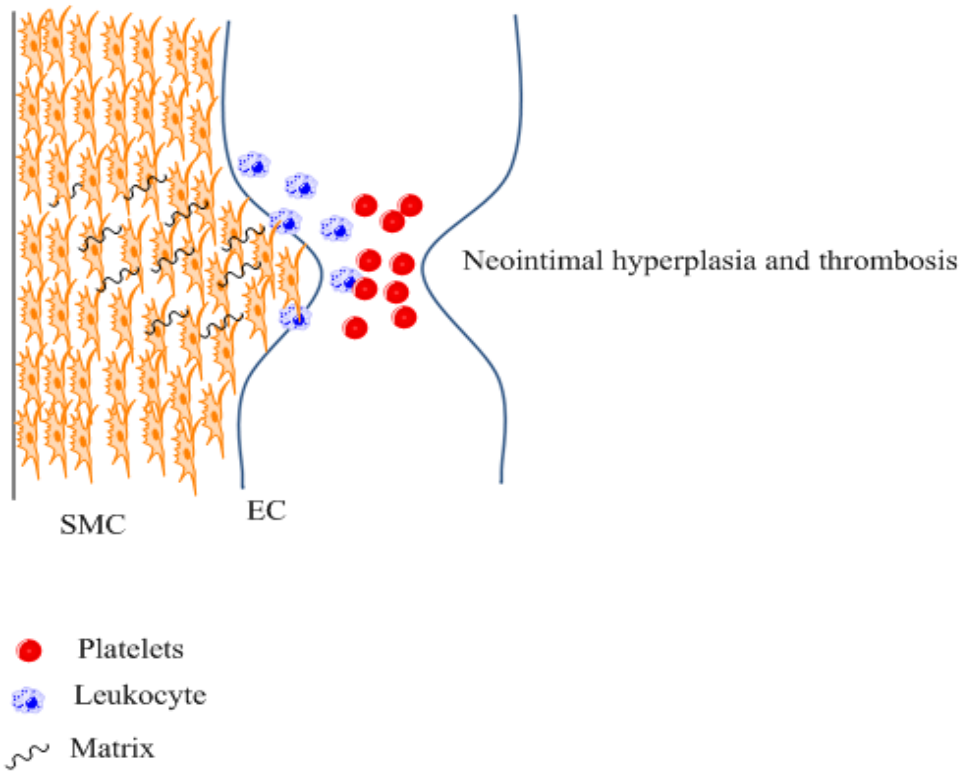

Figure 1.10 *AVF Stenosis. Diagram shows the narrowing of the blood vessel following AVF creation caused by the proliferation of the VSMCs in the medial layer and the activation and recruitment of the platelets and leukocytes.*

1.4 Vascular Smooth Muscle Cell Phenotypes of Stenotic Lesion:

Different cell types were found to exist in a human stenotic lesion from haemodialysis vascular access. This includes contractile smooth muscle cells, myofibroblasts, fibroblasts and macrophages. Some early studies demonstrated the

translocation of adventitial fibroblasts through the media and into the intima where they transform into myofibroblasts and contribute to neointimal hyperplasia (Shi et al., 1996b). More recent investigations suggested that many of the actin positive cells found in the neointima are bone marrow-derived stem cells that have acquired a smooth muscle cell phenotype (Sata and Nagai, 2002). A more detailed analysis of the cellular phenotype present in venous stenosis has been described by Roy-Chaudhury et al (2009). Neointimal cells were primarily viementin positive, SMA positive, desmin negative myofibroblasts and a small proportion of desmin positive cells. This indicates a contractile smooth muscle phenotype as summarized in the table below.

	SMA	Vimentin	Desmin	PGM-1
SMCs	+	_	+	_
Myofibroblasts	+	+	_	_
Fibroblasts	_	+	_	_
Macrophages	_	+	_	+

Table 1.1 *cellular phenotyping in dialysis access stenosis (PGM-1= macrophage marker)*

There is a high likelihood of migration of fibroblasts from the adventitia into the neointima due to the presence of fibroblast-like cells within the venous media (Shi et al., 1996a). This was supported by a study that applied adventitial gene therapy of tissue inhibitor of metalloproteinase (TIMP) which showed a reduction in the neointimal hyperplasia in arteriovenous graft stenosis model (Meng et al., 2006). Thus, targeting migration of adventitial cells can be one effective way of reducing the extent of the stenotic lesion. However, with evidence suggesting other potential role of bone marrow-derived cells binding to the site of vascular injury and then differentiating into smooth muscle cells and myofibroblasts (Caplice et al., 2007), similar approaches could possibly be studied.

It is also thought to be possible, but not yet confirmed, that there could be an ongoing phenotype switching within the lesion. This means that it is possible that the migrating fibroblasts could acquire SMA expression to become myofibroblasts. This also means that contractile smooth muscle cells migrating from the media could lose desmin expression and acquire vimentin expression to become myofibroblasts (Roy-Chaudhury et al., 2009).

1.5 Inflammation Following Vascular Surgery/ Injury:

Mechanical injury to the blood vessel wall including balloon angioplasty, endovascular stent deployment, AVF creation provoke an inflammatory response (Qiu et al., 2014). This acts as a wound healing response involving endothelial denudation, platelet aggregation and expression of adhesion molecules. This also involves inflammatory cell infiltration driven by chemical gradient of chemokines released from smooth muscle cells, release of growth factors from platelets, leukocytes and smooth muscle cells, smooth muscle cell modulation and proliferation, proteoglycan deposition and extracellular matrix remodelling (Hyden and Ghosh, 2004). Many pathological studies reported a strong link between medial damage, inflammation and neointimal thickening (Ghosh et al., 1998). Leukocytes including monocytes, neutrophils and macrophages are recruited as precursors to intimal thickening and are observed clustering around vascular stress or injury areas (Weil and Israel, 2004). Vascular injury is also associated with the recruitment of cytokines such as tumour necrosis factor and interleukins including C reactive protein and IL-6 (Zampetaki et al., 2005). These inflammatory cytokines have effects on endothelial cells, vascular smooth muscle cells, fibroblasts and the extracellular matrix. These circulating cytokines consequently activate inflammatory signalling pathways such as JAK-STAT and NF-κB leading to inflammatory response (Brand et al., 1997). Cytokine interaction with vascular smooth muscle cells activates other signalling pathways including MAPK pathway which promotes cell proliferation and migration. Recent studies have suggested a role for the mitochondria in activating some inflammatory pathways (Madamanchi and Runge, 2007). However, the link between activating inflammatory pathways following vascular injury and vascular

smooth muscle cell proliferation and mitochondrial regulation of these processes is presently poorly understood.

Pro-inflammatory Cytokines in Cardiovascular Disease:

Cytokines are small proteins synthesized by nearly all nucleated cells and they are known to regulate host response to infection, trauma, inflammation and immune response. During the initiation and progression of atherosclerosis and restenosis, a number of pro-inflammatory cytokines including IL-1 and C-reactive protein are recruited. This results in the activation of proliferative signalling pathways such as the mitogen activated protein kinase (MAPK) which phosphorylate the downstream transcription factors and cause VSM cell proliferation and migration (Dinarello, 2000). Some cytokines induce inflammation such as Interleukins-1 (IL-1), Interleukins-6 (IL-6) and Tumour necrosis factor (TNF), those are known as pro-inflammatory cytokines, Whereas, the other group which suppress the inflammation are known as anti-inflammatory cytokines including Interleukin-4, -10 and -13 (IL-4, IL-10, IL-13).

In atherosclerosis and re-stenosis, pro-inflammatory cytokines such as IL-1, IL-6 and TNF interact with specific receptors on target cells such as Toll-like receptor4 (TLR4) and cause phosphorylation of the associated protein kinase. This in turn activates transcription factors such as NF-κB which upon activation synthesise proteins responsible for leukocyte recruitment and adhesion such as E-selectin,VCAM-1 and ICAM- 1, chemokines, growth factors such as vascular endothelial growth factor (VEGF) and platelet derived growth factors (PDGF), and inducible enzymes such as cyclooxygenase-2 (COX2) and inducible nitric oxide synthase (iNOS; (Adrain and Martin, 2001). Synthesis of the growth factors, therefore, activates MAPK signalling pathway which is the main driver of cellular proliferation that follows the inflammatory response (Cortese et al., 1998).

Chemokines are another pro-inflammatory genes including IL-8 which facilitate the migration of leukocytes from circulation into the tissue. IL-1 and TNF induce the adhesion of leukocytes to the endothelial surface and IL-8 facilitates its passage into

the tissue by creating a chemical gradient (Dinarello, 2000). The inflammation process, therefore, is a cascade of gene expression triggered by pro-inflammatory cytokines which is initiated by inflammatory products such as endotoxins as illustrated in the diagram below. These genes include genes for other cytokines, cytokines receptors, growth factors, tissue remodelling enzymes, extracellular matrix components and adhesion molecules (O'Neill, 1995).

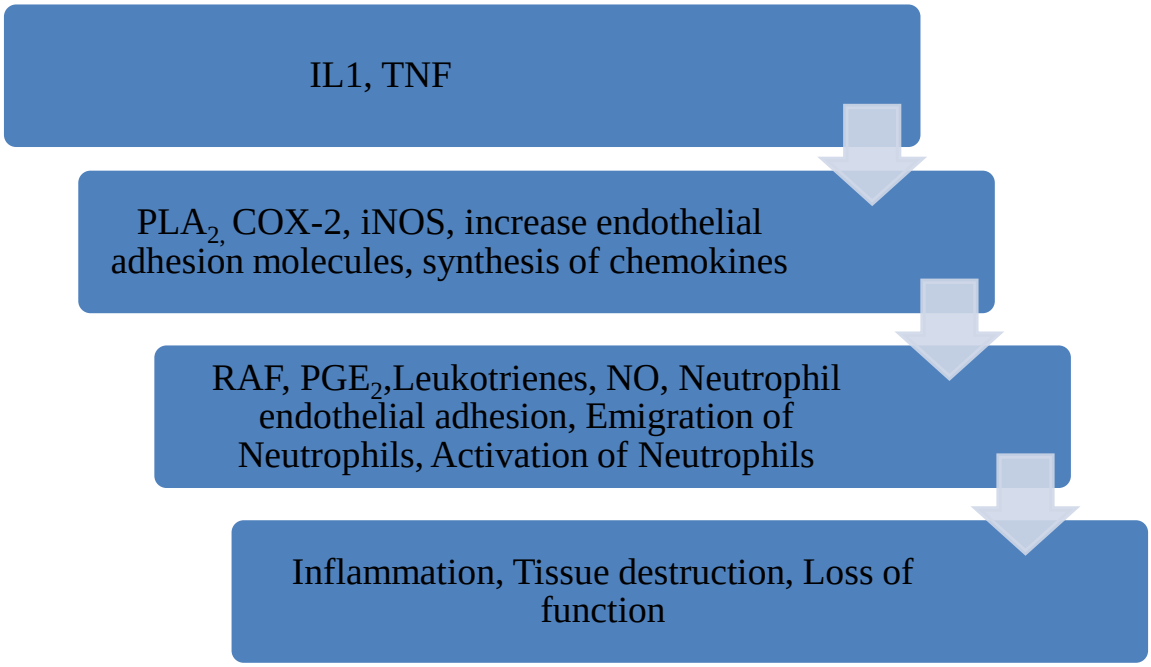

Figure 1.11 *The inflammatory cascade triggered by pro-inflammatory cytokines including IL-1 and TNF*

Pro-Inflammatory Cytokines: Nuclear factor- kappa B (NF-κB)

NF-κB has recently become a very important target for studying pathways involved in inflammatory and immune disorders. Many factors, signalling pathways, adaptor proteins and stimuli lead to the activation of NF-κB which gives it more importance in playing roles in different physiological and pathological conditions both in adaptive and innate immune response (Hyden and Ghosh, 2004). NF-κB proteins are contained in the cytoplasm and their effect is inhibited by IκB molecules which are specific NF-κB inhibitors. When cells are stimulated, another complex called IκB kinase (IKK) becomes activated which in turn phosphorylates IκB molecules.NF-κB

then activates transcription of target genes in the nucleus (Ghosh et al., 1998). Different signalling pathways are associated with the activation of NF-κB. Toll-like receptors (TLRs), for example, detect pathogens of different species and induce pro-inflammatory proteins which trigger innate immunity. T cell and B cell receptors on T and B lymphocytes also sense different antigens and consequently activate NF-κB (Weil and Israel, 2004). Increased activation of NF-κB was detected in many chronic disorders including atherosclerosis (Brand et al., 1997). NF-κB activation was also associated with post-injury trauma where its translocation was significantly increased in trauma patients compared with base line level (Biberthaler et al., 2004).

1.6 Mitogen Activated Protein Kinase (MAPK) Pathway:

MAPK is the main signalling transduction pathway known to mediate smooth muscle cell proliferation. Although many MAPK pathways have been identified, three of them have been the subject of extensive study: extracellular signal-regulated kinases 1/2 (ERK1/2), c-jun amino-terminal kinases (JNK) and P38 MAPK (Figure 1.12). ERK1/2 is the main one responsible for vascular smooth muscle cell proliferation. The cascade begins when a ligand such as a cytokine or a growth factor binds to the extracellular portion of the membrane bound receptor of the family of receptor of tyrosine kinases (RTK). This leads to the dimerisation of two subunits of the receptor (RTK). At the inner sides of the receptors, tyrosine kinase domain catalyses phosphorylation of itself and also the other subunit. Then, the growth factor receptor bound protein-2 (GRB-2) can bind to phosphorylated (RTK). The protein son of sevenless (SOS) is able to bind to membrane bound protein (RAS). Inactive (RAS) is bound to the nucleotide guanosinediphosphate (GDP) against guanosine triphosphate (GTP) (Campbell et al., 1998). This exchange leads to the activation of (RAS) protein which binds to several effector proteins such as A-Raf, B-Raf and Raf-1(Geyer and Wittinghofer, 1997). The kinase B-Raf is one of the most important effectors of (RAS). Regulation of both Raf and Ras is very essential for the maintainance of cell proliferation (Chong et al., 2003). Active B-Raf phosphorylates and activates the kinases (MEK1/2) which phosphorylates and activates (ERK1/2). Finally, the kinase cascade leads to the activation of transcription factors of the activator protein-1 family (AP-1) which includes transcription factors fos and jun.

Fos and jun move to the cell nucleus and bind to AP-1 motif which leads to expression of genes and coding for growth factors, cyclins and cytokines which activates cell proliferation.

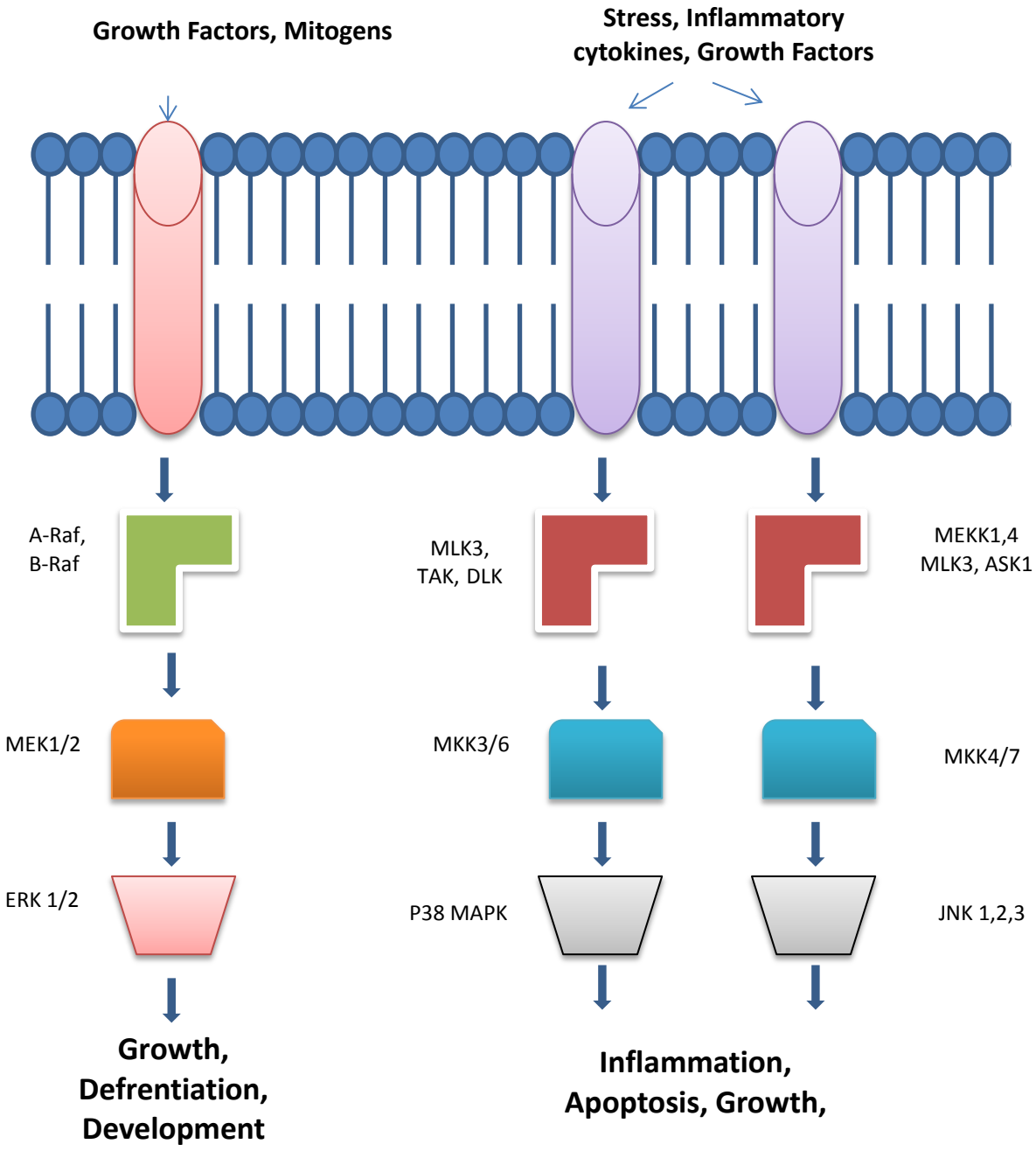

Figure 1.12 *Mitogen Activated Protein Kinase (MAPK) pathway. Schematic shows the three main signalling pathways involved in MAPK; growth factor activated ERK1/2 and stress activated P38 and JNK.*

1.7 Mitochondrial Role in Cardiovascular Disease:

Mitochondria are small organelles enclosed in a membrane inside the cell (Figure 1.13). They were first described in the nineteenth century by botanist Andreas Schimper (Antonsson, 2001). But in 1960, the scientists started to give more attention to study them and their features and functions. Mitochondria are the main source of cellular energy through the production of Adenosine TriPhosphate (ATP). They also function in cell signalling, cell differentiation, apoptosis and cell proliferation and growth (Frohman, 2010).

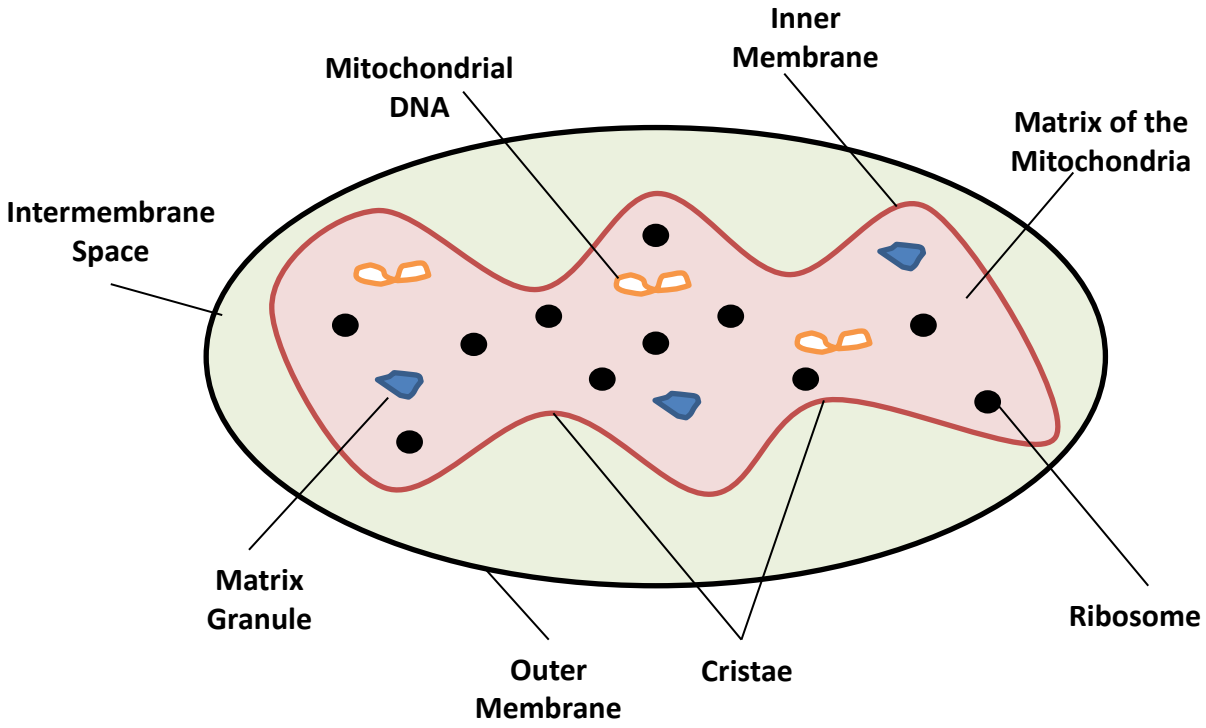

Figure 1.13 *Structure of the mitochondria. Representative diagram showing the different components of the mitochondria*

Recent studies have discovered links between mitochondrial functions and cardiovascular diseases including hyper proliferative disorders through specific signalling pathways such as MAPK and mTOR pathways (Archer, 2010). Mitochondria were long thought to be static organelles but more recent studies revealed that they are dynamic and they undergo fission and fusion to maintain steady state mitochondrial morphology (Suen et al., 2008). These processes are mediated by specific proteins; fission which is the separation of the mitochondria is found to be mediated by DRP1 protein (Wakabayashi et al., 2009) while Mitofusin (Mfn)1 and (Mfn2) mediate fusion of the outer mitochondrial membrane and OPA1 mediates fusion of the inner mitochondrial membrane (Hales and Fuller, 1997). Impaired function of mitochondrial fusion proteins can play a role in developing cardiovascular disease by modulating oxidative stress. Mfn2 has been demonstrated to suppress cell proliferation in vascular smooth muscle cells and might have therapeutic importance in restenosis (Zheng and Xiao, 2010). On the other hand, some studies suggested that inhibiting DRP1 in the heart can protect it from ischemia. It is thought that mitochondrial fusion is important to provide ATP in oxygen poor regions in the cell. It is also essential for calcium buffering across mitochondrial network. It is also required by the cell to overcome the effect of mitochondrial mutations by complementing fused organelles (Skulachev, 2001). Impaired mitochondrial biogenesis has also been shown to result in enhanced activity of renin-angiotensin-aldosterone system, reactive oxygen species production (ROS) and mitochondrial induced apoptosis (Ren et al., 2010). The same study also pointed at a pathological positive feedback pathway between impaired insulin signalling, glucose metabolism and mitochondrial dysfunction. Another study linked ROS production and mitochondrial metabolism and the activity of transcription factors to explain the increase in proliferation in pulmonary artery hypertension. The lower production of ROS has caused resistance to apoptosis due to down regulation of redox-sensitive potassium channels resulting in increase of intracellular potassium and calcium, increase proliferation, activation of transcription factors such as hypoxic inducible factor (HIF) and nuclear factor of activated T-cells (NFAT) (Dromparis et al., 2010). Chalmers et al. (2012) have recently studied the role of mitochondrial dynamics in smooth muscle cell proliferation. They found that when

proliferation of smooth muscle cells was encouraged, the mitochondria became motile and changed its shape into small spheres, short rod-shaped. This led to the conclusion that mitochondrial plasticity is an essential mechanism for the development of smooth muscle cells proliferation (Chalmers et al., 2012). The link between mitochondrial activation, inflammatory signalling pathway and proliferation and migration of smooth muscle cells is still to be further clarified and investigated.

Mitochondrial Cytochrome C:

Mitochondria play a major role in regulating cell death through the mitochondrial apoptotic pathway (Antonsson et al., 2001). The release of cytochrome c from the mitochondria into the cytoplasm in response to growth stimuli activates caspase-9 which activates caspase-3 (Figure 1.14) resulting finally in apoptosis (Orrenius, 2007). Cytochrome C is a redox carrier between complex III and IV in the electron transport chain. This release is facilitated by the opening of the mitochondrial permeability transition pore (MPTP) in response to different stimuli including increased levels of Ca^{2+} and ROS allowing cytochrome c to move from the inter-membrane space into the cytosol (Adrain and Martin, 2001). Cytochrome C in the inter-membrane space can either be loosely tethered to the inner mitochondrial membrane by an electrostatic interaction with anionic phospholipids or partially embedded in the membrane by hydrophobic interactions (Cortese et al., 1998). The release can also be triggered by members of BCL-2 family (Antonsson, 2001).

Mitochondrial Dynamin related protein 1:

Dynamin related protein 1 (DRP1) is a mitochondrial outer membrane protein that, once activated regulates fission and the division of mitochondria (Westermann, 2010). DRP1 is activated as a result of its phosphorylation by cyclin B1 and cyclin dependent kinase 1 (CDK1). Activated DRP1 then moves from the cytosol to the mitochondrial outer membrane where they assemble in helical structure and cause constriction of the mitochondrial membrane followed by mitochondrial division (Ingerman et al., 2005). The importance of DRP1 was studied in different cell types

but it is more essential in highly polarised cells including neurons. Deletion of DRP1 in mice resulted in a decrease in neurites and defective synapse formation (Dickey and Strack, 2011). Mutational defects of DRP1 was also associated with early infant mortality and cardiomyopathy (Ashrafian et al., 2010). DRP1 has also been implicated in myocardial ischemia where the transfection of cells with the dominant negative mutant of DRP1 prevented the effects of ischemia and reperfusion injury (Ong et al., 2010). Recently in a mouse femoral artery wire injury model, neo-intima formation was markedly reduced in transgenic mice expressing DLP1-K38A which was associated with a reduction in ROS level (Wang et al., 2015). In the same study, in-vitro findings also showed that the migratory effect of PDGF was associated with the shortening of the mitochondrial length. Inhibiting mitochondrial fission resulted in the inhibition of VSM cell migration and a reduction in ROS production.

Mitochondrial Mitofusin 2:

Many lines of evidence have been shown to support that Mfn-2 is a major determinant of oxidative stress-mediated cardiomyocyte apoptosis (Shen et al., 2007). Overexpression of Mfn-2 was found to trigger myocyte apoptosis. This was associated with an inhibition of Akt activation without altering ERK1/2 signaling. Inhibition of caspase 9, overexpression of Bcl-xL and activation of phosphatidylinositol reduce the Mfn-2-induced myocyte apoptosis (Shen et al., 2007). This indicates that increased Mfn-2 expression is essential for oxidative stress induced heart muscle cells apoptosis.

Ras-mediated activation of Akt is thought to be one of the signalling pathways that promote cell survival and proliferation (Malumbres and Barbacid, 2003). This signalling pathway has become the focus of many recent studies and many evidences suggested it has a role in cardiovascular diseases including hypertensive vascular proliferative growth (Chien and Olson, 2002). This pathway has been shown to be inhibited by Mfn-2 which caused suppression of cell growth and proliferation in multiple tumour cell lines as well as rat vascular smooth muscle cells both in vivo and in vitro. This is believed to be via inhibition of the Ras-ERK MAPK signaling pathway (Chen et al., 2004). Another strong evidence suggested that Mfn-2 might

have a role in mitochondrial apoptotic signalling after being confirmed that it was associated with Bax which is a pro-apoptotic member of the Bcl-2 family (Zamzami and Kroemer, 2001).

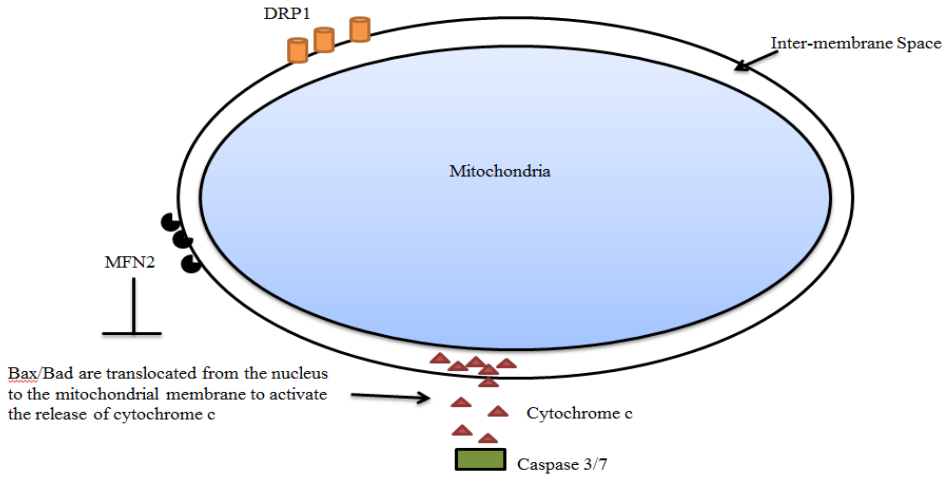

Figure 1.14 *Schematic showing the role played by mitochondrial protein in regulating cellular proliferation and apoptosis. Mfn2 and DRP1 are mitochondrial outer membrane proteins that regulate mitochondrial dynamics needed for cellular proliferation and cytochrome c is a mitochondrial intermembrane protein that is released to stimulate apoptosis.*

A number of studies demonstrate that Mfn-2 protects against Bax-mediated cytochrome c release and reduces free radical-mediated mitochondrial injury (Neuspiel et al., 2005). In addition, protection against apoptotic stimuli can be provided by overexpression of both Mfn-1 and Mfn-2 (Sugioka et al., 2004). This can suggest that high levels of fused mitochondria act as a cell defence mechanism against the accumulation of oxidative lesions (Wei et al., 2001). Moreover, Bax and Bak might undergo conformational changes favouring anti-apoptotic or pro-apoptotic features regulating mitochondrial morphology and apoptosis through their interaction with Mfn-2 and fusion process (Karbowski et al., 2006).

Healthy and Dysfunctional Mitochondria:

Healthy mitochondria have multiple functions of ATP production, cellular growth and apoptosis. They are also known to regulate communication between cells and tissues which can influence organism's physiology (Nunnari and Suomalainen, 2012). Any defect and mutation in the mitochondrial DNA can result in mitochondrial diseases which can affect any organ at any age (Suomalainen, 2011). Mitochondria produce ATP via oxidative phosphorylation. The phosphorylation of ADP to ATP is driven by proton gradient generated by complexes I, III and IV (Okuno et al., 2011). These are the proteins making up the electron transport chain (ETC) (Diaz et al., 2011). The membrane potential is also important for mitochondrial protein import (Neupert and Herrmann, 2007). Complexes I and III are important in generating reactive oxygen species (ROS) such as oxygen radicals and hydrogen peroxide. ROS can cause damage to a cell's lipids and proteins (Murphy, 2009). ROS also have been shown to affect signalling pathways that control cell proliferation and differentiation as well as the hypoxia adaptive stress signalling pathways (Hamanaka and Chandel, 2010). Change in the phenotype from quiescence state to proliferative state was also confirmed in hematopoietic progenitor cells in response to ROS production (Ito et al., 2004).

Dysfunctional mitochondria also affect cellular response to the metabolic status. Even under normal nutrition condition but in mitochondrial dysfunction state, the cells misinterpret decreased ATP synthesis as starvation. Several pathways involving phosphatidylinositol 3-kinase (PI3K) signalling, including Akt/PI3K are activated (Tyynismaa et al., 2010). This can be controlled by AMP-activated protein kinase (AMPK) which is activated by the increase in the AMP:ATP ratio and increased ADP concentrations (Hardie et al., 2011). This triggers the up regulation of the catabolic pathways including oxidative phosphorylation and autophagy and down regulation of anabolic pathways including cell growth and proliferation (Carling et al., 2011). This results in the activation of signalling events that result in initiation of apoptosis and autophagy and inhibition of VSM cell proliferation and migration.

Mitochondrial Signalling:

Many recent lines of evidence show that the mitochondria play an active role in some biological processes such as mitogenic signalling (Arciuch et al., 2012), differentiation and hypoxic stress responses (Chandel, 2010) by being initiators and transducers of cell signalling. They regulate signalling by either acting as a platform on which the protein-protein signalling interaction occurs or by regulating the intracellular signalling molecules such as Ca^{2+} and ROS (Finkel, 2011). Mitochondria have an important signalling role in cell death and apoptosis (Oberst et al., 2008). Cytochrome c proteins which are found in the intermembrane space activate caspase proteases, which are required for apoptosis, when they are released into the cytoplasm (Tait and Green, 2010). In the mitochondria apoptotic pathway, BAX and BAK cause mitochondrial outer membrane permeabilization (MOMP). This results in the release of cytochrome c and SMAC into the cytoplasm where they promote activation of caspase which then leads to apoptosis (Chipuk et al., 2010). In some circumstances, MOMP can be incomplete which can occur because of inhibition of mitochondrial fusion which prevents MOMP of one mitochondrion from causing MOMP in other mitochondria (Westermann, 2010).

Mitochondria are also one of the main sources of damage-associated molecular patterns (DAMPs) and in some studies their DNA was proved to act as an effective DAMPs and induced pro-inflammatory response (Collins et al., 2004). DAMPs are proteins that are released from damaged cells and activate innate immune system by binding to pattern recognition receptors (Medzhitov, 2007). Recognizing DAMPs then up regulates pro-inflammatory cytokines, type I interferons (IFNs) and co-stimulatory molecules (Chen and Nunez, 2010). In a recent study, injection of mitochondria lysates containing mitochondrial DNA induced lung and liver inflammation through activation of TLR-9 (Zhang et al., 2010).

1.8 Mammalian Target of Rapamycin (mTOR) Signalling Pathway:

mTOR signalling is important in regulating cell metabolism, growth, proliferation and survival. This is an important signalling pathway involved in the initiation and progression of VSM cell proliferation which is a key event in atherosclerosis and re-

stenosis (Zhao et al., 2011). mTOR inhibitors are currently used to coat stents used in percutaneous coronary intervention including rapamycin. However, due to their side effects including de-endothelialisation and thrombosis following implantation (Joner et al., 2006), they are used under precaution and there is still a need for more specific inhibitors that would target only the phenotypically switched proliferative VSM cell. This requires the need to identify novel signalling cascade that involves mTOR effector proteins.

The intracellular and extracellular signals are processed through two main complexes (Figure 1.15): mTOR complex1 (mTORC1) and mTOR complex2 (mTORC2) (Laplante and Sabatini, 2009). Cell proliferation and growth is regulated by mTORC1 through promoting biosynthesis of proteins and lipids and limiting autophagy (Guertin and Sabatini, 2007). Protein synthesis is promoted by phosphorylating the eukaryotic initiation factor 4E (eIF4E), binding protein 1 (4E-BP1) and the p70 ribosomal S6 Kinase1 (S6K1) (Richter and Sonenberg, 2005). mTORC1 is stimulated by four major signals; growth factor, energy status, oxygen level and amino acid. Growth factors which stimulate it through the activation of the canonical insulin and Ras signalling pathways which increases the phosphorylation of TSC2 by AKT (Inoki et al., 2002) , by ERK1/2 (Ma et al., 2005) and by p90 ribosomal S6 kinase1 (RSK1) resulting in increased protein synthesis and transcription factors which lead to cellular growth and proliferation (Roux et al., 2004). Hypoxia activates AMPK when the ATP levels drops low and that activates TSC1/2 and inhibits mTORC1 signalling (Arsham et al., 2003). MTORC1 can also be blocked by activating TSC1/2 through transcriptional regulation of DNA damage response (REDD1) in response to hypoxia (DeYoung et al., 2008). MTORC1 can also be stimulated by inflammatory mediators via TSC1/2 complex. Pro-inflammatory cytokines such as tumour necrosis factor TNFα inactivates TSC1 through IκB kinase-β (IKKβ) activation which consequently results in the activation of mTORc1 (Lee et al., 2008).

MTORC1 also regulates mitochondrial metabolism and biogenesis. Mitochondrial membrane potential, oxygen consumption and cellular ATP levels are all lowered

when the mTORC1 is inhibited by rapamycin (Schieke et al., 2006). It was also found that mitochondrial DNA copy number and the expression of many genes which encode the proteins that are involved in oxidative metabolism were reduced by rapamycin and increased by mutations that activate mTORC1 signalling (Cunningham et al., 2007).

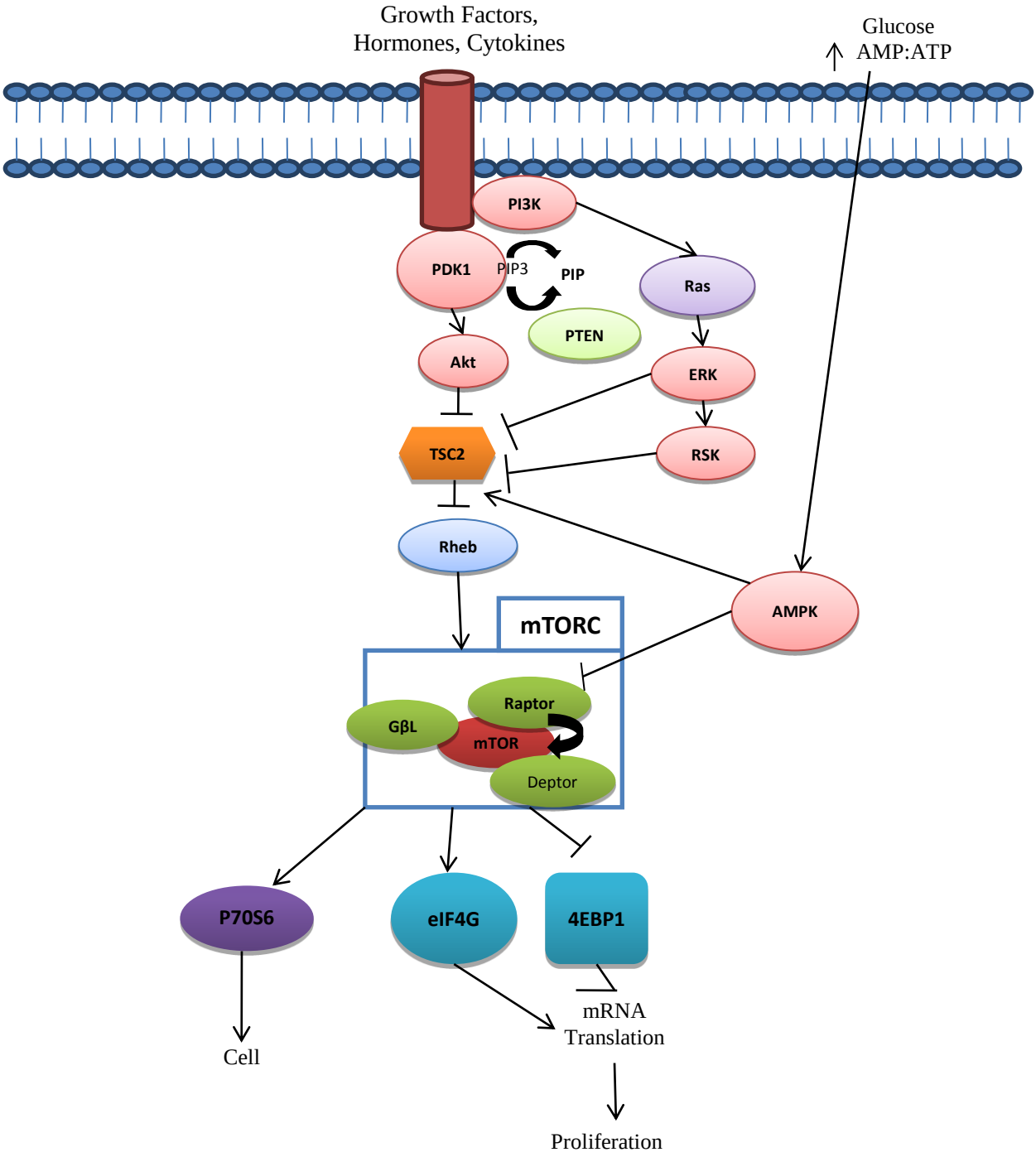

Figure 1.15 *Mammalian Target of Rapamycin (mTOR) signalling pathway. Diagram shows different effector proteins involved in the activation of mTOR signalling pathway both upstream and downstream.*

AMP-activated Protein Kinase (AMPK) and (mTOR) Pathways:

AMPK is known to regulate metabolic processes to maintain cellular energy homeostasis through repression of energy consuming processes and simultaneous enhancement of energy producing processes. mTOR, which is involved in cell growth and division and it is one of the protein kinase regulating protein synthesis pathway has been found to be a target for AMPK as the synthesis consumes a lot of cellular energy (Fingar and Blenis, 2004). Many recent studies have shown that the activation of AMPK is linked to reduction in mTOR signalling. Activation of AMPK using AICAR or any other agents that reduce the intracellular level of ATP was seen to decrease phosphorylation of S6K1 which indicates that mTOR signalling was repressed despite the amino acid-induced activation of mTOR (Dubbelhuis and Meijer, 2002). Another study also showed that mTOR signalling was repressed in skeletal muscles of rats when treated with AICAR. Increase in the AMPK phosphorylation was observed along with the dephosphorylation of 4E-BP1 and S6K1 which are believed to be directly phosphorylated by mTOR (Bolster et al., 2002).

1.9 Regulation of Signalling Pathways by micro RNA (miRNA):

Vascular diseases such as atherosclerosis and restenosis initiate and progress via well-established signalling pathways including MAPK, mTOR and NFκβ signalling pathways. However, new molecules that contribute to the initiation and progression of these signalling cascades are continuing to be discovered. One of these is a class of gene regulators known as micro RNAs (miRNAs). MiRNAs are negative regulators of gene synthesis that inhibit mRNA translation or cause a post transcriptional degradation of specific mRNA targets. They regulate the synthesis of over 30% of the genes in the cell and therefore control cell physiology and pathogenesis. Changes in the miRNA expression profile in VSM cell has been linked to changes in cell differentiation, proliferation and migration that are involved in angiogenesis and neointimal formation underlying vascular diseases including atherosclerosis and restenosis (Weber et al., 2010).

In atherosclerosis, the endothelial cell layer is in direct contact with haemodynamic forces including shear stress. In cultured endothelial cells, expression of miR-21 was induced in response to the exposure to oscillatory shear stress (Zhou et al., 2011). This has led to inflammatory response mediated by peroxisome proliferators-activated receptor-α. Oscillatory shear stress was also found to upregulate the expression of miR-92a which targets KLF-2. KLF-2 has athero-protective properties and regulates the expression of other athero-protective genes including eNOS and thrombomodulin (Wu et al., 2011). Expression of other miRNAs have also been found to be regulated by shear stress in endothelial cells including miR-663 (Ni et al., 2011) and miR-19a (Qin et al., 2010). MiR/mRNA expression profile conducted in atherosclerotic plaques obtained from patients revealed an increase in the expression of a number of miRNAs including miR-21, -43a, -146a and -210. Bioinformatics analysis identified a number of mRNA targets involved in different signalling pathways including metabolism, immunodeficiency, P53 and cell proliferation (Raitoharju et al., 2011). MiR-43a was found to be one of the key players in the development of atherosclerosis by regulating apoptosis and cell cycle. Likewise, the increase in the expression of miR-221 and miR-222 seen in balloon-injured carotid arteries play a major role in the regulation of p27(Kip1) and p57(Kip2) which are negative regulators of VSM cell proliferation through cell cycle control (Liu et al., 2009). The importance of miR-145 in VSM cell differentiation and its role in cardiovascular diseases has been the focus of some studies recently. MiR-145 was found to be highly expressed in the smooth muscle cells of the aorta postnatally (Cordes et al., 2009). MiR-145 was also found to target genes that are involved in the dedifferentiation and proliferation of VSM cell including KLF-4 and ELK-1 (Elia et al., 2009). Another equally important miRNA is miR-21 which is an oncomir found at significantly elevated levels in neointimal lesions (Bonci, 2010). miR-21 enhances VSM cell proliferation and neointimal formation by blocking apoptotic signalling pathways through the direct targeting of PTEN and PDCD4 (Lin et al., 2009).

miR	Function	Effect	Potential Targets
miR-21	Vascular Remodelling	Increase VSM cell proliferation	PTEN, BCL2
miR-26	Vascular Remodelling	Decrease VSM cell proliferation	SMAD
miR-145	Vascular Remodelling	Decrease VSM cell proliferation	KLF4, KLF5
miR-146a	Vascular Remodelling	Increase VSM cell proliferation	KLF4
miR-221/222	Vascular Remodelling	Increase VSM cell proliferation	P27/ P57
miR-126	Atherosclerosis	Increase EC cell proliferation	Spred1, PI3K
miR-146	Atherosclerosis	Increase VSM cell proliferation	KLF4

Table 1.2 *Lists key miRNAs involved in cardiovascular diseases, their function, cellular effect and potential gene targets.*

1.10 Regulation of Mitochondrial Bioactivity by miRNAs:

Different cellular functions played by mitochondria including supply of energy, calcium homeostasis, apoptosis and the production of reactive oxygen species all require synthesis of genes that regulate these pathways. Although limited, some of these genes are synthesised within the mitochondria using mitochondrial genome whereas others are synthesised in the nucleus and transported to the mitochondria (Cannino et al., 2007). This means that mitochondria can play an important role in miRNA sourcing as well as being a target for miRNAs synthesised either by their own genome or nuclear genome. MiR-338 is one of the miRNAs found to target cytochrome c oxidase IV (COXIV) which is a key regulator of the electron transfer chain and ATP production. Overexpression of miR-338 associated with neuronal diseases was seen to reduce mitochondrial oxygen consumption, mitochondrial metabolic activity and ATP production (Aschrafi et al., 2008). This is also important for the proliferation and migration of VSMCs during the initiation and progression of atherosclerosis and re-stenosis. Another miRNA known to target mitochondrial ATP

synthesis is miR-23a/b which targets glutaminase. Glutaminase converts glutamine to glutamate which is catabolised to produce ATP in the tricarboxylic acid cycle in the mitochondria (Gao et al., 2009). Mitochondrial biogenesis was seen to be regulated by miR-696 through targeting peroxisome proliferator-activated receptor gamma co activator 1-alpha (PGC-1α) (Aoi et al., 2010).

MiRNAs also regulate mitochondrial intrinsic apoptotic pathway. MiR-15a and miR16-1 regulate apoptosis through the downregulation of the expression of Bcl-2 and Mcl-1(Gao et al., 2010). This leads to the translocation of Bax and Bad from the cytosol into mitochondrial outer membrane and results in mitochondrial membrane permeabilisation and the release of cytochrome c. The miR-143 is another miRNA associated with mitochondrial-dependent apoptotic pathway. miR-143 targets ERK5 which regulates cell proliferation and results in an induction of apoptotic pathway (Nakagawa et al., 2007).

Mitochondrial morphology and dynamics are also regulated by miRNAs. The miR-30 family has been associated with mitochondrial fission through targeting p53 (Li et al., 2010a). P53 is required for the transcriptional activation of dynamin related protein-1 (DRP-1) which regulates mitochondrial fission by acting on the mitochondrial outer membrane. This is also important in atherosclerosis and re-stenosis as mitochondrial fission is required for the initiation of VSM cell proliferation and migration (Chalmers et al., 2012).The miR-499 is another miRNA that regulates mitochondrial fission by targeting calcinurin which negatively regulates DRP-1. The increase in miR-499 expression is also transcriptionally regulated by p53 and results in an increase in mitochondrial fission (Wang et al., 2011).

MiRNAs can either exert their effect on their target mRNAs of the same cell or be transported to another cell where they become functionally active. They are transported via extracellular vesicles including exosomes and taken up by the recipient cell where they act either on the cytoplasmic mRNAs or mitochondrial mRNAs.

It is now clear that mitochondrial health/ bioactivity/ bioenergetics are important in determining cellular health. Cellular functions including growth, differentiation, proliferation and apoptosis is closely associated with mitochondrial functions. Any change in mitochondrial essential functions including ATP supply, Calcium homeostasis and ROS production will result in a vital change in cellular biology leading to pathological changes including VSM cell proliferation and migration which give rise to diseases including atherosclerosis and re-stenosis. Interestingly, these changes could be driven by miRNAs which are transported within circulating exosomes.

1.11 Cellular Communication and Initiation of Proliferation and Migration Cascades through Exosomes:

Information transmission between one cell and another is important in the initiation and progression of VSM cell proliferation and migration and the development of cardiovascular diseases such as atherosclerosis and restenosis. One way of this communication is through the release of extracellular vesicles including exosomes.

Exosomes are vesicles that are released by the endosomal system and carries membrane and cytosolic components within their cargo. The cargo contains proteins, mRNAs, miRNAs and lipids (Belting and Wittrup, 2008). The transfers of these membrane and nucleic components from one cell to another makes exosomes an important player in many physiological functions and pathological conditions (Simons and Raposo, 2009). Exosomes range in size between 30- 120 nm and are released in body fluids including blood, urine, milk and seminal fluid (Gonzales et al., 2009). Although mitochondrial proteins and genes have been detected in exosomes, it is still not well understood whether mitochondria have a role in exosomes biogenesis and cargo content in VSM cell. This could be potentially be a therapeutic target in atherosclerosis and restenosis if mitochondria shown to be important in the formation and sorting of exosomes.

1.12 Hypothesis and Aims:

The working hypothesis in this project aims to establish a relationship between vascular injury and activation of mitochondrial-dependent signalling pathways regulated by specific miRNAs contained in exosomes which in part drive VSM cell proliferation and migration.

The general aim of this study was to gain better understanding of the mechanisms underpinning VSM cell phenotype switching from a contractile cell to a proliferative, migratory cell. Defining the role of mitochondria in the proliferative, migratory phenotype and relationship in atherogenesis.

Chapter 2

Materials & Methods

2.1 Materials:

- Foetal calf serum (Sigma, UK)
- Ham's F12 medium (Gibco, UK)
- Paraformaldehyde (Sigma, UK)
- Penicillin streptomycin (Gibco, UK)
- Sodium hydroxide (Sigma, UK)
- Sodium lauryl sulphate (Sigma, UK)
- Trichloroacetic acid (Sigma, UK)
- Triton X 100 (Sigma, UK)
- Tryple Express (Gibco, UK)
- Emulsifier-safe scintillation fluid (PerkinElmer, USA)
- MAPK inhibitor U0126 (Sigma, UK)
- mTOR inhibitor everolimus (Sigma, UK)
- Mitochondrial inhibitor Mdivi-1 (Sigma, UK)
- Anti ERK antibody (Cell Signalling, UK)
- Anti P38 antibody (Cell Signalling, UK)
- Anti GAPDH antibody (abcam, UK)
- Anti-cytochrome C antibody (abcam, UK)
- Anti Akt antibody (abcam,UK)
- Anti mTOR antibody (Invitrogen, UK)
- Anti 4EBP1 antibody (Invitrogen, UK)
- Anti-Cyclin D antibody (Santa Cruz, UK)
- Anti α-smooth muscle actin (Sigma, UK)
- Anti-CD9 antibody (Life Technologies, Paisley, UK)
- Anti-CD63 antibody (Life Technologies, Paisley, UK)
- Anti-CD81 antibody (Life Technologies, Paisley, UK)
- Mitochondria/cytosol Fractionation kit (abcam, UK)
- ^{3}H thymidine solution (Amersham, UK)
- Waymouth's medium (Gibco, UK)
- Anti-mitochondria antibody (abcam, UK)
- Anti-mouse IgG HRP-linked secondary antibody (Cell Signalling, UK)

- Anti-rabbit IgG HRP-linked secondary antibody (Cell Signalling, UK)
- Thermo Scientific Luminaris Color HiGreen High ROX qPCR Master Mix (Life Technologies, Paisley, UK)
- Platelet Derived Growth Factor (PDGF) (Sigma,UK)
- ApoTox-Glo reagent (Promega, Madison, USA)
- ROS-Glo H_2O_2 reagent (Promega, Madison, USA)
- ToxGlo reagent (Promega, Madison, USA)
- Ethidium Bromide (Life Technologies, Paisley, UK)
- Sodium Pyruvate (Sigma, UK)
- Uridine (Sigma, UK)
- Isolate II RNA mini kit (Bioline, London, UK)
- Tetro cDNA synthesis kit (Bioline, London, UK)
- Mitochondrial array RT^2 profiler PCR array (QIAGEN, USA)
- RT^2 SYBR Green Mastermix (QIAGEN, USA)
- MicroAmp tubes (Applied Biosystems, Paisley,UK)
- mirVana miRNA 21 mimic (Life Technologies, Paisley, UK)
- mirVana miRNA 21 inhibitor (Life Technologies, Paisley, UK)
- mirVana miRNA 145 mimic (Life Technologies, Paisley, UK)
- mirVana miRNA 145 inhibitor (Life Technologies, Paisley, UK)
- mTOR siRNA silencer (Life Technologies, Paisley, UK)
- Exosomal RNA and protein extraction kit (101 Bio, USA)
- 96 well plates (Applied Biosystems, Paisley, UK)
- Taqman master mix (Applied Biosystem, Paisley, UK)
- Wheat germ agglutinin conjugates (Life Technologies, Paisley, UK)
- Balloon catheter (Boston Scientific, Ireland)
- Propodium iodide (Sigma, UK)
- miRNeasy min isolation kit (Qiagen, USA)
- miRNA reverse transcription kit (Applies biosystem, Paisley, UK)
- vector-shield containing DAPI (Vector laboratories, USA)
- Tris (2-carboxyethyl) phosphine (TCEP, Sigma, UK)
- iodacetamide (IOA, Sigma, UK)
- L-Cysteine (Sigma, UK)

Methods:

2.2 Cell culture:

All cell culture procedures were conducted in class II biological safety cabinet and following strict aseptic conditions.

Vascular smooth muscle cells were explanted from rat's aorta. The rings were placed in T25 flasks in 10% FCS made from 50: 50 Waymouth and F12. The medium was changed 48-72 hourly and growth was monitored using a light microscope until they reached ~70% confluency (Passage 0). Cells were then split into T75 flasks and allowed to grow to ~70% confluency (Passage 1). Cells were then again split into six well plates, 24 well plates or 96 well plates for further analysis.

- Six well plates were seeded at $2x10^5$ density then treated with four different concentrations of the mitochondrial inhibitor MDivi-1 (0.1 μM, 1 μM, 5 μM and 10 μM). The first two wells had the quiesced 0.1% FCS and the stimulated 10% FCS without MDivi-1. Cells were quiesced for 24 hours then stimulated for 15 minutes using 10% foetal calf serum or 20ng/ml PDGF. Treatment was added 30 minutes prior to stimulation. The cells were then lysed using 1x sample buffer and stored in -20^oC for western blotting.

- Additional six well plates were prepared by adding 1 mm glass cover slips and seeded with P1 vascular smooth muscle cells at $2x10^5$ density then treated with MDivi-1 as above. The first two wells had the quiesced 0.1% FCS and the stimulated 10% FCS without MDivi-1. Cells were quiesced for 24 hours then stimulated 15 minutes using 10% FCS or 20ng/ml PDGF. Treatment with MDivi-1 was added 30 minutes prior to stimulation with FCS or PDGF. The cells were then fixed in 4% paraformaldehyde and stored in 4^oC for immunohistochemistry.

- 24-well plates were seeded at $2x10^4$ and cells were allowed to grow until they were 70% confluent. MDivi-1 was used as outlined above. The experiment was done in quadruplicate where the first four wells contained the quiesced

cells in 0.1% FCS and the second four wells had the stimulated 10% FCS or 20ng/ml PDGF. Cells were quiesced for 24 hours, treated 30 minutes prior to stimulation with MDivi-1 then stimulated for 24 hours with either 10% FCS or 20 ng/ml PDGF.

2.3 Western blotting:

Preparation of whole cell extracts were from rat aortic VSMCs. Cells were grown up to 70% confluency in 6 well plates using 10% FCS media. Cells were then washed twice with warm sterile PBS and serum starved for 24 hours using 0.1% FCS media. Different concentrations of MDivi-1 were added 30 minutes prior to stimulation. Cells were then stimulated using 10% FCS or 20 ng/ml PDGF for the desired period of time. Following stimulation, 200 µl of pre-heated sample buffer was added (63mM Tris-HCL (pH6.8), 2 mM $Na_4P_2O_7$, 5mM EDTA, 10% (v/v) glycerol, 2% (w/v) SDS, 50mM DTT, 0.007% (w/v) bromophenol blue). The cells were then scraped from the well and the lysate transferred to labelled microcentrifuge tubes and boiled for 5 minutes for protein denaturation before storing at -20^{o}C.

2.4 SDS-Polyacrylamide Gel Eletrophoresis (SDS-PAGE):

Gel preparation components were cleaned in 70% ethanol and dried before assembly. Running component was prepared at 10% (w/v) acrylamide as follows: (N, N'-methylenebis-acrylamide (30: 0.8), 0.375 M Tris (pH 8.8), 0.1% (w/v) SDS and 10% (w/v) ammonium persulfate (APS). Acrylamide polymerisation was commenced by the addition of 0.05% (v/v) N, N, N', N'-tetramethylethylenediamine (TEMED) and quickly poured between two glass plates assembled according to manufacturer's instruction (Bio-Rad) and left to set for ~15 minutes at 40^{o}C in a drying oven. Following polymerisation, loading component was prepared containing (10% (v/v) N, N'-methylenebis-acrylamide (30: 0.8), 125 mM Tris (pH 6.8), 0.1% (w/v) SDS, 0.05% (w/v) ammonium persulfate (APS) and 0.05 (v/v) TEMED. The acrylamide was poured on top of the running component and 9 well comb was placed to shape the loading wells. The acrylamide was left to set (polymerise) at room temperature for ~45 minutes. Thereafter, the combs were removed and up to 25 µl of sample was

loaded to each well. The first well was typically loaded with 10 µl of molecular weight marker. Samples were electrophoresed at 200V for 45 minutes or until the bromophenol dye had reached the bottom of the gel in running buffer (25mM Tris, 129mM glycine, 0.1% (w/v) SDS).

2.5 Electrophoretic Transfer of proteins to Nitrocellular Membrane:

The separated proteins by SDS-PAGE were transferred to nitrocellulose membrane by electrophoretic blotting. The gel was sandwiched against nitrocellulose sheet and assembled in transfer cassette between two pieces of Whatman 3M paper and two sponge pads. The cassette was placed in a Bio-Rad Mini Trans-Blot ^{TM} tank filled with transfer buffer (25 mM Tris, 19 mM glycine, 20% (v/v) methanol). A constant voltage of 100 V was applied for 60 minutes and the tank was cooled by the insertion of an ice pack.

2.6 Immunological detection of Proteins:

Following Transfer, the nitrocellulose membranes were then carefully removed from the cassettes and placed in 25 mls of 3% (w/v) BSA in TTBS buffer (150 mM NaCl, 20 mM Tris, 0.2% Tween-20; pH 7.4) at room temperature for 1 hour on a slow rocking plate. The membranes were then removed from the blocking buffer and incubated overnight with antibodies specific to the target proteins diluted in TTBS buffer containing 1% BSA and left in the cold room. The concentrations of the primary antibodies were prepared according to manufacturer's instruction. Thereafter, the nitrocellulose membranes were removed and placed in a small plastic dish and washed with TTBS four times for ~15 minutes on a rocking plate. The membranes were then incubated for 1 hour at room temperature with secondary horseradish peroxidase-conjugated antibody directed against the primary immunoglobulin and diluted according to manufacturer's instruction in TTBS containing 1% BSA. The nitrocellulose membranes were then washed with TTBS three times of 10 minutes each at room temperature on rocking plate. Enhanced Chemiluminescence reagent (ECL) mixture was prepared in the dark room and applied to each nitrocellulose membrane for 1 minute with agitation, lifted from the tray onto a paper towel to remove any excess ECL. The membranes were then placed

in exposure cassettes with an X-ray film on top (Kodak Ls X-OMAT) for the required exposure time under dark room conditions and developed using X-OMAT (KODAK M35-M X-OMAT processor).

2.7 Nitrocellulose membrane stripping and re-probing:

Nitrocellulose membranes were stored in the fridge in sealed dishes containing TTBS for further detection of other proteins. Antibodies were stripped from nitrocellulose membranes by incubation in 15 ml stripping buffer containing (0.05 M Tris-HCL, 2% SDS and 0.1 M of β-mercaptoethanol) for 60 minutes at 70^{o}C on a rocking plate. This was followed with three washes of 15 minutes each with TTBS buffer to remove any residual stripping buffer from the membranes. The membranes were then incubated again overnight with primary antibody prepared in TTBS buffer with 1% BSA. Following day, membranes were washed four times with TTBS buffer and incubated with the secondary for 1 hour in TTBS containing 1% BSA followed by three washes with TTBS. The blots were then ready for immunological detection as described previously.

2.8 Scanning Densitometry:

All data obtained from western blotting were scanned using GS-800 Calibrated Densitometer (Bio-Rad) and values were normalised against loading control values.

2.9 Cell proliferation ^{3}H thymidine incorporation assay:

Cells were quiesced for 24- 48 hours in 0.1% FCS. Thereafter, cells in the 24-well plates were stimulated using 10% foetal calf serum for 24 hours. 18 hours through the stimulation, 10µl of thymidine was added into each well and left for the remaining 6 hours. After completing the 6 hours, the wells were washed with ice-cold PBS for 10 minutes followed by four washes with ice-cold 10% TCA for 10-15 minutes each. 250 µl of 2% SDS was added into each well after the washes. The contents of each well was then transferred into the scintillation vials which was prefilled with 2ml of Emulsifier-safe scintillation fluid, labelled and analysed using protocol 2 in the scintillation analyser machine.

2.10 Cell migration assay:

Passage 1 vascular smooth muscle cells were plated in six well plate at $2x10^5$ density and incubated until ~ 90% confluency. Cells were then quiesced using 0.1% FCS for 24 hours. A vertical scratch was then created using a sterile 200µl tip which crosses a horizontal black mark which was drawn at the bottom of each well that marks the middle of the well. Cells were stimulated after that using 10% FCS or 20 ng/ml PDGF, which are the same stimulants used to drive VSM cell proliferation, and treated with the MDivi-1. Images were taken at 0 hour, 6 hours, 24 hours and 48 hours using Motic inverted light microscope. The captured images were analysed and the scratch gap closure (distance travelled by the cells) was measured using ImageJ software.

2.11 Generation of mitochondrial incompetent (Rho) cells:

VSMCs were cultured in T75 flasks in 10% FCS supplemented media. Mitochondrial DNA was depleted by co-incubation with 50 ng/ml of Ethidium Bromide supplemented with 50 ng Uridine and 1mM of sodium pyruvate for 21 days. The efficiency of the mitochondrial loss of bioactivity was measured by the level of expression of mitochondrial markers at the end of the 21 days incubation.

2.12 RNA isolation for PCR work:

VSMCs were cultured in three different conditions: 0.1% FCS, 21 days cultured in 10% FCS and cells cultured with ethidium bromide to generate mitochondrial incompetent Rho cells as described in previous section. After the incubation period, total RNA was isolated using isolate II RNA mini kit (Bioline, London, UK). Cells were lysed by adding 350 µl lysis buffer with 3.5µl of β-Mercaptoethanol into each well. The lysate was transferred into isolate II violet filter and centrifuged at 11000 g for 1 minute at room temperature. 350 µl of 70% ethanol was added to the flow through and mixed by pipetting up and down ~5 times. Each sample was then loaded into one RNA mini column and centrifuged at 11000 g for 30 seconds at room temperature. The silica membrane was then desalted by adding 350 µl of membrane desalting buffer and centrifuged at 11000 g for 1 minute to dry the membrane. The DNA was then digested by adding 95 µl of DNase I reaction mixture (made up by

adding 10 µl of reconstituted DNase I to 90 µl of reaction buffer for DNase I) to the centre of the silica membrane of each column and was incubated for 15 minutes at room temperature. The silica membrane was then washed three times with 200 µl wash buffer RW1 and spun for 30 seconds at 11000 g, 600 µl wash buffer RW2 and spun for 30 seconds at 11000 g and finally 250 µl wash buffer RW2 and spun for 2 minutes at 11000 g. The final step was eluting the RNA with 60 µl RNase free water and the column was spun at 11000 g for 1 minute. RNA concentration was then measured using Nano Drop spectrophotometer.

2.13 cDNA preparation:

To quantify the mRNA transcripts of target genes, total RNA was reversed transcribed to complementary DNA (cDNA) using a Tetro cDNA synthesis kit (Bioline, London, UK). All RNA concentrations were normalised to 500 ng in all reactions. The mixture was prepared by adding 1µl of oligo-dT primer mixture as the first strand synthesis primer and 1µl of dNTP mixture (10mM). 4 µl of 5x RT buffer was also added to the mixture followed by 1 µl of RiboSafe RNase inhibitor and 1 µl of Tetro Reverse Transcriptase diluted to 20 µl with DEPC-treated water. The samples were mixed gently by pipetting, reactions incubated at 45C^{o} for 30 minutes and terminated by incubating at 85^{o}C for 5 minutes followed by chilling on ice.

2.14 Mitochondrial PCR array:

The qRT-PCR assay was performed by preparing reaction mixtures of the cDNA to be loaded into each well of the 96 well plate format of the mitochondrial array RT^{2} profiler PCR array (Qiagen, USA). The 20µl of the prepared cDNA was added to 91µl of RNase free water to make up the cDNA synthesis reaction. The PCR components mix was then prepared by adding 1350 µl of 2x RT^{2} SYBR Green Mastermix (Qiagen, USA) to 102 µl of the cDNA synthesis reaction and 1248 µl of RNase free water to make a total volume of 2700 µl which is sufficient for the 96 well plate. 25 µl of the mixture was added into each well. The plate was then sealed using the optical adhesive film and centrifuged for 1 minute at 1000 g at room temperature to remove bubbles. The thermal cycling and detection was performed on an applied Biosystems StepOne Plus real-time PCR system (Table 2.1)

Hold stage	Cycling stage (40 cycles)	Final extension stage
DNA polymerase activation 10 minutes at 95C^{o}	Melt Step 15 seconds at 95C^{o}	Cooling down at 4C^{o} to stop PCR reaction
	Anneal/Extend step 1 minute at 60C^{o}	

Table 2.1 *shows the thermal cycle conditions used to run PCR array plates*

2.15 Quantitative real time polymerase chain reaction amplification of individual primer genes:

The qRT-PCR assay was performed in PCR fast reaction MicroAmp tubes (Applied Biosystems, Paisley,UK). The PCR reaction was carried out in a volume of 20 µl containing 19 µl of PCR master mix and 1 µl of each template cDNA sample. The master mix contained 1 µl of 10 pmol/µl Forward primer, 1 µl of 10 pmol/µl Reverse primer, 10 µl of thermo scientific Luminaris Color HiGreen High ROX qPCR Master Mix (Life Technologies, Paisley, UK) and 7 µl RNAase free water. Two technical and three biological replicates were conducted for each assay. The thermal cycling and detection was performed on an applied Biosystems StepOne Plus real-time PCR system (Table 2.2)

Hold stage	Cycling stage (40 cycles)	Final extension stage
DNA polymerase activation 10 minutes at 95C^{o}	Melt Step 15 seconds at 95C^{o}	Cooling down at 4C^{o} to stop PCR reaction
	Anneal/Extend step 1 minute at 60C^{o}	

Table 2.2 *shows the thermal cycle conditions used to run QRTPCR for individual primers*

2.16 Relative quantification [ΔΔCt] method for real time PCR:

The quantification method used with the PCR results was the relative quantification (ΔΔCt) method. This method normalises Ct values of the target gene to Ct value of the reference gene in order to get the fold change in gene expression between the control and treated samples according to the following equations:

1- $(\Delta Ct) = Ct_{target} - Ct_{reference\ gene}$ (This is to calculate the difference between the treated and control samples).
2- $(\Delta\Delta Ct) = (Ct_{target} - Ct_{reference})$ treated $- (Ct_{target} - Ct_{reference})$ control (This is to calculate the difference between the ΔCts of the treated and control samples).
   $\Delta\Delta Ct = \Delta Ct_{treated} - \Delta Ct_{control}$
3- The fold change in the samples = $2_{-\Delta\Delta Ct}$

2.17 PCR primers for SYBR green based real time assays:

Primers were designed to ensure that they only bind to their target genes and avoid non-specific products in SYBR green assays. All primers were designed as described in the following process:

- Sequences of the genes were obtained from GeneBank.
- To identify potential primer pairs, the sequences were imported into the PrimerQuest web tool (http://eu.idtdna.com/Primerquest/Home/Index) in the Integrated DNA Technologies (IDT) website (http://eu.idtdna.com/site).
- "qPCR – 2 Primers and Intercalating dye" was chosen in the setting.
- Amplicon size between 90 – 140 was chosen to maximise PCR efficiency.
- Primer sequences were generated and only the one with good specificity was selected and validated using Primer-BLAST (Basic Local Alignment Search Tool) in the National Centre for Biotechnology Information (NCBI) website (http://ncbi.nlm.nih.gov/tools/primer-blast/index.cgi).
- Melting temperature (Tm) of all primers was selected between 47 - 62^{o}C and the ΔTm between the forward and the reverse was ≤ 1^{o}C.

Primers lengths were selected between 18-30 bases and the primers GC content was between 35% - 70%

Gene	Forward Sequence
GAPDH	5′-GCTCTCTGCTCCTCCCTGTTCT-3′
COXII	5′-GGCTTACCCATTTCAACTTGGC-3′
Tfam	5′-AGTTCATACCTTCGATTTTC-3′
16S	5′-TCCGCTGCAGTCCGTTCAAGTCTT-3′
MHC	5′-GACACCAGCGCCCACCTG-3′
CNN1	5′-TTGAACTTGTCTGGGTCATCTC-3′
Gene	**Reverse Sequence**
GAPDH	5′-CAGGCGTCCGATACGGCCAAA-3′
COXII	5′-CACCTGGTTTTAGGTCATTGGTTG-3′
Tfam	5′-TGACTTGGAGTTAGCTGC-3′
16S	5′-GCCAAACTTCTTGGATTCGCAGCG-3′
MHC	5′-ATAGCAACAGCGAGGCTCTTTCTG-3′
CNN1	5′-TGGGCCAGCTTGTTCTTTAC-3′

Table 2.3 *Primers used to characterise mitochondrial-depleted Rho cells*

2.18 Data and statistical analysis:

Values are presented as mean ± standard error of the mean (SEM). Statistical analysis of the data was performed using Microsoft Excel 2010 and minitab 16 statistical software. Comparison of different culture conditions was by one-way analysis of the variance (ANOVA). Where appropriate a post hoc test for multiple comparisons or Dunnett's comparison of all vs. control was chosen. Significance was assumed if $p<0.05$.

Chapter 3

Mitochondrial-dependent mechanisms underlying vascular smooth muscle cell proliferation and migration

3.1 Introduction

One key feature seen in the cardiovascular hyper- proliferative disorders is the change in the phenotype of vascular smooth muscle cells from the contractile to the synthetic phenotype (Milewicz et al., 2010). This underpins vascular remodelling, increase in wall thickness and reduction in lumen size associated with atherosclerosis and re-stenosis (Schwartz et al., 1995). Therefore, the contribution of VSM cell proliferation in the pathophysiology of atherosclerosis and re-stenosis is important and inhibiting this has been a focus of treatment strategy (Dzau et al., 2002). Although the mechanisms that drive this change is not fully understood, emerging evidence suggests that mitochondria play an important role in this process (Chang et al., 2010). Mitochondria have an impact on many cellular functions. ATP production, ROS synthesis, inhibition of pro-apoptotic mediator proteins such as cytochrome c and mitochondrial dynamics all have been shown to be important and directly related to the progression and development of cardiovascular hyper-proliferative diseases (Chen and Zweier, 2014). The balance between apoptosis and cell proliferation is, in part, regulated by mitochondria and mitochondrial dysfunction could potentially result in either increase in cellular growth or an increase in apoptosis (Li et al., 1997). Despite that the exact signalling mechanism mediated by the mitochondria are not completely understood, it has become evident that key proteins including Akt, PI3K and mTOR are involved (Parra et al., 2014). Parra et al reported that treating cardiomyocytes with insulin increased the level of Opa-1 protein and promoted mitochondrial dynamics. They also reported that treatment with insulin resulted in increased mitochondrial membrane potential and elevated levels of intracellular ATP and oxygen consumption. They also confirmed that altering mitochondrial dynamics which consequently altered metabolic effects triggered by insulin was driven by Akt/ mTOR/ NFκB signalling pathway.

The study of mitochondrial dynamics suggested that mitochondrial morphology and the process of mitochondrial fission and fusion are important in determining mitochondrial bioactivity and mitochondrial biogenesis. Different molecules were previously used to try and inhibit mitochondrial activities including ATP production and mitochondrial biogenesis. More recently, MDivi-1 has been used to inhibit mitochondrial fission process through the inhibition of DRP1 (Cassidy-Stone et al.,

2008). Inhibition of mitochondrial dynamics, via MDivi-1/ DRP1 resulted in reduction in the proliferation of VSM cells (Lackner and Nunnari, 2010). These results led to further investigations in an attempt to understand the signalling mechanisms blocked by MDivi-1.

3.2 Mitochondrial motility and biogenesis:

Mitochondrial motility and bioactivity have been linked to changes in VSM cell phenotype switching from the native contractile to disease associated synthetic phenotype. However, relatively little is known about mitochondrial movement in cardiovascular tissues, cardiac or vascular (Beraud et al., 2009). Mitochondrial fission and fusion are linked to mitochondrial motility and any disturbance to mitochondrial dynamics leads to a change in mitochondrial and cell function. Mitochondria in native non-proliferative cells exist in a static form but upon the exposure to stimulants they become mobile towards the nucleus and organelles as part of the cell proliferative progression (Chalmers et al., 2012).

3.3 Mitochondrial division inhibitor-1 MDivi-1:

This DRP1 inhibitor MDivi-1 was first characterised by Cassidy et al (2008) following the screening of compounds that affect mitochondrial morphology (Cassidy-Stone et al., 2008). MDivi-1 selectively inhibits DRP1 by binding to an allosteric binding site and stabilising a conformational form of unassembled DRP1 that binds GTP. This conformational change stops DRP1 from assembling into spiral filaments and blocks their polymerisation. Inhibiting DRP1 leads to the inhibition of mitochondrial fission which has been recently associated with VSM cell proliferation, migration and cell cycle progression. The differences in the structure of mitochondria are important in determining cellular physiology (McCarron et al., 2013). This change in the morphology is determined by the energetic requirements of the cell (Westermann, 2010). Change in mitochondrial morphology then influences other important cellular functions including Ca^{2+} and ROS signalling which are associated with VSM cell proliferation and migration (Szabadkai et al., 2004).

3.4 Chapter Aims:

The aims of the work described in this chapter:

- To evaluate the effect of balloon injury on blood vessel structure and the effect following mitochondrial inhibition.
- To measure the effect of mitochondrial inhibition on VSM cell proliferation and migration.
- To study possible signalling pathways involved in mitochondrial-dependent proliferation and migration.
- To investigate the effect of mitochondrial inhibition on mitochondrial gene expression.

3.5 Specific Methods:

3.6 Histological sectioning and staining of balloon injured vascular tissues:

Rat aortic blood vessels were harvested and exposed to balloon catheter injury using 2.5 x 24 mm balloon catheter in an in-vitro setting. The catheter was inserted in the blood vessel and inflated at 9 ATM for 20 seconds. The catheter was then deflated and removed from the blood vessel. The blood vessel was then cultured in 10% foetal calf serum (FCS) for 21 days without treatment or with one of the following treatments: 100 nM Rapamycin, 10 μM MDivi-1, 50 ng/ml Ethidium bromide and 100 nM Wortmannin. These treatments were introduced to the cultured vessels every time the media was changed during the 21 days.

3.7 Fixation, wax embedding and cutting of vascular tissues:

Following 21 day culture, vessels were fixed in 4% paraformaldehyde for 24 hours. Tissues were then processed in a citadel 1000 (Thermo Shandon, UK) processor overnight using the following programme:

Step	Duration (hours)
1. 70% ethanol	3
2. 90% ethanol	3.5
3. 100% ethanol	2
4. 100% ethanol	1
5. 1:1 (v/v) ethanol: histoclear	1
6. 100% histoclear	1
7. 100% histoclear	1
8. Paraffin wax	2
9. Paraffin wax	2

Tissues were then embedded in paraffin wax using a leica EG1140H (Leica microsystems, UK) embedder and 4 μm sections were cut using a Leica RM2125RTF (Leica microsystems, UK) microtome. Tissue sections were floated onto silanated slides using a water bath at 60^{o}C. Slides were silanated using the following steps:

Step	Duration (minutes)
1. Acetone wash	10
2. Submersion in 3-aminopropyltriethoxysilane (APES) solution (0.1% APES in acetone)	10
3. Running tap water	10
4. Covered and air dried	~48 hours

Wax embedded sections were mounted on salinated slides and placed in a drying oven at 60^{o}C for 30 minutes.

3.8 Rehydration and dehydration of tissue slides:

Prior to histological staining, tissue sections were rehydrated using a varistain 24-4 auto stainer (Thermo Shandon, UK) using the following steps:

Step	Duration (minutes)
1. Histoclear	10
2. Histoclear	10
3. Histoclear	10
4. 100% ethanol	5
5. 100% ethanol	5
6. 100% dH_2O	5

At the end of staining, the slides were dehydrated using the following steps:

Step	Duration (minutes)
1. 100% ethanol	10
2. 100% ethanol	10
3. 100% ethanol	10
4. Histoclear	5
5. Histoclear	5
6. Histoclear	5

3.9 Haematoxylin and eosin staining:

Following rehydration, the slides were placed into metal racks for staining with haematoxylin and eosin (H&E) using the following steps:

Step	Duration (minutes)
Haematoxylin	6
dH_2O	1
Acid alcohol (1%)	3 sec
dH_2O	1
Scots tap water substitute	2
dH_2O	1
Eosin	1
dH_2O	1

Slides were then dehydrated and mounted using histomount and 24 x 50mm coverslips and left to dry overnight before analysis.

3.10 Image analysis and quantification of histological sections:

A digital image of each section was captured with the same magnification using Adobe Photoshop v5 on a leica DMLB2 microscope fitted with a Leica DFC320 camera (Leica microsystems, UK). Images were then quantified using Image J; the thickness of the blood vessel, the lumen diameter and blood vessel area, the wall: lumen ratio was calculated and the statistical significance was calculated using one way ANOVA on minitab v15, a p value of <0.05 was considered significant. Graphs were plotted using Microsoft Excel 2010.

3.11 Immunocytochemistry of histological sections:

Immunocytochemistry was undertaken to characterise the expression of vascular smooth muscle cells such as α-smooth muscle actin as well as looking at the localisation of mitochondria within the cell following treatment with mitochondrial fission inhibitor MDivi-1 and stimulation with 10% FCS. Cells were fixed at the end of the treatment period using 4% paraformaldehyde. The 4% paraformaldehyde was then removed from the wells and the glass cover slips were washed in PBS three times followed by permeabilising the cells using 0.1% Triton X-100 in PBS for 5 minutes. 10% goat serum was prepared in PBS and added to the cover slips for 60 minutes at room temperature to block the unspecific binding. This was removed and followed by adding anti-α-SMA raised in mouse (1/400; Sigma, UK) and anti-mitochondria (1/500; Sigma, UK) primary antibodies and incubated overnight at 4°C. Next day, the slides were washed in three times with PBS before adding a fluorescent anti-mouse secondary antibody (1/1000; Sigma, UK) at room temperature for 45 minutes. Coverslips were then mounted using hard set vector-shield containing DAPI (Vector laboratories, USA) and visualised under an epi-fluorescent microscope.

3.12 Fluorescence-activated cell sorting (FACS) analysis:

MDivi-1 (0.1 μM, 1 μM, 5 μM and 10 μM) was added when cells reached ~50% confluency. A background where cells were cultured in 0.1% FCS and a maximum stimulation in 10% FCS in the absence of MDivi-1 were measured as reference. All cells were quiesced for 24 hours followed by stimulation with 10% FCS for 24 hours, the exception being the background control in 0.1% FCS. Cells were then lifted from the culture plates using Triple E Express and centrifuged at 2500 g for 10 minutes at 4^{o}C. The supernatant was removed and 300 μl of ice cold PBS was added and the cells were re-suspended. 700 μl of ice cold ethanol was added drop wise with a gentle vortex. The vials were then stored in the fridge. The following day, 1ml of PBS was added to each vial and the cells were spun at 2500 g for 10 minutes. The supernatant was removed and another 1ml of PBS was added and spun at 2500 g for 10 minutes. The PBS was removed and 250 μl of PBS was added back with gentle vortex. The cells were then transferred to FACS tubes and 5 μl of RNAse A (Sigma, UK) was added to each tube and left in the incubator for 1 hour covered in tin foil. 13.5 μl of propodium iodide (Sigma, UK) was finally added to each tube and analysed on (FACS CANTO, Becton Dickinson, Oxford, UK) flow cytometer using FACS Diva software. A total of 10,000 events were measured per sample.

3.13 Cell apoptosis assay:

VSMCs were cultured in 96 well plates until they reached ~70% confluency. Cells were quiesced for 24 hours using 0.1% FCS and subsequently stimulated with 10% FCS or 20 ng/ml PDGF for 24 hours. MDivi-1 was added to the treated cells 30 minutes before stimulation. As a positive apoptotic control one well of cells was treated with 1 μM of paclitaxel. At the end of the 24 hours stimulation, 100 μl of ApoTox-Glo reagent (Promega, Madison, USA) was added to each well and incubated at room temperature for 1 hour. The luminescence of each sample was then measured in a polar star plate reader which corresponds to the caspase 3/7 activity within the cells.

3.14 Reactive oxygen species (ROS) assay:

VSMCs were cultured in 96 well plates until they reached ~70% confluency, quiesced for 24 hours (0.1%FCS) and stimulated with 10% FCS or 20 ng/ml PDGF for 24 hours. MDivi-1 was added to the treated cells 30 minutes before stimulation. At the end of the 24 hours stimulation, 100 µl of ROS-Glo H_2O_2 reagent (Promega, Madison, USA) was added to each well and incubated at room temperature for 20 minutes. The luminescence of each sample was then measured in a polar star plate reader which corresponds to the level of ROS released by the cells in each treatment.

3.15 Cellular ATP assay:

VSMCs were cultured in 96 well plates until they reached ~70% confluency, quiesced for 24 hours (0.1%FCS) and stimulated with 10% FCS or 20 ng/ml PDGF for 24 hours. MDivi-1 was added to the treated cells 30 minutes before stimulation. At the end of the 24 hours stimulation, 100 µl of mitochondrial ToxGlo reagent (Promega, Madison, USA) was added to each well and incubated at room temperature for 30 minutes. The luminescence of each sample was then measured in a polar star plate reader which corresponds to the level of ATP released by the cells in each treatment.

3.16 Results

3.17 Effect of MDivi-1 on balloon-injured whole artery:

Balloon injured artery haematoxylin & Eosin staining results showed differences in the wall thickness and wall: lumen ratio between different conditions (Figure 3.1). The wall thickness measured in the 21 days cultured artery was 10 ± 4.1 μm greater than the freshly fixed artery (Figure 3.3). The wall thickness and the wall: lumen ration was seen to increase more with the balloon injured artery in comparison to the freshly fixed and the 21 days cultured artery. The wall thickness in the injured and cultured artery was 35 ± 10 μm higher than the freshly fixed artery and the wall: lumen ratio was doubled in the injured and cultured artery compared to the freshly fixed (Figure 3.2). The wall thickness was reduced to 93 ± 2 μm, 87 ± 2 μm, 84 ± 0.9 μm and 87 ± 2 μm following treatment with 100 nM Rapamycin, 10 μM mitochondrial fission inhibitor MDivi-1, 50 ng/ml Ethidium Bromide and 100 nM Wortmanin respectively. The wall: lumen ratio was also decreased to 0.8 ± 0.02, 0.7 ± 0.02, 0.7 ± 0.02 and 0.8 ± 0.03 in the balloon injured artery following treatment with 100 nM Rapamycin, 10 μM mitochondrial fission inhibitor MDivi-1, 50 ng/ml Ethidium Bromide and 100 nM Wortmanin respectively. Lumen diameter reduced from 1347 ± 39 μm in the freshly fixed artery to 1148 ± 47 μm in the injured-cultured artery. The lumen diameter was increased to 1414 ± 65 μm, 1419 ± 48 μm, 1407 ± 53 μm and 1383 ± 60 μm following treatment with 100 nM Rapamycin, 10 μM mitochondrial fission inhibitor MDivi-1, 50ng/ml Ethidium Bromide and 100 nM Wortmanin respectively (Figure 3.4).

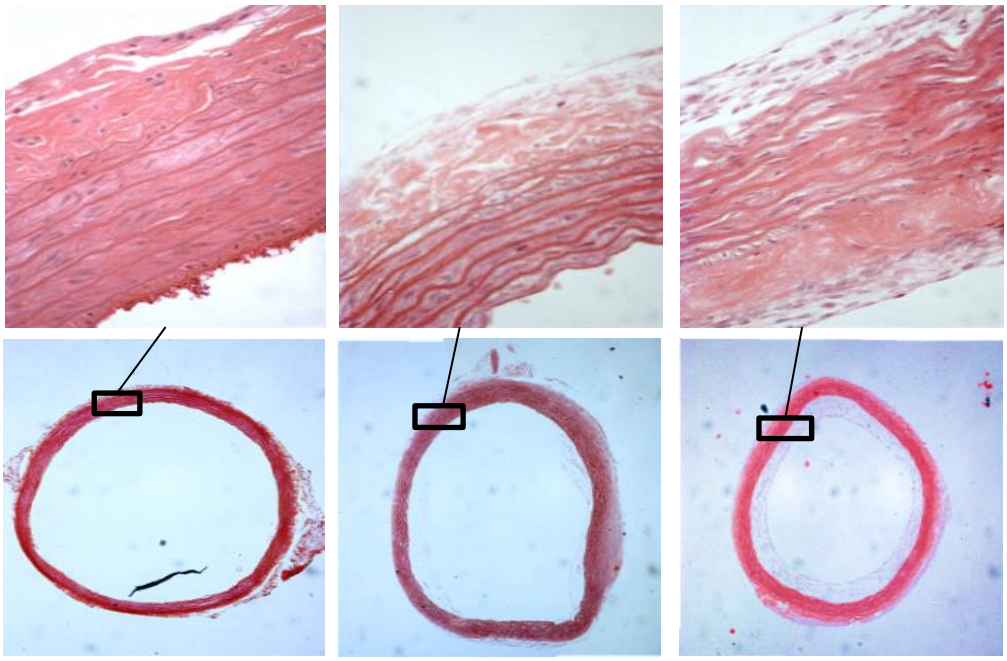

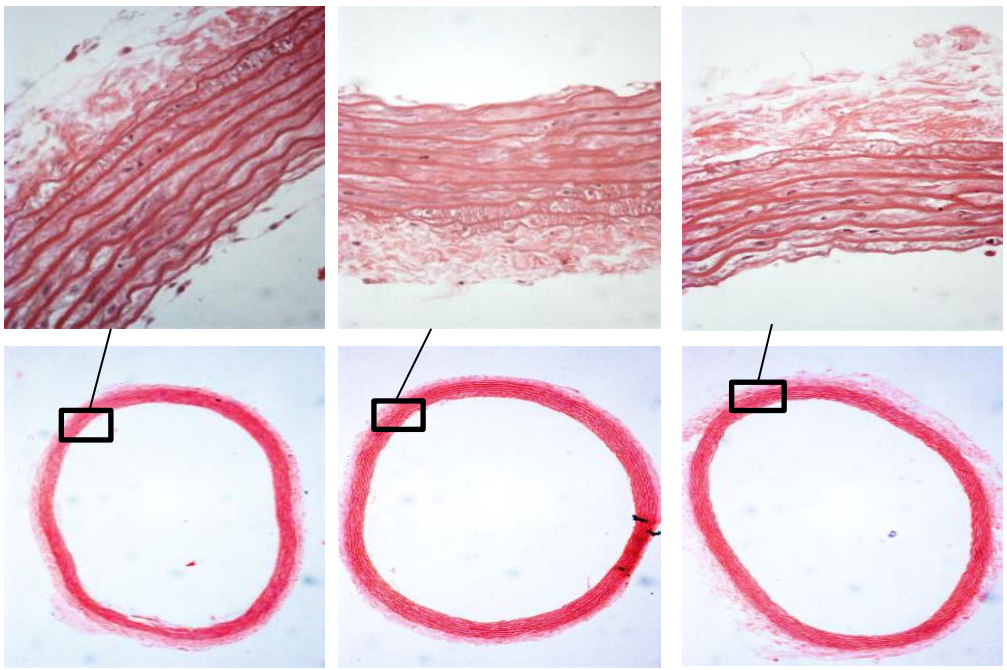

Figure 3.1 *shows the change in the vascular wall thickness following balloon injury and the reduction following different treatments. Haematoxylin & Eosin staining show the increase in wall thickness following balloon injury and no increase in the vascular thickness following balloon injury when treated with rapamycin, MDivi-1, ethidium bromide.*

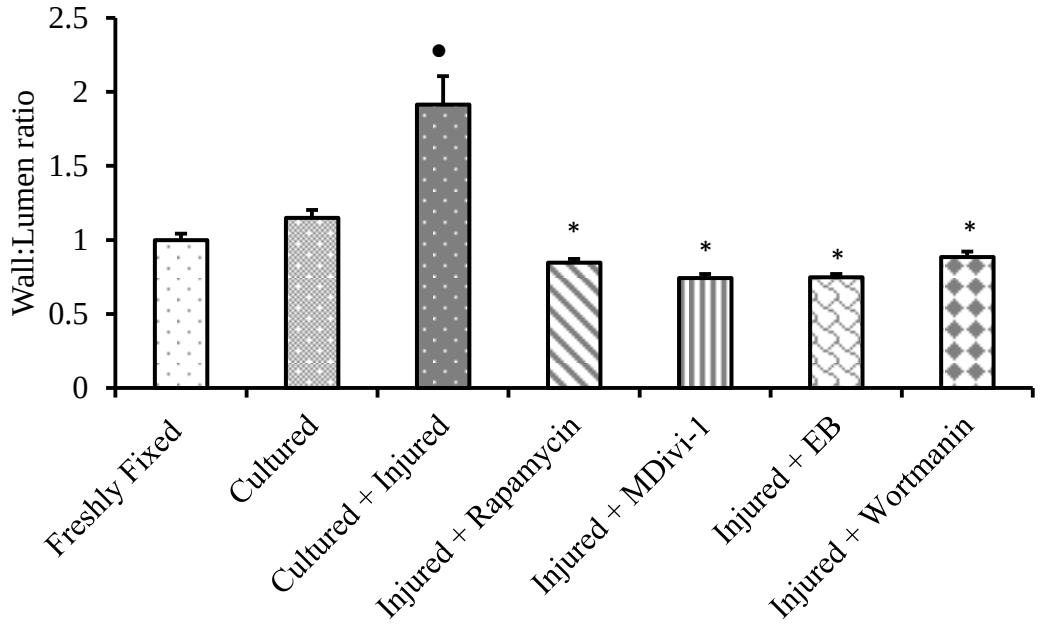

Figure 3.2 *shows the change in the vascular wall: lumen ratio following balloon injury and the change in cultured + injured, injured + rapamycin, injured + MDivi-1, injured + EB (ethidium bromide) and injured + wortmanin (n=6).* ●$p<0.05$ *cultured + injured vs the freshly fixed,* *$p<0.05$ *different treatments vs cultured + injured.*

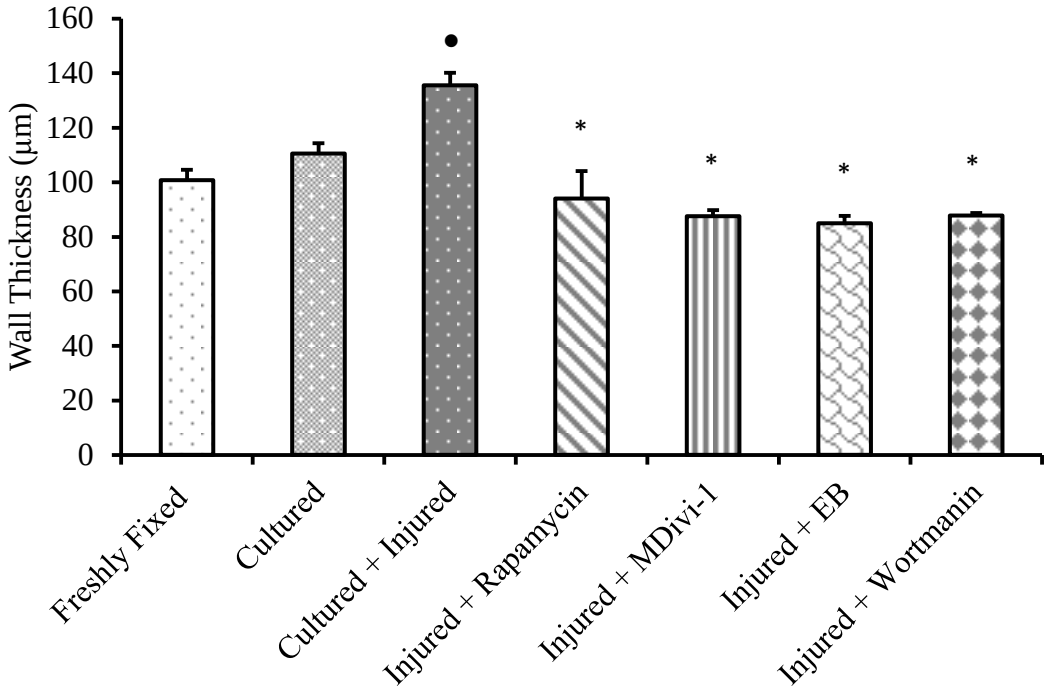

Figure 3.3 *shows the change in the vascular wall thickness following balloon injury and the change in cultured + injured, injured + rapamycin, injured + MDivi-1, injured + EB (ethidium bromide) and injured + wortmanin (n=6).* ●*p<0.05 cultured + injured vs the freshly fixed, *p<0.05 different treatments vs cultured + injured.*

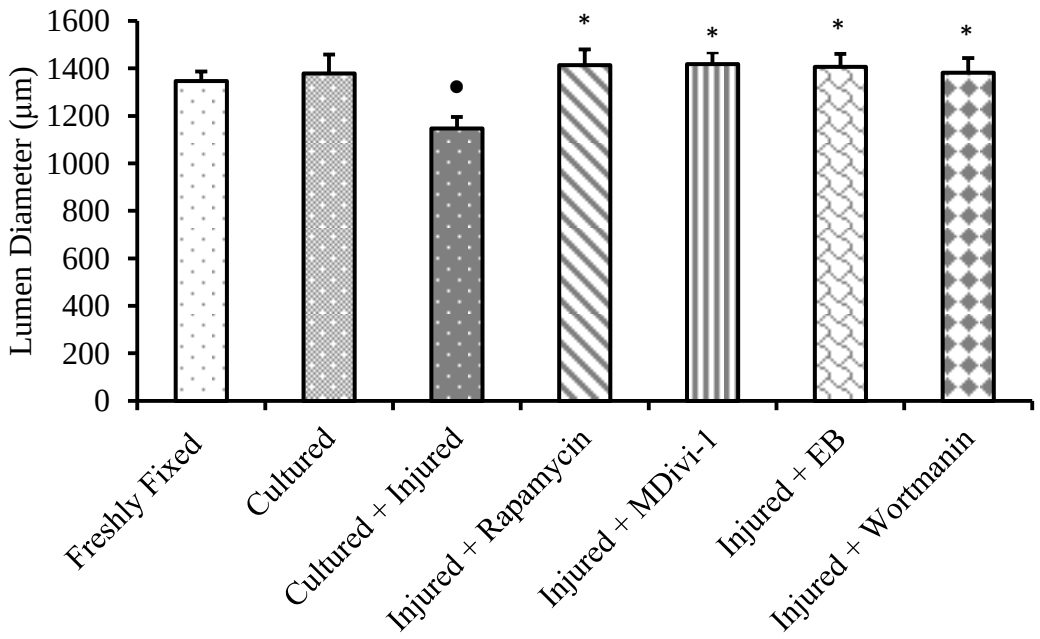

Figure 3.4 *shows the change in the vascular lumen diameter following balloon injury and the change in cultured + injured, injured + rapamycin, injured + MDivi-1, injured + EB (ethidium bromide) and injured + wortmanin (n=6).* ●*p<0.05 cultured + injured vs the freshly fixed, *p<0.05 different treatments vs cultured + injured.*

3.18 VSM Cell Morphology:

Vascular smooth muscle cells were characterised by their morphology under the bright field microscope (figure 3.5A). They were also classified by some specific markers including smooth muscle actin using the epi-fluorescent microscope (figure 3.5B). The cells expressed actin filaments which are shown in green and the nuclei were visualised using DAPI stain which is shown in blue. The expression of actin confirms that these are vascular smooth muscle cells.

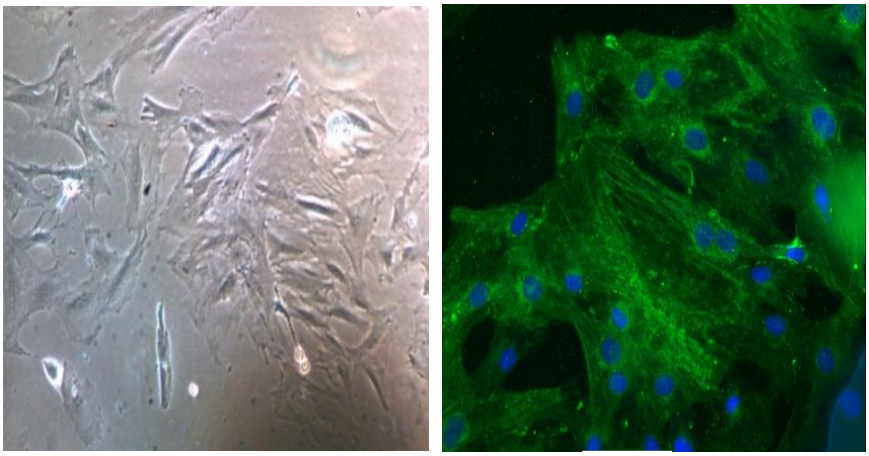

(A) (B)

Figure 3.5 *The bright field microscope was used at x20 magnification to visualise vascular smooth muscle cells pattern (Hills and Valleys) (A). The epi-fluorescent image shows vascular smooth muscle cell actin filaments labelled with smooth muscle actin antibody (green) and nucleus stained with DAPI (blue). Image was taken at x20 magnification (B).*

3.19 Effect of MDivi-1 on mitochondrial morphology and localisation:

The localisation, density and morphology of the mitochondria within the cell was investigated using the fluorescent anti-mitochondrial antibody recognising the 60 KDa non glycosylated protein component of mitochondria found in human cells. Images were taken to show the distribution of mitochondria in the cytoplasm for the different treatments used. The images show that the mitochondria were scattered around the cell with the 0.1% FCS (quiesced) with a longer size 0.6 ± 0.1 μm (figure 3.6) and when stimulated using 10% FCS they fragment and become shorter in size 0.1 ± 0.1 μm, migrate and accumulate around the nuclei (figure 3.7). Mitochondrial fission inhibition with MDivi-1 resulted in a network formation and an increase in mitochondrial length 0.5 ± 0.07 μm (figure 3.8).

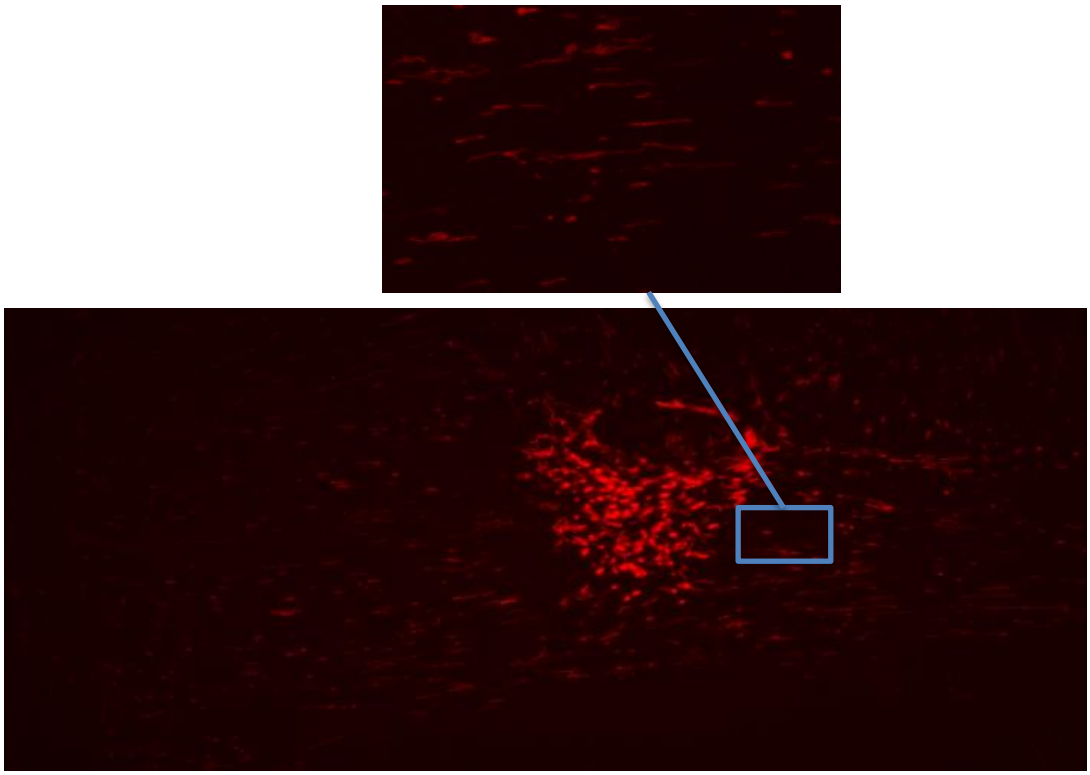

Figure 3.6 *The mitochondria were visualised using anti-mitochondria antibody (red). The distribution of the mitochondria was measured by the intensity of the red fluorescence. The mitochondria were scattered evenly with low density around the nuclei in the quiesced cells x60.*

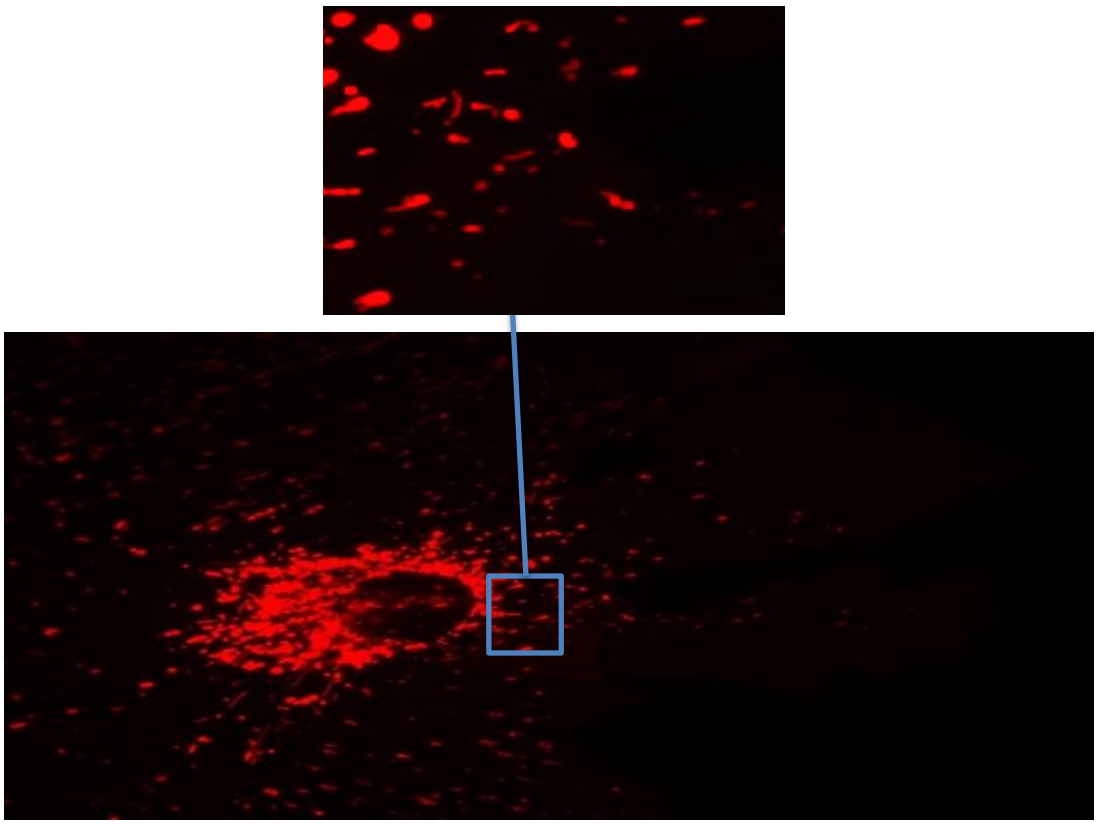

Figure 3.7 *The mitochondria were visualised using anti-mitochondria antibody (red). The distribution of the mitochondria was measured by the intensity of the red fluorescence. The mitochondria were seen to fragment and accumulate in higher density around the nuclei when they were stimulated with 10% FCS x60.*

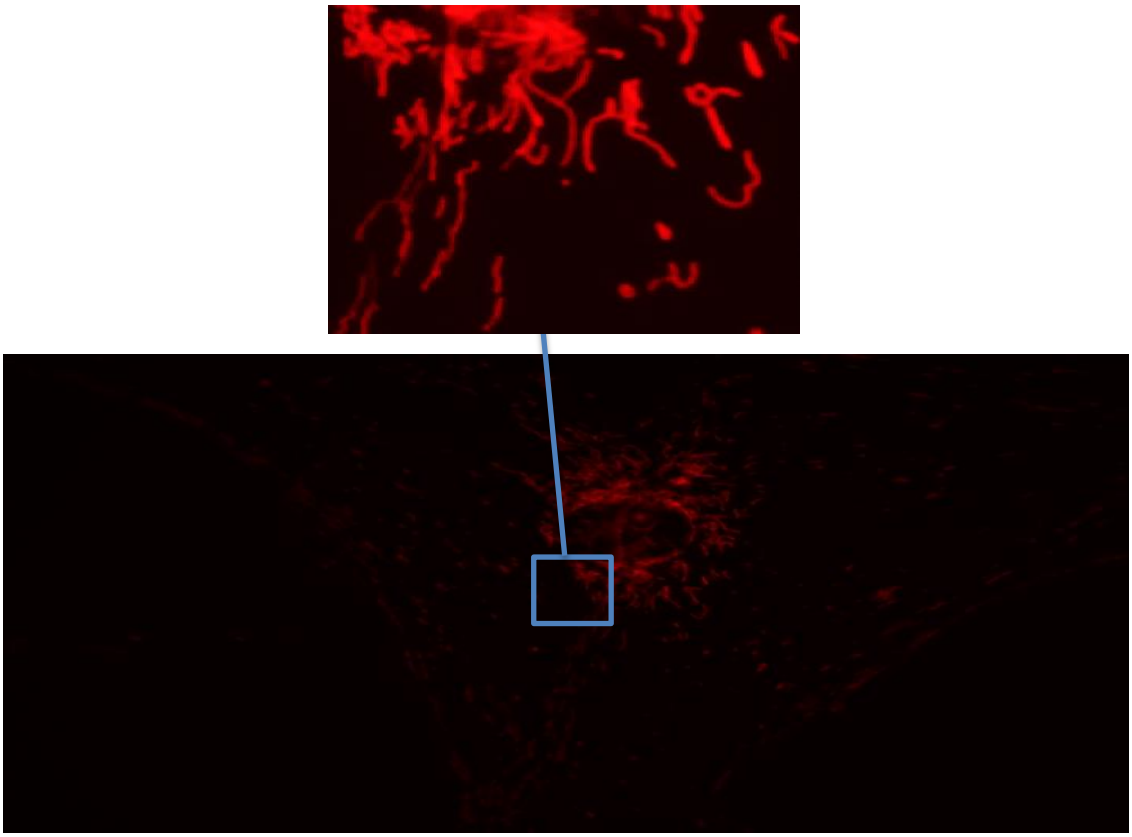

Figure 3.8 *The mitochondria were visualised using anti-mitochondria antibody (red). The distribution of the mitochondria was measured by the intensity of the red fluorescence. 10 μM treatments with MDivi-1 reduced mitochondrial density and restored mitochondrial network structure x60.*

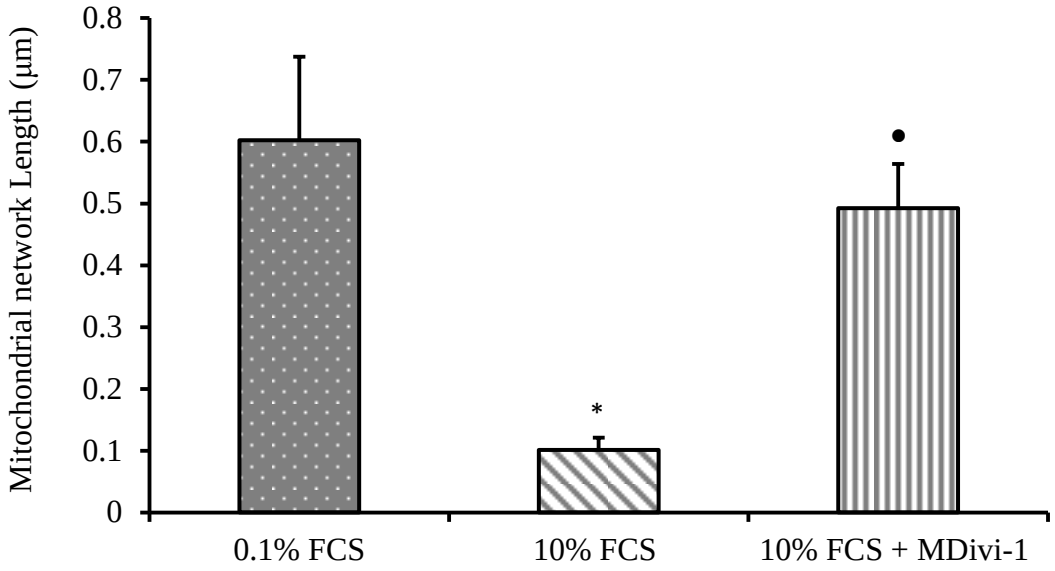

Figure 3.9 *shows the graph representation of mitochondrial length in the quiesced 0.1% FCS, 10% stimulated cells and stimulated + MDivi-1 treated cells (n=3). *p<0.05 10% FCS stimulated cells vs 0.1% FCS cultured cells, ●p<0.05 stimulated + MDivi-1 treated cells vs 10% FCS stimulated cells.*

3.20 Effect of MDivi-1 on VSM cell proliferation:

The proliferation of VSM cells and the effect of MDivi-1 treatment were measured using ^{3}H Thymidine incorporation assay. The inhibition in VSM cell proliferation using 10 μM of Mdivi-1 was assessed following stimulation with 10% FCS (Figure 3.10) and 20 ng platelet derived growth factor (PDGF) (Figure 3.11). Inhibiting mitochondrial fission in the 10% FCS stimulated cells resulted in a 24 ± 10% reduction in proliferation whereas inhibiting mitochondrial fission in the PDGF stimulated cells resulted in a 55 ± 2% reduction in proliferation.

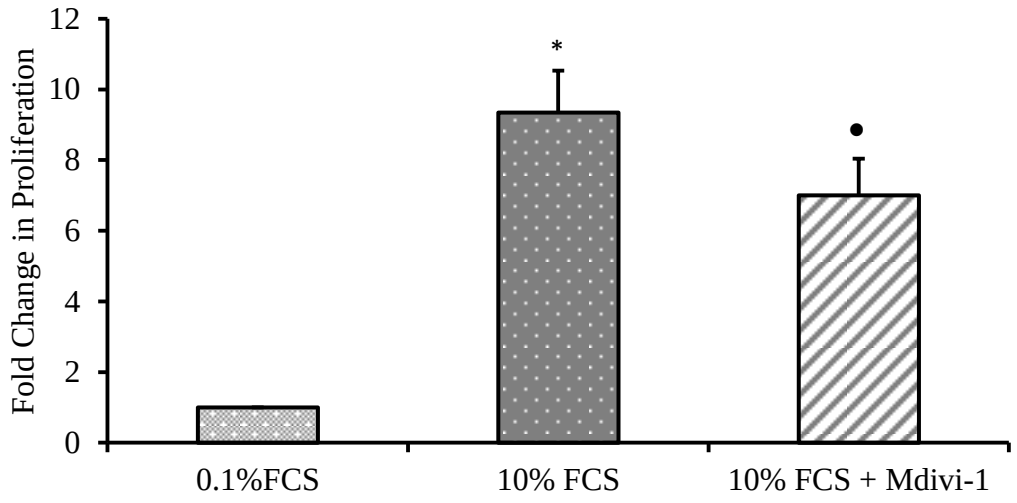

Figure 3.10 Shows the e*ffect of proliferation inhibition using 10 μM of Mdivi-1 following 10% FCS stimulation (n=7). *p<0.05 cells cultured in 10% FCS vs cells cultured in 0.1% FCS, ●p<0.05 cells cultured in 10% FCS + MDivi-1 vs cells cultured in 10% FCS.*

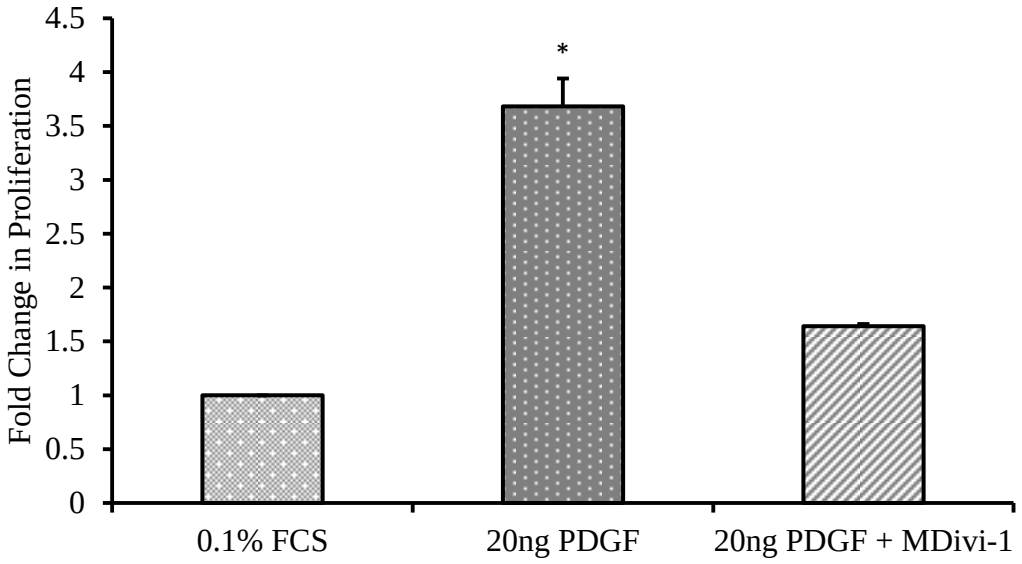

Figure 3.11 Shows the e*ffect of proliferation inhibition using 10 μM of Mdivi-1 following 20 ng PDGF stimulation (n=7). *p<0.05 cells cultured in PDGF vs cells cultured in 0.1% FCS, ●p<0.05 cells cultured in PDGF + MDivi-1 vs cells cultured in PDGF.*

3.21 Effect of MDivi-1 on VSM cell migration:

The migration of VSM cells was measured using a scratch assay to assess the impact of mitochondrial fission inhibition on VSM cell migration. Treating VSM cells with 10 μm of the mitochondrial inhibitor MDivi-1 inhibited cell migration and gap closure following stimulations with 10% FCS and 20 ng PDGF. Results show that the scratch area was reduced by 79 ± 4% after 24 hours of 10% FCS stimulation. However the scratch area was only reduced by 10 ± 2% following stimulation with 10% FCS and treatment with 10 μM of MDivi-1 (Figure 3.12). Results also show that scratch area was reduced by 50 ± 2% following 20 ng/ml PDGF stimulation. However when cells were treated with 10 μM of MDivi-1, the scratch area was reduced by 14 ± 4% (Figure 3.13).

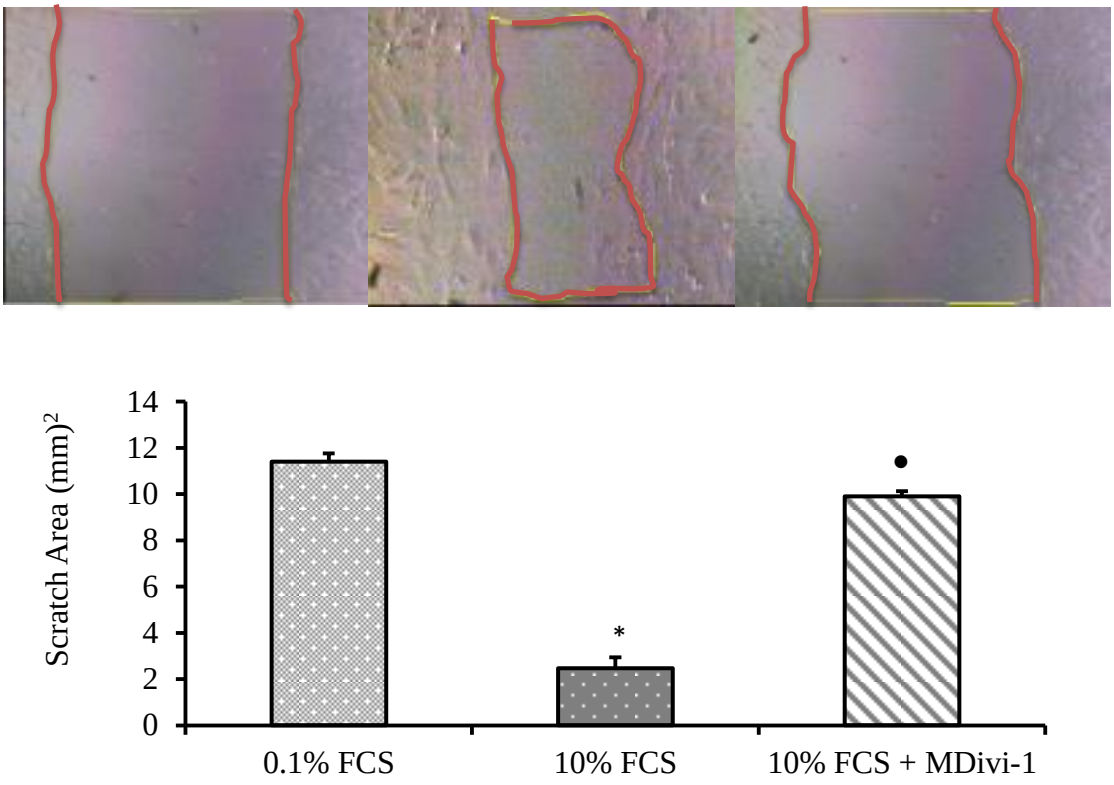

Figure 3.12 *Microscope images using x 5 magnification of the scratch assay showing the magnitude of vascular smooth muscle cells migration following stimulation with 10% FCS and the consequent inhibition following Mdivi-1 treatment (n=3). *p<0.05 cells cultured in 10% FCS vs cells cultured in 0.1% FCS, ●p<0.05 cells cultured in 10% FCS + MDivi-1 vs cells cultured in 10% FCS.*

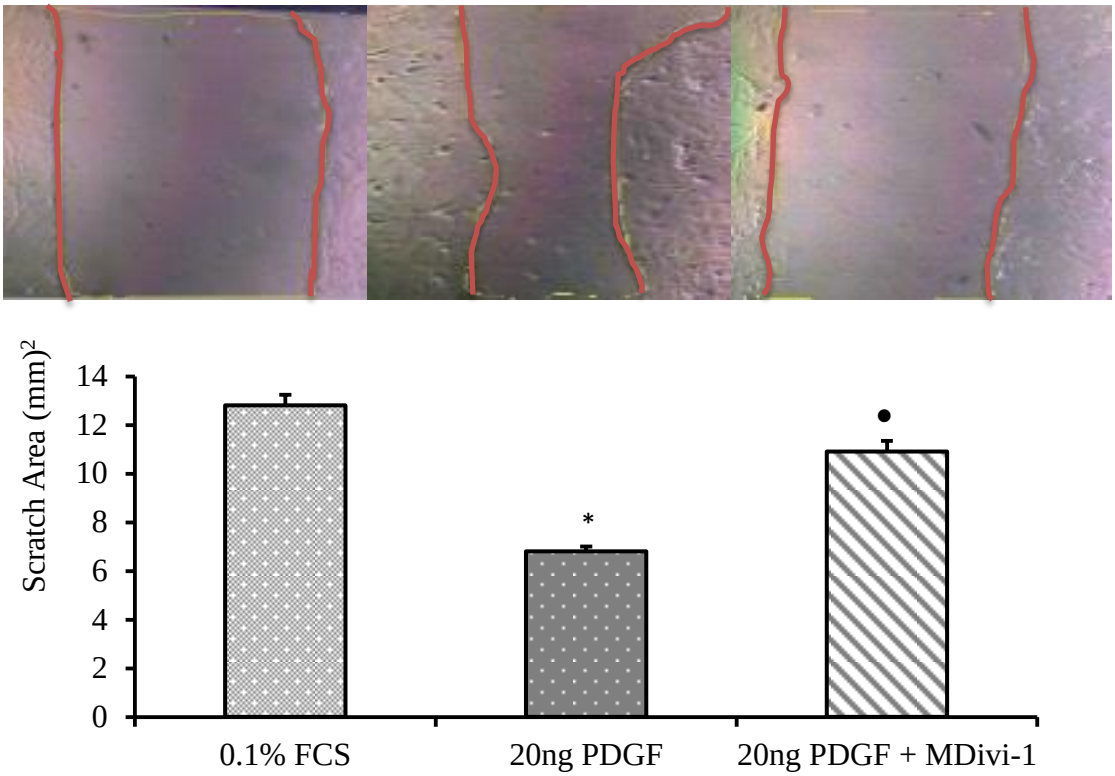

Figure 3.13 *Microscope images using x 5 magnification of the scratch assay showing the magnitude of vascular smooth muscle cells migration following stimulation with 20 ng/ml PDGF and the consequent inhibition following Mdivi-1 treatment (n=3). *p<0.05 cells cultured in 20 ng PDGF vs cells cultured in 0.1% FCS, ●p<0.05 cells cultured in 20 ng PDGF + MDivi-1 vs cells cultured in 20 ng PDGF.*

3.22 Effect of MDivi-1 on protein expression:

Phosphorylation and expression of different proteins were investigated by western blots after treating the cells with MDivi-1 to measure the effect of inhibiting mitochondria dynamics on MAPK signalling pathway, mTOR signalling pathway and cell cycle progression. Figure 3.14 showed no difference in the phosphorylation of ERK1/2 at tyrosine 204 site following treatment with MDivi-1.

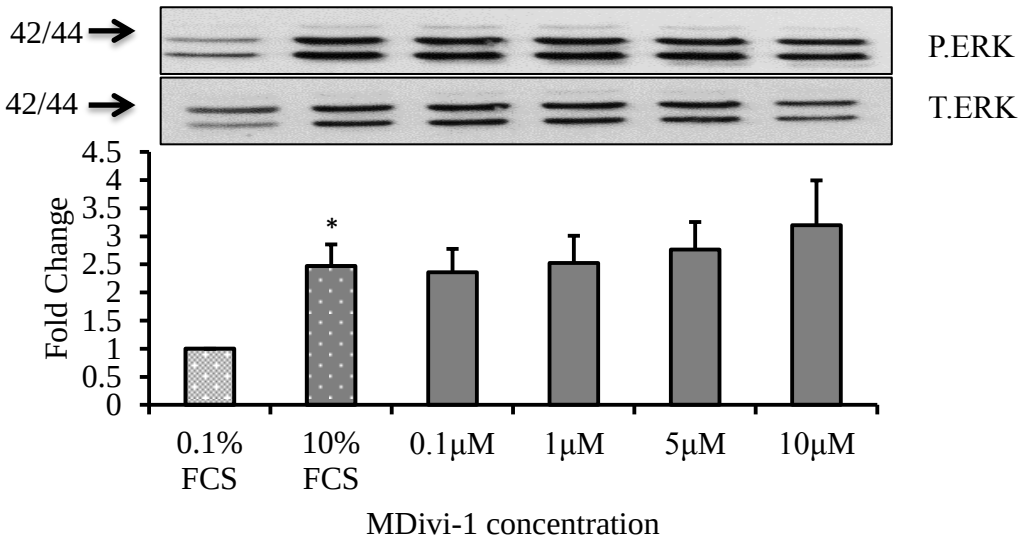

Figure 3.14 *shows the phosphorylation of ERK1/2 following 10% FCS stimulation and MDivi-1 treatment. The ERK1/2 was measured relative to Total ERK (n=3). *p<0.05 cells cultured in 10% FCS vs cells cultured in 0.1% FCS.*

However, increased phosphorylation was measured between the quiesced vs. 10% FCS and 20 ng PDGF (Figures 3.14 & 3.15).

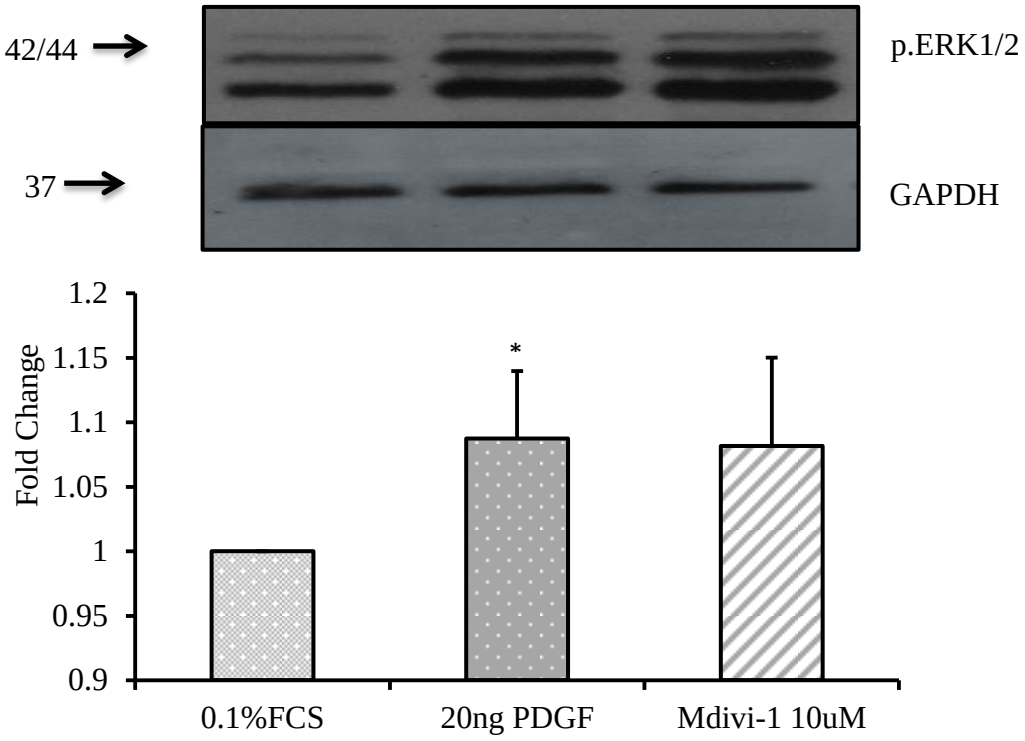

Figure 3.15 *shows the phosphorylation of ERK1/2 following 20ng PDGF stimulation and MDivi-1 treatment. The ERK1/2 was measured relative to GAPDH (n=3). *p<0.05 cells cultured in 20 ng PDGF vs cells cultured in 20 ng PDGF + MDivi-1.*

Cell cycle protein Cyclin D1 showed a decrease in their expression by 60 ± 10% following treatment with MDivi-1 (Figure 3.16).

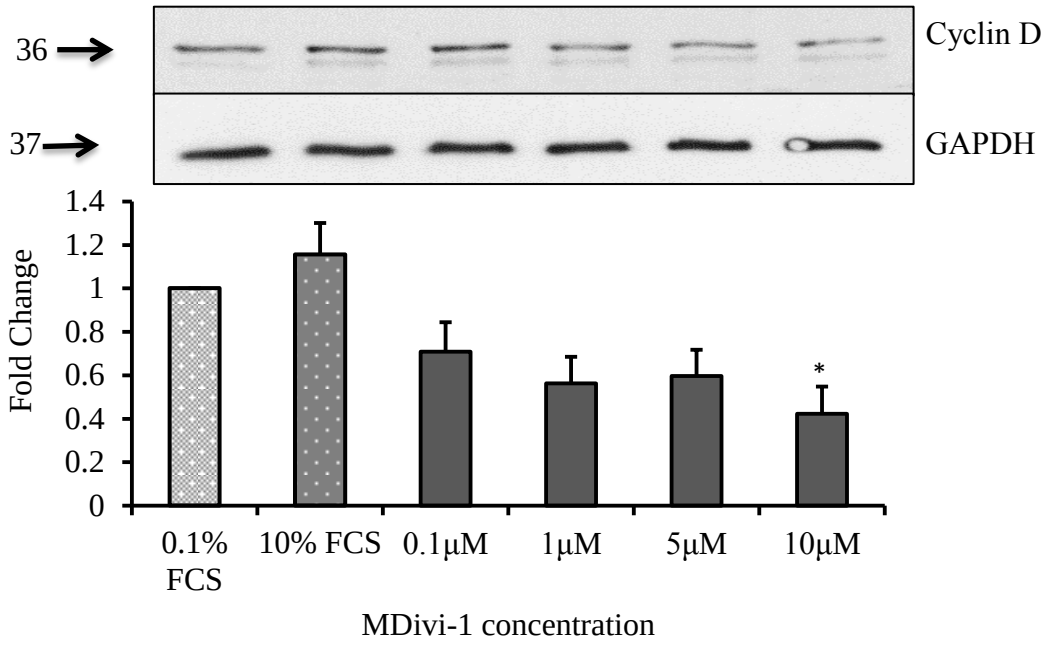

Figure 3.16 *shows the expression of cyclin D following 10% FCS stimulation and MDivi-1 treatment. Level of cyclin D was measured relative to GAPDH (n=3). *p<0.05 cells treated with 10 µM of MDivi-1 vs cells cultured in 0.1% FCS.*

The effect of mitochondrial inhibition on mTOR pathway was assessed by the phosphorylation of upstream Akt and the phosphorylation of the downstream 4EBP1. Akt phosphorylation at the ser-473 site was increased following stimulation with both 10% FCS and 20 ng PDGF. MDivi-1 showed a concentration-dependent inhibition of phosphorylation. The maximum reduction of phosphorylation was measured at 10 μM. At this concentration MDivi-1 inhibited phosphorylation by 57 ± 9% in the 10% stimulated cells (Figure 3.17) and by 23 ± 6% in the PDGF stimulated cells (Figure 3.18).

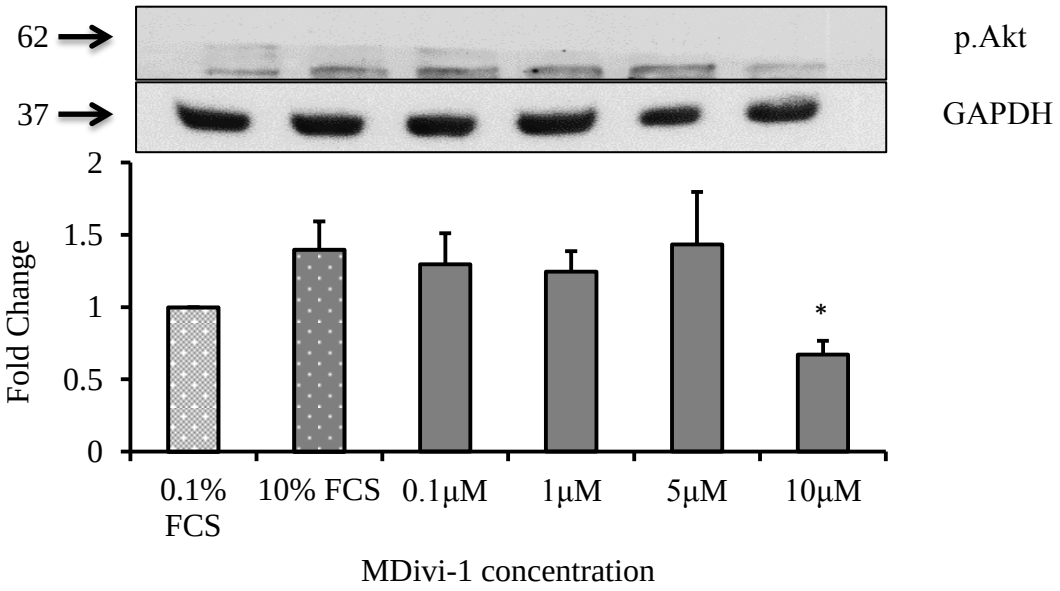

Figure 3.17 *shows the phosphorylation of Akt following 10% FCS stimulation and MDivi-1 treatment. Akt was measured relative to GAPDH (n=3). *p<0.05 cells treated with 10 μM of MDivi-1 vs cells cultured in 0.1% FCS.*

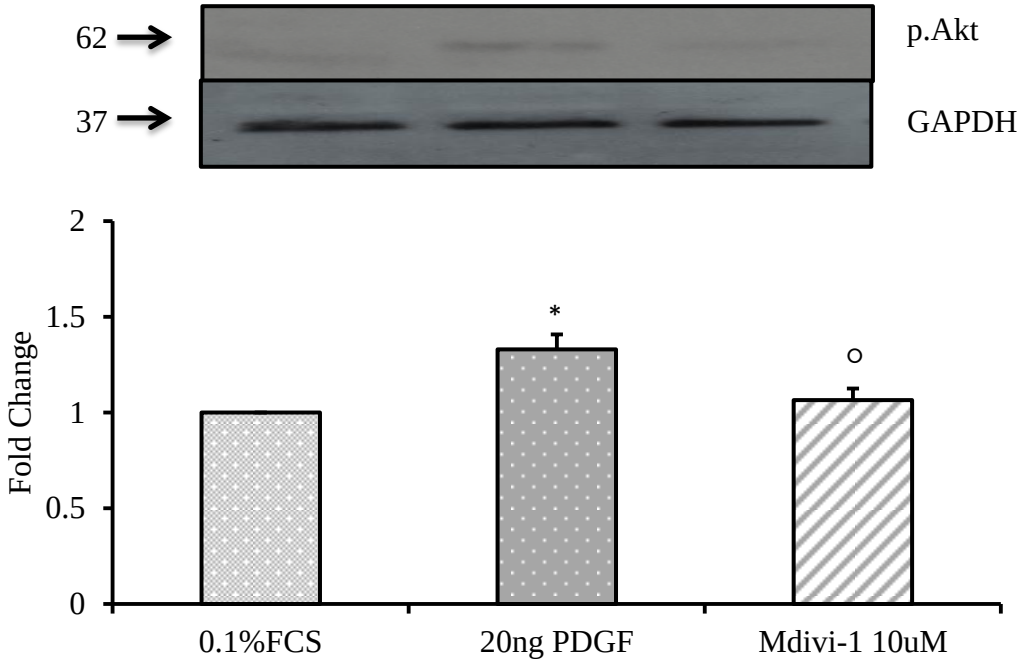

Figure 3.18 *shows the phosphorylation of Akt following 20 ng PDGF stimulation and MDivi-1 treatment. The phosphorylation of Akt was measured relative to GAPDH (n=3). *p<0.05 cells cultured in 20 ng PDGF vs cells cultured in 0.1% FCS, ○p<0.05 cells cultured in 20 ng PDGF + MDivi-1 vs cells cultured in 20 ng PDGF.*

The downstream 4EBP1 also showed a reduction in the phosphorylation at tyrosine 37 site by 50 ± 7% following mitochondrial inhibition in both 10% FCS and 20 ng PDGF (Figures 3.19 & 3.20).

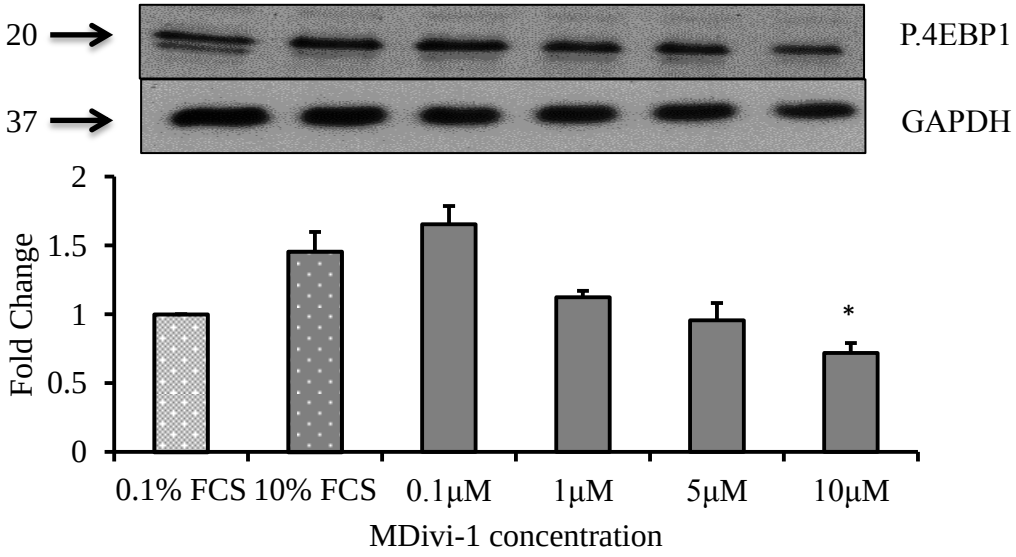

Figure 3.19 shows the p*hosphorylation of 4EBP1 following 10% FCS stimulation and MDivi-1 treatment. 4EBP1 was measured relative to GAPDH (n=3). * p<0.05 cells treated with 10 μM of MDivi-1 vs cells cultured in 0.1% FCS.*

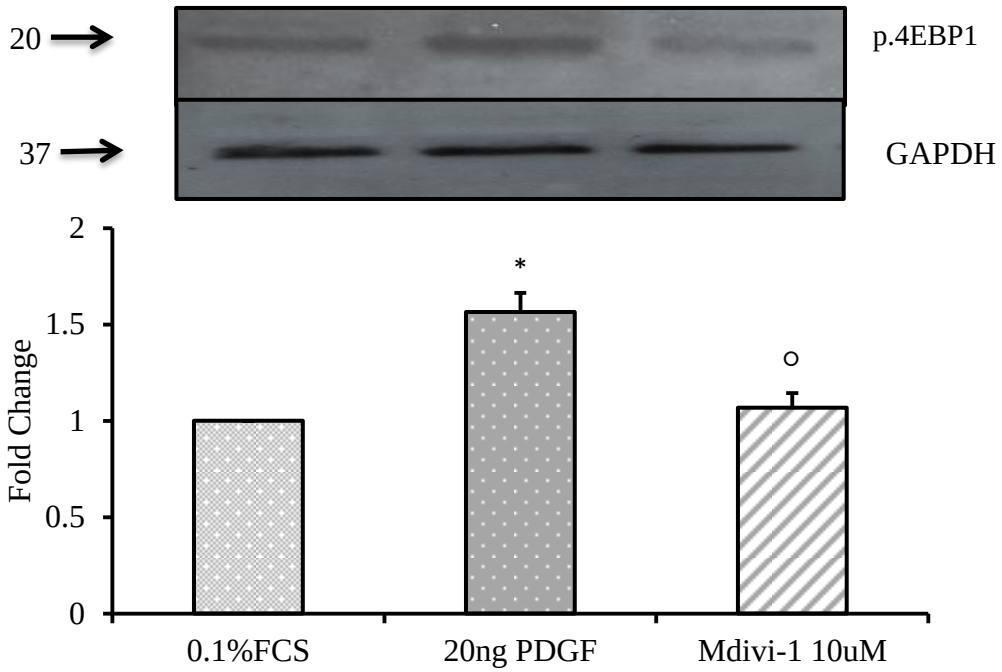

Figure 3.20 *shows the phosphorylation of 4EBP1 following 20 ng PDGF stimulation and MDivi-1 treatment. The phosphorylation of 4EBP1 was measured relative to GAPDH (n=3). *p<0.05 cells cultured in 20 ng PDGF vs cells cultured in 0.1% FCS, ○p<0.05 cells cultured in 20 ng PDGF + MDivi-1 vs cells cultured in 20 ng PDGF.*

The effect of MDivi-1 on the bioenergetics of the mitochondria, reflected by the release of Cytochrome C, was assessed and showed no difference in the total Cytochrome C levels with all the different concentrations of MDivi-1 (Figures 3.21 & 3.22).

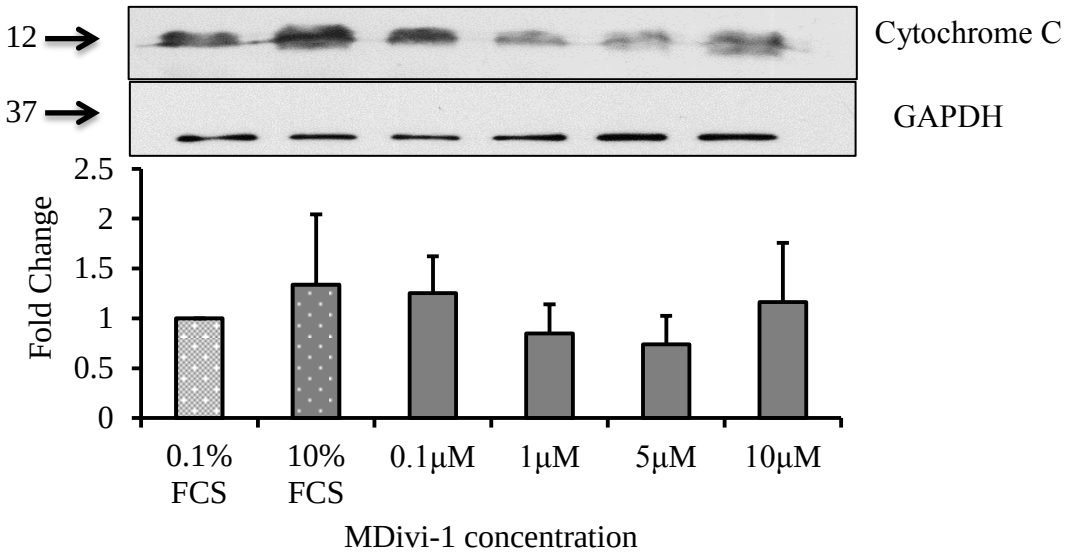

Figure 3.21 *shows the expression of cytochrome c following 10% FCS stimulation and MDivi-1 treatment. Level of cytochrome c was measured relative to GAPDH (n=3).*

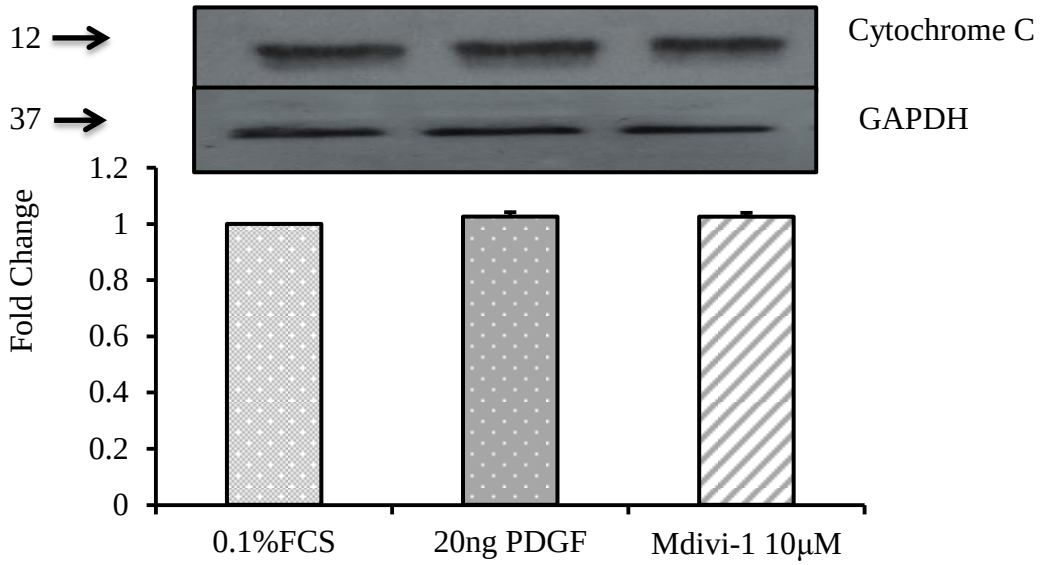

Figure 3.22 *shows the expression of cytochrome c following 20 ng PDGF stimulation and MDivi-1 treatment. The expression of cytochrome c was measured relative to GAPDH (n=3).*

3.23 Effect of MDivi-1 on cell cycle progression:

The percentage of cells in each phase of the cell cycle following MDivi-1 treatment was measured to determine the phase at which the drug works (Figure 3.23). The results showed 76 ± 4% increase in G2 phase following 10 µM MDivi-1 treatment compared to the 10% stimulated control (Figure 3.24).

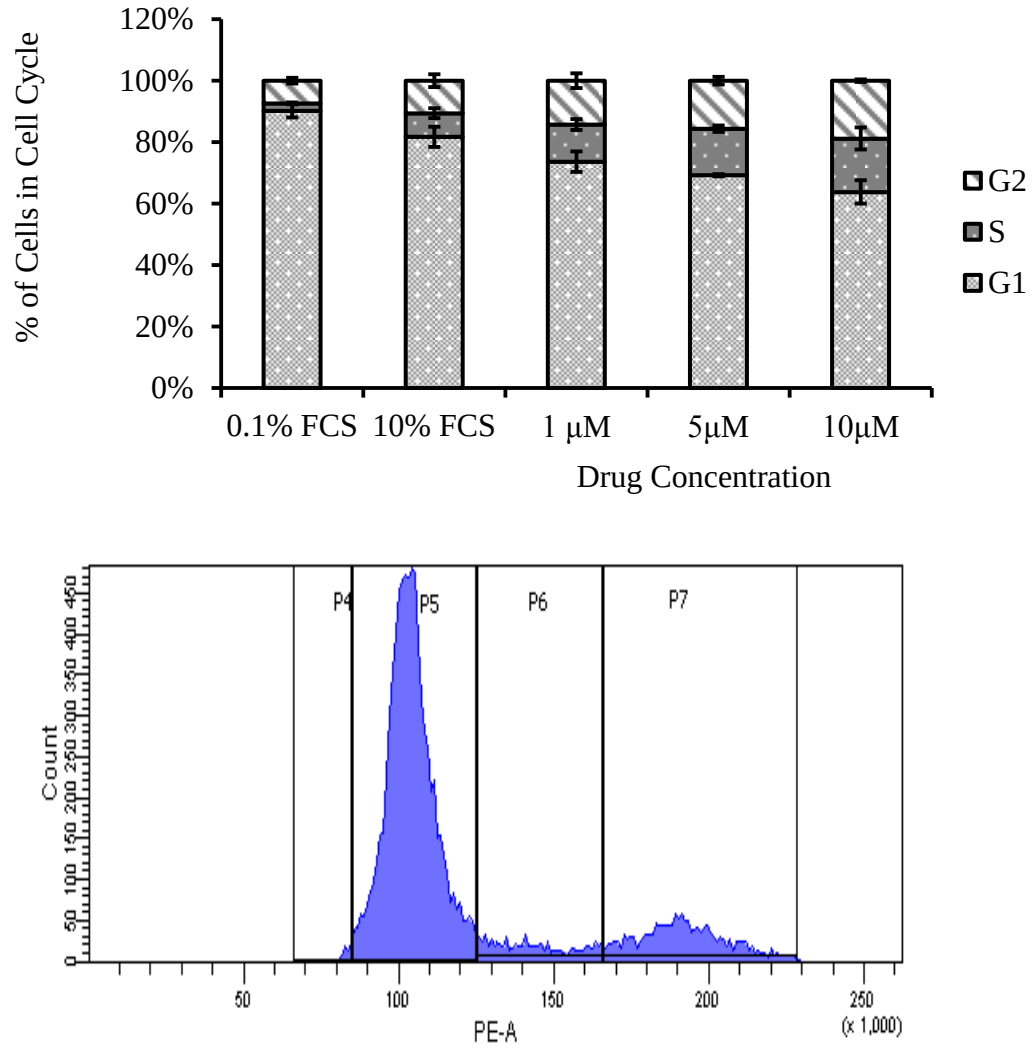

Figure 3.23 *Shows percentage of cells in different phases of the cell with different concentrations of MDivi-1 compared to the background cells 0.1% FCS and control cells 10% FCS (n=3).*

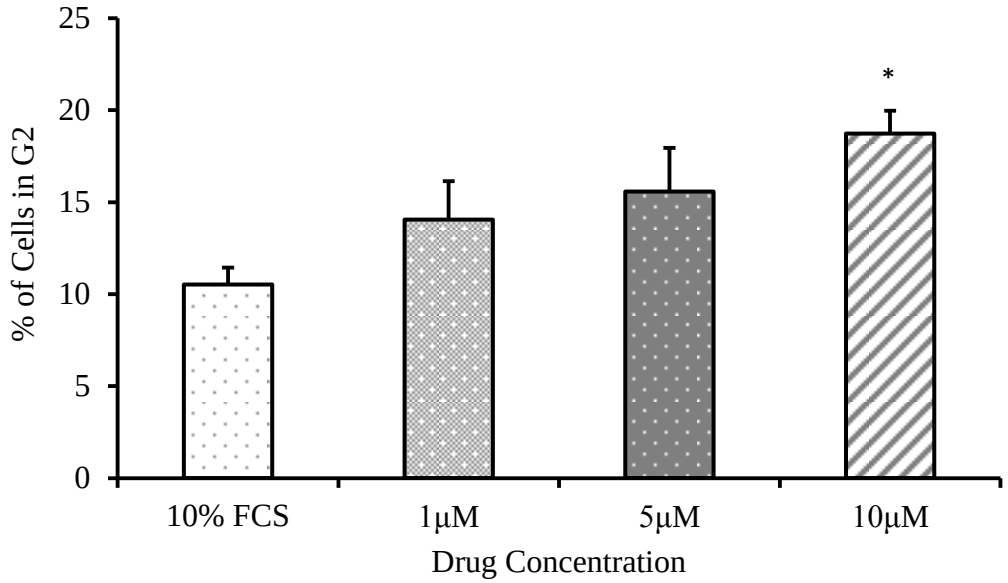

Figure 3.24 *Shows percentage of cells in G2 with increasing MDivi-1 concentration to 10 μM compared to the control cells 10% FCS (n=3) *p<0.05 cells treated with 10 μM of MDivi-1 vs cells cultured in 10% FCS.*

3.24 Effect of MDivi-1 on the level of caspase 3/7 in VSM cells:

Apoptosis was assessed by measuring caspase 3/7 activity. The release of caspase 3/7 was not seen to change significantly following stimulation with 10% FCS and 20 ng/ml PDGF. However, the level of caspase was increased following treatment with 10 μM mitochondrial fission inhibitor MDivi-1 by 3 fold in the 10%FCS stimulated cells and 0.5 fold in the PDGF stimulated cells (Figure 3.25).

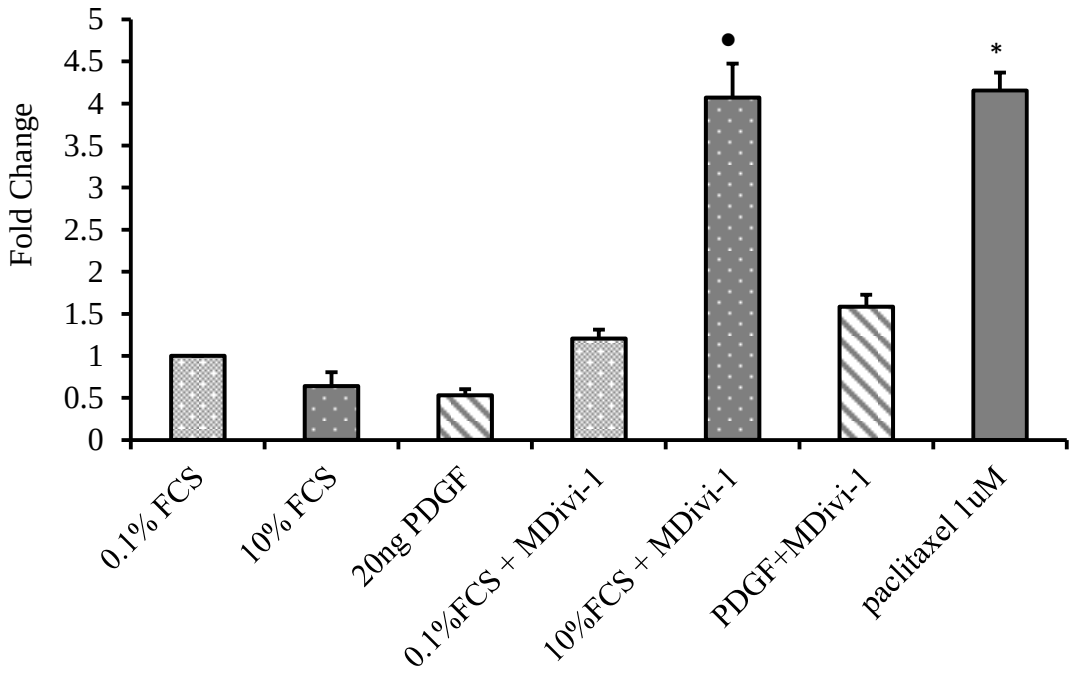

Figure 3.25 *Shows the differences in apoptotic activity measured by caspase 3/7 activity under different treatments. The release of caspase 3/7 was measured in background 0.1% FCS and compared with the level following stimulation with 10% FCS and 20 ng PDGF. The level was also measured following treatment with MDivi-1 in cells cultured in 0.1% FCS, 10% FCS and 20 ng PDGF. The level was compared to the level of caspase activity measured following treatment with paclitaxel (n=3) •p< 0.05 cells cultured in 10% FCS + MDivi-1 vs cells cultured in 10% FCS, *p< 0.05 cells cultured in 10% FCS + treated with paclitaxel vs cells cultured in 10% FCS.*

3.25 Mitochondrial functions (ROS &ATP):

Mitochondrial bioactivity was measured by the generation of ROS and ATP turnover. Results highlighted that the generation of ROS in the mitochondrial-depleted Rho cells did not differ significantly between 0.1 % FCS, 10% FCS and 10% FCS + MDivi-1. However the total ROS measured was lower when compared with control (wild type) VSM cell (Figures 3.26 & 3.27).

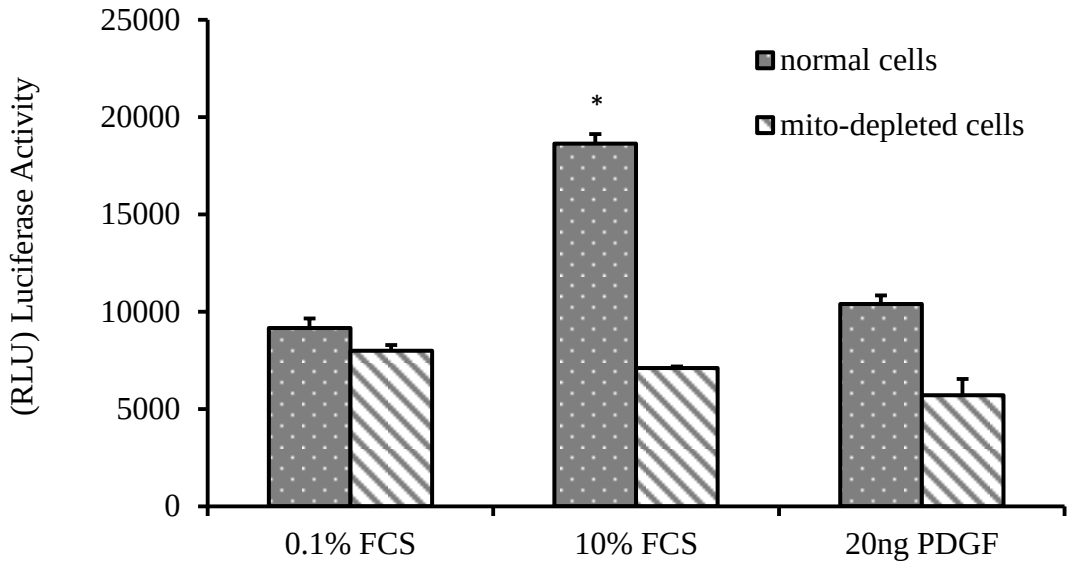

Figure 3.26 *Shows the difference in ROS release between normal cells and Rho cells following stimulation with 10% FCS and 20 ng/ml PDGF (n=3) *p < 0.05 cells cultured in 10% FCS vs cells cultured in 0.1% FCS.*

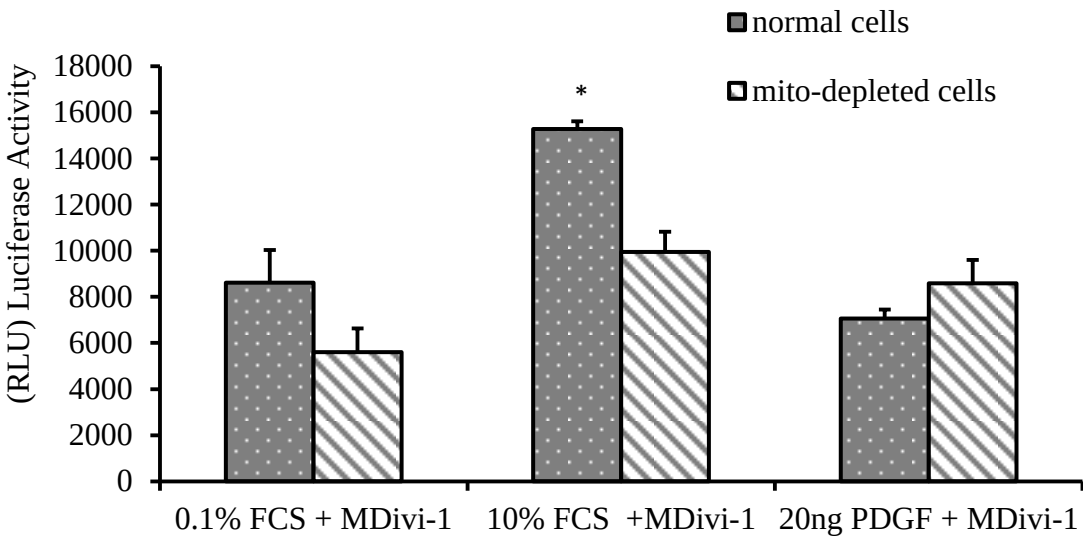

Figure 3.27 *Shows the difference in ROS release between normal cells and Rho cells following stimulation with 10% FCS and 20 ng/ml PDGF in VSM cell treated with MDivi-1(n=3), *p < 0.05 cells cultured in 10% FCS + MDivi-1 vs cells cultured in 0.1% FCS + MDivi-1.*

The generation of ROS was seen to be increased by 100% ± 13% and 10% ± 2% in stimulated cells with both 10% FCS and 20ng/ml PDGF respectively. Inhibiting mitochondrial fission using MDivi-1 significantly reduced the level of ROS released in VSM cell. A 20% ± 5% reduction in the 10% FCS stimulated cells and 36% ± 5% reduction in the PDGF stimulated cells were measured (Figure 3.28).

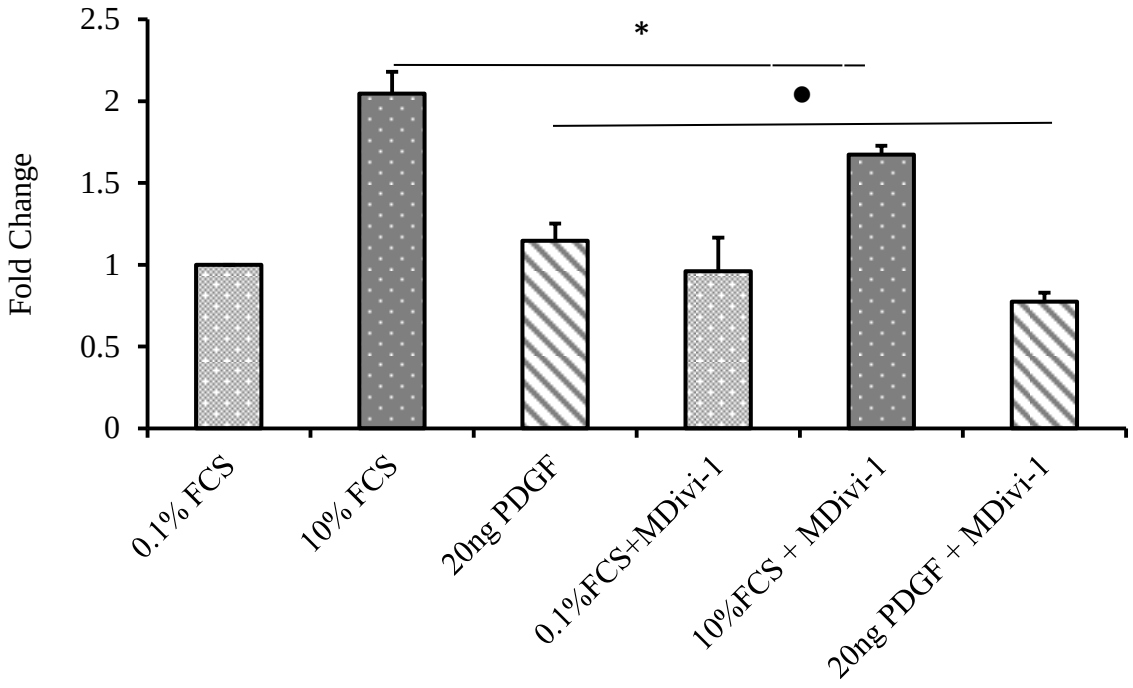

Figure 3.28 *Shows the release of ROS in 0.1% FCS cultured cells, 10% FCS stimulated cells, 20 ng PDGF stimulated cells, 0.1% FCS + MDivi-1 treated cells, 10% FCS + MDivi-1 treated cells and 20 ng PDGF + MDivi-1 treated cells (n=3), *p < 0.05 cells cultured in 10% FCS + MDivi-1 vs cells cultured in 10% FCS. ●p < 0.05 Cells cultured in 20 ng PDGF + MDivi-1 vs cells cultured in 20 ng PDGF.*

The production of ATP was also significantly increased in the stimulated vs. control VSM cell by 34% ± 12% following 10% FCS stimulation and by 36% ± 13% following PDGF stimulation. ATP level was reduced following treatment with MDivi-1 by 7% in the 10%FCS stimulated cells and by 12% in the PDGF stimulated cells (Figure 3.29).

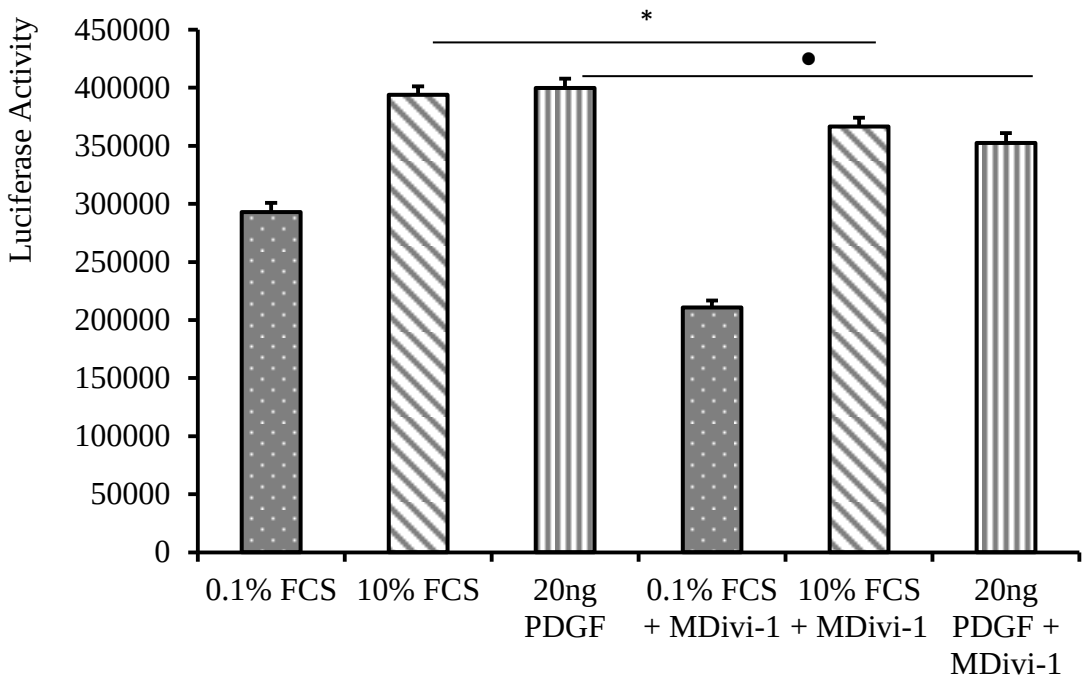

Figure 3.29 *Shows the production of ATP in 0.1% FCS cultured cells, 10% FCS stimulated cells, 20 ng PDGF stimulated cells, 0.1% FCS + MDivi-1 treated cells, 10% FCS + MDivi-1 treated cells and 20 ng PDGF + MDivi-1 treated cells (n=3), *p < 0.05 cells cultured in 10% FCS + MDivi-1 vs cells cultured in 10% FCS. ●p < 0.05 Cells cultured in 20 ng PDGF + MDivi-1 vs cells cultured in 20 ng PDGF.*

3.26 Generation of Rho cells:

To inhibit the mitochondria non-pharmacologically, mitochondrial-depleted Rho cells were generated. These cells were characterised by the absence of mitochondrial activity markers including Tfam and cytochrome c oxidase II. The results showed that the level of Tfam was reduced to half the normal level (Figure 3.30) and the level of cytochrome c oxidase II was almost abolished (Figure 3.31).

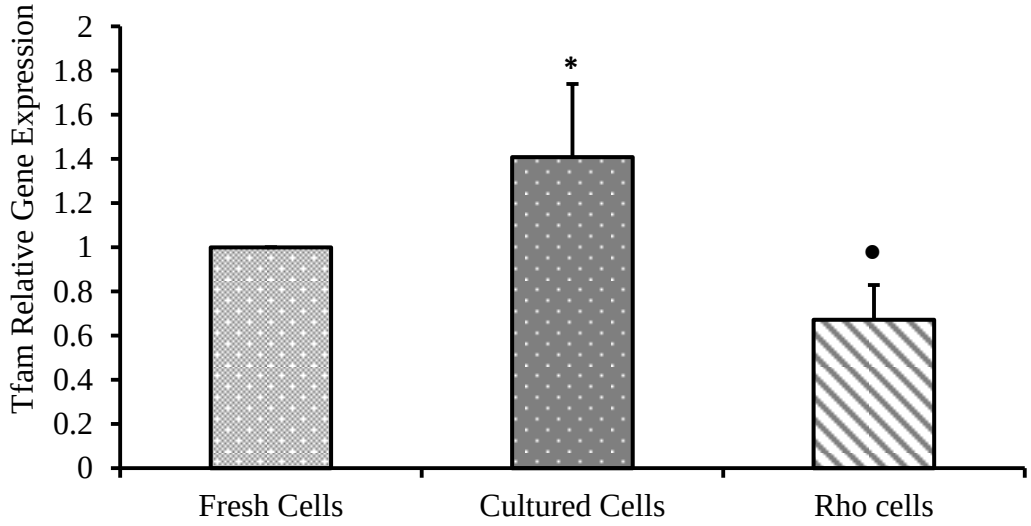

Figure 3.30 *Shows the loss of mitochondrial marker Tfam in the mitochondrial depleted Rho cells in comparison to 21 days cultured cells (n=3), *p < 0.05 cells cultured for 21 days vs freshly isolated cells. ●p < 0.05 Rho cells vs 21 days cultured cells.*

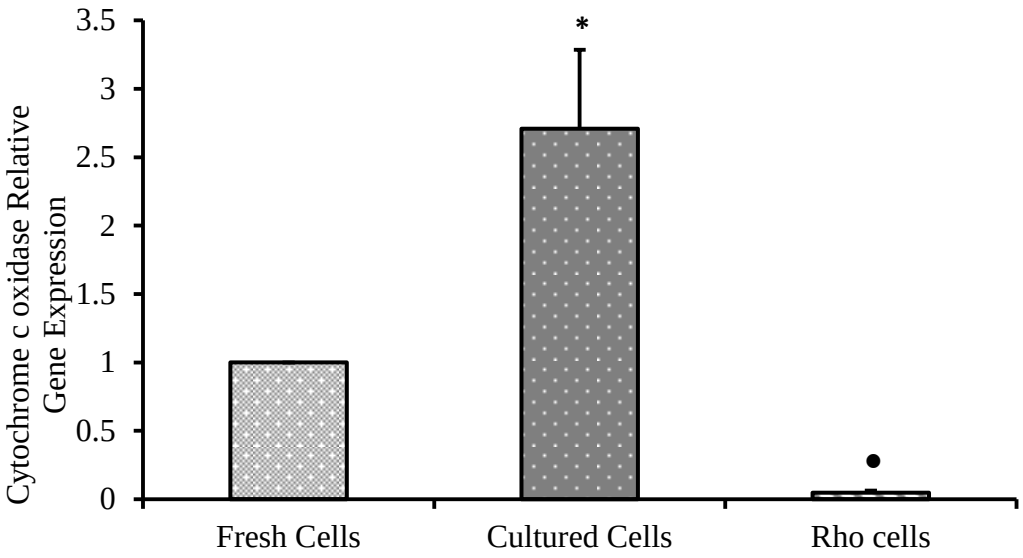

Figure 3.31 *Shows the loss of mitochondrial marker cytochrome c oxidase II in the mitochondrial depleted Rho cells in comparison to 21 days cultured cells (n=3), *p < 0.05 cells cultured for 21 days vs freshly isolated cells. ●p < 0.05 Rho cells vs 21 days cultured cells.*

Contractile markers including Calponin and myosin heavy chain were also seen to be lost in Rho cells (Figures 3.32 & 3.33).

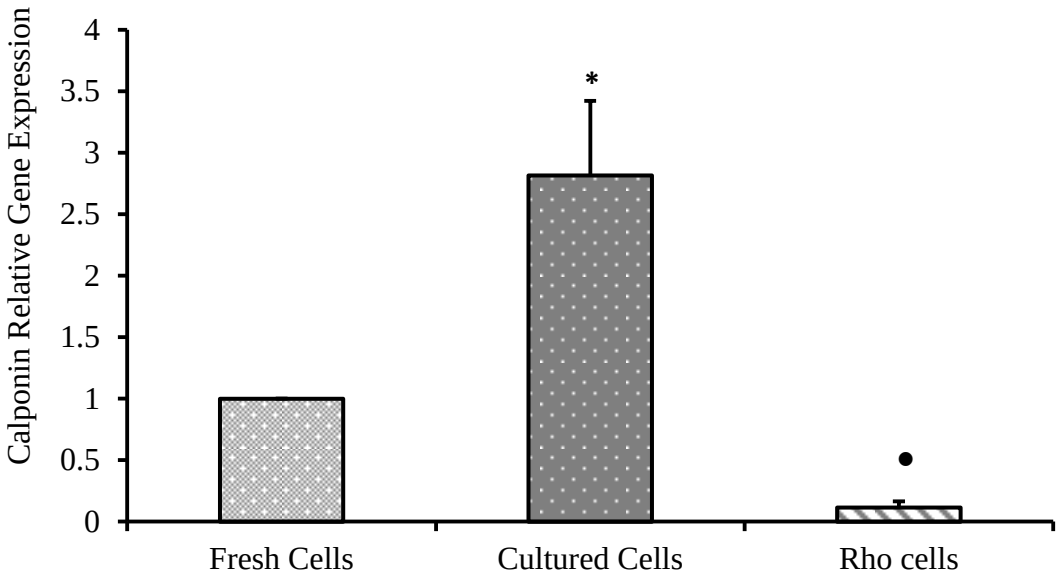

Figure 3.32 *Shows the loss of mitochondrial marker calponin in the mitochondrial depleted Rho cells in comparison to the 21 days cultured cells (n=3),*p < 0.05 cells cultured for 21 days vs freshly isolated cells. ●p < 0.05 Rho cells vs 21 days cultured cells.*

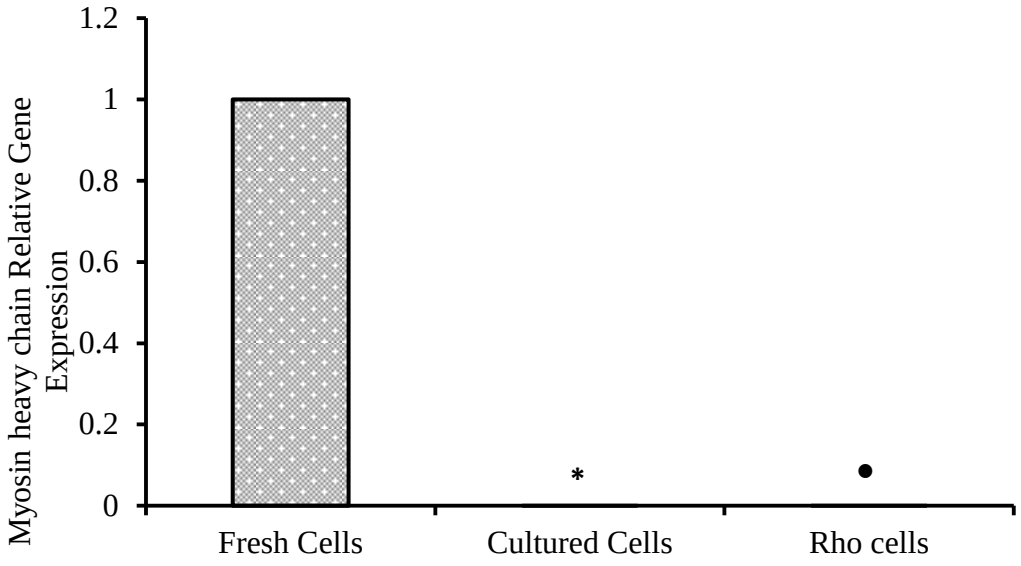

Figure 3.33 *Shows the loss of mitochondrial marker Myosin heavy chain in the mitochondrial depleted Rho cells in comparison to the 21 days cultured cells (n=3), *p < 0.05 cells cultured for 21 days vs freshly isolated cells. ●p < 0.05 Rho cells vs 21 days cultured cells.*

These cells were also imaged by epi-fluorescent microscope and the mitochondria seem to be fragmented and distributed in the cytoplasm (Figure 3.34).

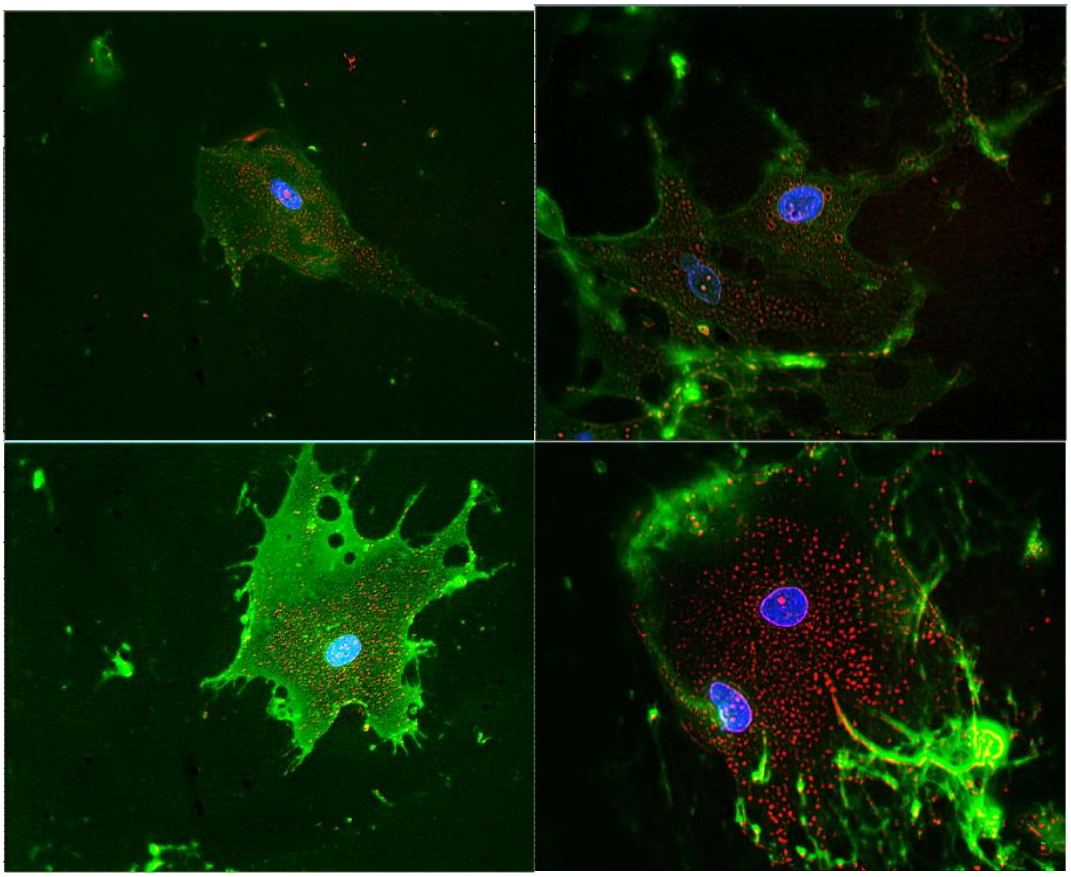

Figure 3.34 *Shows mitochondrial morphology and distribution in Rho cells using epi-fluorescent microscope x 60 magnification. Results showed that mitochondria stained with mitochondrial antibody (red) tend to be fragmented in Rho cells and spread across the cytoplasm with no concentration around the nuclei which is stained with DAPI (blue). Plasma membrane was stained using wheat germ agglutinin conjugate (green).*

3.27 Mitochondrial PCR array:

Mitochondrial PCR array was done to measure the difference in mitochondrial gene profile between 21 days cultured VSM cells and Rho cells (Figure 3.35).

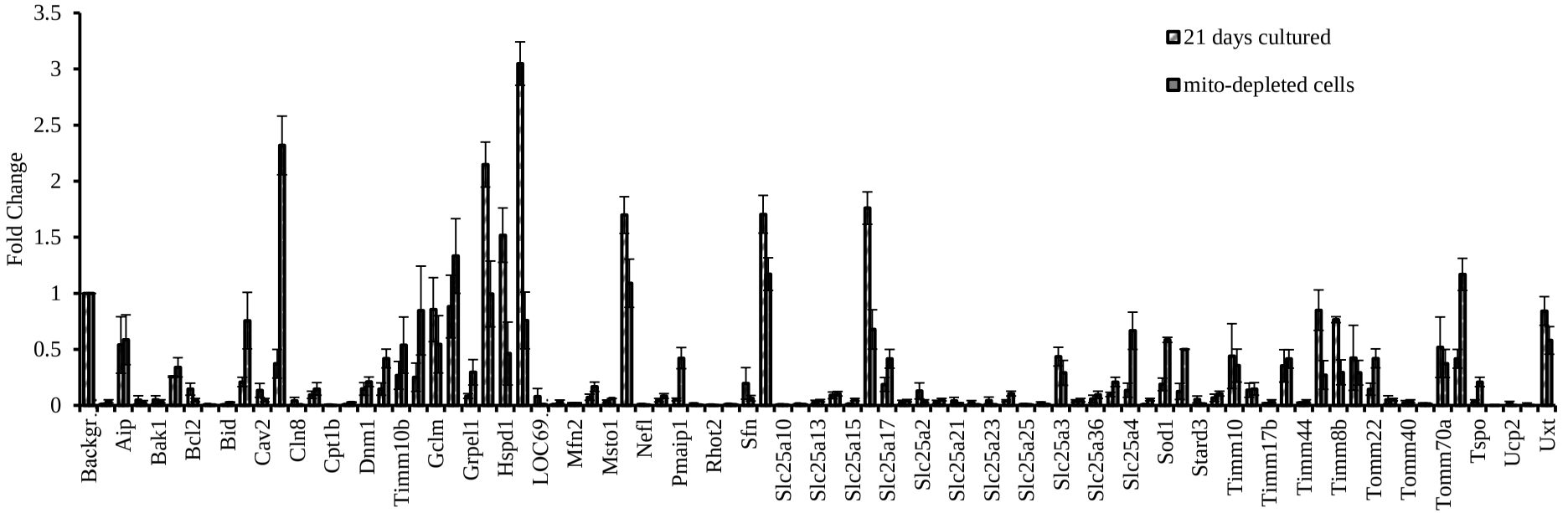

Figure 3.35 *Shows mitochondrial PCR array results comparing the expression of mitochondrial genes in Rho cells compared to 21 days cultured cells (n=3).*

Generating mitochondrial-depleted Rho cells resulted in an increase in the expression of pro-apoptotic proteins such as Bnip3, cdkn2a, Pmaip1 and P53 compared to 21 days cultured VSMCs. The expression of Bnip3 was reduced by 80 ± 4% in the 21 days cultured VSM cells compared to the freshly isolated VSM cells and increased by 73 ± 2.5% in the Rho cells compared to the 21 days cultured VSM cells (Figure 3.36).

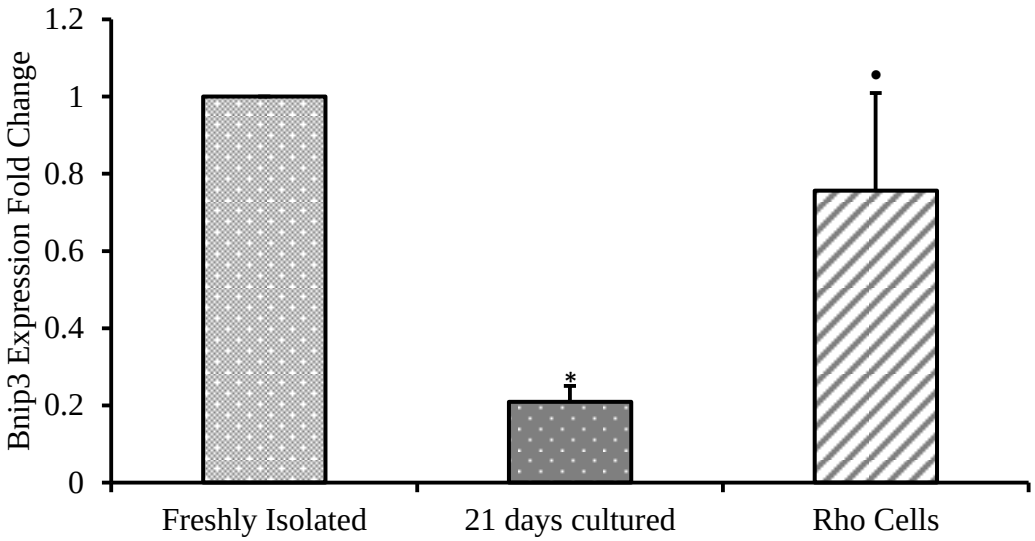

Figure 3.36 *Shows the expression of pro-apoptotic gene Bnip3 in freshly isolated cells, 21 days cultured cells and Rho cells. (n=3), *p <0.05 21 days cultured cells vs freshly isolated cells, ●p <0.05 Rho cells vs 21 days cultured cells.*

The expression of cdkn2a was reduced by 63 ± 2% in the 21 days cultured VSM cells compared to the freshly isolated VSM cells and increased by 73 ± 3% in the Rho cells compared to the 21 days cultured VSM cells (Figure 3.37).

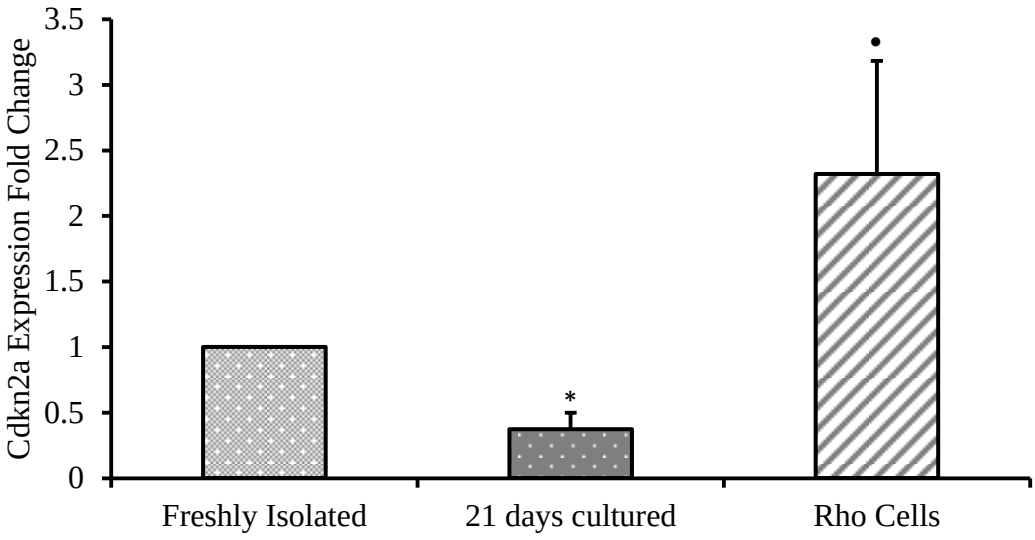

Figure 3.37 *Shows the expression of cell cycle inhibitor gene Cdkn2a in freshly isolated cells, 21 days cultured cells and Rho cells (n=3), *p <0.05 21 days cultured cells vs freshly isolated cells, ●p <0.05 Rho cells vs 21 days cultured cells.*

The expression of pmaip1 was reduced by 95 ± 10% in the 21 days cultured VSM cells compared to the freshly isolated VSM cells and increased by 38 ± 4% in the Rho cells compared to the 21 days cultured VSM cells (Figure 3.38).

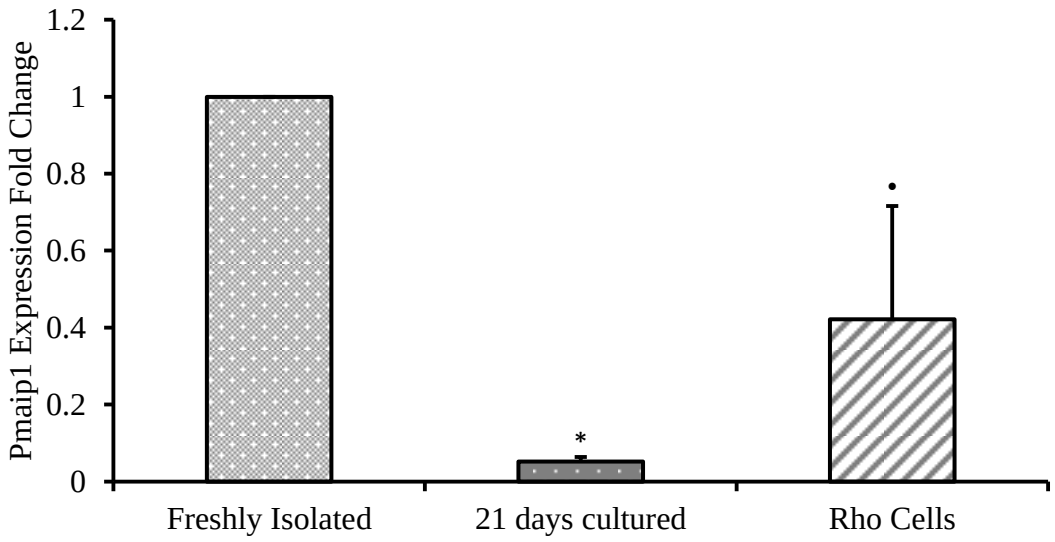

Figure 3.38 *Shows the expression of pro-apoptotic gene Pmaip1 in freshly isolated cells, 21 days cultured cells and Rho cells (n=3), *p <0.05 21 days cultured cells vs freshly isolated cells, ●p <0.05 Rho cells vs 21 days cultured cells.*

The expression of P53 was reduced by 60 ± 8% in the 21 days cultured VSM cells compared to the freshly isolated VSM cells and increased by 63 ± 4% in the Rho cells compared to the 21 days cultured VSM cells (Figure 3.39).

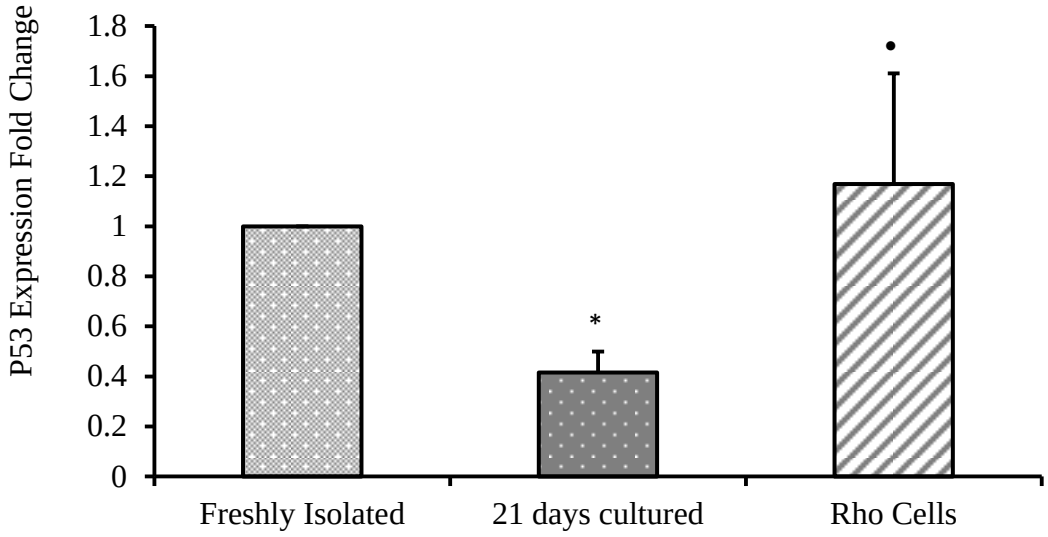

Figure 3.39 *Shows the expression of pro-apoptotic gene in freshly isolated cells, 21 days cultured cells and Rho cells (n=3), *p <0.05 21 days cultured cells vs freshly isolated cells, ●p <0.05 Rho cells vs 21 days cultured cells.*

Results also showed that expression of mitochondrial transport proteins such as Hsp90aa1, Hspd1 and slc25a16 were reduced in Rho cells compared to 21 days cultured cells. The expression of Hsp90aa1 was increased by 100 ± 12% in the 21 days cultured VSM cells compared to the freshly isolated VSM cells and decreased by 51 ± 29% in the Rho cells compared to the 21 days cultured VSM cells (Figure 3.40).

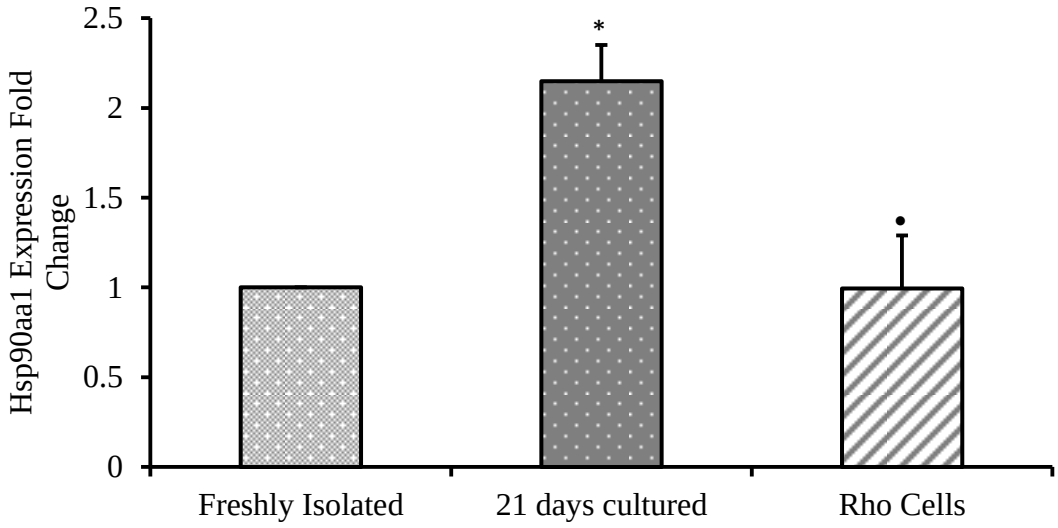

Figure 3.40 *Shows the expression of mitochondrial transport gene Hsp90aa1 in freshly isolated cells, 21 days cultured cells and Rho cells (n=3), *p <0.05 21 days cultured cells vs freshly isolated cells, ●p <0.05 Rho cells vs 21 days cultured cells.*

The expression of Hspd1 was decreased by 75 ± 28% in the Rho cells compared to the 21 days cultured VSM cells (Figure 3.41).

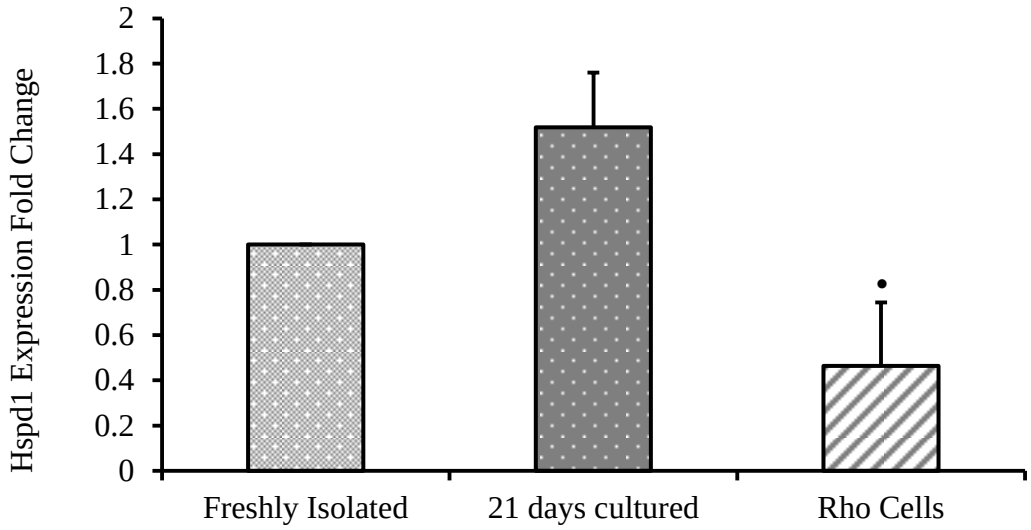

Figure 3.41 *Shows the expression of mitochondrial transport gene Hspd1 in freshly isolated cells, 21 days cultured cells and Rho cells (n=3), ●p <0.05 Rho cells vs 21 days cultured cells.*

The expression of Slc25a16 was increased by 70 ± 15% in the 21 days cultured VSM cells compared to the freshly isolated VSM cells and decreased by 61 ± 22% in the Rho cells compared to the 21 days cultured VSM cells (Figure 3.42).

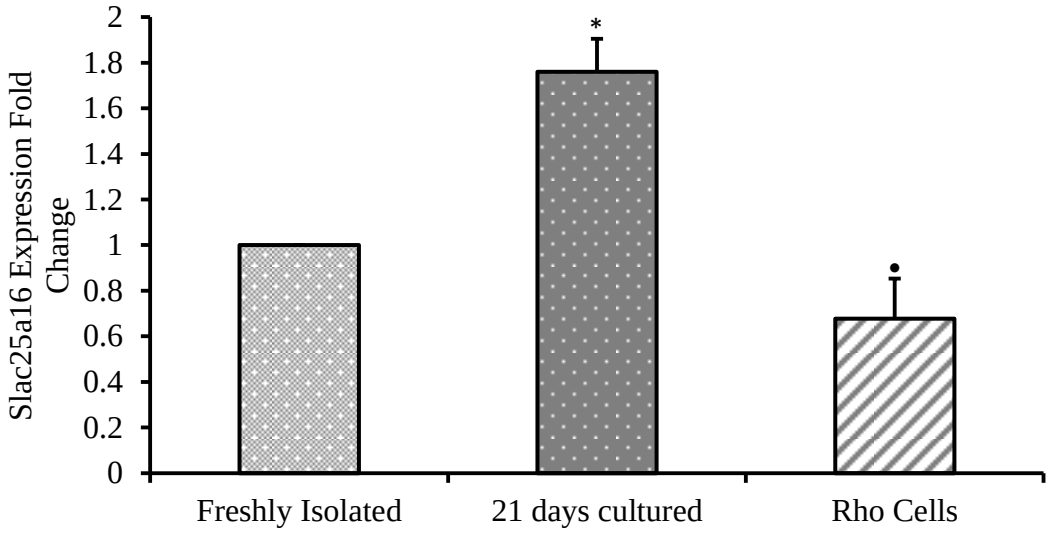

Figure 3.42 *Shows the expression of mitochondrial transport gene in freshly isolated cells, 21 days cultured cells and Rho cells (n=3), *p <0.05 21 days cultured cells vs freshly isolated cells, ●p <0.05 Rho cells vs 21 days cultured cells.*

We also found that the expression of both SOD1 and SOD2 were increased in Rho cells in comparison to 21 days cultured cells. The expression of SOD1 was decreased by 80 ± 7% in the 21 days cultured VSM cells compared to the freshly isolated VSM cells and increased by 40 ± 1% in the Rho cells compared to the 21 days cultured VSM cells (Figure 3.43).

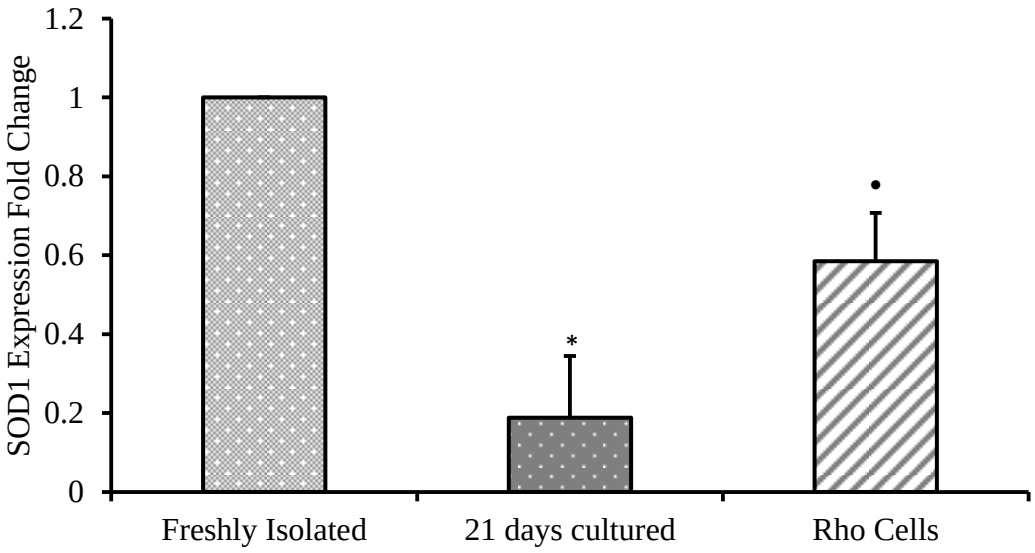

Figure 3.43 *Shows the expression of ROS scavenging gene SOD1 in freshly isolated cells, 21 days cultured cells and Rho cells (n=3), *p <0.05 21 days cultured cells vs freshly isolated cells, ●p <0.05 Rho cells vs 21 days cultured cells.*

The expression of SOD2 was decreased by 90 ± 7% in the 21 days cultured VSM cells compared to the freshly isolated VSM cells and increased by 40 ± 0.01% in the Rho cells compared to the 21 days cultured VSM cells (Figure 3.44).

Figure 3.44 *Shows the expression of ROS scavenging gene SOD2 in freshly isolated cells, 21 days cultured cells and Rho cells (n=3), *p <0.05 21 days cultured cells vs freshly isolated cells, ●p <0.05 Rho cells vs 21 days cultured cells.*

3.28 Discussion

3.29 Effect of MDivi-1 on the balloon injured artery:

Restenosis following stent insertion is a major challenge limiting the use of bare-metal stents. On the other hand, drug-eluting stents containing mTOR inhibitors including Rapamycin have undesirable effects on proliferative as well as normal healthy cells which also limit its use in coronary angioplasty. In this experiment, we investigated the effect of balloon injury on the blood vessel structure. Results showed that culturing the blood vessel in media containing 10% FCS for 21 days resulted in an increase in the blood vessel wall compared to the thickness of a normal freshly fixed blood vessel (Figure 3.1). When the blood vessel was injured using a balloon catheter, the increase in the thickness was seen to be bigger and the wall: lumen ratio was significantly higher than the normal blood vessel or blood vessel which was cultured in serum-containing media alone (Figure 3.2). This suggests that the balloon injury resulted in a damage to the endothelial cell layer which resulted in an exposure of the medial layer containing smooth muscle cells to growth factors in the media. The de-endothelialisation is followed by a loss of endothelial layer to release antithrombotic factors including nitric oxide, prostacyclin and tissue plasminogen activator (Farb et al., 2002). This contributes to platelet adhesion and aggregation which release mitogens like platelet derived factors and thromboxane A_2 (Pakala et al., 1997). This results in a shift in VSMCs phenotype from contractile to synthetic and an initiation of VSMCs proliferation and migration which led to the increase in the wall thickness we have reported (Miano et al., 1993). The increase in the wall thickness (Figure 3.3) and wall: lumen ratio leads to a decrease in the lumen diameter of the blood vessel which we saw in both cultured blood vessel and cultured and injured blood vessel (Figure 3.4). This leads to a reduction in blood flow and ischaemic disorders.

Measuring the effect of inhibiting identified mitogenic or mitochondrial signalling pathways in balloon injury artery model resulted in a reduction in the wall thickness and the wall: lumen ratio. The most remarkable resolution of injury-dependent vascular wall remodelling was attributable to use of the mTOR inhibitor rapamycin,

mitochondrial fission inhibitor MDivi-1, the PI3K inhibitor wortmanin and ethidium bromide used to inhibit mitochondrial genome.

The addition of MDivi-1 had a similar effect in reducing blood vessel wall thickness and improving lumen diameter as rapamycin and wortmanin. However, because both rapamycin and wortmanin have serious side effects on healthy cells, it will be of a great interest to study the toxic effect of MDivi-1 on the un-proliferative healthy cells.

3.30 VSM cell characterisation:

Vascular smooth muscle cells are characterised by their morphology which is described as the "Hill and Valley" as well as some specific markers which are highly expressed in the contractile phenotype such as α- smooth muscle actin and heavy chain myosin which was clearly seen in the cells explanted from rat aorta (Figure 3.5). Change in the phenotype following stimulation of VSM cells causes a decrease in these markers.

3.31 Effect of inhibiting mitochondrial fission on the morphology and localisation of mitochondria:

Mitochondria have been thought for long to be static organelles acting as a power house to the cell by producing ATP. However, other roles have been recently widely recognised are proliferation and apoptosis. The localisation of the mitochondria in the cytoplasm differs depending on the status of the cell (Eapen et al., 1998). They are normally localised in certain areas of the cytoplasm, however, their locations change based on the cellular stimulation followed by cellular growth and proliferation (Weakley, 1976). The higher density of mitochondria shown in the image obtained from stimulated vascular smooth muscle cells (Figure 3.7) when compared to the quiesced cells (Figure 3.6). This perhaps suggests that the number of mitochondria increase upon stimulation to meet the demand for higher cellular energy needed to complete cell cycle and cellular growth (Naokatu arakaki et al., 2006) (Arakaki et al 2006). This increase in the number of mitochondria is accompanied by a change in their location. Not surprisingly mitochondria are

observed to translocate from the cytoplasm to the nucleus. This suggests that mitochondrial number and location within the cell is an important determinant of cellular functions and growth. Treatment with MDivi-1 which is a selective inhibitor of the mitochondrial division dynamin (DRP1) prevented mitochondrial fragmentation and resulted in the formation of mitochondrial network as seen in (Figure 3.8). This could be due to low cellular turn over caused by an increase in the apoptotic pathway or a reduction in the cellular growth leading to lower rate of proliferation. The mitochondria play a major role in both apoptosis and proliferation and any imbalance could finally lead to the uncontrolled proliferation. Mitochondria control these cellular functions by undergoing dynamical changes of fission and fusion which are regulated by proteins including DRP1, MFN1 and MFN2. DRP1 is thought to enhance mitochondrial fragmentation which results in apoptosis whereas MFN1 and MFN2 are thought to enhance network formation and cell survival. It was clear that 10 μm of MDivi-1 maintained long filamentous mitochondrial network around the nucleus (Figure 3.8).

3.32 Effect of mitochondrial fission inhibition on VSM cell proliferation:

The ^{3}H thymidine incorporation assay shows that the cultured VSM cells have a proliferative capacity when compared with quiesced VSM cells in 0.1% FCS. Upon stimulation with 10% FCS, the cells enter the cell cycle and start proliferating (Rzucidlo et al., 2007). This, however, was reduced when MDivi-1 was incubated for 24 hours. As the concentration of MDivi-1 was increased, the proliferation was shown to be decreased in a concentration dependent manner. This suggests that mitochondrial movement and fission process are important for the cells to proliferate. And following the inhibition of DRP-1, mitochondrial movement was restricted by inhibiting fission process and forming a fused mitochondrial network which resulted in the reduction in proliferation (Chalmers et al., 2012).

The inhibition in vascular smooth muscle cells proliferation was greater following stimulation with platelet derived factor (PDGF) compared to the inhibition seen when the cells were stimulated using 10% FCS which could suggest that mitochondria stimulate vascular smooth muscle cells through specific pathways including PDGF but not the others. This greater inhibition following PDGF

stimulation goes in line with the reduction in Akt and 4EBP1 phosphorylation which are mTOR upstream and downstream substrates suggesting that inhibiting mitochondria results in inhibiting vascular smooth muscle cell proliferation through PI3k/ Akt/ mTOR signalling pathway. PDGF was previously reported to initiate VSM cell proliferation and migration through the activation of PI3K/Akt/mTOR signalling pathway (Goncharova et al., 2002). However, our results suggest that mitochondria mediate this activity and inhibiting mitochondria results in PI3K/ Akt/ mTOR inhibition.

3.33 Migratory capacity of VSM cells following mitochondrial fission inhibition:

The migratory feature seen in VSM cells following their stimulation with 10% FCS and PDGF indicates that these cells have undergone phenotypic switch from being contractile to being synthetic. This switch is accompanied with a release of growth factors, cytokines and extracellular matrix components which activate some signalling pathways and promote cell's migration (Carrillo-Sepulveda and Barreto-Chaves., 2010). Some of the signalling pathways that have already been identified include Mitogen Activated Protein Kinase (MAPK) (Yamboliev and Gerthoffer, 2001), Rho-activated protein kinase, P21-activated protein kinases (Dechert et al., 2001), calcium- dependent protein kinase and phosphatidyl-inositol 3-kinases (PI3K) (Yamboliev et al., 2001). Both stimuli used help promote VSM cell migration through the activation of different signalling cascades. Blocking mitochondrial division using MDivi-1 and the resulting effect seen in restricting VSM cell migration further supports that the mitochondria play an essential role in mediating these signalling cascades. It also supports the involvement of PI3K/ Akt/ mTOR signalling pathway through which mitochondria signal activates the migration process. The reduction in PI3K/ Akt/ mTOR signalling seen following mitochondrial inhibition could contribute to the inhibition of VSM cell migration. Previous study has reported that PDGF-induced VSM cell proliferation and migration was seen to be mediated by PI3K/ Akt/ mTOR signalling pathway (Goncharova et al., 2002). Our results take this further by showing that mitochondria mediate VSM cell migration following stimulation through PI3K/ Akt/ mTOR signalling pathway.

3.34 Proteins expression and phosphorylation following mitochondrial fission inhibition:

The MAP Kinases (ERK1/2, P38 and JNK) are considered common signalling cascades in VSM cell proliferation (Sprague and Khalil, 2009). Interestingly, blotting for ERK1/2 phosphorylation showed no significant differences when the mitochondrial fission process was inhibited. This suggests that mitochondria signal independent of ERK1/2 and that any role mitochondria might have in inducing proliferation is signalled through another pathway.

Inhibiting mitochondrial DRP1 using MDivi-1 reduced the expression of cell cycle protein Cyclin D. This reduction suggests cell cycle arrest at G1 phase of the cell cycle. This could result in reduction in cell growth and proliferation as it is one of the important mitogenic sensors that responds to different growth factors and results in cell cycle progression (Tchakarska et al., 2011). It also attaches to transcription factors and chromatin remodelling proteins which control cell proliferation and migration (Li et al., 2006). The reduction in the expression of cyclin D correlates with the reduction in proliferation and migration we see in later sections. This suggests that the inhibition of VSM cell proliferation we see when we inhibit mitochondrial fission could be in part due to the cell cycle arrest.

Phosphorylated Akt was reduced as a result of inhibiting mitochondrial activity (Sun Young Ahn et al., 2010). This leads to the inactivation of downstream mTOR effector proteins such as 4EBP1 resulting in inhibition of mRNA translation and protein synthesis. This signalling cascade is mediated by phosphoinositide-3-OH kinase (PI3K) which indirectly activates mTOR signalling pathway (Mendez et al., 1996). Full activation of Akt requires the phosphorylation of both 3-phosphoinositide-dependent kinase-1 (PDK1) and PI3K-dependent kinase (Gingras et al., 1998). This activation is responsible for the control of many cellular functions including proliferation and migration. The activation of this signalling pathway is also implicated in the activation of other signalling cascades involved in VSM cell proliferation and migration such as ERK1/2 and P38. Therefore, the inhibition of Akt phosphorylation may result in partial inhibition of PI3K, mTOR, ERK1/2 and P38. However, because ERK1/2 involvement was rolled out based on initial results

obtained from western blot, PI3K and mTOR may still be a potential pathway inhibited as a result of inhibiting mitochondrial fission.

Cytochrome c is released from mitochondria to induce apoptosis in response to cellular proliferation and differentiation (Orrenius, 2004). The inhibition of mitochondrial fission resulted in reduction of cytochrome c level in the cell. This suggests that fission process regulated by DRP-1 is important for the release of cytochrome c (Youle and Karbowski, 2005). Cytochrome c release was also inhibited following the expression of the negative mutant DRP-1 which also inhibited mitochondrial fragmentation (Frank et al., 2001). Although the release of cytochrome c is blocked when the DRP-1 is inhibited, release of other pro apoptotic factors is unaffected such as Smac/DIABLO and the apoptosis process is not inhibited (Estaquier and Arnoult, 2007). This could explain the reduction in proliferation seen despite the decrease in the level of cytochrome release seen following treatment with MDivi-1.

3.35 Cell cycle analysis:

The increase in the percentage of cells in G2 phase of the cell cycle seen with the increase concentrations of MDivi-1 suggest that this drug causes cell cycle arrest at G2/M phase. This was also seen when MDivi-1 was used to inhibit DRP-1 protein in cells cultured from pulmonary arterial hypertensive subjects (Marsboom et al., 2012). DRP-1 is phosphorylated by Cyclin B1 and cyclin-dependent kinase-1 (CDK1) which regulate the G2 phase of the cell cycle resulting in its activation (Chang and Blackstone, 2007). Once activated, DRP-1 moves from the cytosol to the mitochondria where it exerts its effect by dividing the mitochondria. One action of MDivi-1 is to lock the mitochondria in a fusion status and stop cell cycle progression from G2 to mitosis. The net result being a reduction/ inhibition of VSM cells proliferation (Rehman et al., 2012). This observation of cell cycle highlights that the fission of mitochondria is an important determinant of cell cycle progression and cellular growth and proliferation. Inhibiting mitochondrial fission resulted in a cell cycle arrest which leads to inhibition of VSM cell proliferation.

3.36 The effect of inhibiting mitochondrial fission on VSM cell apoptosis:

The activation of the intrinsic apoptotic signalling pathway was studied by measuring the level of caspase 3/7 release in VSM cells. Results show that caspase 3/7 did not change significantly in 10% FCS and 20 ng PDGF stimulated cells. However, following mitochondrial fission inhibition using 10 μM of MDivi-1, the level of caspase 3/7 increased significantly similar to the level seen in paclitaxel treated cells. Mitochondrial division regulated by DRP1 is an essential cellular process that maintains normal cellular function (Parone et al., 2008) and the increase in the level of caspase 3/7 activity is linked with the increase in Mfn2 expression level in the cell as a result of the inhibition of DRP1. The pro-apoptotic effect of DRP1 inhibition seen here is mediated by the inhibition of the Akt signalling which results in the activation of the mitochondrial apoptotic pathway and increased mitochondrial Bax/Bcl-2 ratio (Xiaomei Guo et al., 2007). This then leads to the activation of apoptosis through the release of cytochrome c or the activation of other pro-apoptotic proteins including Smac/DIABLO which then results in reduction in cell number and inhibition in proliferation.

3.37 VSM cell ROS generation and ATP activity:

Both ROS cellular level and ATP production were measured to assess mitochondrial activity under different treatment conditions. Level of H_2O_2 was significantly increased following stimulation with both 10% FCS and 20 ng PDGF (Figure 3.12 A&B). The increase is due to the increase in the mitochondrial bioactivity required to produce cellular energy which we see in the corresponding ATP levels (Figure 3.14). When the mitochondrial fission was inhibited using MDivi-1, H_2O_2 and ATP levels were significantly reduced. This finding confirms that the increase in ROS level which correlates to the increase in VSM cell proliferation following stimulation is due to the increase in cellular energy demand which leads to an increase in ROS in the electron transport chain (Yoshida et al., 2005). These results suggest that mitochondrial fission is an important process during VSM cell proliferation and migration required to produce ATP. Results also suggest that ROS is also important in driving VSM cell proliferation further and that inhibiting mitochondrial fission limited both ATP and ROS level within the cell (Lee et al., 2007).

3.38 Mitochondrial gene profiling of wild type VSM cells vs. Rho cells:

To further evaluate signalling pathways involved in the mitochondrial-dependent VSM cell proliferation, qRT-PCR was performed. Mitochondrial function was compromised using a non-pharmacological approach. Loss of mitochondrial activity was confirmed by measuring gene expression of Tfam and cytochrome c oxidase. Tfam is mitochondrial transcription factor A which is required for VSM cell proliferation during the progression of atherosclerosis (Yoshida et al., 2005). The level of Tfam was seen to increase in VSM cells of balloon-injured rat carotid artery model in response to an increased energy demand in proliferating VSM cells. Cytochrome c oxidase is another mitochondrial gene involved in mitochondrial oxidative phosphorylation to produce ATP required for cellular functions (Aurelio et al., 2001). Our results showed a reduction in the expression of both genes. Mitochondrial gene expression proteins showed that there is an increase in the pro-apoptotic gene expression in the Rho cells in comparison to the 21 days cultured hyper-proliferative cells. These genes include BBC3, Bnip3, cdkn2a, Pmaip1 and P53. These proteins have been previously seen to inhibit cellular proliferation

through the inhibition of mTOR and the activation of autophagy (Spencer, 2010). Similarly, P53 responds to the DNA damage caused by increased level of ROS and initiates autophagy to maintain cellular health (Mazure and Pouysségur, 2010). This was reflected in the increase of P53 following the depletion of mitochondrial DNA in Rho cells which could have initiated cellular apoptotic or autophagic signalling pathway resulting in the inhibition in VSM cell proliferation we reported earlier in this chapter. Results also showed that there is a decrease in the mitochondrial transporter genes in the Rho cells compared to 21 days cultured cells. These genes include Hsp90aa1, Hspd1 and Mtx2. Hsp90 is highly expressed in mitochondria of tumour cells to regulate the permeability transition pores. The shutting down of these pores stops essential apoptotic proteins from moving outside the mitochondria therefore inhibiting mitochondrial apoptotic signalling pathway (Kang et al., 2011). The reduction of the mitochondrial transporter genes in Rho cells suggest that permeability transition pores are open and there is a possible movement of pro-apoptotic proteins from the mitochondria to the cytosol which inhibits VSM cell proliferation. The expression of proteins regulating the transport of small molecules between the cytosol and the mitochondria including sh3glb1 and slc25a16 were also different. In Rho cells there is a decrease in their expression compared to the hyper-proliferative cells. Sh3glb1 is a protein that localises between the cytosol and the mitochondrial protein depending on the cell's status. It is required for mitochondrial fission following VSM cell growth stimulation (Karbowski et al., 2004). Its subcellular distribution is an essential determinant of whether the cells undergo autophagy or apoptosis (Takahashi et al., 2007, Takahashi et al., 2005). It is therefore important in mitochondrial fission regulation during autophagy through DRP1 modulation (Twig et al., 2008). This resulted in the inhibition of VSM cell proliferation which we reported earlier. Furthermore, the expression of ROS scavenging proteins including SOD1 and SOD2 is increased in Rho cells in comparison to the 21 days cultured cells. This ties in with our previous finding that level of ROS was significantly reduced when the mitochondria was inhibited using MDivi-1. This also goes in line with other clinical findings where SOD2 expression was seen to be reduced in Pulmonary artery hypertension disease (Archer et al., 2010). It was also found to be a major element in other diseases including cancer

(Hitchler et al., 2008). The increase in SOD1 and SOD2 levels contributes to ROS scavenging therefore limits the proliferative effect of ROS on VSM cells.

These results suggest that inhibiting mitochondrial bioactivity results in cell cycle arrest and initiation of apoptosis which was seen in the increase in pro-apoptotic gene expression and the reduction in the cell cycle regulatory protein (Figure 3.45). The reduction in proliferation could also partly be due to the decrease in ROS and ATP production which play a major role in VSM cell proliferation and migration. These events were driven by PI3K/ Akt/ mTOR signalling pathway which was downregulated following mitochondrial inhibition.

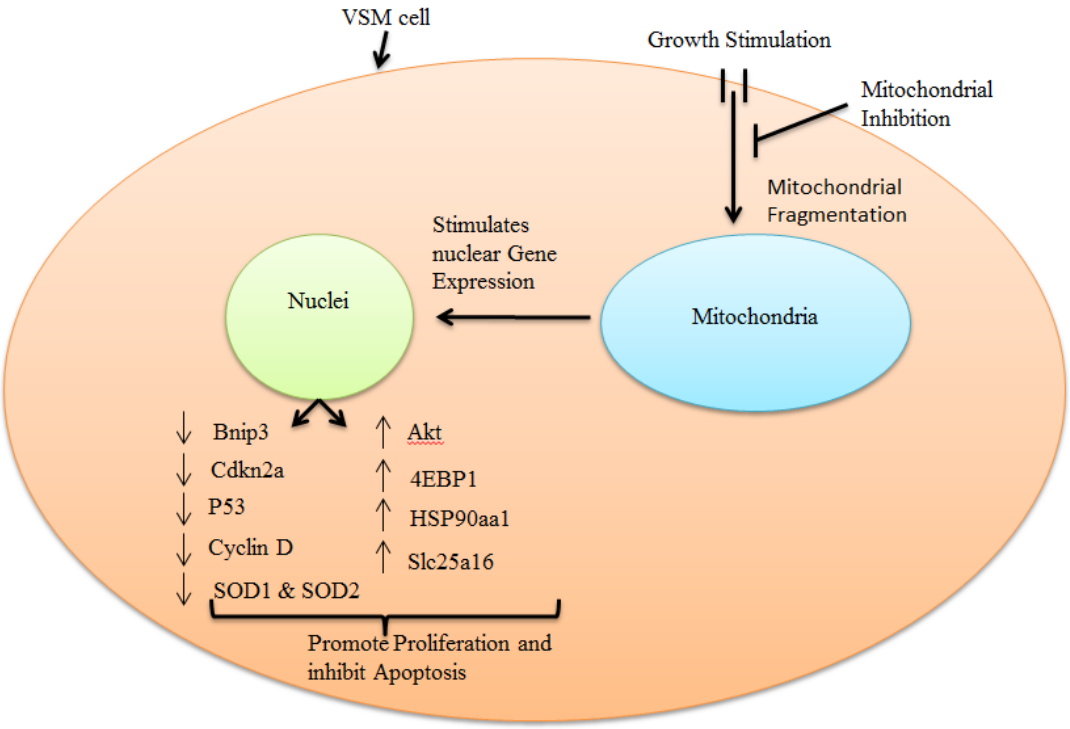

Figure 3.45 *Shows a summary of the main findings of this chapter. Inhibiting mitochondrial dynamics and bioenergetics results in a reduction in the proliferation inducing genes including Akt, 4EBP1, HSP90aa1 and Slc25a16. It also results in an increase in the pro-apoptotic, cell cycle inhibitory genes and ROS scavenging genes including Bnip3, Cdkn2a, P53, Cyclin D, SOD1 and SOD2.*

Summary of the primary experimental findings reported in this chapter:

- Inhibiting mitochondrial dynamics and bioactivity reduces neo-intimal formation in an ex-vivo setting.
- Inhibiting mitochondrial dynamics reduces VSM cell proliferation and migration in an in-vitro setting.
- Inhibiting mitochondrial dynamics induces cell cycle arrest at G2/M phase.
- Mitochondrial inhibition results in down-regulation of PI3K/ Akt/ mTOR-dependent signalling pathway.
- Inhibiting mitochondrial bioactivity results in a down-regulation of mitochondrial transportation genes and increase in the expression of pro-apoptotic genes, cell cycle inhibitory genes and ROS scavenging genes.

Chapter 4

Role of vascular smooth muscle cell mitochondrial-dependent regulation of miRNA associated with cell proliferation and migration

4.1 Introduction

Micro RNAs (miRNA) are small non coding RNAs that have been found to contribute in different cellular processes such as embryonic development, cell differentiation, proliferation and apoptosis. They were first discovered in 1993 when *Lin-4* was the first miRNA to be characterised (Lee et al., 1993). Despite this, miRNAs were only relatively recently recognised as active gene regulators (Bartel, 2004). miRNAs are approximately 20 nucleotides long and regulate gene expression post transcriptionally by binding to the 3´untranslated regions (UTR) or the 5´ untranslated region (UTR) of the messenger RNA leading to inhibition of translation or degradation of the target messenger RNA (Filipowicz et al., 2008). miRNA have also been shown to activate translation of targeted mRNA (Vasudevan et al., 2007).

miRNA synthesis starts with the primary miRNA (pri-miRNA) which is transcribed by RNA polymerase II. Pri-miRNA is then cleaved in the nucleus by the nuclear RNAse III-type protein Drosha and the cofactor the DiGeorge syndrome critical region gene 8 (DGCR8) to release a small hairpin structure called precursor miRNA (pre-miRNA) (Lee et al., 2002). Pre-miRNA is then transported from the nucleus to the cytoplasm by the exportin-5/RAN-GTP complex. This results in activation of Dicer which is another type-III RNAse and consequent cleavage of the pre-miRNA into a small double stranded RNA which has the mature miRNA in one strand and the complementary sequence on the strand (Lund et al., 2004). miRNA duplex is then assembled into the RNA induced silencing complex (RISC) which separates the two miRNA strands (Figure 4.1) then selects and recruits one strand whereas the other strand is excluded and degraded. RISC complex with miRNAs then initiates translational inhibition or mRNA degradation (Kim et al., 2009).

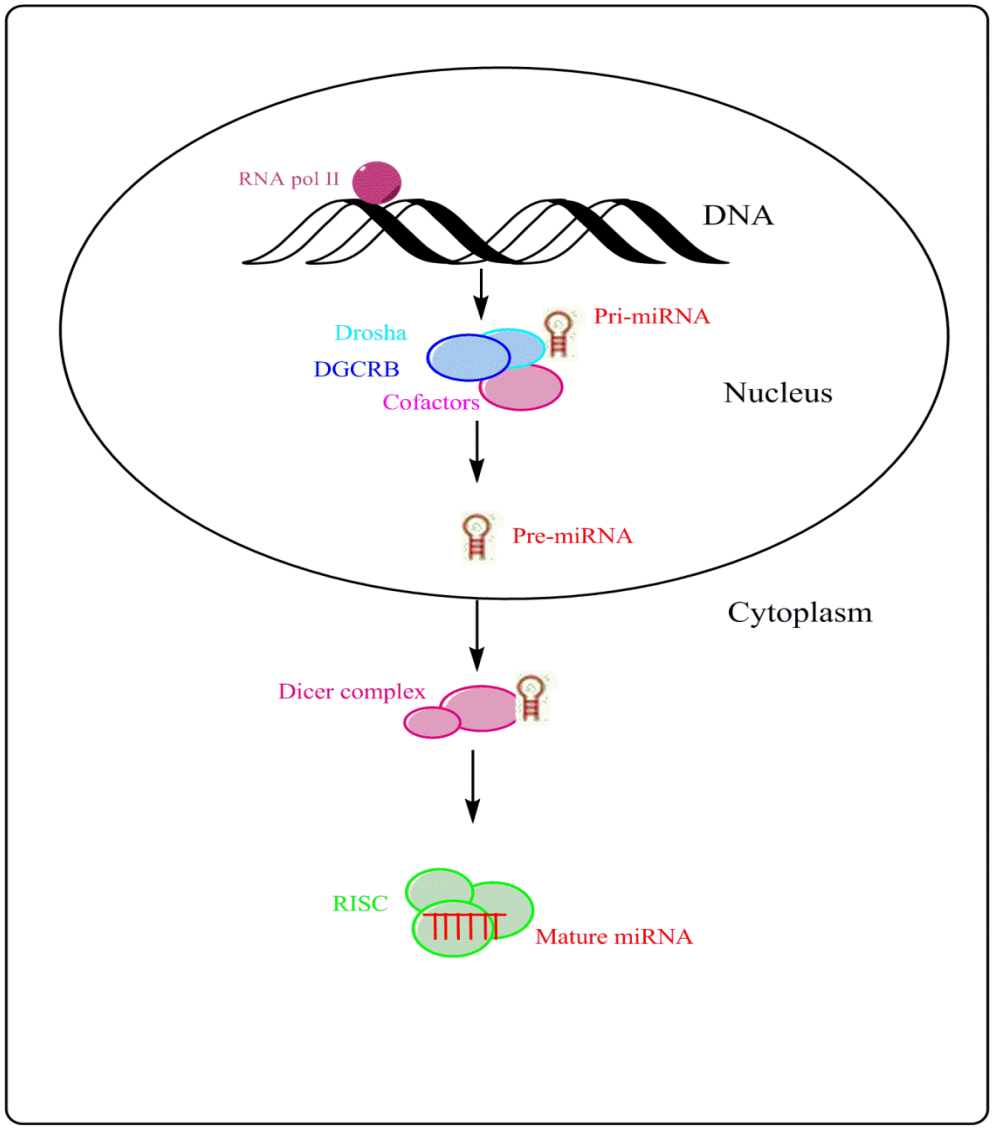

Figure 4.1: *Schematic showing miRNA biogenesis. Diagram shows the synthesis of miRNA inside the nuclei to form the primary miRNA and the precursor miRNA which is then transported to the cytoplasm to form the mature miRNA.*

The produced miRNAs bind their targets between their second and eighth nucleotides of their 5´extremity. The binding also occurs between the ninth and the twentieth nucleotides but their complementarity is not as important (Lewis et al., 2005). This imperfect complementarity allows one single miRNA to regulate the expression of different messenger RNAs and control different biological functions (Baek et al., 2008). miRNAs can be considered as biomarkers for a wide range of

diseases being found in urine, saliva, circulating blood and other biological fluids (Weber et al., 2010). miRNAs have also been found to act as hormones since they not only regulate gene expression in the mother cell where they are expressed, but circulating miRNAs can regulate gene expression in other cells distant from the mother cell (Hu et al., 2012).

4.2 Role of miRNAs in vascular diseases:

Many growth factors have been shown to regulate vascular development and angiogenesis including vascular endothelial growth factor and platelet derived growth factor (Hoch and Soriano, 2003). However, the upstream regulation of gene expression and translation is not fully understood. Endothelial cell functions and angiogenesis have been demonstrated to be regulated by miRNAs such as Let7-f, miR-27b and miR-130a (Kuehbacher et al., 2007). On the other hand, miRNAs have been seen to inhibit endothelial cell migration, proliferation and angiogenesis by miR-221 and miR-222. These miRNAs were seen to target stem cell factor receptor c-kit and endothelial nitric oxide synthase (Suarez et al., 2007). Other miRNAs including miR-21 were found to increase VSM cell proliferation through targeting pro-apoptotic proteins such as PTEN (Ji et al., 2007a). miR-21 was also found at significantly elevated levels in neo-intimal lesions suggesting an important role in the development of re-stenosis (Bonci, 2010). MiR-126 was also found to inhibit the expression of vascular cell adhesion molecule 1 (VCAM-1) resulting in decreased leukocyte adherence to endothelial cells (Harris et al., 2008). Moreover, miR-145 was seen to reduce atherosclerotic plaque rupture and to limit atherosclerotic plaque morphology and cellular composition (Lovren et al., 2012). MiR-145 was also found to target genes that are involved in the dedifferentiation and proliferation of VSM cell including KLF-4 and ELK-1 (Elia et al., 2009). Deng et al (2015) also found that miR-143 modulated cellular proliferative response in pulmonary vascular cells (Deng et al., 2015).

4. 3 Mitochondria as a potential destination of miRNAs:

Although mitochondria contain around 1500 different proteins, only 13 of those are encoded by the mitochondrial genome and are involved in the regulation of the

mitochondrial electron transport chain (Lopez et al., 2000). Other proteins are encoded by nuclear genome in the nucleus and translocated into mitochondria or nuclear RNA is trafficked into mitochondria and translated into proteins. Proteins trafficking into mitochondria are mediated by TOM/TIM complexes through well-studied signalling pathways such as carrier protein transport pathway, redox-regulated import pathway and oxidative folding pathway (Becker et al., 2012). Some miRNAs have repeatedly been reported to be enriched in the mitochondria such as let-7 family which regulate cell cycle, proliferation and apoptosis by targeting c-Myc, ras, STAT3 and P53 (Sripada et al., 2012). The let-7 family includes hsa-miR-107, hsa-miR-145, hsa-miR-134, hsa-miR-503 and hsa-miR-21 (Barrey et al., 2011).

4.4 Transporting miRNAs:

Emerging evidence has recently shown that RNA is transported between the cytosol and mitochondria by ATP or voltage dependent anion channels located in the mitochondrial outer membrane (Rubio et al., 2008). Polynucleotide phosphorylase (PNPASE) which is an inter membrane space protein is also important for transport of miRNA (Wang et al., 2012a). Furthermore, proteins involved in miRNA biogenesis such as Ago2 were found to play a key role in the transportation of tRNA Met to mitochondria (Maniataki and Mourelatos, 2005).

A number of studies have shown that a small number of nuclear encoded miRNAs target mitochondrial proteins and the majority target nuclear encoded mRNAs (Barrey et al., 2011). The same was also seen with the mitochondrial encoded miRNAs which prefer to target nuclear genes more than mitochondrial genes (Kren et al., 2009). miRNAs are transported from one cell to another via exosomes (Hu et al., 2012). Exosomal transportation prevents the miRNAs from undergoing degradation when moving from one cell to another (Hu et al., 2012). These exosomal miRNAs play a vital role in the recipient cell by preventing mRNA translation of the target genes therefore causing a change in the cellular functions of the target cell. However, it is not fully understood how these miRNAs are sorted into the exosomes. Four potential different mechanisms have been suggested for sorting miRNAs into the exosomes. The first is the neural sphingomyelinase2-dependent pathway (nSMase2; (Kosaka et al., 2013). The second is the miRNA motif and sumoylated

heterogeneous nuclear ribonucleoproteins-dependent pathway (hnRNPs: (Villarroya-Beltri et al., 2013). Thirdly, the 3`-end of the miRNA sequence-dependent pathway (Koppers-Lalic et al., 2014). The fourth mechanism is the miRNA induced silencing complex-dependent pathway (miRISC; (Frank et al., 2010).

4.5 Chapter Aims:

The aims of this chapter are:

- To measure the expression levels of miR-21 and miR-145 in VSM cells following stimulation and mitochondrial inhibition.
- To study the effect of miR-21 and miR-145 on mitochondrial network formation.
- To study the role of miR-21 and miR-145 in VSM cell proliferation and migration.
- To investigate and evaluate mRNA potential targets for miR-21 and miR-145.

4.6 Specific Methods:

4.7 miRNA isolation from cultured VSM cell*:*

MiRNAs from VSMCs were isolated using miRNeasy mini kit (Qiagen, USA). VSMCs in the 6 well plates were washed with sterile PBS. 700 µl of lysis reagent Qiazol was added into each well and left for 5 minutes at room temperature. It was then gently scraped and the content was removed into Eppendorf tubes. 140 µl of chloroform was added into each Eppendorf and homogenised vigorously using vortex for 15 seconds. Samples were then left for 5 minutes at room temperature to separate the three layers. Samples were then centrifuged at 12000 RPM for 30 minutes at 4^{o}C. The top clear layer only was collected into a new 1.5 ml tube and added to 1.5 volume of 100% ethanol. The mixture was re-suspended using pipette then transferred to labelled columns. Samples in the columns were then spun at 12000 RPM for 30 seconds at room temperature and the flow through liquid was discarded. 350 µl of RWT buffer was added into each column to wash the DNA and spun at 12000 RPM for 1 minute at room temperature (Qiagen, USA). The liquid in collection tube was discarded and 80 µl of DNAse I was added to each column to get rid of the DNA and incubated at room temperature for 15 minutes. Another 350 µl of RWT buffer was added to each column and spun at 12000 RPM for 1 minute at room temperature. 500 µl of RPE buffer was added into each column and spun at 12000 RPM for 1 minute at room temperature. The liquid in the collection tube was discarded and another 500 µl of RPE buffer was added to each column and spun at 12000 RPM for 2 minutes at room temperature. The used collection tube was exchanged for a new one and re-spun at 12000 RPM for 1 minute at room temperature. The column was transferred into an Eppendorf tube and 40 µl of RNase free water was added into each column. Columns were spun twice at 12000 RPM for 30 seconds at room temperature. RNA yield was measured by absorbance at 260 nm using Nano Drop spectrophotometer.

4.8 miRNA reverse transcription preparation*:*

To quantify the miRNA transcripts of target genes, miRNA yield was reverse transcribed using miRNA reverse transcription kit (Applied Biosystem, Paisley, UK) following the manufacturer's manual. miRNA concentrations were normalised to 5 ng in all samples. For each reaction, 0.075 µl of dNTPs was added followed by 0.5 µl of multiscribe and 0.75 µl of the 10 x RT buffer and 10 reactions were prepared at each time to avoid pipetting errors associated with measuring very small volumes. 0.095 µl of RNA inhibitor was also added with 2.08 µl of RNase-free water and 1.5 µl of the 5 x RT primer. This was followed by adding 2.5 µl of the RNA stock diluted to 2 ng/µl to make up a total reaction volume of 7.5 µl. The reaction was then run in a thermal cycler at 16^{o}C for 30 minutes, 42^{o}C for 30 minutes and the reaction was terminated by heating to 85^{o}C for 5 minutes. The resulting RT product was then used for quantitative real-time PCR to measure miRNA expression under different treatment conditions.

4.9 Quantitative real time polymerase chain reaction amplification of miR-21 and miR-145*:*

The qRT-PCR assay was performed by placing the samples in 96 well plates (Applied Biosystems, Paisly, UK). The PCR reaction was carried out in a volume of 10µl containing 8.5 µl of PCR master mix and 1.5 µl of each template cDNA sample. The PCR master mix contained 5 µl of (2x) Taqman master mix (Applied Biosystem, Paisly, UK), 0.5 µl of the miRNA probe, 3 µl RNase free water and 1.5 µl of the RT product to make a total reaction volume of 10 µl. Two technical and three biological replicates were conducted for each assay. The thermal cycling and detection was performed on an applied Biosystems StepOne Plus real-time PCR system (Table 4.1).

Hold stage	Cycling stage (40 cycles)	Final extension stage
DNA polymerase activation 10 minutes at 95C^{o}	Melt Step 15 seconds at 95C^{o}	Cooling down at 4C^{o} to stop PCR reaction
	Anneal/Extend step 1 minute at 60C^{o}	

Table 4.1 *shows the thermal cycle conditions used to run QRTPCR for miRNA*

4.10 miR-21 and miR-145 transfection*:*

VSMCs were cultured in 6 well plate until they were ~60% confluent. Cells were then transfected using 30 nM of mirVana miRNA inhibitors and mirVana miRNA mimics for both miR-21 and miR-145 (Life Technologies, Paisley, UK). Cells were washed with sterile PBS to remove any media containing antibiotics and 1.8 ml of Optimem media was added into each well. Two solutions were prepared in two different tubes and added at the end. Solution A contains 90 pmol of the mirVana in 100 µl Optimem media and solution B contains 6 µl in 100 µl of Optimem media. The two solutions were added together and incubated at room temperature for 5 minutes. The final 200 µl of the mixture was added into the well to make it up to total volume of 2 ml. Cells were incubated in Optimem for 24 hours after which cells were put back in normal media for another 48 hours. Cells were then lysed and RNA was isolated for further PCR analysis.

4.11 Proliferation assay following miRNA transfection:

VSMCs were cultured in 24 well plates until they were 60% confluent. Cells were then transfected with miR-21 inhibitor, miR-21 mimic, miR-145 inhibitor and miR-145 mimic for 72 hours. Cells were then quiesced using 0.1% FCS for 24 hours followed by a stimulation using 20ng/ml PDGF for 24 hours. 3H labelled thymidine was added 18 hours through the stimulation. At 24 hour, cells were washed with an ice cold PBS once for 10 minutes followed by 4 washes with 10% ice cold TCA 10 minutes each. Cells were then lysed using 250µl of 0.2% SDS and the lysate is added into scintillation vials containing 2ml of scintillation emulsifier. Measurement of

disintegration per minute of each sample was taken using protocol 2 in the scintillation analyser machine.

4.12 Migration assay following miRNA transfection:

VSMCs were cultured in 6 well plate until they are 90% confluent. Cells were then transfected with miR-21 inhibitor, miR-21 mimic, miR-145 inhibitor and miR-145 mimic for 72 hours. Cells were then quiesced using 0.1% FCS for 24 hours. A scratch was made using 200µl tip and cells were then stimulated using 20ng PDGF. Pictures of the scratch were taken at 0hour, 6 hour, 12 hour and 24 hour. Area of the scratch was measured using ImageJ software.

4.13 mTOR siRNA silencing:

VSMCs were cultured in 6 well plate until they were 60% confluent. Cells were then transfected using 40 nM of mTOR siRNA for 72 hours (Life Technologies, Paisly, UK). Cells were washed with sterile PBS to remove any media containing antibiotics and 1.8 ml of Optimem media was added into each well. Two solutions were prepared in two different tubes and added at the end. Solution A contains 75 pmol of the siRNA in 100 µl Optimem media and solution B contains 6 µl in 100 µl of Optimem media. The two solutions were added together and incubated at room temperature for 5 minutes. The final 200 µl of the mixture was added into the well to make it up to total volume of 2 ml. Cells were incubated in Optimem for 24 hours, thereafter replaced with basal media for 48 hours. Cells were then lysed and RNA was isolated for further PCR analysis of the genes in (Table 4.2).

Gene	Forward Sequence
PI3K	5′-CGCCCCCTTAATCTCTTACA-3′
Akt	5′-CTTCGTGAACATTAACGACAGGGCC-3′
mTOR	5′-TTGAGGTTGCTATGACCAGAGAGAA-3′
4EBP1	5′-TAGCCCTACCAGCGATGAGCCT-3′
P70s6k	5′-GGAGCCTGGGAGCCCTGATGTA-3′
Cdkn2a	5' - GGCACCAGAGGCAGTAACCAT- 3'
P53	5'-AACGGTACTCCGCCACC-3'
Gene	**Reverse Sequence**
PI3K	5′-TGGATGTTCTCCTAACCATCTG-3′
Akt	5′-AATGGCCACCCTGACTAAGGAGTGG-3′
mTOR	5′-TTACCAGAAAGGACACCAGCCAATG-3′
4EBP1	5′-GTATCAACAGAGGCACAAGGAGGTAT-3′
P70s6k	5′-GAAGCCCTCTTTGATGCTGTCC-3′
Cdkn2a	5' - GACCTTCCGCGGCATCTATG- 3'
P53	5'-CGTGTCACCGTCGTGGA-3'

Table 4.2 *Primers used to validate targets of miR21 and miR145*

4.14 Results

4.15 Effect of mitochondrial fission inhibition on VSM cell miRNA expression:

RT-qPCR results showed that VSM cells express different levels of miR-21, miR-143 and miR-145 in the quiesced 0.1% FCS cultured VSM cells, PDGF stimulated VSM cells and following treatment with mitochondrial fission inhibitor MDivi-1. Expression of miR21 following stimulation with 20 ng PDGF resulted in a 3 ± 0.2 fold over basal level of miR-21 (Figure 4.2). Following addition of MDivi-1 the effect of PDGF on expression of miR-21 was negated (Figure 4.2).

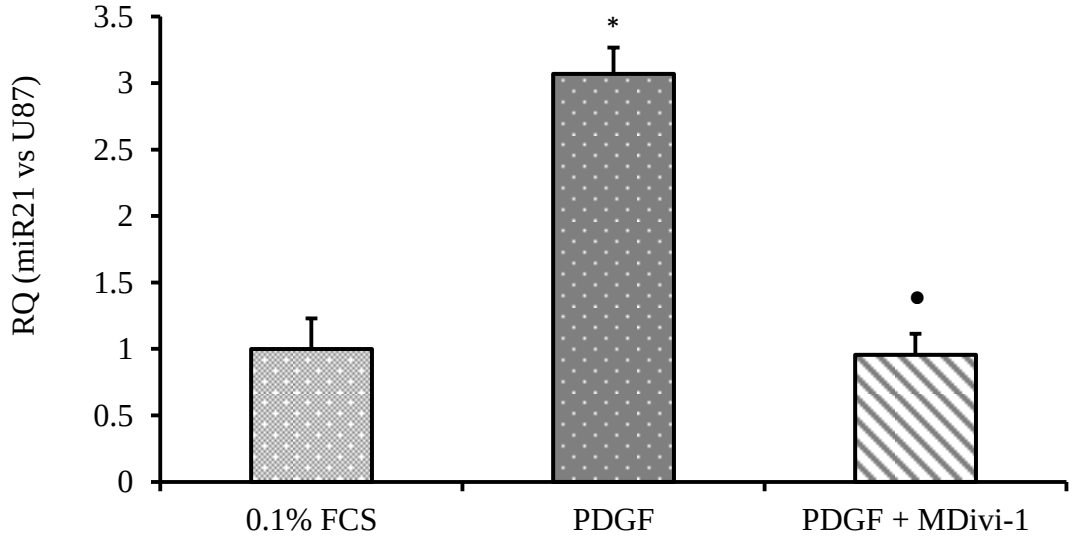

Figure 4.2 *Shows miR-21 expression following stimulation with 20 ng PDGF and the reversed effect following 10 μM treatment with MDivi-1, expression of miRNA was measured relative to the VSM cell endogenous control U87 (n=3), *p<0.05 PDGF stimulated VSM cells vs 0.1 % FCS cultured VSM cells. ●p<0.05 PDGF + MDivi-1 treated VSM cells vs PDGF stimulated VSM cells.*

The expression of both miR-143 and miR-145 were reduced by 50 ± 16% following stimulation with 20 ng PDGF. Similar to miR-21, addition of MDivi-1 returned miR-143/ 145 expressions to near baseline (Figure 4.3 & 4.4).

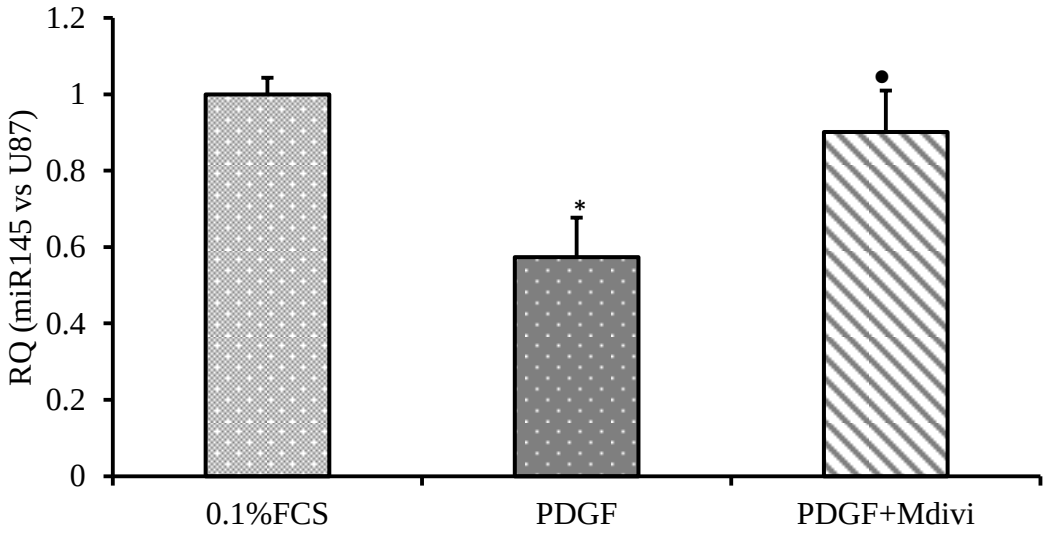

Figure 4.3 *Shows miR-145 expression following stimulation with 20ng PDGF and following incubation with 10 μM MDivi-1, expression of miRNA was measured relative to the VSM cell endogenous control U87 (n=3), *p<0.05 PDGF stimulated VSM cells vs 0.1 % FCS cultured VSM cells. ●p<0.05 PDGF + MDivi-1 treated VSM cells vs PDGF stimulated VSM cells.*

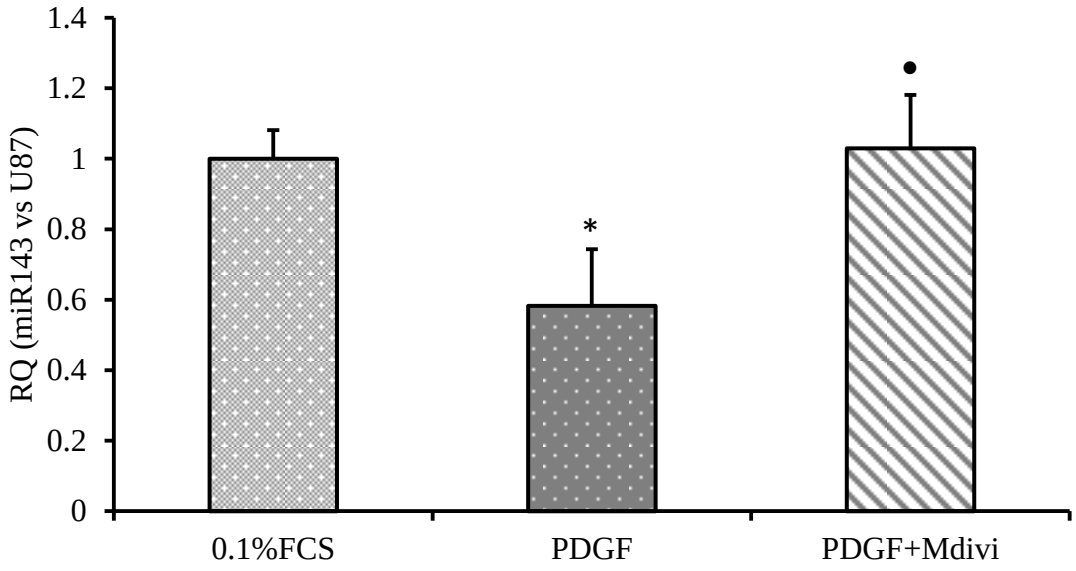

Figure 4.4 *Shows miR-143 expression following stimulation with 20 ng PDGF and the reversed effect following 10 μM treatment with MDivi-1 , expression of miRNA was measured relative to the VSM cell endogenous control U87 (n=3), *p<0.05 PDGF stimulated VSM cells vs 0.1 % FCS cultured VSM cells. ●p<0.05 PDGF + MDivi-1 treated VSM cells vs PDGF stimulated VSM cells.*

4.16 MiRNA transfection efficiency:

MiRNA transfection with miRNA mimics and inhibitors showed a difference in the level of expression following the transfection. Levels of expression of both miR-21 and miR-145 were almost zero following transfection with miR-21 and miR-145 inhibitors (Figure 4.5 and 4.6).

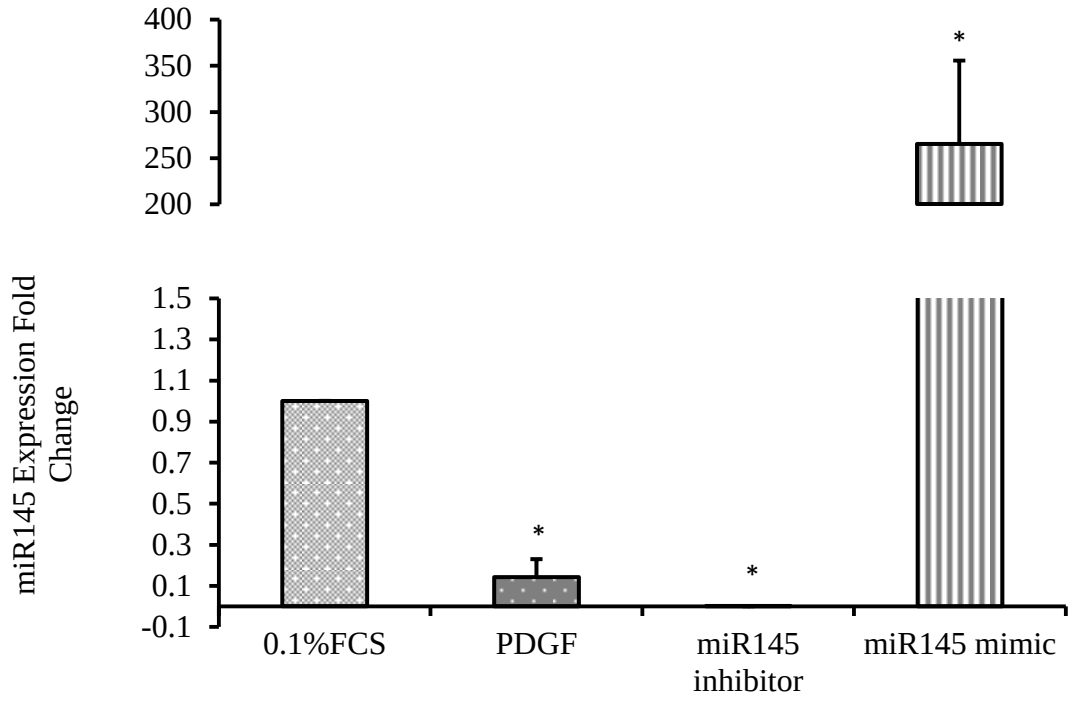

Figure 4.5 *Shows the transfection efficiency of miR-145 using miR mimics and miR inhibitors. Expression of miR-145 increased 265 folds with miR-145 mimic and decreased to almost 0 with miR-145 inhibitor (n=3), *p<0.05 PDGF stimulated cells, miR-145 inhibitor, miR-145 mimic vs 0.1% FCS cultured VSM cells.*

On the other hand, transfection with miR-21 and miR-145 mimics resulted in 1868 ± 762 and 265 ± 90 fold increase respectively in the expression of these miRNAs (Figure 4.5 and 4.6).

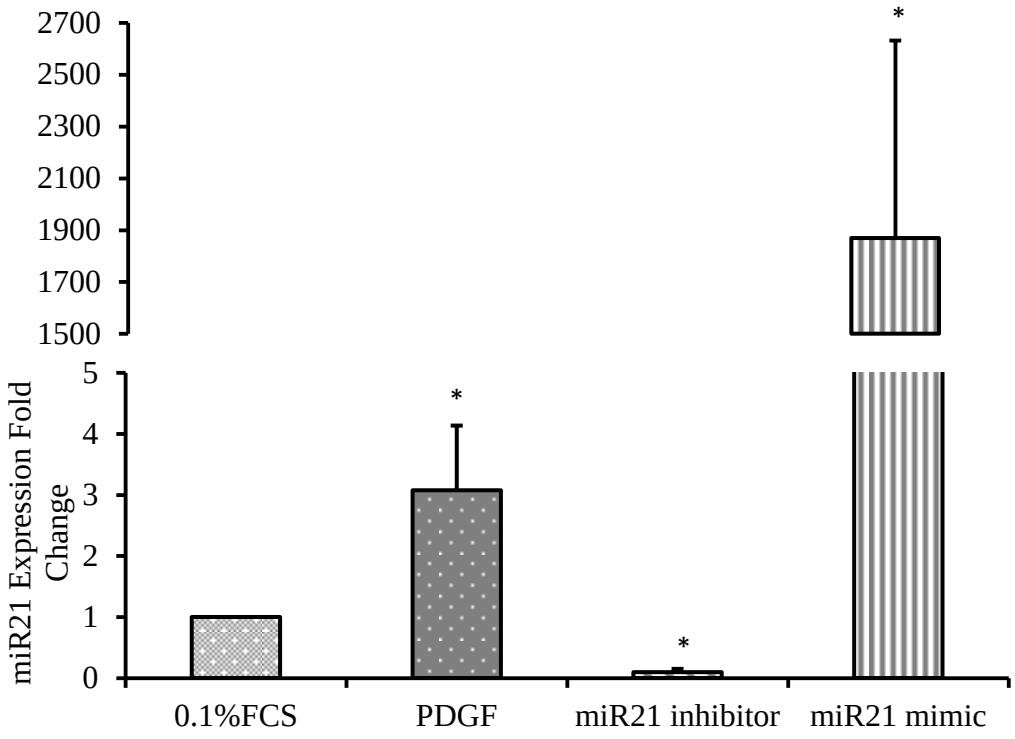

Figure 4.6 *Shows the transfection efficiency of miR-21 using miR mimics and miR inhibitors (n=3), *p<0.05 PDGF stimulated cells, miR-145 inhibitor, miR-145 mimic vs 0.1% FCS cultured VSM cells.*

4.17 Effect of miR-21 and miR-145 on mitochondrial morphology:

Images obtained from epi-fluorescent microscope for mitochondria using mito-tracker following transfection with miR-21 and miR-145 inhibitors and mimics show that miR-21 enhances mitochondrial fragmentation whereas miR-145 promotes mitochondrial elongation and fusion (Figure 4.11). Images show that mitochondrial length in cells transfected with miR-21 mimic is 0.48 ± 0.03 μm (Figure 4.7) whereas the length of mitochondria in cells transfected with miR-21 inhibitor is 3.5 ± 0.2 μm (Figure 4.8).

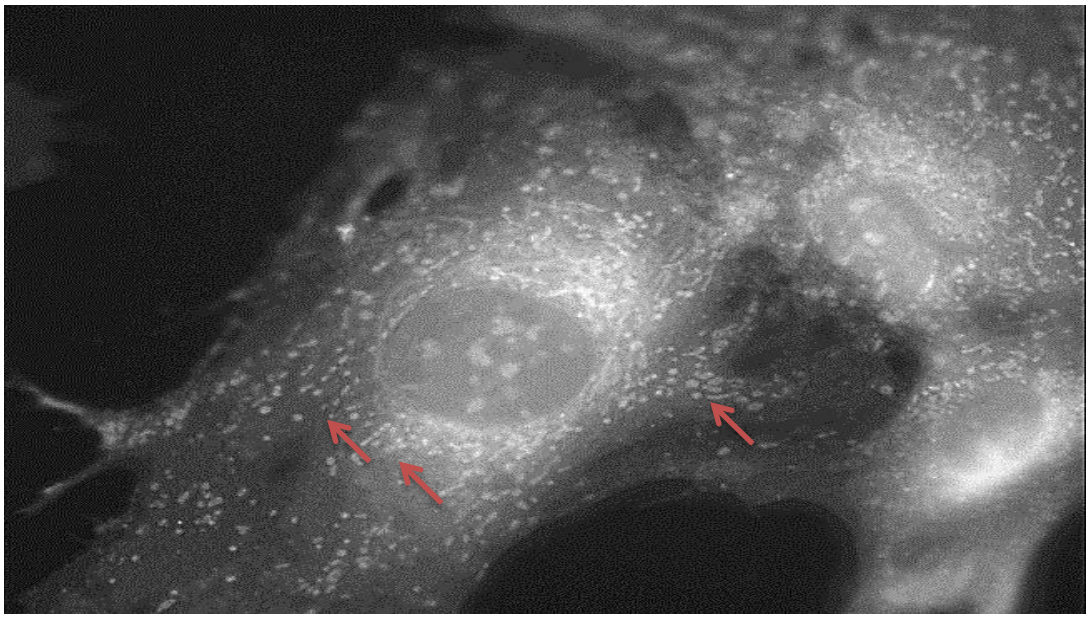

Figure 4.7 *shows VSM cell mitochondrial change in morphology following miRNA transfection. Results show that transfection with miR-21 mimic leads to fragmentation of mitochondria, mitochondria were stained using mito-tracker and imaged using x 60 magnification in the epi-fluorescent microscope.*

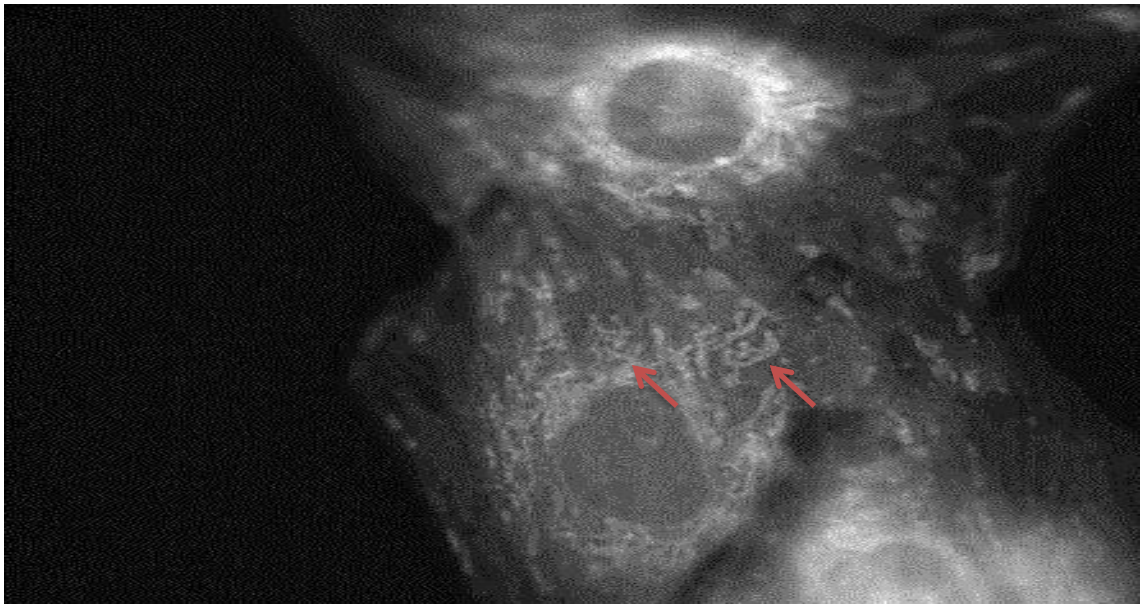

Figure 4.8 *shows VSM cell mitochondrial change in morphology following miRNA transfection. Results show that transfection with miR-21 inhibitor leads to elongation of mitochondria, mitochondria were stained using mito-tracker and imaged using x 60 magnification in the epi-fluorescent microscope.*

On the other hand, the length of mitochondria in cells transfected with miR-145 mimic is 4.1 ± 0.1 μm (Figure 4.9) and in the cells transfected with miR-145 inhibitor is 0.6 ± 0.04 μm (Figure 4.10).

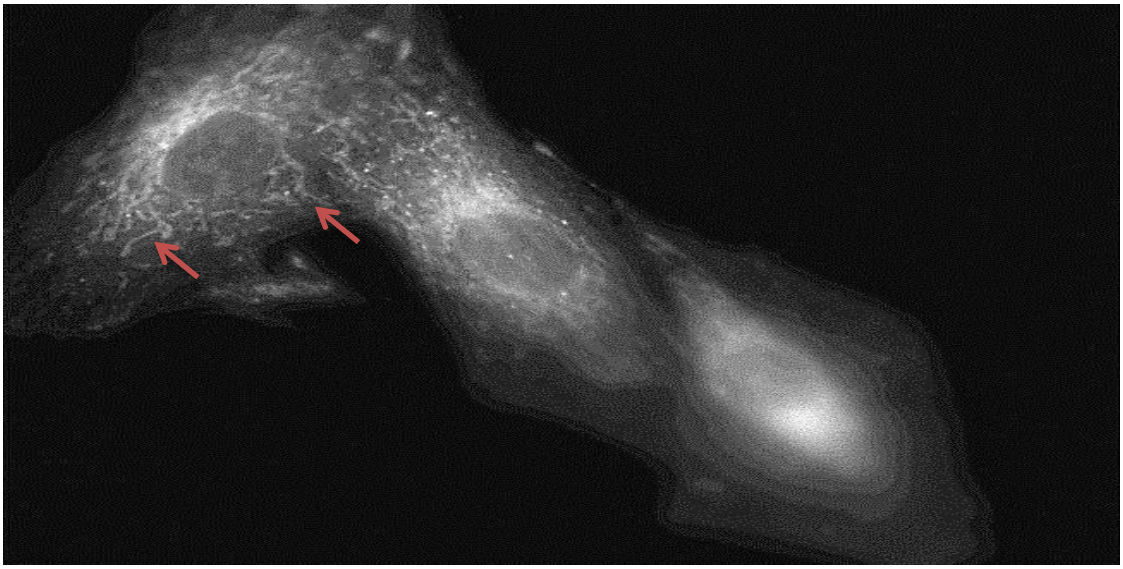

Figure 4.9 *shows VSM cell mitochondrial change in morphology following miRNA transfection. Results show that overexpressing miR-145 leads to formation of elongated mitochondria, mitochondria were stained using mito-tracker and imaged using x 60 magnification in the epi-fluorescent microscope.*

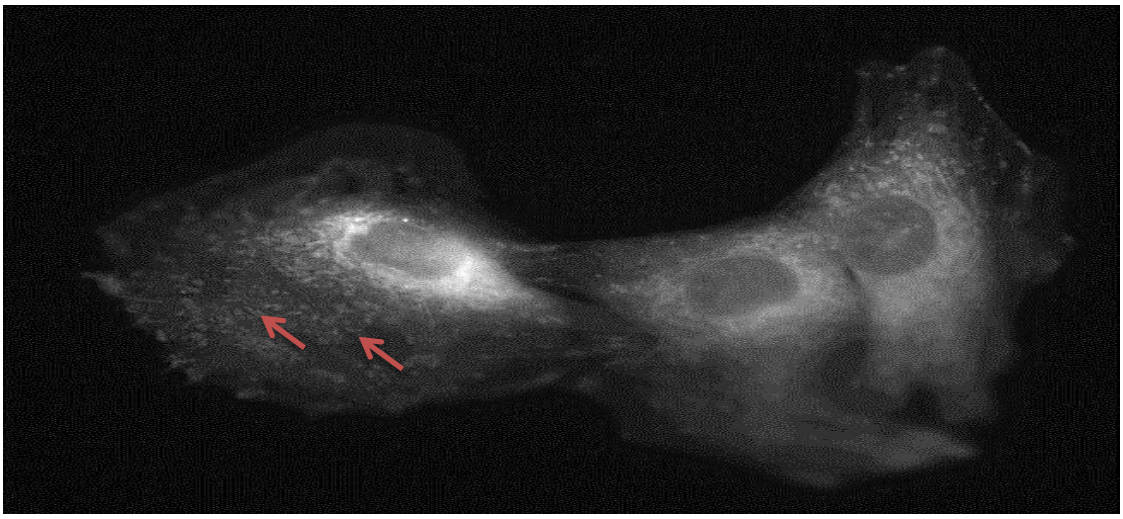

Figure 4.10 *shows VSM cell mitochondrial change in morphology following miRNA transfection. Results show that knocking down miR-145 leads to mitochondrial fragmentation; mitochondria were stained using mito-tracker and imaged using x 60 magnification in the epi-fluorescent microscope.*

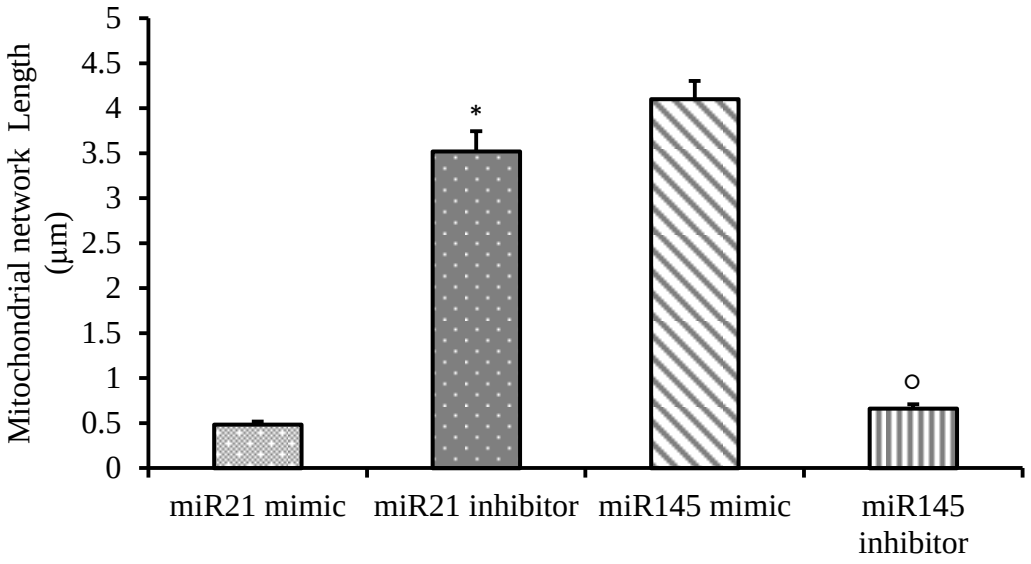

Figure 4.11 *shows mitochondrial length following miRNA transfection with miR-21 inhibitor, miR-21 mimic, miR-145 inhibitor and miR-145 mimic (n=3), * $p<0.05$ miR-21 inhibitor vs miR-21 mimic, ○$p<0.05$ miR-145 inhibitor vs miR-145 mimic.*

4.18 miR-21 and miR-145 potential gene targets in VSM cells:

RT-qPCR results showed that miR-21 and miR-145 could potentially target a selected number of genes related to ROS scavenging, mTOR signalling and cell cycle regulation. The expression of these selected genes was measured at basal 0.1% FCS level and following 20 ng/ml PDGF stimulation and compared to the level of expression following transfection with either miRNA inhibitor or mimic. Results showed that miR21 could potentially target ROS scavenging gene SOD1 and cell cycle regulatory genes P53 and cdkn2a. Although the level of SOD2 did not change significantly with miR-21 inhibitor and miR-21 mimic (Figure 4.12B), the level of SOD1 expression in cells transfected with miR-21 inhibitor is 40 ± 14% higher than what is seen in the PDGF stimulated cells. However, the level of SOD1 expression in miR-21 mimic transfected cells is 20 ± 8% lower than what is seen in the PDGF stimulated cells (Figure 4.12A).

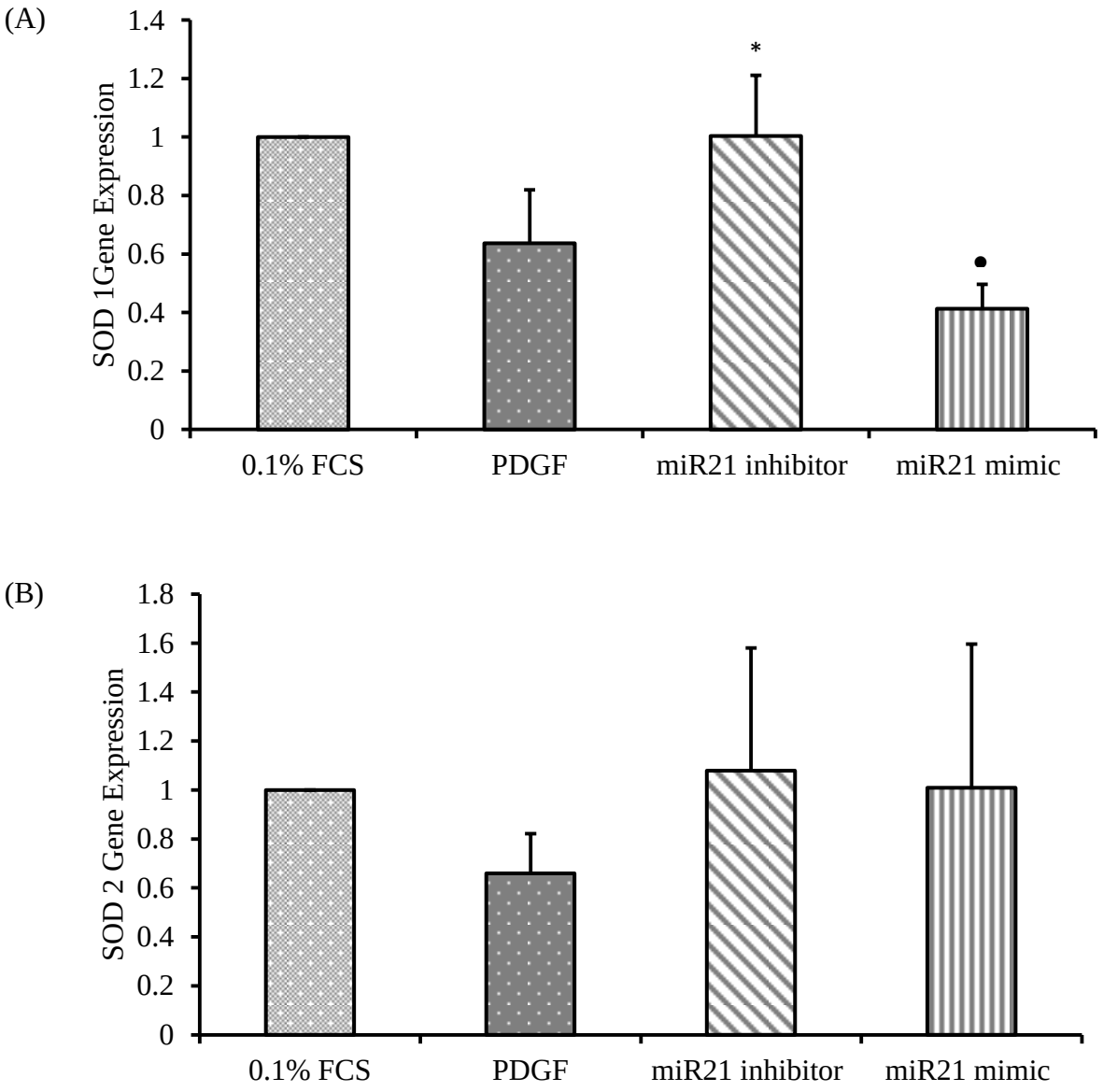

Figure 4.12 *shows the expression of ROS scavenging proteins SOD1 (A) and SOD2 (B) in VSM cells following transfection with miR-21inhibitor and miR-21 mimic (n=3), *p<0.05 miR-21 inhibitor transfected VSM cells vs PDGF stimulated VSM cells. ●p<0.05 miR-21 mimic transfected VSM cells vs PDGF stimulated VSM cells.*

Although there was an increase in the expression of PI3k, Akt, 4EBP1 and mTOR following stimulation with PDGF, their level did not change significantly following transfection with miR-21 inhibitor or miR-21 mimic (Figures 4.13 – 4.16).

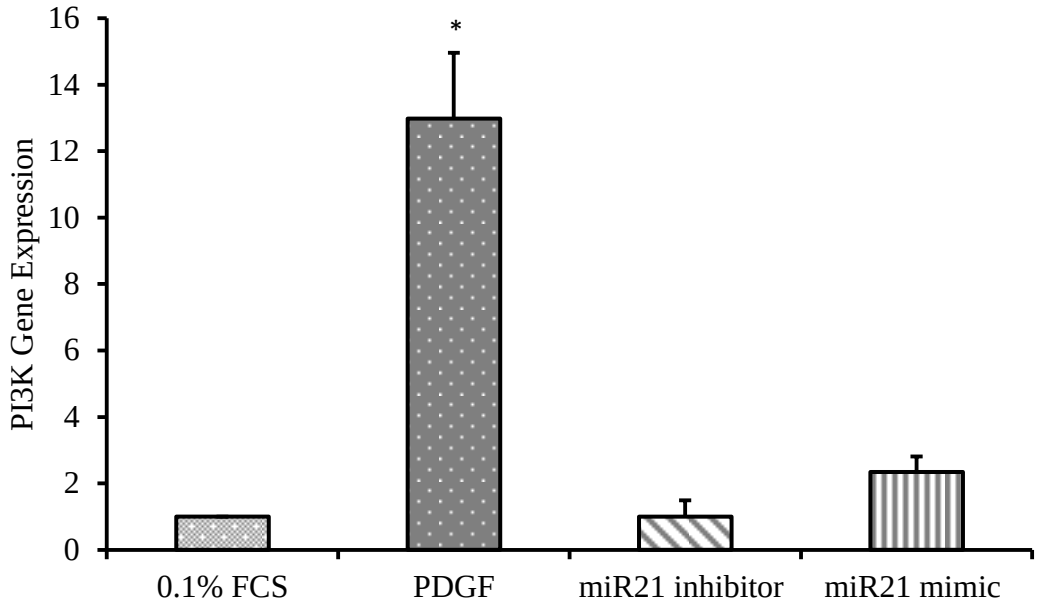

Figure 4.13 *shows the expression of PI3K gene in VSM cells following transfection with miR-21inhibitor and miR-21 mimic (n=3), *p<0.05 PDGF stimulated VSM cells vs 0.1% FCS cultured VSM cells.*

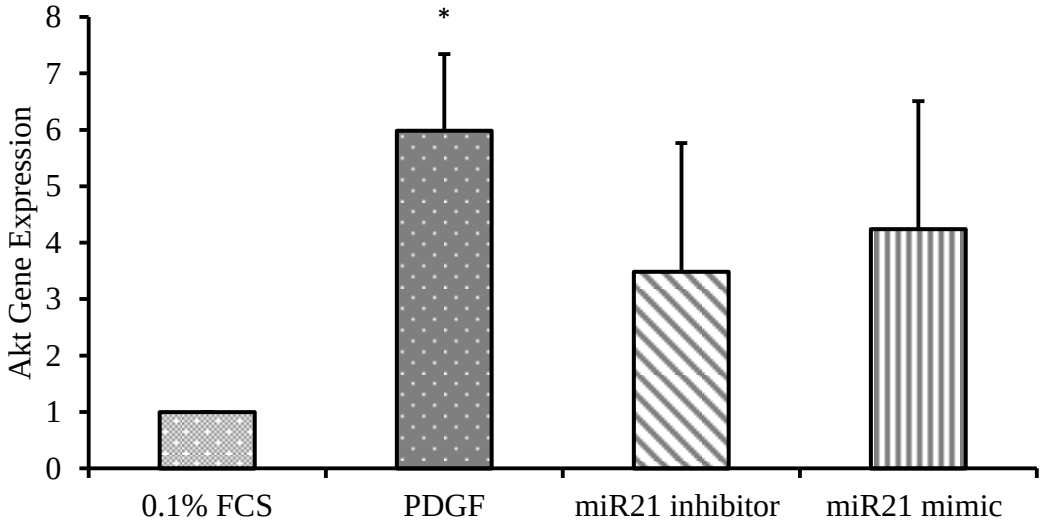

Figure 4.14 *shows the expression of Akt gene in VSM cells following transfection with miR-21inhibitor and miR-21 mimic (n=3), *p<0.05 PDGF stimulated VSM cells vs 0.1% FCS cultured VSM cells.*

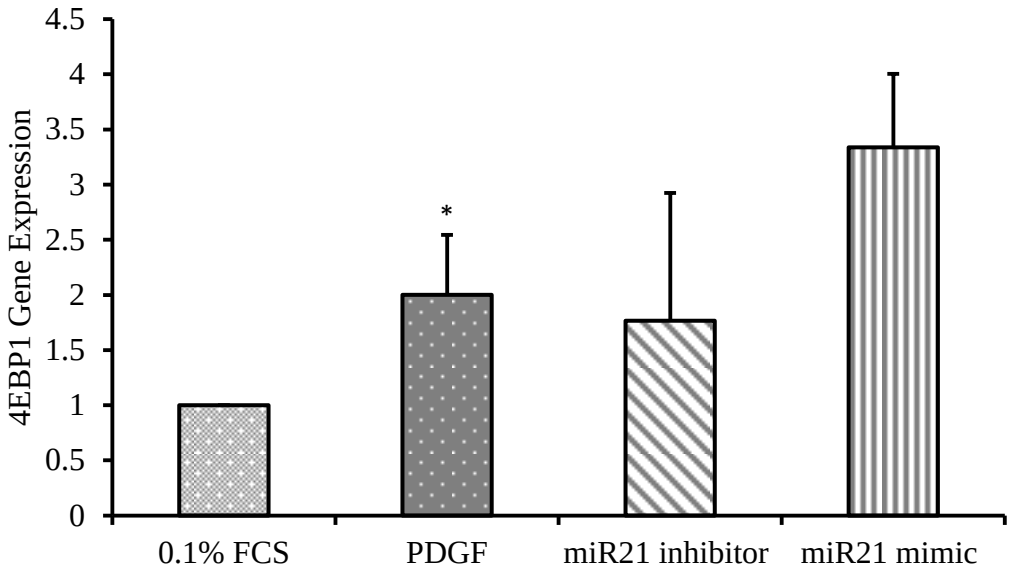

Figure 4.15 *shows the expression of 4EBP1 gene in VSM cells following transfection with miR-21inhibitor and miR-21 mimic (n=3), *p<0.05 PDGF stimulated VSM cells vs 0.1% FCS cultured VSM cells*

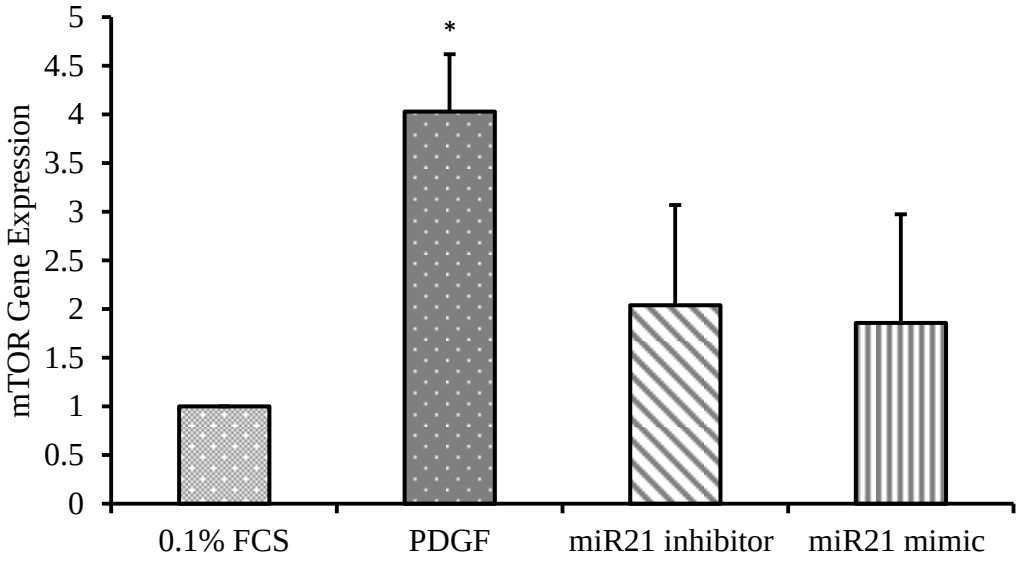

Figure 4.16 *shows the expression of mTOR gene in VSM cells following transfection with miR-21inhibitor and miR-21 mimic (n=3), *p<0.05 PDGF stimulated VSM cells vs 0.1% FCS cultured VSM cells.*

Furthermore, the level of P53 in the cells transfected with miR-21 inhibitor is 100 ± 10% higher than the PDGF stimulated cells, whereas the level of P53 in the cells transfected with miR-21 mimic is only 30 ± 6% higher than the PDGF stimulated cells (Figure 4.17).

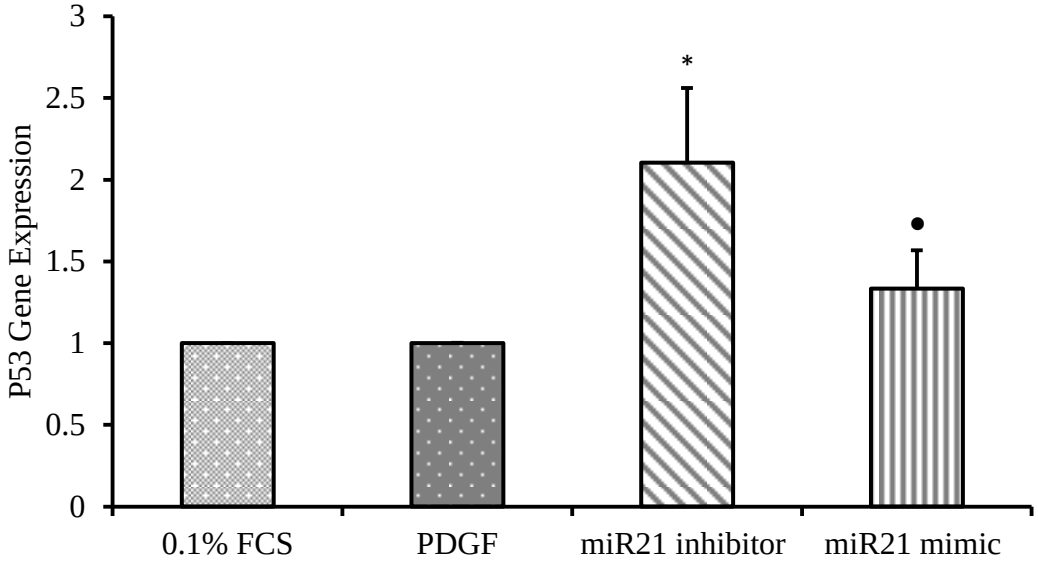

Figure 4.17 *shows the expression of Tumour suppressor gene P53 in VSM cells following transfection with miR-21inhibitor and miR-21 mimic (n=3), *p<0.05 miR-21 inhibitor transfected VSM cells vs PDGF stimulated VSM cells. ●p<0.05 miR-21 mimic transfected VSM cells vs miR-21 inhibitor transfected VSM cells.*

The level of cell cycle inhibitory gene cdkn2a in the cells transfected with miR-21 inhibitor is 100 ± 16% higher than the PDGF stimulated cells, whereas the level of cdkn2a in the cells transfected with miR-21 mimic is similar to the background level seen in 0.1% FCS cultured cells (Figure 4.18).

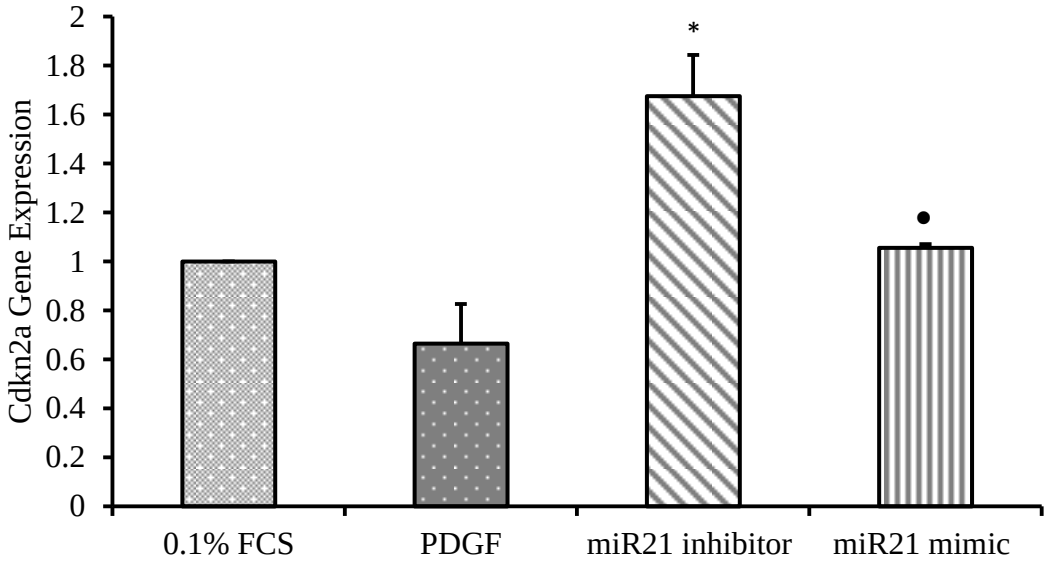

Figure 4.18 *shows the expression of cell cycle inhibitory gene Cdkn2a in VSM cells following transfection with miR-21 inhibitor and miR-21 mimic (n=3), *p<0.05 miR-21 inhibitor transfected VSM cells vs PDGF stimulated VSM cells. ●p<0.05 miR-21 mimic transfected VSM cells vs PDGF stimulated VSM cells.*

The expression of mitochondrial DNA synthesis gene Tfam did not change significantly in the PDGF stimulated cells when compared with 0.1% FCS cultured cells. The expression level did not change significantly when cells were transfected with miR-21 inhibitor or miR-21 mimic (Figure 4.19).

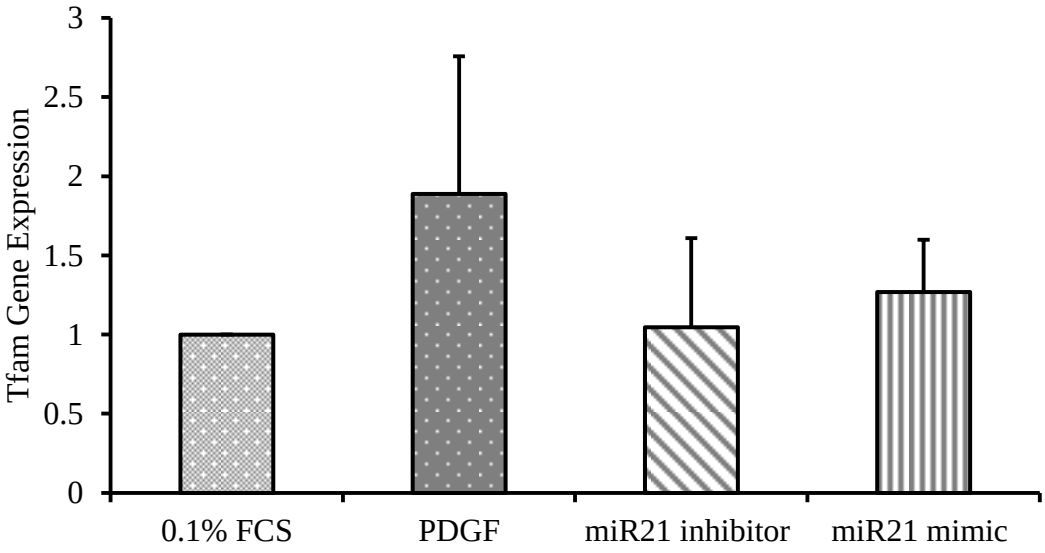

Figure 4.19 *shows the expression of mitochondrial DNA synthesis gene Tfam in VSM cells following miR-21 inhibitor and miR-21 mimic transfection (n=3).*

The expression levels of both SOD1 and SOD2 did not change significantly when VSM cells were transfected with miR-145 inhibitor or miR-145 mimic (Figure 4.20).

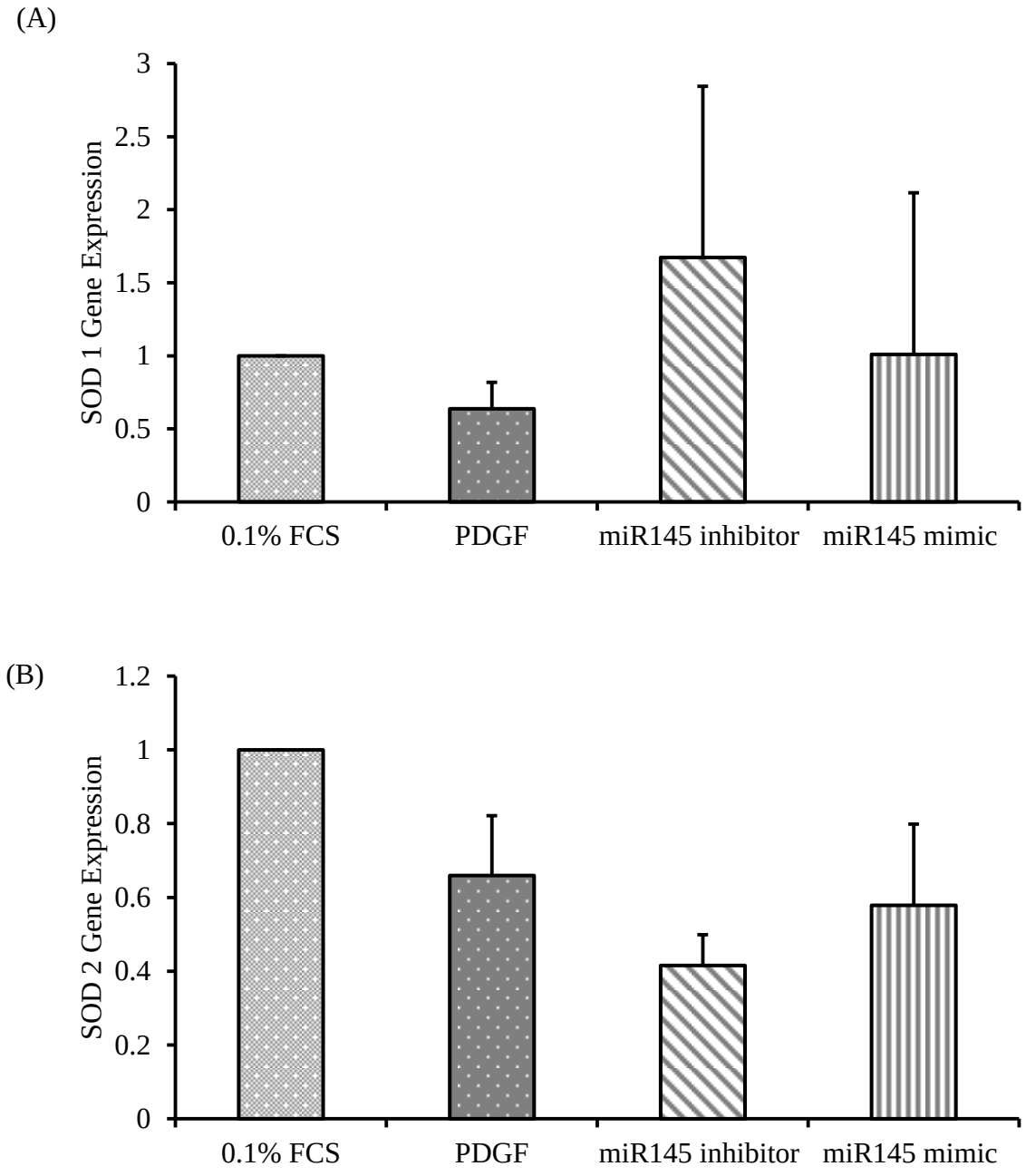

Figure 4.20 *Shows the expression of ROS scavenging proteins SOD1 (A) and SOD2 (B) in VSM cells following transfection with miR-145inhibitor and miR-145 mimic (n=3).*

Results also showed that mTOR signalling genes including PI3K, Akt, 4EBP1 and mTOR could potentially be targets for miR145. The level of expression of PI3K, Akt, 4EBP1 and mTOR is 2.6 ± 1 fold, 0.3 ± 0.1 fold, 0.3 ± 0.1 fold and 11.7 ± 1 fold higher in the cells transfected with miR-145 inhibitor than the expression in 0.1% FCS cultured cells respectively (Figures 4.21 – 4.24). However, the level of their expression following miR-145 mimic transfection is 0.5 ± 0.2 fold lower than the 0.1% FCS cultured cells for Akt and 4EBP1 and almost back to base line level for PI3K and mTOR.

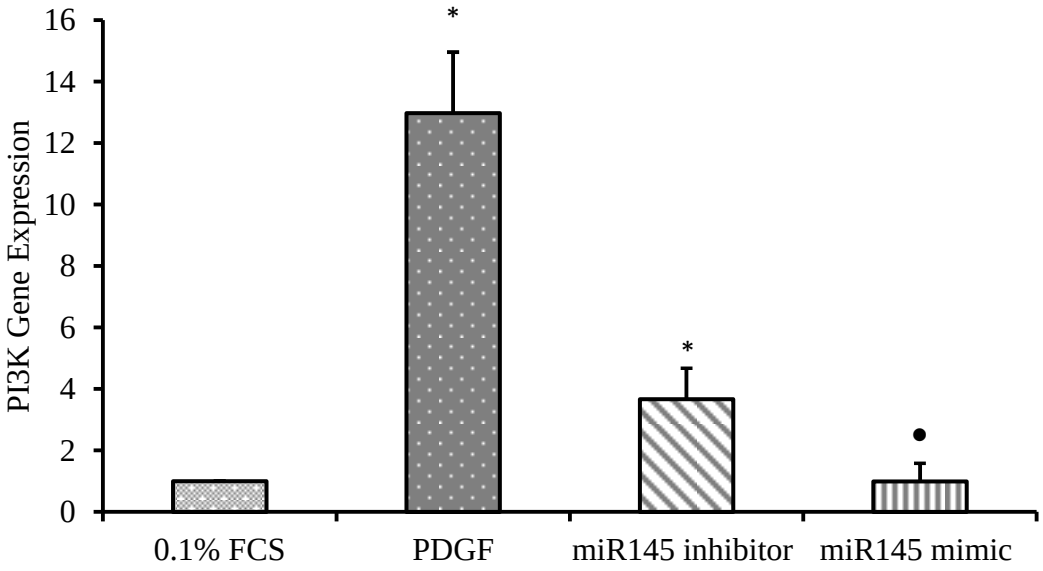

Figure 4.21 *shows the expression of PI3K gene in VSM cells following transfection with miR-145 inhibitor and miR-145 mimic (n=3), *p<0.05 PDGF stimulated VSM cells and miR-145 inhibitor transfected VSM cells vs 0.1% FCS cultured VSM cells. ●p<0.05 miR-145 mimic transfected VSM cells vs PDGF stimulated VSM cells.*

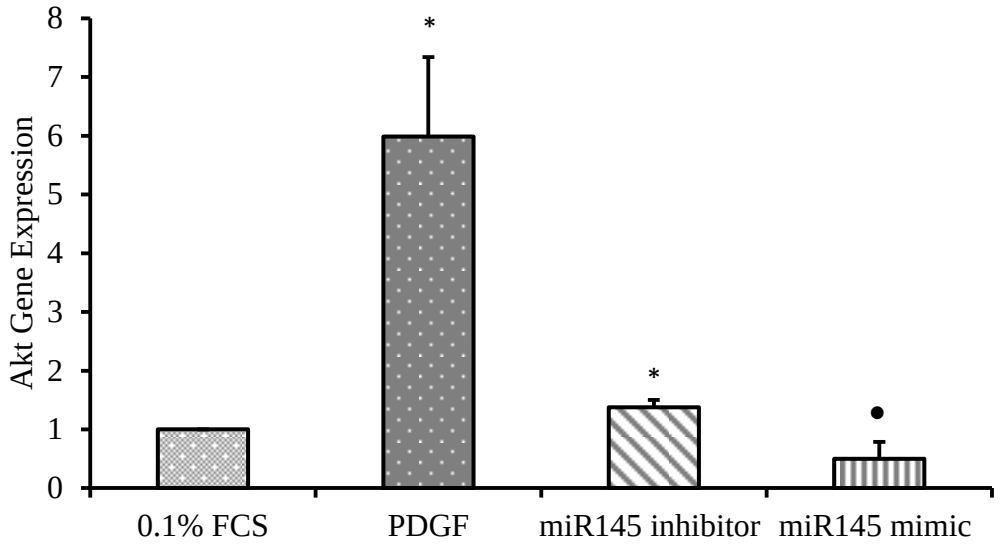

Figure 4.22 *shows the expression of Akt gene in VSM cells following transfection with miR-145 inhibitor and miR-145 mimic. (n=3),*p<0.05 PDGF stimulated VSM cells and miR-145 inhibitor transfected VSM cells vs 0.1% FCS cultured VSM cells. ●p<0.05 miR-145 mimic transfected VSM cells vs PDGF stimulated VSM cells.*

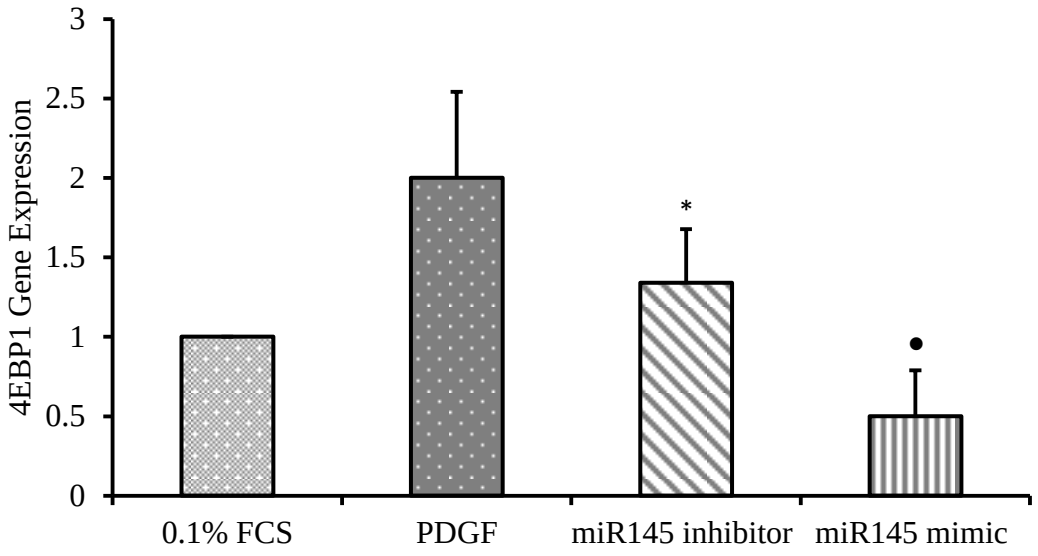

Figure 4.23 *shows the expression of 4EBP1 gene in VSM cells following transfection with miR-145 inhibitor and miR-145 mimic (n=3),*p<0.05 miR-145 inhibitor transfected VSM cells vs 0.1% FCS cultured VSM cells. ●p<0.05 miR-145 mimic transfected VSM cells vs PDGF stimulated VSM cells.*

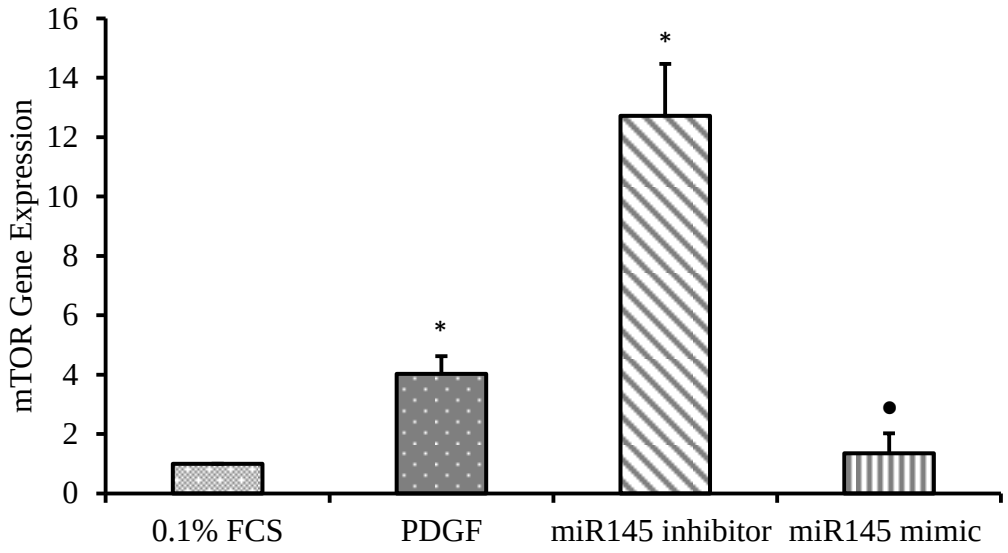

Figure 4.24 *shows the expression of mTOR gene in VSM cells following transfection with miR-145 inhibitor and miR-145 mimic (n=3), *p<0.05 PDGF stimulated VSM cells and miR-145 inhibitor transfected VSM cells vs 0.1% FCS cultured VSM cells. ●p<0.05 miR-145 mimic transfected VSM cells vs PDGF stimulated VSM cells.*

The expression level of the tumour suppressor gene P53 (Figure 4.25), the expression of the cell cycle inhibitory gene cdkn2a (Figure 4.26) and the expression level of the mitochondrial DNA synthesis gene Tfam (Figure 4.27) did not change significantly following transfection of VSM cells with miR-145 inhibitor or miR-145 mimic.

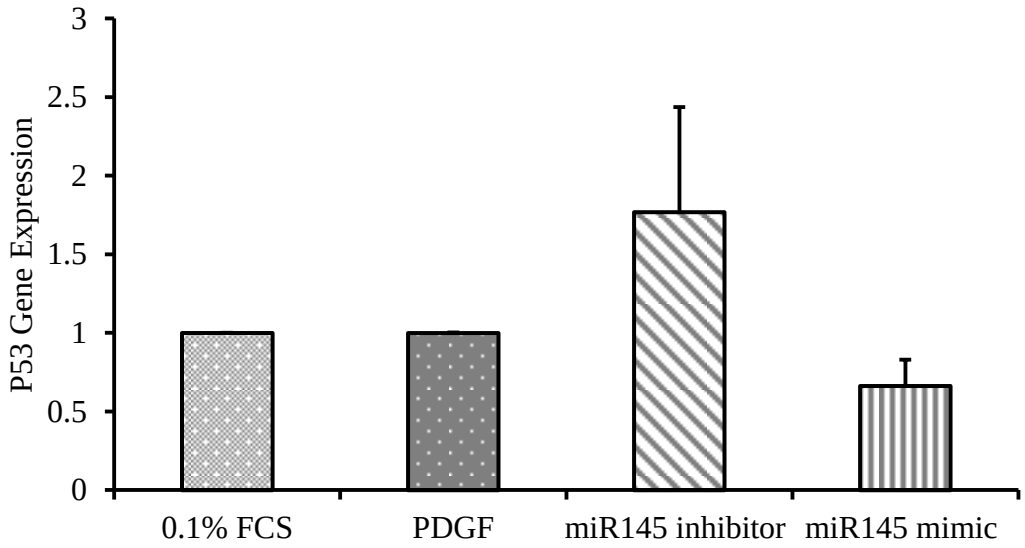

Figure 4.25 *shows the expression of tumour suppressor gene P53 in VSM cells following transfection with miR-145 inhibitor and miR-145 mimic (n=3).*

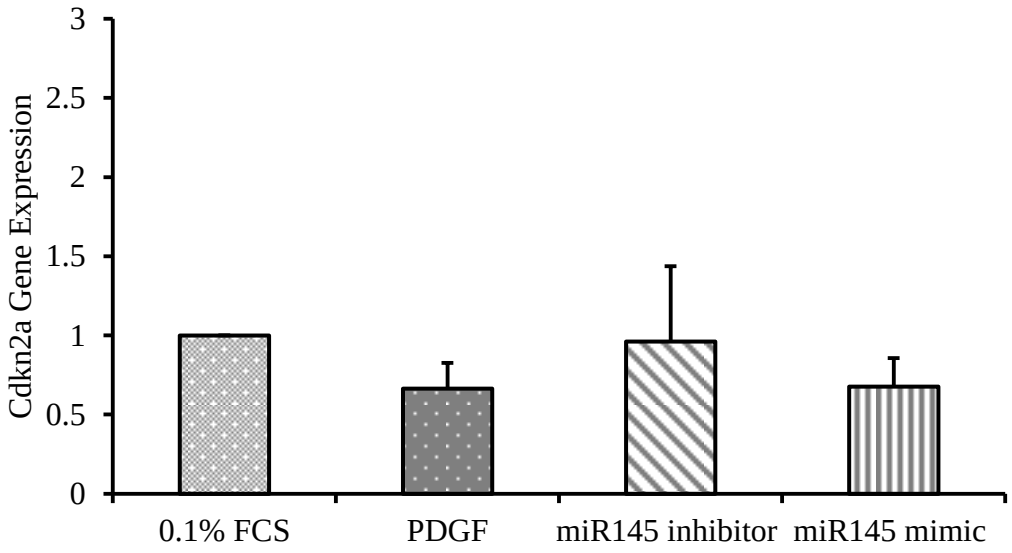

Figure 4.26 *shows the expression of cell cycle inhibitory gene Cdkn2a in VSM cells following transfection with miR-145 inhibitor and miR-145 mimic (n=3).*

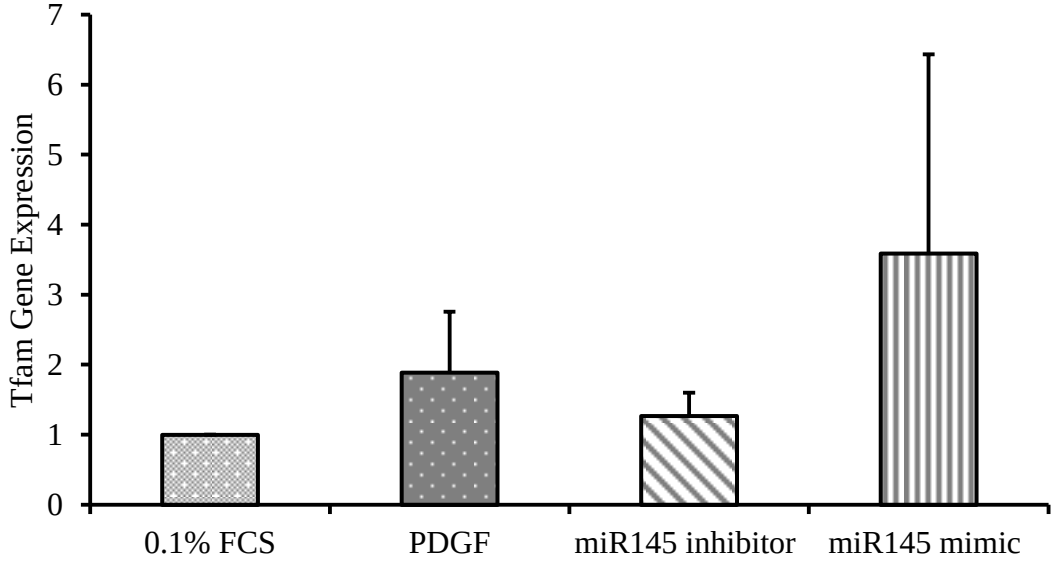

Figure 4.27 *shows the expression of mitochondrial DNA synthesis gene Tfam in VSM cells following miR-145 inhibitor and miR-145 mimic transfection (n=3).*

4.19 Effect of miR-21 and miR-145 on VSM cell proliferation:

Thymidine incorporation assay following transfection with miRNA inhibitors and mimics showed 4 ± 0.5 fold increases in VSM cell proliferation following transfection with miR-21 mimic and no significant change following transfection with miR-21 inhibitor (Figure 4.28).

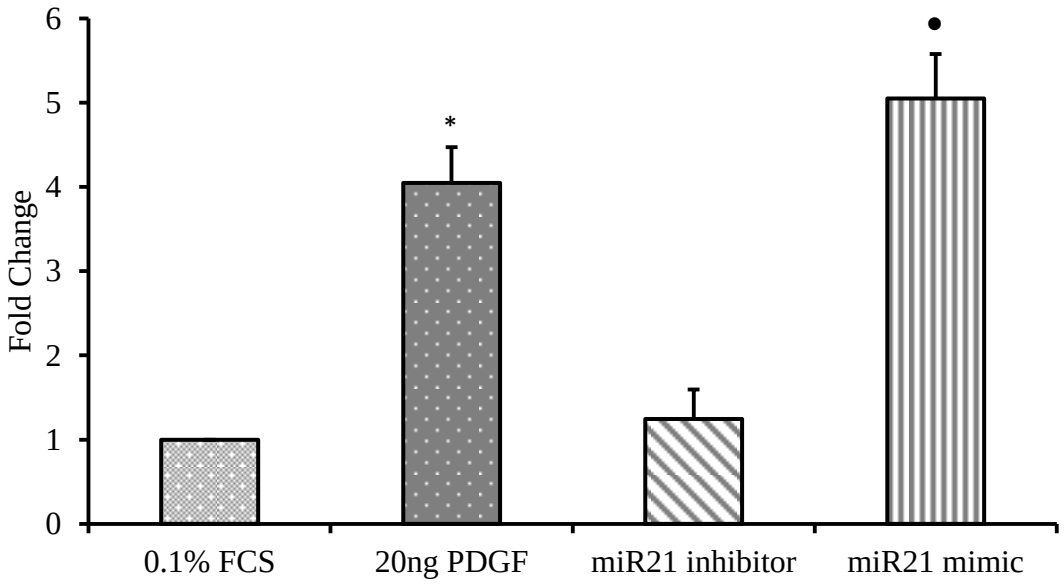

Figure 4.28 *shows the proliferation of VSM cell following transfection with miR-21inhibitor and miR-145 mimic (n=3),*p<0.05 PDGF stimulated VSM cells vs 0.1% FCS cultured VSM cells. ●p<0.05 miR-21 mimic transfected VSM cells vs 0.1% FCS cultured VSM cells.*

Results also showed that transfecting VSM cells with miR-145 inhibitor resulted in 3.7 ± 0.5 fold increase in proliferation whereas transfection with miR-145 mimic did not significantly change the proliferation of VSM cells (Figure 4.29).

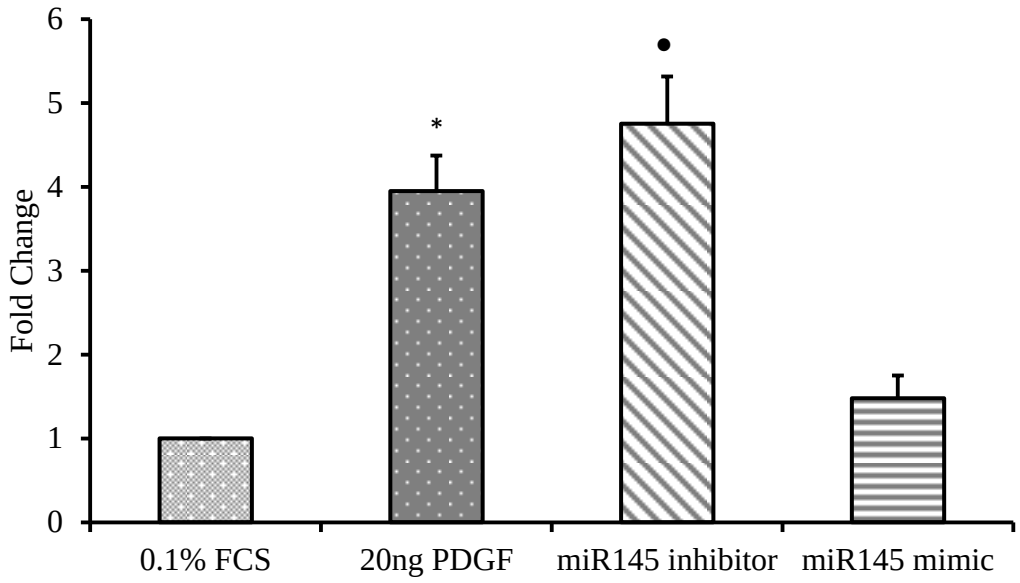

Figure 4.29 *shows the proliferation of VSM cell following transfection with miR-145 inhibitor and miR-145 mimic (n=3), *p<0.05 PDGF stimulated VSM cells vs 0.1% FCS cultured VSM cells. ●p<0.05 miR-145 inhibitor transfected VSM cells vs 0.1% FCS cultured VSM cells.*

4.20 Effect of miR21 and miR145 on VSM cells migration:

Wound healing assay results following transfection of VSM cells with miRNA inhibitors and mimics showed an increase in the migratory effect of VSM cells following transfection with miR-21 mimic (Figure 4.31). Transfection with the miR-21 inhibitor resulted in inhibition of cell migration and scratch closure (Figure 4.30). The scratch area was reduced by 50 ± 2% after 24 hour in cells stimulated with 20 ng/ml PDGF. Scratch area in cells transfected with miR-21 mimic were also reduced by 46 ± 4% after 24 hour following transfection. miR-21 inhibitor transfected in cells stimulated with 20 ng/ml PDGF resulted in no significant change in the scratch area 24 hour following transfection (Figure 4.31).

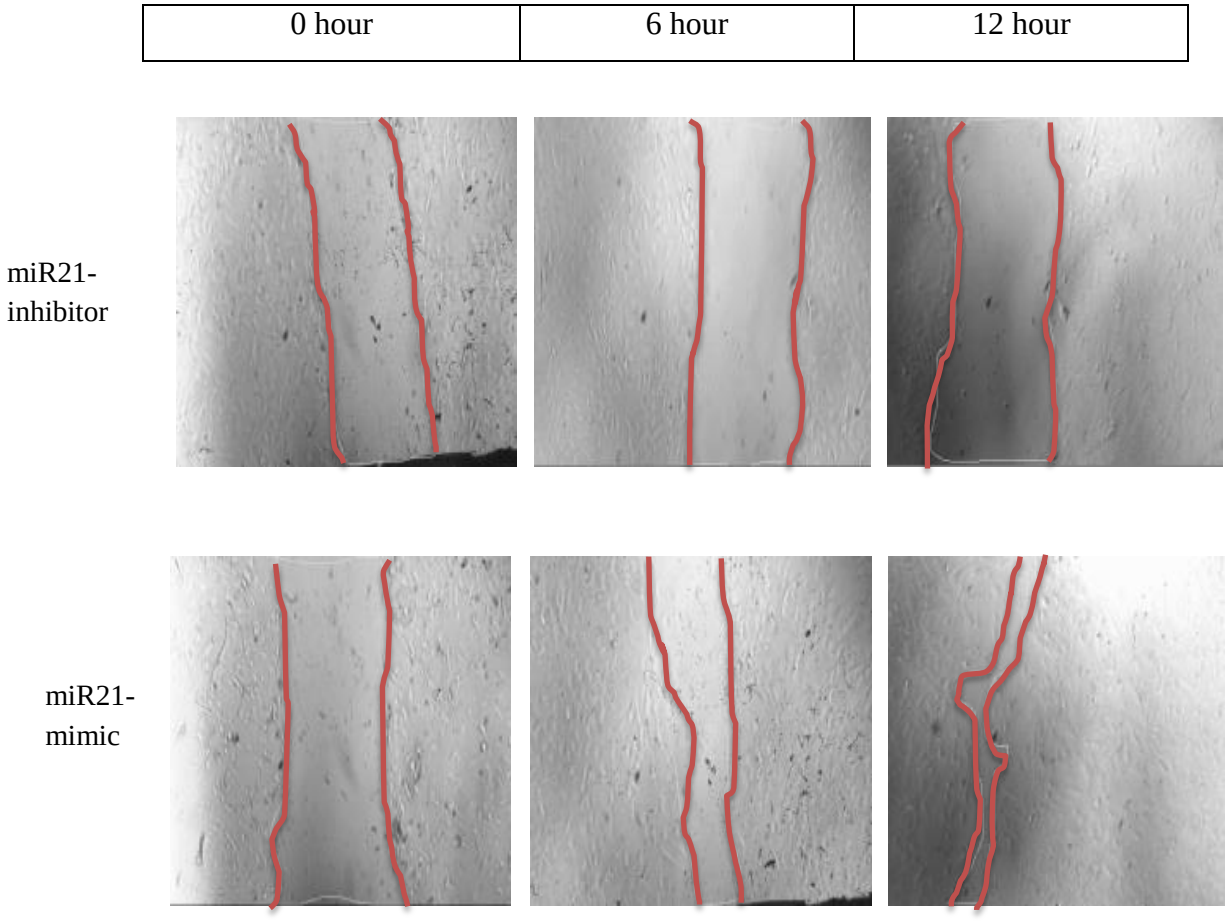

Figure 4.30 *shows the images of wound healing assay of VSM cell following transfection with miR-21inhibitor and miR-21 mimic. Results show that the wound area did not change significantly following miR-21 inhibitor transfection and significantly reduced with miR-21 mimic after 6 and 12 hour (n=3).*

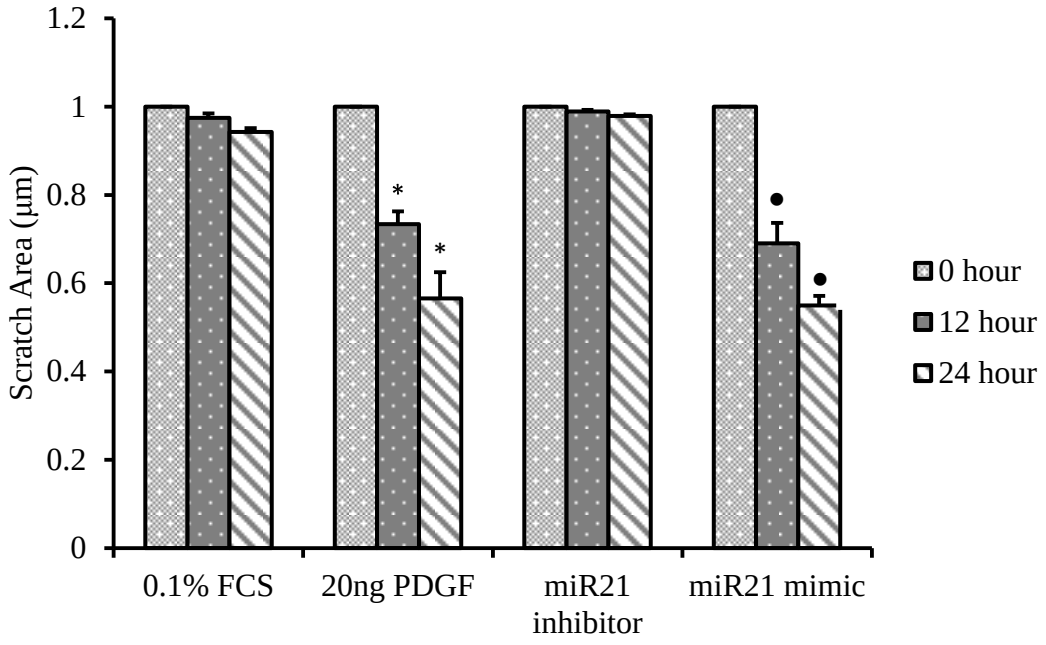

Figure 4.31 *shows the migratory capacity of VSM cell following transfection with miR-21inhibitor and miR-21 mimic (n=3),*p<0.05 PDGF stimulated VSM cells vs 0.1% FCS cultured VSM cells. ●p<0.05 miR-21 mimic transfected VSM cells vs 0.1% FCS cultured VSM cells.*

Results also show an increase in VSM cells migratory capacity following transfection with miR-145 inhibitor and a decrease following transfection with miR-145 mimic. Scratch area was reduced by 50 ± 3% in cells transfected with miR-145 inhibitor after 24 hour following transfection; however, there was no significant change in the scratch area in the cells transfected with miR-145 mimic (Figure 4.33).

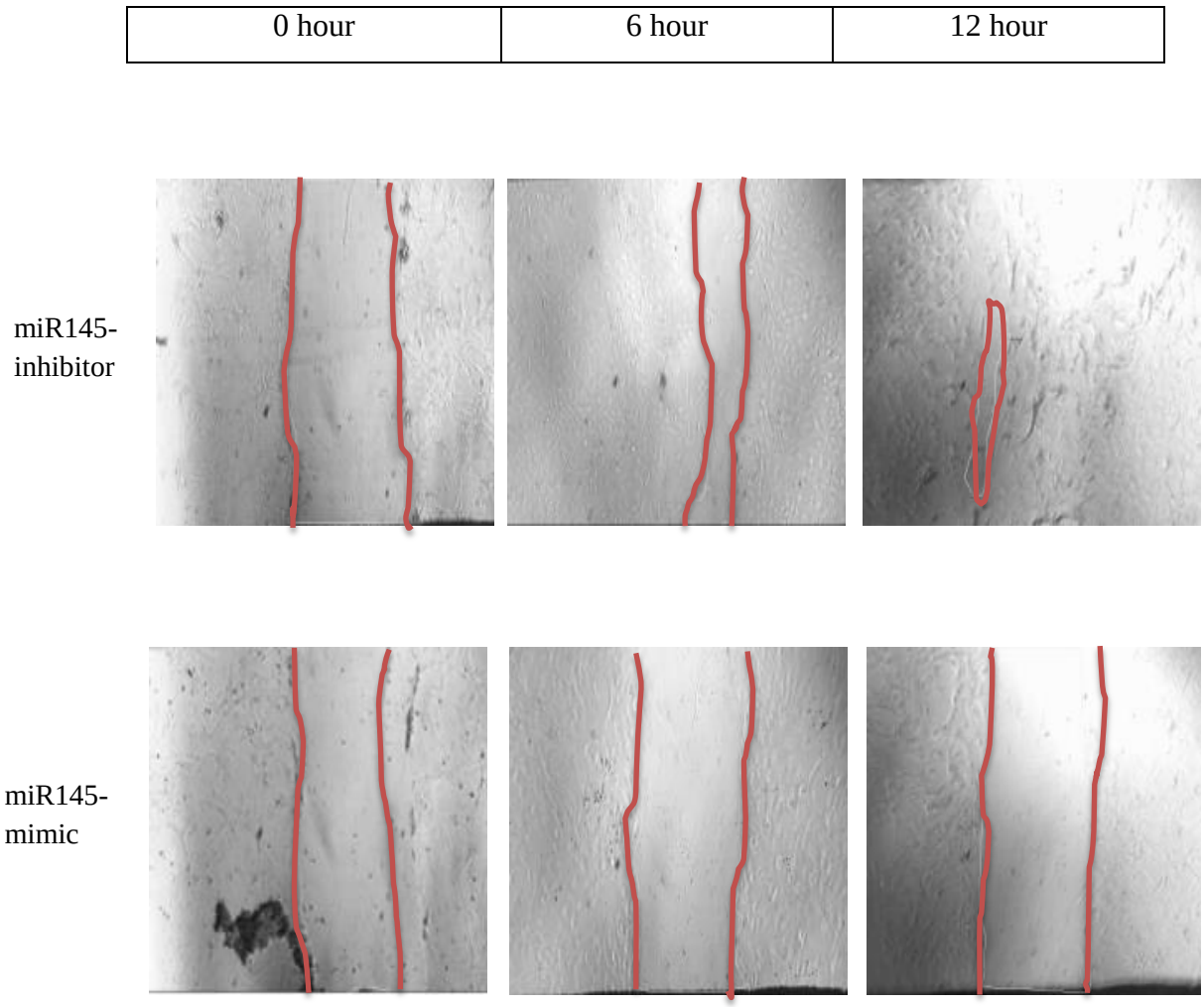

Figure 4.32 *shows the images of wound healing assay of VSM cell following transfection with miR-145 inhibitor and miR-145 mimic. Results show that the wound area significantly decreased following miR-145 inhibitor and did not change following miR-145 mimic transfection after 6 and 12 hour (n=3).*

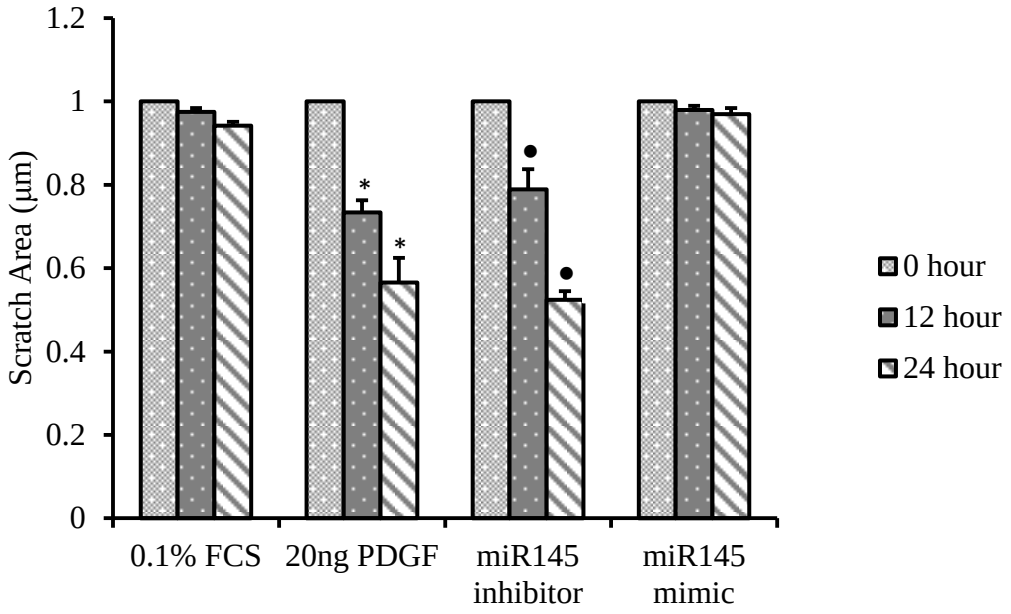

Figure 4.33 *shows the migratory capacity of VSM cell following transfection with miR-145inhibitor and miR-145 mimic (n=3), *p<0.05 PDGF stimulated VSM cells vs 0.1% FCS cultured VSM cells. ●p<0.05 miR-145 inhibitor transfected VSM cells vs 0.1% FCS cultured VSM cells.*

4.21 mTOR silencing transfection efficiency:

RT-qPCR results showed that the expression of mTOR following transfection with mTOR siRNA was reduced to basal level in comparison to the expression level following 20 ng/ml PDGF stimulation. Results also showed that co-transfection of mTOR siRNA with miR-145 inhibitor resulted in a further decrease in the mTOR expression (Figure 4.34).

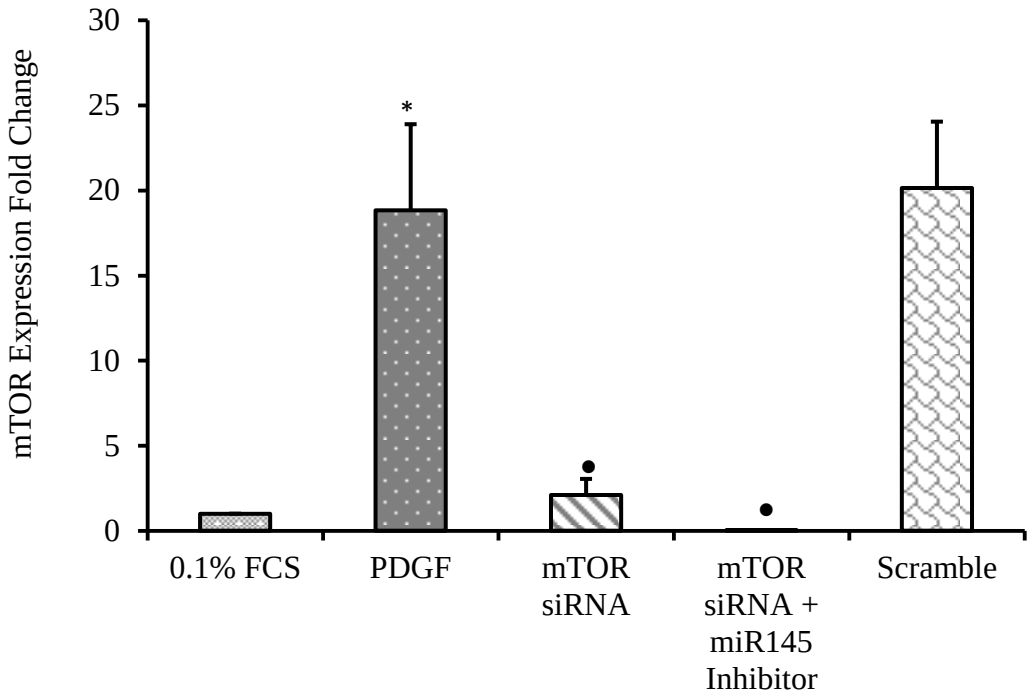

Figure 4.34 *shows the transfection efficacy of mTOR siRNA and transfection of VSM cells with mTOR siRNA + miR-145 inhibitor (n=3), *p<0.05 PDGF stimulated VSM cells vs 0.1% FCS cultured cells. ●p<0.05 mTOR siRNA and mTOR siRNA + miR-145 inhibitor vs PDGF stimulated VSM cells.*

4.22 Target validation of miR-145:

Results of the co-transfection of mTOR with miR145 inhibitor to validate mTOR as a potential target for miR145 show that transfecting VSM cells with miR-145 inhibitor alone resulted in 3.5 ± 1 fold increase in VSM cell proliferation. However, when mTOR was knocked down using siRNA, miR-145 inhibitor did not increase VSM cell proliferation (Figure 4.35).

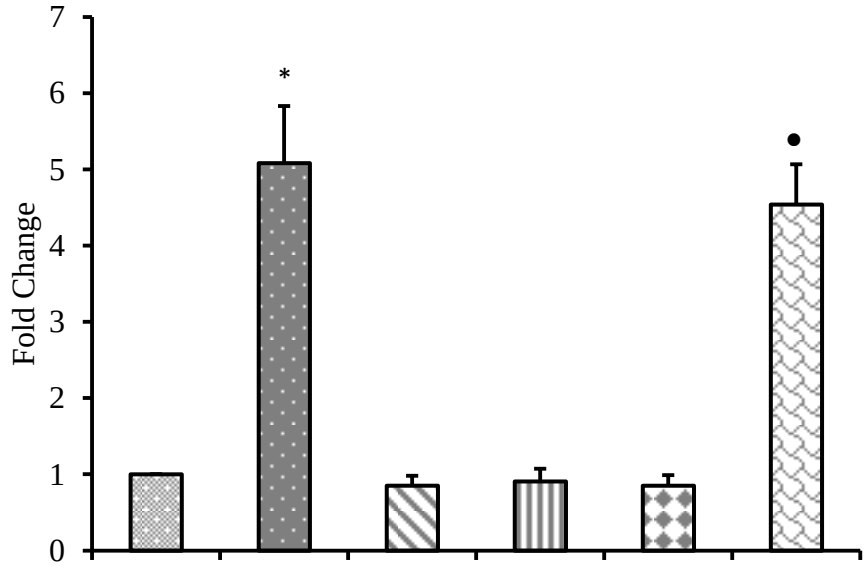

PDGF	-	+	+	-	+	-
mTOR siRNA	-	-	+	+	+	-
miR145 Inhibitor	-	-	-	+	+	+

Figure 4.35 *shows the fold change in VSM cell proliferation following transfection with mTOR siRNA and miR-145 inhibitor to validate potential targets of miR-145 (n=3),*p<0.05 PDGF stimulated VSM cells vs 0.1% FCS cultured VSM cells. ●p<0.05 miR-145 inhibitor transfected VSM cells vs 0.1 % FCS cultured VSM cells.*

Results also show the validation of PDGF receptor as a potential target for miR145. Transfecting VSM cells with miR-145 inhibitor did not increase proliferation when PDGF receptor was blocked using 10 μM PDGF receptor inhibitorimatinib (Figure 4.36).

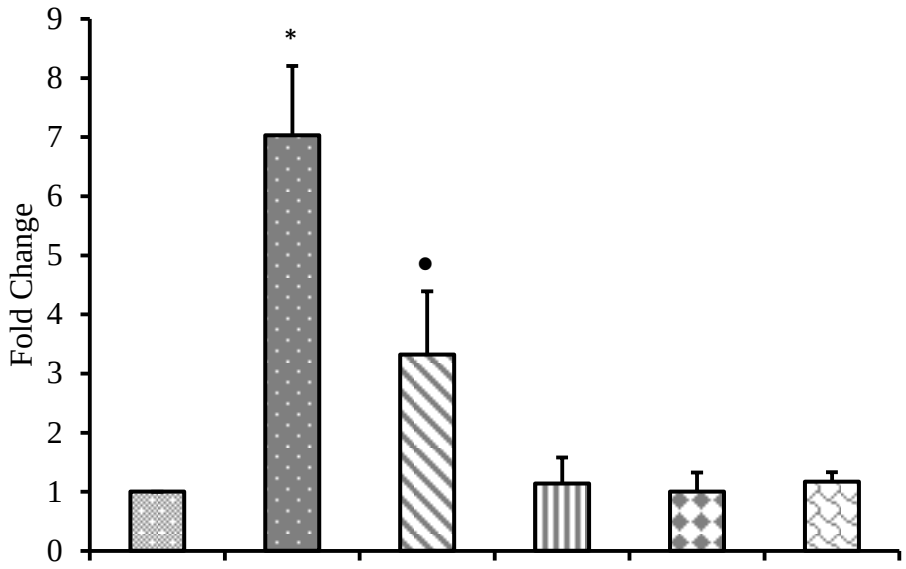

PDGF	-	+	-	+	-	+
miR145 Inhibitor	-	-	+	-	+	+
Imatinib	-	-	-	+	+	+

Figure 4.36 *shows the fold change in VSM cell proliferation following transfection with miR-145 inhibitor and treatment with 10 μM PDGF receptor inhibitor Imatinib to validate potential targets of miR-145 (n=3),*p<0.05 PDGF stimulated VSM cells vs 0.1% FCS cultured VSM cells. ●p<0.05 miR-145 inhibitor transfected VSM cells vs 0.1 % FCS cultured VSM cells.*

4.23 Discussion

4.24 Effect of mitochondrial fission inhibition on VSM cell miRNA expression:

The expression of miRNAs is a continuous dynamic event and changes with any change in the cellular or environmental function (Zhang, 2008). miR-21 and miR-145 are smooth muscle cells-associated, well characterised miRNAs that have been linked to vascular development, physiology and injury (Albinsson et al., 2010). During quiescence, the expression of miR-21 in vascular smooth muscle cells is lower than the expression following stimulation with PDGF (Figure 4.2). This increase in the expression indicates the important role played by miR-21 in the regulation of important genes involved in the initiation and progression of VSM cell proliferation and migration. This increase in miR-21 expression was previously reported to be involved in the early development of vascular occlusive disease and was a tropomyosin 1-dependent process (Wang et al., 2011). Similar studies also reported the upregulation of miR-21 following acute vascular injury leading to neo-intimal formation (Ji et al., 2007a) and in pulmonary vasculature following exposure to hypoxia (Sarkar et al., 2010). Here we have confirmed a potentially significant role for miR-21 as the expression of miR-21 decreased to near baseline level following the inhibition of mitochondria fission (Figure 4.2).

miR-145 was downregulated and reduced by half following stimulation with PDGF when compared with unstimulated cells (Figure 4.3). This suggests that miR-145 may suppresses genes responsible for VSM Cell proliferation. These observations are further supported as when miR-145 was inhibited, VSM cell proliferation increases (Figure 4.29). This observation was also seen in other studies such as (Cordes et al., 2009) who found that miR-145 regulates smooth muscle cells fate and plasticity through targeting transcription factors such as krupple like factor 4 (KLF4) myocardin and Elk-1 leading to the promotion of differentiation and repression of proliferation of VSM cells. Other groups have also found that miR-145 is the most abundant miRNA in normal vascular wall and that its expression was downregulated in vascular walls with neo-intimal lesion which supports our observation (Cheng et al., 2009). The expression of miR-145 was significantly increased following the inhibition of mitochondrial fission using MDivi-1. An increase in miR-145

expression was reported to be associated with the increase in caspase 3 mediated apoptosis in colon cancer by targeting DNA fragmentation factor 45 (Zhang et al., 2010). This finding is in keeping with our observation whereby inhibiting mitochondrial fission using MDivi-1 resulted in an increase in caspase 3/7 activity and correlates with an increase in miR-145 expression (Figure 3.25).

4.25 Effect of miR-21 and miR-145 in mitochondrial morphology:

There was a clear correlation between mitochondrial network formation and miRNA expression level in cells (Figure 4.2). Overexpressing miR-21 which is seen to increase during VSM cell proliferation resulted in a distinct fragmentation of mitochondrial networks whereas down regulating miR-21 resulted in their formation. Similarly, studies have previously looked at potential targets for miR-145 including targets that affect VSM cell plasticity (Cordes et al., 2009). However, it is not understood what determines the level of miR-145 within the cell. In this present work, we show that overexpressing miR-145 resulted in formation of mitochondrial network and more elongated mitochondria whereas the down regulation of miR-145 resulted in shorter mitochondria being formed and fragmentation of mitochondrial network. Although previous studies have reported that mitochondrial fission/ fusion are important in VSM cell proliferation, the mechanism driving this are poorly understood (Chalmers et al., 2012). Following this present work we are somewhat clearer as to mechanisms linked to mitochondrial fission/ fusion and VSM cell proliferation. VSM cell proliferation is determined by the mitochondrial network formation and inhibiting mitochondrial fission results in a reduction in miR-21 expression and increase in miR-145 expression. This in turn affects the target genes such as mTOR which then result in a reduction in mTOR signalling pathway (Figures 3.17, 3.18, 3.19 & 3.20). The end result will be an inhibition in VSM cell proliferation and migration. This is novel evidence that mitochondrial fission/ fusion could play a vital role in the transfer of gene information through the synthesis of specific miRNAs.

4.26 Gene targets for miR-21 and miR-145 in VSM cells:

Considering the relevance of miR-21 and miR-145 we aimed to identify the potential pro-mitogenic signalling pathway targets of miR-21 and miR-145. Thus following manipulation of miR-21/ miR-145 signalling gene expression of Akt, PI3K and mTOR was measured. We confirmed the transfection success by measuring the level of expression of these miRNAs. Results showed there was a significant decrease in the expression of miR-21 and miR-145 following transfection with the miRNA inhibitors. Results also confirmed that the level of expression of miR-21 and miR-145 was significantly increased following the transfection with miRNA mimics. The expression of pro-apoptotic cell cycle inhibitory genes was modulated when the expression of miR-21 was either increased or decreased in the cell. The expression of both p53 and cdkn2a was significantly increased when the cells were transfected with miR-21 inhibitor. However, their expression was significantly reduced when the cells were transfected with miR-21 mimic. This change in the expression of these genes suggests a possible link between miR-21, p53 and cdkn2a. miR-21 could potentially target p53 and cdkn2a and thus inhibit cell cycle progression and consequently VSM cell proliferation. Although the expression of SOD2 did not change significantly following miR-21 transfection, ROS scavenging gene SOD1 was seen to change. Overexpressing miR-21 in VSM cell resulted in a decrease in the expression of SOD1. Whereas miR-21 knock down resulted in an increase in SOD1 expression. Thus SOD1 may be another target for miR-21. These results highlights the importance of ROS induced VSM cell proliferation through the overexpression of miR-21. miR-21 was previously seen to decrease the activity of superoxide dismutase which led to the activation of ERK pathway and increase in ROS production and migration in angiogenic progenitor cells (Fleissner et al., 2010). Previous studies have identified other targets for miR-21 including tropomyosin-1 which is responsible for maintaining cellular phenotype of VSM cell (Wang et al., 2011). A number of studies published validated pro-apoptotic targets for miR-21 including CDK2AP1 (Zheng et al., 2011). In this study they found that miR-21 inhibited the tumour suppressor gene CDK2AP1 and stimulated proliferation and migration of the human immortalized keratinocyte cell line. Our finding clearly points at a possible mechanism of targeting SOD1 and Cdkn2a by miR-21 which

promotes VSM cell proliferation. Inhibiting mitochondria reduces the expression of miR-21 which consequently increases the expression of SOD1 and Cdkn2a and shifts the balance towards apoptosis and reduction in proliferation.

The expression of mTOR signalling genes including PI3K, Akt, mTOR and 4EBP1 were all modulated by the change in the expression of miR-145. The expression of all four genes was significantly reduced when cells were transfected with miR-145 mimic. Their expression was, however, increased when miR-145 was knocked down. Thus miR-145 may be important in the genes responsible for the initiation of mTOR signalling cascade. Many targets have been identified previously for miR-145 including genes involved in cellular proliferation, invasion and differentiation. Phenotypic regulatory VSM cell KLF4 has been found to be one of the targets for miR-145 (Cordes et al., 2009). Likewise, miR-145 has been reported to target the mTOR effector gene P70S6K1 (Wu et al., 2013). The investigators found that miR-145 negatively regulated the expression of P70S6K1 in ovarian cancer cells leading to a significant reduction in cell proliferation and migration. Their results highlight the important role played by miR-145 in regulating mTOR signalling pathway. Likewise data from this work similarly supports this observation in VSM cell proliferation and migration.

Both miR-21 and miR-145 have an important role in VSM cell proliferation and migration through the regulation of cell cycle progression, ROS production and cellular protein synthesis by mTOR signalling pathway. Therefore, the inhibition in proliferation and migration seen previously following the inhibition of mitochondrial bioactivity could be due to mitochondria regulation of miRNA synthesis as reported in this work (Figures 3.10 & 3.11). Mitochondria have been observed to be enriched in miRNA suggesting that mitochondria are one of the main miRNA destinations within the cell (Mercer et al., 2011). Although mitochondrial genome encodes for only 13 mitochondrial proteins because of its limited size, there are more than 1500 proteins present in the mitochondria (Lopez et al., 2000). Emerging evidence has shown that the nuclear RNA is transported into the mitochondria (Duchene et al., 2009). Thus it is highly plausible that inhibiting mitochondrial activity results in the

inhibition of miRNA synthesis. This in turn affects gene synthesis targeted by these miRNA which regulate VSM cell proliferation and migration.

4.27 Effect of miR-21 and miR-145 on VSM cell proliferation and migration:

To validate the functional role of miR-21 and miR-145 VSM cell proliferation and migration assays were undertaken following transfection with miR-21 and miR-145 both inhibitors and mimics. Results clearly confirm that overexpressing miR-21 resulted in a significant increase in the VSM cell proliferation more than the increase following PDGF stimulation alone. This suggests that overexpression of miR-21 has a stimulatory effect on VSM cell proliferation similar to PDGF stimulated proliferation. On the other hand, miR-21 knockdown resulted in a reduction in proliferation when compared with PDGF stimulated proliferation. This again supports the role of miR-21 in promoting VSM cell proliferation and the importance of their expression following PDGF stimulation. Similar effects were observed with VSM cell migration assays (Figures 4.31 & 4.33). Overexpressing miR-21 resulted in a faster closure of the cell gap and a higher VSM cell motility after 12 and 24 hours in comparison to the PDGF stimulated VSM cells. Whereas miR-21 knockdown resulted in no VSM cell movement and the area of the gap did not significantly change after 12 and 24 hours. Similar observations have been reported previously (Ji et al., 2007b). In this study the authors demonstrated that miR-21 modulates VSM cell proliferation in a balloon injured rat carotid artery model. They reported that miR-21 controls VSM cell proliferation through the regulation of PTEN and BCL-2 genes which have been reported to be involved in apoptosis (Ji et al., 2007b). A similar study reported that miR-21 was an important determinant of endothelial cell proliferation and migration (Sabatel et al., 2011). They linked miR-21 to the expression of RhoB which is involved in the regulation of actin cytoskeleton.

miR-145 knockdown however resulted in an increase in VSM cell proliferation when compared with PDGF stimulated VSM cells. This increase in proliferation was significantly reversed following overexpression of miR-145. Similarly, knocking down miR-145 resulted in a significant increase in VSM cell migration after 12 and 24 hours in comparison to the rate of migration seen with PDGF stimulation.

Increasing the expression of miR-145, however, resulted in inhibition of VSM cell motility with little change in motility following stimulation with PDGF.

miR-145 was also seen to be involved in the proliferation and migration of VSM cells. It was seen to be required for the maintenance of contractile phenotype by murine arterial smooth muscle cells through the regulation of angiotensin converting enzyme (Boettger et al., 2009). MiR-145 was also previously seen to be involved in the migration of VSM cell through the maintenance of their cytoskeletal structure. One group concluded that miR-145 is required for maintenance of actin stress fibres in SMCs. The spindle-like morphology was lost with the knockdown of miR-145 and the cells became migratory and proliferative (Xin et al., 2009).

4.28 Validating mTOR and PDGFR as a target for miR-145:

To validate mTOR and the PDGF receptor as potential targets for miR-145, we performed proliferation assay with mTOR knock down and co-transfected miR-145 inhibitor (Figures 4.35 & 4.36). The increase in proliferation seen earlier with miR-145 inhibitor was completely diminished when mTOR was knocked down. This finding confirms that the increase in proliferation we report with miR-145 inhibitor involves mTOR. This also strongly suggests mTOR as a target for miR-145 as the presence of high levels of miR-145 results in degradation of mTOR mRNA and correlates with a reduction in VSM cell proliferation.

Another target for miR-145 we aimed to validate was the PDGF receptor. We inhibited the PDGF receptor with imatinib. Following transfection with miR-145 inhibitor, proliferation of VSM cell was not increased and stayed at the same background level. This finding links the effect of miR-145 in targeting essential effector genes that result in the reduction of VSM cell proliferation. miR-145 here might work as a ligand that blocks PDGF receptor and therefore stops the downstream stimulation of other signalling proteins including mTOR. Or perhaps miR-145 inhibits the mTOR signalling pathway.

These results confirm that during VSM cell proliferation and migration, reduction of miR-145 results in an increase in PDGF receptors and mTOR genes. The increase of these genes promotes VSM cell proliferation and migration. However, when

mitochondria are inhibited, the expression of miR-145 is increased and the proliferation and migration of VSM cells are consequently inhibited.

The results obtained from this chapter highlight the importance of mitochondria in the expression of miRNAs involved in the initiation and progression of vascular diseases. The change in the expression of miR-21 and miR-145 following mitochondrial inhibition correlates with the reduction in proliferation and migration we reported in chapter 3 following the inhibition of mitochondrial bioactivity.

The increase in the level of miR-145 following mitochondrial inhibition along with previous data showing reduction in mTOR effector genes following mitochondrial inhibition provide further evidence of the mitochondrial role in the regulation of mTOR signalling pathway possibly through miR-145 regulation.

Looking at the gene targets we identified including mTOR and cell cycle regulatory genes and the functional analysis, we see a correlation between inhibiting mitochondrial bioactivity, reduction in miR-21 and increase in miR-145, alteration of gene expression and VSM cell modulation in proliferation and migration. miR-21 modulates genes that are involved in the activation of the apoptotic signalling pathway including SOD1 and Cdkn2a. Whereas miR-145 regulates genes that are involved in VSM cell proliferation and migration including PI3K/Akt/mTOR. This is another evidence that mitochondria could potentially target mTOR signalling pathway through the regulation of miR-145 expression within the cell. Mitochondria could also target cell cycle and apoptosis through the regulation of mR-21 expression in VSM cell.

Summary of the primary experimental findings reported in this chapter:

- Inhibiting mitochondrial dynamics results in a decrease in the expression of miR-21 and increase in the expression of miR-145.
- The decrease in miR-21 expression and the increase in miR-145 expression correlate with the decrease in VSM cell proliferation and migration.
- miR-21 induces fragmentation of mitochondria and increases VSM cell proliferation and migration

- miR-145 promotes mitochondrial fusion and reduction in VSM cell proliferation and migration.
- miR-21 could potentially target pro-apoptotic proteins including p53 and ROS scavenging proteins including SOD1
- miR-145 likely targets mTOR effector genes including PI3K, Akt and mTOR as well as targeting PDGF receptor.

Chapter 5

Mitochondrial Regulation of Exosomal MicroRNA Cargo in Vascular Smooth Muscle Cell Proliferation

5.1 Introduction

Cells of different types secrete vesicles which differ in their size and composition. They are classified into three main groups: apoptotic blebs, micro-vesicles and exosomes.

Exosomes are extracellular organelles of endocytic origin released by different cell types into the extracellular space. Their size ranges between 40-100 nm in diameter and they perform different biological functions through mediating cell to cell communication (Simpson et al., 2008). They are also considered another class of signal mediators as they carry proteins and nucleic acids such as mRNA and miRNA which regulate gene expression of some signalling cascades. Exosomes can be found in many body fluids such as blood, saliva, cerebrospinal fluids, urine, breast milk and seminal fluid (Mathivanan and Simpson, 2009). Their ability to transfer proteins and nucleic acids from one cell to another emphasises their potential role in different pathological and physiological conditions (Schorey and Bhatnagar, 2008).

Exosomes are physically characterised by their size which ranges between 30-120 nm in diameter and the cup-like morphology seen in transmission electron microscope or round well delimited vesicles as seen in cryo-electron microscope (Conde-Vancells et al., 2008). Sucrose gradient is also used to purify exosomes which float at a density range 1.13-1.19 g/ml (Thery et al., 2006). Exosomes are also characterised based on their protein and lipid composition. They contain proteins involved in membrane transport and fusion such as flotillins and annexins, proteins involved in multivesicular body formation such as alix and tetraspanins such as CD9, CD63 and CD81 (Wubbolts et al., 2003). Exosomes are also rich in cholesterol, ceramide, glycerophospholipids and sphingolipids (Subra et al., 2007).

5.2 Biogenesis of exosomes:

Exosomes originate from cellular endosomes that fuse with the membrane and form inwardly budding vesicles that is then released into body fluids. They originate in the intraluminal vesicles (ILVs) of the multivesicular bodies (MVBs) which fuse with the plasma membrane releasing exosomes into the extracellular space (Simons and Raposo, 2009). This requires contractile force to bring the opposing membranes together which is regulated by soluble NSF attachment protein receptor (SNARE) (Sudhof and Rothman, 2009). This protein then forms a complex which anchors the interacting proteins in the membrane (Fukuda et al., 2000). The SNARE complex vesicle associated membrane protein7 (VAMP7) has also been demonstrated to participate in exocytosis by mediating the fusion of MVBs with the plasma membrane (Fader et al., 2009). Endosomal sorting complex required for transport (ESCRT) is also essential for the formation of MVBs. It is recruited to the cytosolic side of the endosomal membrane to sort selected proteins to the ILVs (Katzmann et al., 2002). The process starts with the recruitment of Tsg101 which belongs to the ESCRT-I complex to form a complex that binds the ubiquitinated cargo proteins and activates the ESCRT-II complex (Figure 5.1). ESCRT-II complex then initiates the formation of ESCRT-III complex which helps in the sequestration of MVB proteins and recruits an enzyme to remove the ubiquitin tag from the protein cargo before sorting them into ILVs (Raiborg et al., 2003). ESCRT-III is then degraded by ATPase.

Other proteins involved in the release of exosomes are the Rab family proteins including Rab27a, Rab27b and Rab35 (Ostrowski et al., 2010). These Rab family members have been implicated in determining the size of the MVBs, the distribution of the MVBs in the cytoplasm and the release of exosomes into the extracellular environment (Hsu et al., 2010). Tumour repressor protein p53 and its downstream effector TSAP6 were also found to play vital role in regulating the production of exosomes possibly through regulating the transcription of other genes involved in the production and secretion of exosomes (Yu et al., 2006).

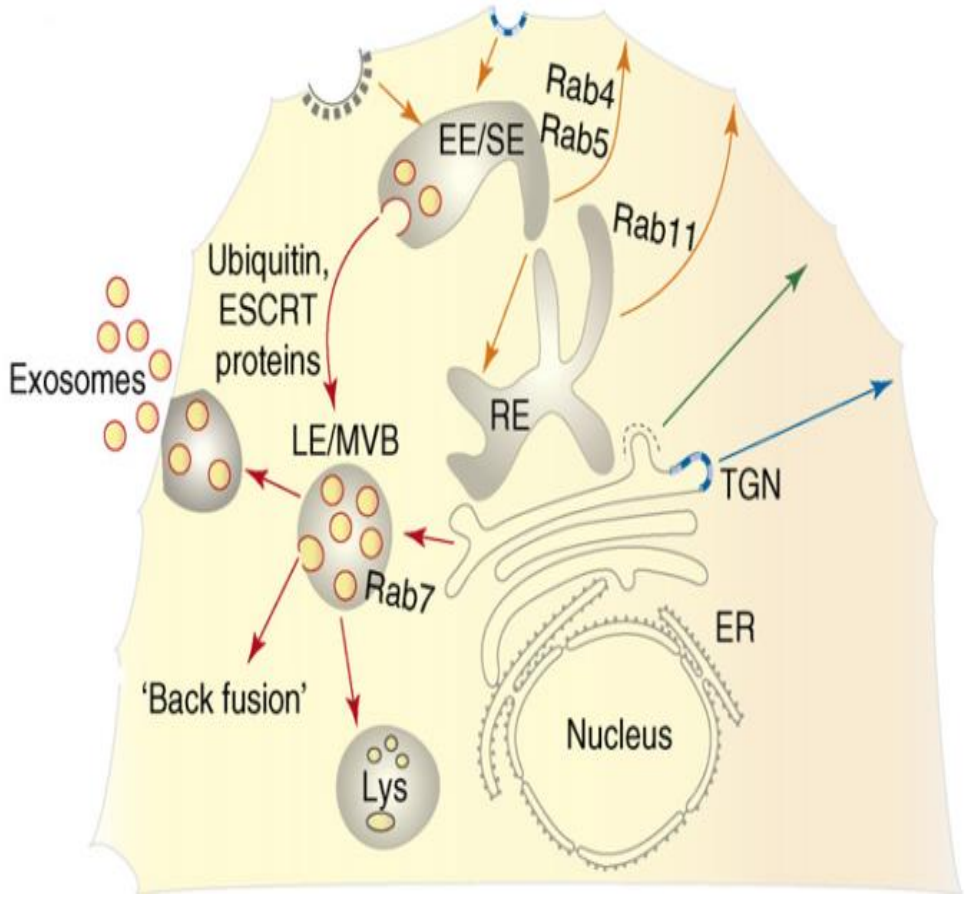

Figure 5.1 *schematic diagram showing the biogenesis of exosomes involving proteins such as Rab family and ESCRT, adapted from (Lakkaraju and Rodriguez-Boulan, 2008). ESCRT: Endosomal sorting complex required for transport, ER: Endoplasmic Reticulum, Lys: Lysosomes, MVB: Multi-vesicular Body, EE: Early Endosome, SE: Sorting Endosome, RE: Recycling Endosome, TGN: Trans-Golgi Network.*

5.3 Trafficking of exosomes:

Exosomes released by one cell might exert their biological effect through one of three possible mechanisms (Figure 5.2). The proteins in the exosomal transmembrane might directly interact with signalling receptors of the recipient cell after being cleaved by proteases and soluble fragments act as soluble ligands. This

could trigger the activation of specific signalling pathways leading to functional changes in the cell (Munich et al., 2012). Exosomes could also fuse to the membrane of the target cell and deliver the cargo into the cytosol including mRNAs, miRNAs and proteins. This cargo then activates or inhibits signalling pathways (Mulcahy et al., 2014). Furthermore, exosomes could be engulfed by the target cell where they will be merged with endosomes and released into other neighbouring cells. Or they will mature into lysosomes and undergo degradation (Tian et al., 2013).

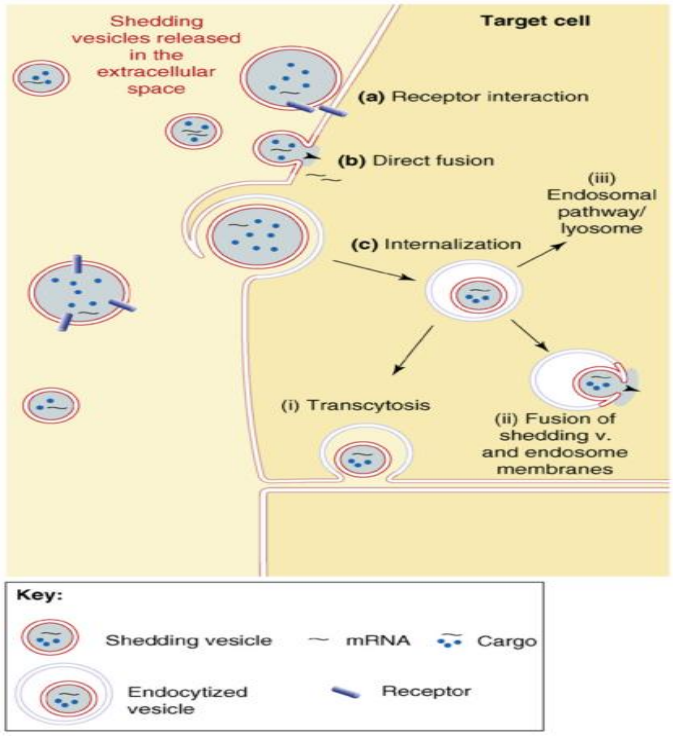

Figure 5.2 *schematic diagrams showing the three different ways through which the exosomes exert their effect in the recipient cell (Cocucci et al., 2009).*

A number of factors have been reported to influence the uptake of exosomes by the recipient cells. one of these factors is the presence of proteins that are important for adhesion and growth on the exosomal surface including annexins (Koumangoye et al., 2011). Exosomal internalisation was also seen to be affected when cells and their derived exosomes were treated with protease k. This suggests that the proteins that

are important in the uptake of exosomes are present in the surface of the cell and the exosomes (Escrevente et al., 2011).

Exosomes are being used as bio markers for many disease conditions because of their unique cargo of mRNAs, miRNAs and proteins (Hu et al., 2012). Exosomes isolated from diseased subjects including ovarian cancer patients contained different miRNAs than exosomes isolated from healthy subjects (Taylor and Taylor, 2008). The unique gene profile of exosomes isolated from cancer cells makes it one of the ways in identifying tumour development (Rabinowits et al., 2009).

5.4 Functionality of exosomal Cargo:

Increasing evidence demonstrates that exosomes play a vital role in regulating cellular bioactivities (Pant et al., 2012). Exosomes derived from cells stimulated by growth factors were reported to increase proliferation and chemoinvasion in lung adenocarcinoma cell line (Janowska-Wieczorek et al., 2005). The study found that these exosomes stimulated proliferation through the upregulation of expression of cyclin D and the phosphorylation of ERK1/2 and Akt. The metastasis was also induced by the expression of membrane type 1-matrix metalloproteinase. Exosomes have been shown to promote proliferation of gastric cancer cell line (Qu et al., 2009) and endothelial cell angiogenesis in epithelial ovarian cancer cells (Millimaggi et al., 2007). Exosomes also change cellular phenotype of the recipient cells through the exosomal cargo of TGF-β. Exosomes isolated from cancer cell lines including prostate cancer, bladder cancer, colorectal cancer and breast cancer were incubated with primary fibroblasts and transformed them to myofibroblasts (Webber et al., 2010). TFG-β was seen to drive SMAD-dependent signalling which contributes to the modulation of the stromal-extracellular matrix. Although the full mechanism is not understood, TFG-β was seen to trigger changes in the actin cytoskeleton and an increase in the structural α-SMA which contributes to the change in the phenotype.

The content of the exosomes is the key factor that plays the major role in regulating the biological functions of the recipient cells. Although all different components of the exosomal cargo are important in regulating biological functions of the cell including proteins and mRNAs, miRNAs are considered the main contributor to this

functional regulation (Zhang et al., 2015) and their expression can be higher in exosomes than in their parental cells (Goldie et al., 2014). Exosomal miRNAs exert their effect either by negatively regulating their target genes on the recipient cell and changing the cellular biological functions or by acting as a ligand binding the receptor and activating certain signalling pathways (Fabbri et al., 2012).

Functional mRNAs are also an important component of the exosomal cargo that can be translated into functional proteins in the target cell (Valadi et al., 2007). The inclusion of mRNAs from the parental cell into the released exosomes seems to be selective and not all mRNAs are included (Urbanelli et al., 2013). Mitochondrial DNA was also found to be carried in exosomes. This DNA is thought to be transferred to the mitochondria of the recipient cell where they exert their effect. This finding is very important as it suggests a link between mitochondrial bioactivity and exosomal cargo (Guescini et al., 2010).

Exosomes were also found to play important role in the development of cardiovascular diseases including atherosclerosis and re-stenosis (Su et al., 2017). A study by Lightell et al. (2017) revealed that exosomes isolated from VSM cells from a diabetic mouse contained high level of miR-221 and miR-222. Both miRNAs are involved in the initiation and progression of atherosclerosis when compared to the exosomes isolated from non-diabetic mouse. When these exosomes were administered to $ApoE^{-/-}$ mice, atherosclerosis lesions was reported to develop faster (Lightell and Woods, 2015). Exosomes isolated from cultured human VSM cell calcification model were also reported to be enriched in calcium-binding and extracellular matrix proteins (Kapustin et al., 2015). VSM cell calcification is a component of late atherogenesis. This was seen to be triggered by TNF-α and PDGF leading to increased calcification of VSM cells. Furthermore, administration of exosomes isolated from endothelial progenitor cells resulted in acceleration of the re-endothelialisation process in a rat model of balloon-induced vascular injury (Fadini et al., 2012). This finding highlights potential positive and negative roles played by exosomal content in atherogenesis and vascular repair following injury.

5.5 Chapter Aims:

The aims of this chapter are:

- To isolate exosomes released by VSM cells cultured under 0.1% FCS, PDGF, PDGF + MDivi-1, 21 days cultured and Rho cells.
- To measure mRNA cargo levels contained in these exosomes.
- To measure miRNA cargo levels contained in these exosomes.
- To identify protein cargo contained in these exosomes.

5.6 Specific Methods

5.7 Cell culture for exosomes isolation:

Vascular smooth muscle cells were cultured in T75 flasks at Passage 1. The cells were then divided into five treatment groups as follows: 0.1% FCS, 20ng/ml PDGF, 20ng/ml PDGF + 10μM MDivi-1, 21 days cultured in 10% FCS, and mitochondrial-depleted cells. Six T75 flasks were used for each treatment with 10ml of culture media in each flask. Serum containing media was removed and cells were washed twice with Opti-MEM media to remove any traces of the serum. The cells were then incubated in Opti-MEM for 48 hours before the media was collected for ultracentrifugation.

5.8 Exosome isolation*:*

Media from all six T75 flasks of each treatment was divided into two 50 ml tubes. The tubes are spun at 2000 g for 10 minutes to remove large dead cells. The resulting pellet was discarded and the supernatant re-spun at 10000 g for 30 minutes at 4^{o}C to remove large cell debris. The pellet again was discarded and the supernatant run through a 0.2 μm filter to exclude any microvesicles and apoptotic blebs. The flow was again re-spun at 100,000 g for 70 minutes at 4^{o}C. The resulting pellet was considered to contain exosomes and potential contaminating proteins. The pellet was washed in 1 ml PBS and re-spun again at 100,000 g for 70 minutes at 4^{o}C. The resulting final pellet was now considered to contain exosomes. The pellet was finally re-suspended in 250 μl of PBS and stored at -80^{o}C.

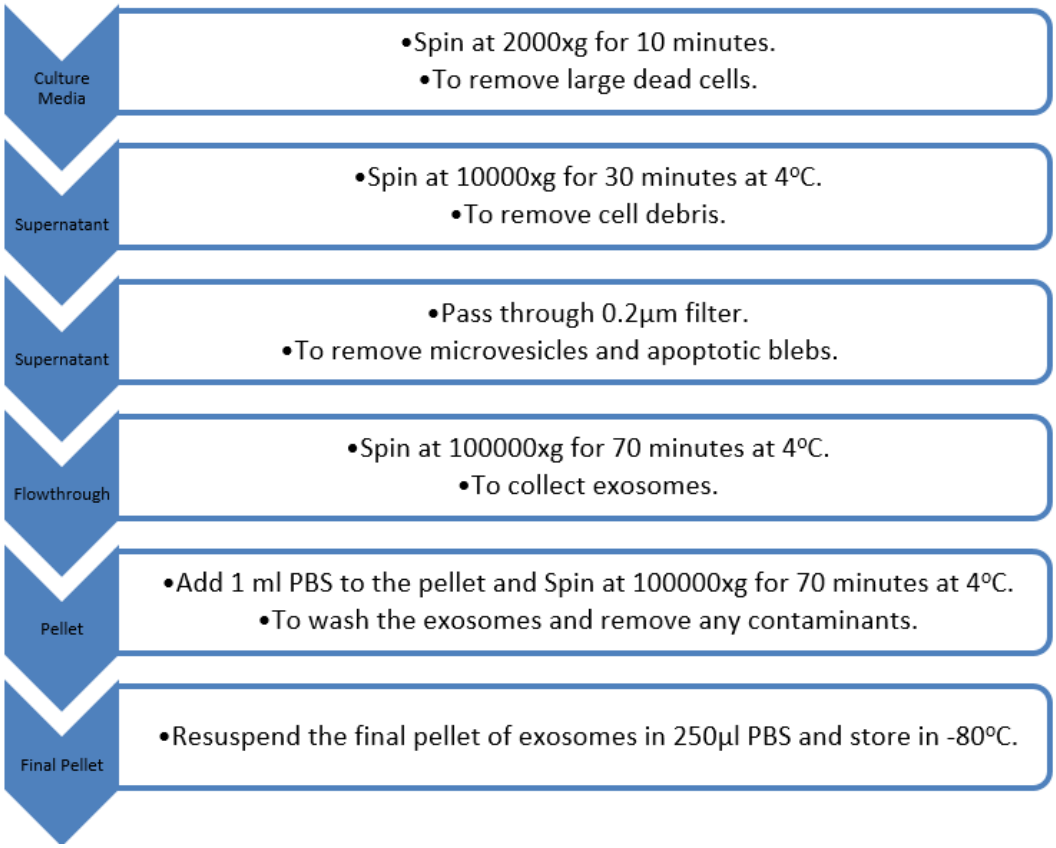

Figure 5.3 *shows the process of exosomes isolation using ultracentrifugation method*

5.9 Samples protein concentration determination*:*

Protein concentration in each sample was measured using Bradford assay standard curve. 10µl of each sample was diluted in 790 µl of PBS and 200 µl of protein assay reagent to make a total volume of 1 ml in a cuvette. Absorbance of each sample was then read at 595nm in a spectrometer and the corresponding protein concentration was recorded.

5.10 Exosome size distribution:

25 µg/ml of the exosome sample was analysed using the zeta sizer to measure particles size distribution. 20 µl of the sample was added to 980 µl of PBS in zeta sizer cuvette and measured for particle size using Malvern zetasizer.

5.11 Confirmation of exosomes by western blotting*:*

20μg of the total protein was loaded and run in 10%SDS-PAGE at 200V for 45 minutes. The proteins were then transferred onto a nitrocellulose membrane at 100V for 60 minutes. This was followed by blocking the membranes using 5% milk. The membranes were incubated overnight at 4^{o}C in the following primary antibodies: CD9 (1:2000; Life Technologies, Paisly, UK), CD63 (1:2000; Life Technologies, Paisly, UK) and CD81 (1:2000; Life Technologies, Paisly, UK). The following day the membranes were washed four times of 10 minutes each with TTBS. The membranes were incubated in anti-mouse secondary antibody (1:10000; sigma,UK) for 60 minutes at room temperature. This was followed with four washes of 10 minutes each with TTBS. Enhanced Chemiluminescence Reagent (ECL) mixture was prepared in the dark room and applied to each nitrocellulose membrane for 1 minute with agitation, lifted from the tray onto a paper towel to remove any excess ECL. The membranes were then placed in exposure cassettes with an X-ray film on top (Kodak Ls X-OMAT) for the required exposure time under dark room conditions and developed using X-OMAT (KODAK M35-M X-OMAT processor).

5.12 Imaging of exosomes using confocal microscopy:

10 μl of the exosomes suspension was taken and added to 990 μl of Hanks Balanced Salt Solution (HBSS). 1 mg/ml of labelling solution of wheat germ agglutinin conjugates was prepared and added to the exosomal mixture at a concentration of 10 μg/ml and incubated for 30 minutes at 37^{o}C. The labelled exosomes were visualised using confocal microscope for alexa-fluor 488.

5.13 Exosomal RNA isolation*:*

150 μg of exosomes re-suspended in 200 μl of PBS was used to isolate RNA using exosomal RNA and protein extraction kit (101 Bio, USA). One volume of 2 x denaturing solution was added to each exosome sample and mixed. The mixture was incubated on ice for 5 minutes. One volume of acid-phenol: chloroform was added to each sample. The sample was mixed by vortexing for 60 seconds. The sample was then centrifuged at 10000 g for 5 minutes at room temperature to separate the mixture into aqueous and organic phases. The upper aqueous phase was removed and

transferred into a fresh tube. Thereafter, 1.25 volumes of 100% ethanol was added to the aqueous phase and mixed thoroughly. The mixture was then passed through filter cartridge, centrifuged at 10000 g for 15 seconds and collected in a collection tube. The flow-through was discarded and the filter cartridge was washed using 700µl miRNA wash solution and centrifuged at 10000 g for 15 seconds. The filter cartridge was washed with 500 µl wash solutions 2&3 twice and centrifuged at 10000 g for 1 minute to remove residual fluid from the filter. RNA was eluted by applying 50 µl of preheated (95^{o}C) elution solution to the centre of the filter and centrifuged for 30 seconds to remove the RNA. Elution step was repeated once more with another 50 µl of elution solution. RNA was collected in a tube and stored in -80^{o}C.

5.14 Protein content identification using mass spectrometry, tryptic digestion*:*

40 µg of the sample was added to 10 µl of 0.5 mg/ml myoglobin solution with 10 µl of acetonitrile and mixed gently. This was followed with the addition of 10 µl of 0.1 M Tris (2-carboxyethyl) phosphine (TCEP, Sigma, UK) in water to each sample and the samples were incubated for 30 minutes at room temperature. 10 µl of 0.2 M iodacetamide (IOA, Sigma, UK) in water was then added to each sample and the samples were incubated for further 30 minutes at room temperature. This was followed with the addition of 10 µl of 0.2 M L-Cysteine (Sigma, UK), 145 µl of digestion buffer (pH 7.9) and 10 µl of trypsin in 50 mM acetic acid and the samples were incubated overnight at 37^{o}C. The samples were then diluted 1:1 with 20% acetonitrile after centrifugation for 10 minutes at 7000 rpm. Samples were then transferred to auto sampler vials for analysis.

5.15 ESI-LCMS analysis*:*

Samples were analysed using an LTQ Orbitrap classic equipped with an electrospray ionization source (Thermo Fisher Scientific, Hemel Hempstead, UK). 50 mL of filtrate samples were added to 50 mL of a solution composed of 2% ACN and 0.1% formic acid. Chromatographic separation of peptides was performed using a C18 column (phenomenex x 100 x 4.6 mm 130 A). The ESI interface was operated in a positive ion mode with a spray voltage of 4.5 kV. The temperature of the ion transfer capillary was 275^{o}C and the flow rates of the sheath and auxiliary gases were 50 and 17 arbitrary units respectively. Mobile phase A consisted of (water/acetonitrile 98/2

vol/vol, 0.1% formic acid) and the flow rate was 300 nL/min. Runs were performed under a 60 min linear gradient from 10 to 45% of solvent B (water/acetonitrile 2/98 vol/vol, 0.1% formic acid) followed by a 10 min purge step at 95% of B before a 20 min re-equilibration step to the starting conditions.

5.16 LCMS/MS analysis*:*

The fragmentation mass spectra results were obtained using collision energy of 35 V. The full-scan mass spectrum was followed by a data dependent MS^2 scan of the marker peptide m/z values. Peptides were identified manually with the use of a theoretical list obtained from the bioinformatics resource portal ExPASy© website. Xcalibur 2.1.0 mass spectrometry software (Thermo Fisher Scientific) was used to quantify the results.

5.17 Results

5.18 Characterisation of exosomes:

Exosomes isolated using ultracentrifugation method were characterised by their size, morphology and the presence of exosomal protein markers. Results show that exosomes ranged in size between 37 nm – 255 nm depending on the culture conditions (Figures 5.4 – 5.8).

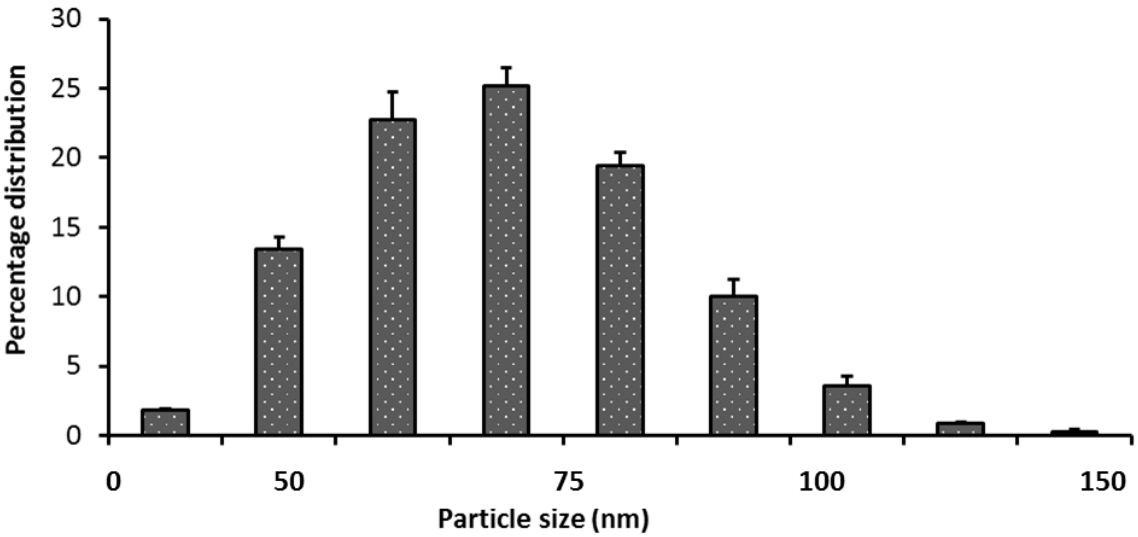

Figure 5.4 *Graph shows size distribution of secreted vesicles in the 0.1% FCS treated media (n=3).*

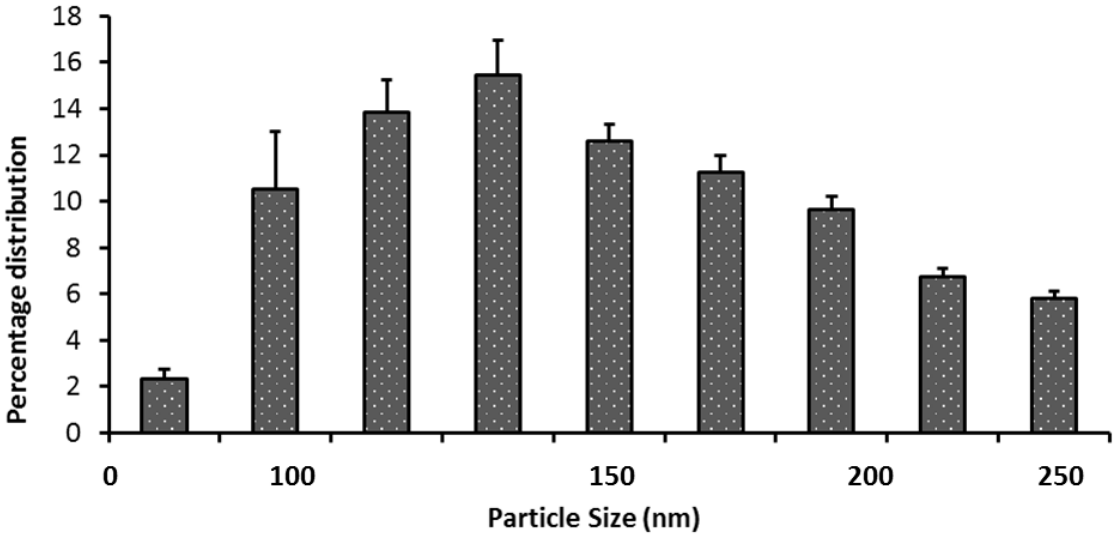

Figure 5.5 *Graph shows size distribution of secreted vesicles in the 20ng PDGF stimulated cells (n=3).*

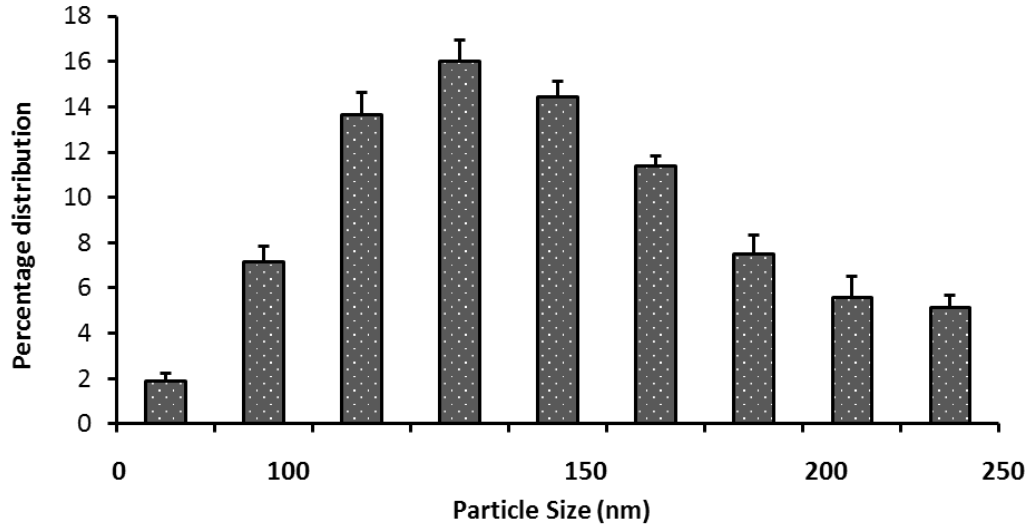

Figure 5.6 *Graph shows size distribution of secreted vesicles in the 20ng PDGF stimulated cells treated with mitochondrial fission inhibitor MDivi-1 (n=3).*

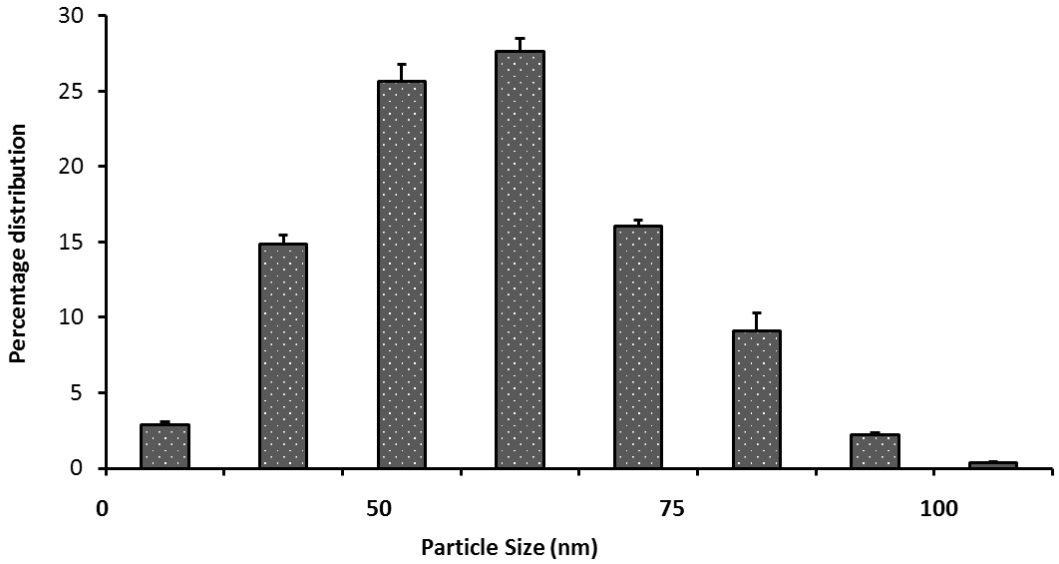

Figure 5.7 *Graph shows size distribution of secreted vesicles in the 21 days cultured cells (n=3).*

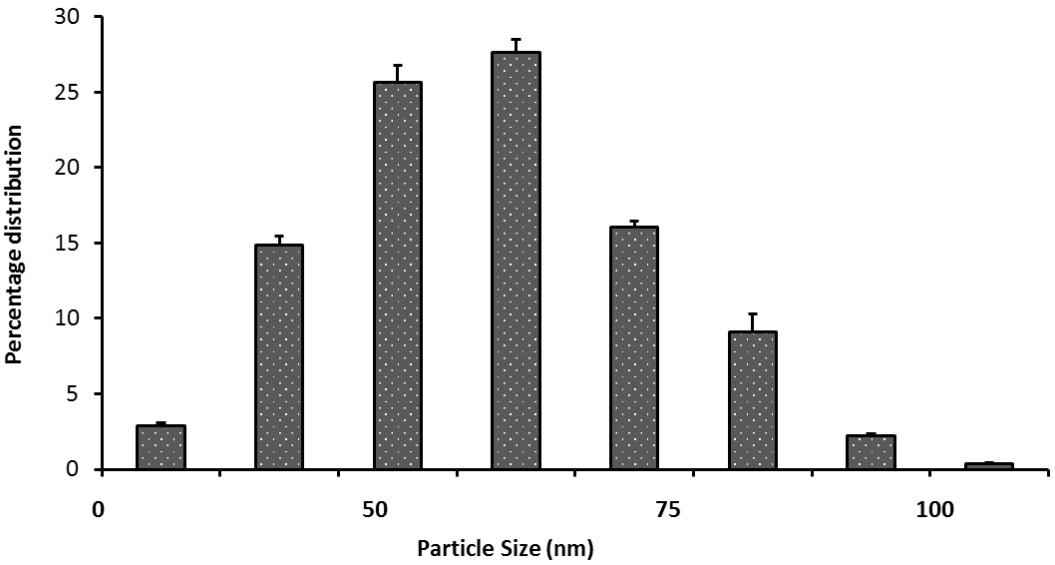

Figure 5.8 *Graph shows size distribution of secreted vesicles in the mitochondrial-incompetent Rho cells (n=3).*

Western blotting results also showed the presence of exosomes-specific protein markers CD9 and CD81 (Figure 5.9).

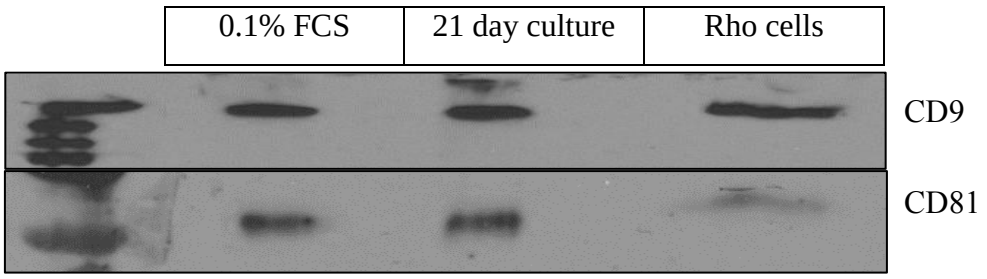

Figure 5.9 *shows the presence of exosome-specific tetraspanin protein markers in 0.1%FCS, 21 days cultured cells and mitochondrial-depleted cells. (A) Confirms the presence of CD9 in all three treatments and (B) confirms the presence of CD81 in all three treatments (n=3).*

Images obtained from confocal microscopy also confirmed the size of exosomes between 20 nm -120 nm (Figure 5.10).

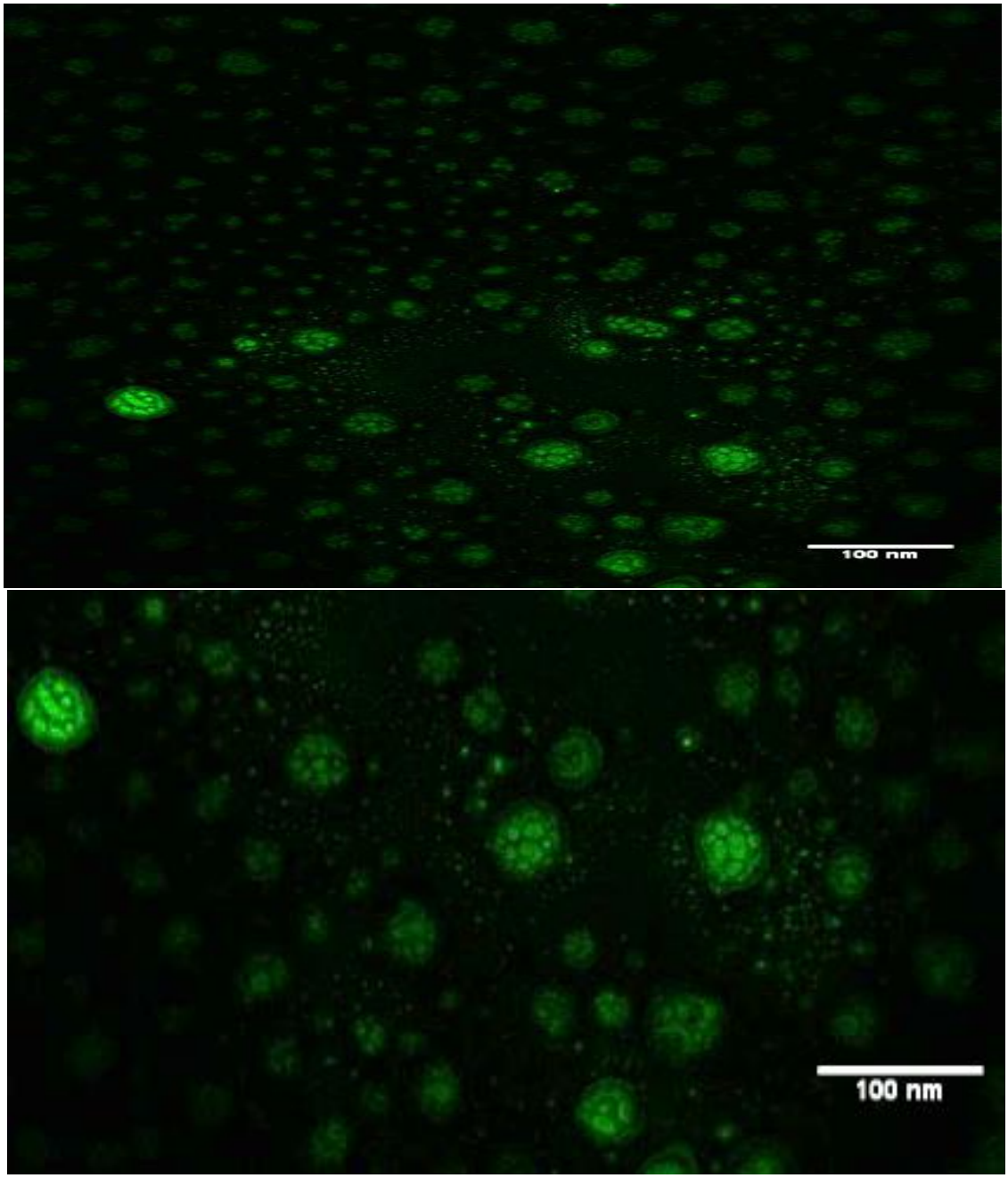

Figure 5.10 *Images show the size and the round shape of the exosomes isolated from 21 day cultured VSM cells using confocal microscope x 315 magnification. Exosomes were stained by wheat germ agglutinin conjugate and visualised at wavelength 488 nm.*

RNA concentration isolated from exosomes released by VSM cells cultured under different conditions varied significantly. The concentration of RNA isolated from 0.1% FCS 70.2 ± 10.2 ng/µl was similar to the concentration isolated from Rho cells 70.8 ± 4.7 ng/µl. However, the concentration of RNA was remarkably higher in exosomes isolated from 21 days cultured cells 118.7 ± 2.4 ng/µl (Table 5.1)

Condition	RNA Yield (ng/µl)
0.1% FCS	70.2 ± 10.2
21 day cultured	118.7 ± 2.4
Mito-depleted (Rho)	70.8 ± 4.7

Table 5.1 *Table lists the mean RNA yield extracted from isolated from VSMC cultured in 0.1% FCS, 21 days cultured cells and mitochondrial-depleted cells (n=3).*

Protein concentration isolated from exosomes released by VSM cells cultured under different conditions was also different. The concentration of protein isolated from 0.1% FCS was 120 ± 5 µg/250µl and the protein concentration in exosomes isolated from Rho cells was 105 ± 2.5 µg/250µl. However, the concentration of protein in exosomes isolated from 21 days cultured cells was 130 ± 2.5 µg/250µl (Table 5.2)

Condition	Size (nm)	Protein (µg/250µl)
0.1% FCS	84.6 ± 0.8	120 ± 5
21 day cultured	66.2 ± 0.5	130 ± 2.5
Mito-depleted (Rho)	97.4 ± 0.6	105 ± 2.5

Table 5.2 *Table lists the mean size of exosomes and the mean protein concentration extracted from exosomes isolated from VSMC cultured in 0.1% FCS, 21 days cultured cells and mitochondrial-depleted cells (n=3).*

5.19 Effect of inhibiting mitochondria on exosomes mRNA cargo of VSM cells:

RT-qPCR results show different levels of mRNA cargo in exosomes. The level varied greatly depending on the culture conditions. Results show that the level of PI3K in exosomes isolated from 20 ng/ml PDGF stimulated cells is 9 ± 4 fold higher than the level in exosomes isolated from 0.1% FCS cultured cells. However, the level of PI3K gene in exosomes following treatment with mitochondrial fission inhibitor MDivi-1 is reduced to 0.9 ± 0.07 fold. Results also show that the level of PI3K gene in exosomes isolated from 21 days cultured cells is 6.7 ± 1 fold higher than the level in exosomes isolated from 0.1% FCS cultured cells. Furthermore, the level of PI3K in exosomes isolated from Rho cells was reduced to near basal level (Figure 5.11)

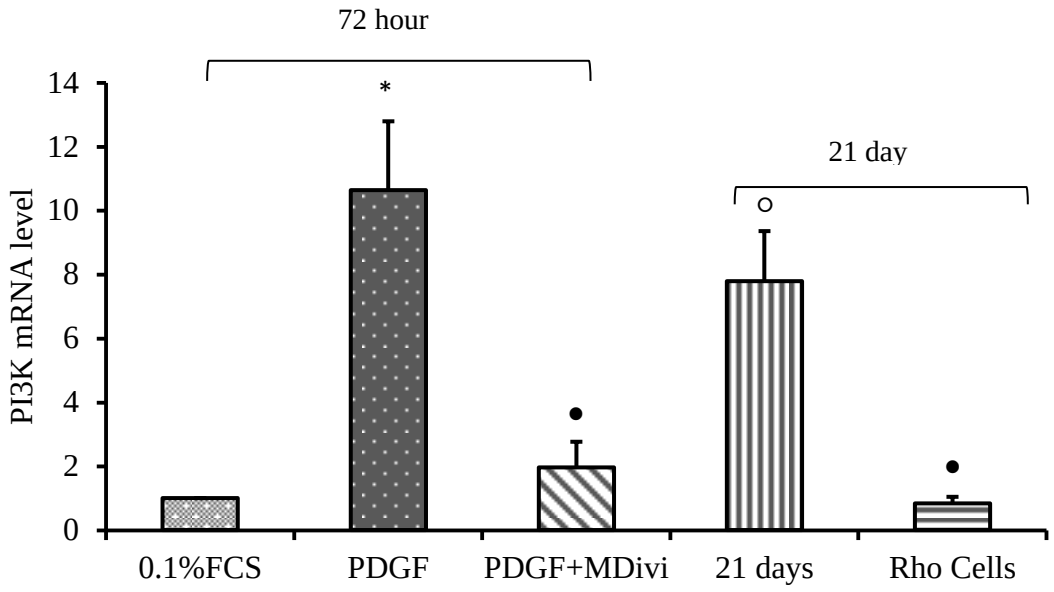

Figure 5.11 *level of PI3K inside the exosomes was measured using QPCR for 0.1% FCS cultured cells, PDGF stimulated cells, PDGF + MDivi-1 treated cells, 21 days cultured cells and Rho cells (n=3), *p<0.05 compares PDGF stimulated VSM cells vs 0.1% FCS cultured VSM cells, ○p<0.05 compares 21 days cultured VSM cells vs 0.1% FCS cultured VSM cells, ●p<0.05 compares PDGF + MDivi-1 and Rho cells vs PDGF stimulated cells and 21 days cultured VSM cells.*

Results also show that the level of Akt in exosomes isolated from 20 ng/ml PDGF stimulated cells is 141 ± 19 fold higher than the level in exosomes isolated from 0.1% FCS cultured cells. The level of Akt in exosomes following treatment with mitochondrial fission inhibitor MDivi-1 is reduced to 15 ± 7 fold increase for Akt compared with exosomes isolated from 0.1% FCS cultured cells. Results also show that the level of Akt in exosomes isolated from 21 days cultured cells is 3.4 ± 1 fold higher than the level in exosomes isolated from 0.1% FCS cultured cells. Furthermore, the level of Akt in exosomes isolated from Rho cells was reduced to near basal level (Figures 5.12)

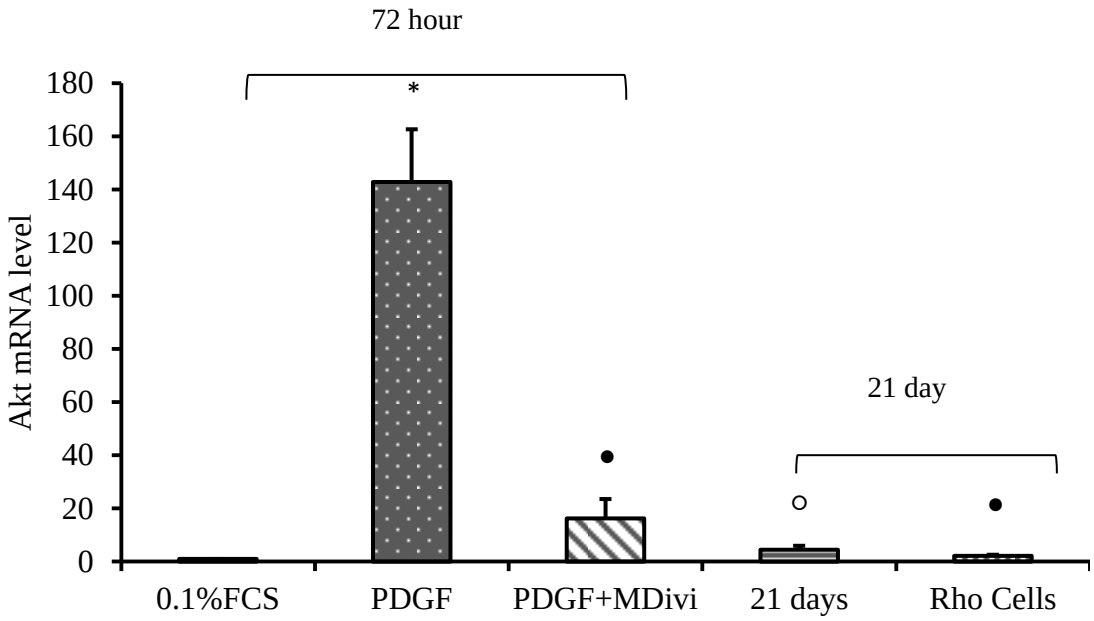

Figure 5.12 *level of Akt inside the exosomes was measured using QPCR for 0.1% FCS cultured cells, PDGF stimulated cells, PDGF + MDivi-1 treated cells, 21 days cultured cells and Rho cells (n=3), *p<0.05 compares PDGF stimulated VSM cells vs 0.1% FCS cultured VSM cells, ○p<0.05 compares 21 days cultured VSM cells vs 0.1% FCS cultured VSM cells, ●p<0.05 compares PDGF + MDivi-1 and Rho cells vs PDGF stimulated cells and 21 days cultured VSM cells.*

Results show that the level of 4EBP1 in exosomes isolated from 20 ng/ml PDGF stimulated cells is 0.3 ± 0.05 fold higher than the level in exosomes isolated from 0.1% FCS cultured cells. However, the level of 4EBP1 in exosomes following treatment with mitochondrial fission inhibitor MDivi-1 did not change significantly when compared with exosomes isolated from 0.1% FCS cultured cells. Results also show that the level of 4EBP1 in exosomes isolated from 21 days cultured cells is 5.6 ± 0.9 fold higher than the level in exosomes isolated from 0.1% FCS cultured cells. The level of these genes in exosomes isolated from Rho cells was reduced to near basal level (Figures 5.13).

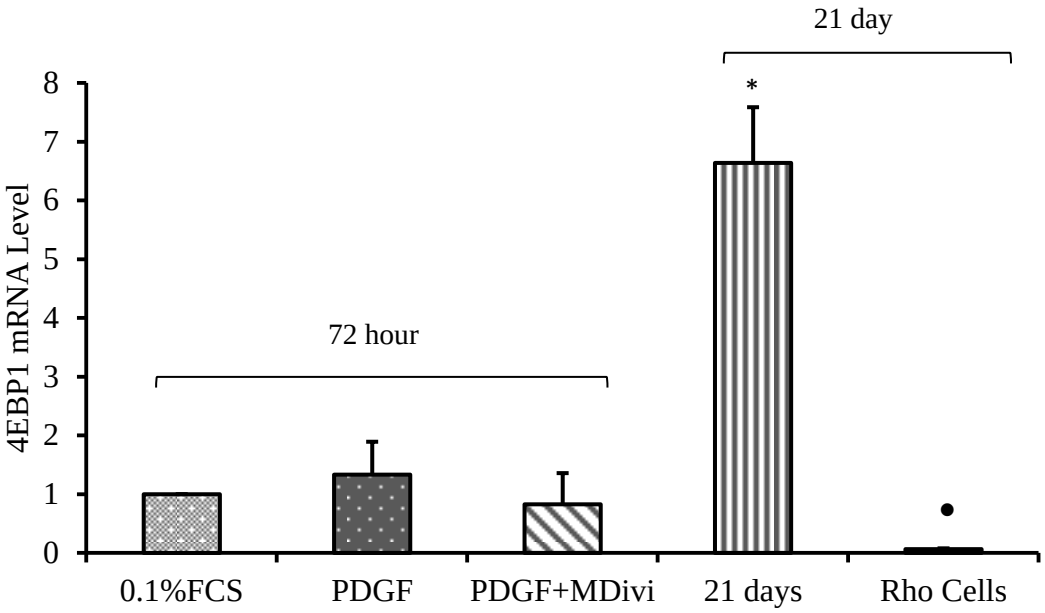

Figure 5.13 *level of 4EBP1 inside the exosomes was measured using QPCR for 0.1% FCS cultured cells, PDGF stimulated cells, PDGF + MDivi-1 treated cells, 21 days cultured cells and Rho cells (n=3), *p<0.05 compares 21 days cultured VSM cells vs 0.1% FCS cultured VSM cells, ●p<0.05 compares Rho cells vs 21 days cultured VSM cells.*

Results also show that the level of cell cycle inhibitory gene cdkn2a is 50 ± 1% lower in exosomes isolated from 20 ng/ml stimulated cells and 90 ± 7% lower in exosomes isolated from 21 days cultured cells compared to the level in exosomes isolated from 0.1%FCS cultured cells. The level of expression of cdkn2a is 100 ± 30% higher in exosomes isolated from Rho cells compared to exosomes isolated from 0.1%FCS cultured cells (Figure 5.14).

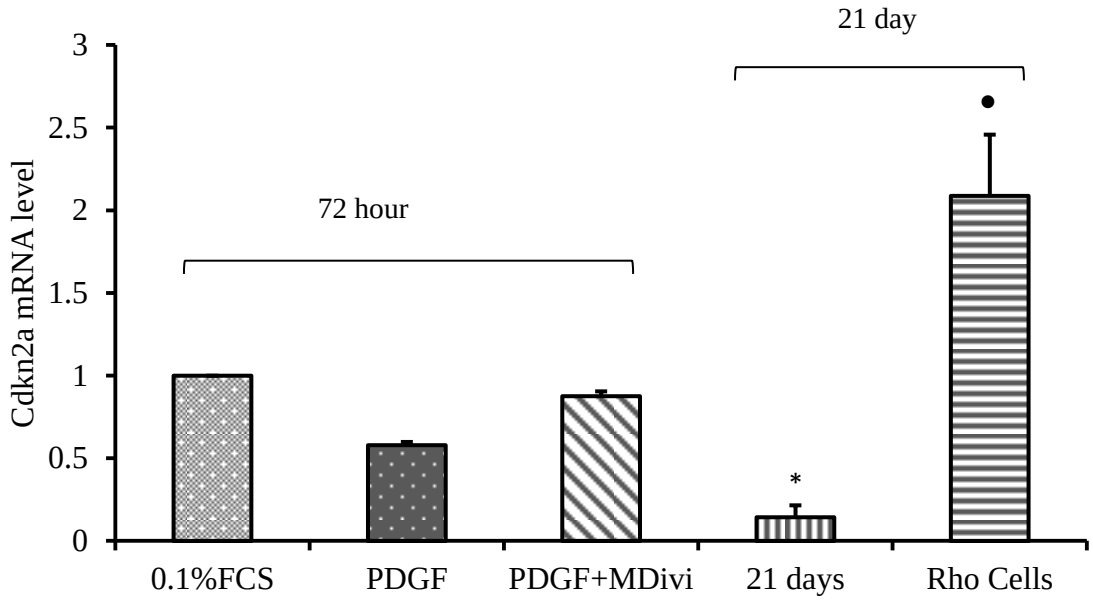

Figure 5.14 *level of Cdkn2a inside the exosomes was measured using QPCR for 0.1% FCS cultured cells, PDGF stimulated cells, PDGF + MDivi-1 treated cells, 21 days cultured cells and Rho cells (n=3), *p<0.05 compares 21 days cultured VSM cells vs 0.1% FCS cultured VSM cells, ●p<0.05 compares Rho cells vs 21 days cultured VSM cells.*

5.20 Effect of mitochondrial inhibition on exosomal miRNA cargo in VSM cells:

RT-qPCR results show different levels of miRNA cargo in exosomes. Results show that the level of miR-21 in exosomes isolated 21 days cultured cells is 7.8 ± 1 fold higher than the level in exosomes isolated from 0.1% FCS cultured cells. Their level in exosomes isolated from Rho cells show a significant reduction by 8 ± 0.5 fold (Figure 5.15).

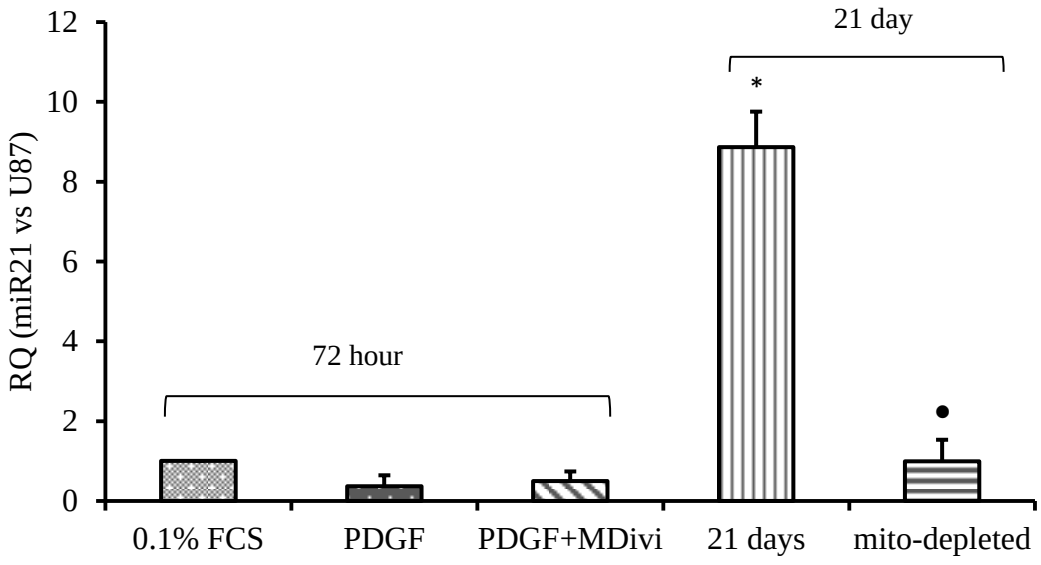

Figure 5.15 *level of miR21 inside the exosomes was measured using QPCR for 0.1% FCS cultured cells, PDGF stimulated cells, PDGF + MDivi-1 treated cells, 21 days cultured cells and Rho cells (n=3), *p<0.05 compares 21 days cultured VSM cells vs 0.1% FCS cultured VSM cells, ●p<0.05 compares Rho cells vs 21 days cultured VSM cells.*

Results also show that the level of miR145 is lower by 70 ± 10% and 40 ± 10% in exosomes isolated from 20 ng/ml stimulated cells and 21 days cultured cells respectively. The level of miR-145 is 2 ± 0.5 fold and 1.5 ± 0.5 fold higher in exosomes isolated from MDivi-1 treated cells and Rho cells respectively (Figure 5.16).

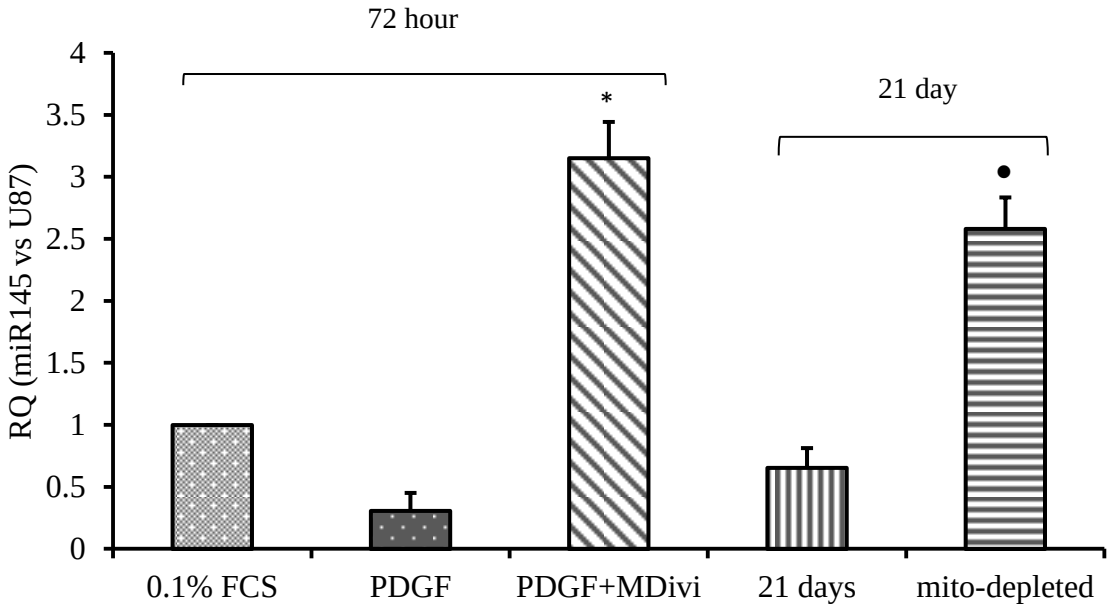

Figure 5.16 *level of miR145 inside the exosomes was measured using QPCR for 0.1% FCS cultured cells, PDGF stimulated cells, PDGF + MDivi-1 treated cells, 21 days cultured cells and Rho cells (n=3), *p<0.05 compares PDGF + MDivi-1 treated cells vs PDGF stimulated VSM cells, ●p<0.05 compares Rho cells vs 21 days cultured VSM cells.*

5.21 Effect of mitochondrial inhibition on exosomal protein content in VSM cells:

Results from mass spectrometry show that there were significant differences in the protein cargo within exosomes isolated from VSM cells (Figure 5.17). Different protein have been identified in exosomes isolated from 0.1% FCS, 21 days cultured cells and Rho cells (Table 5.3).

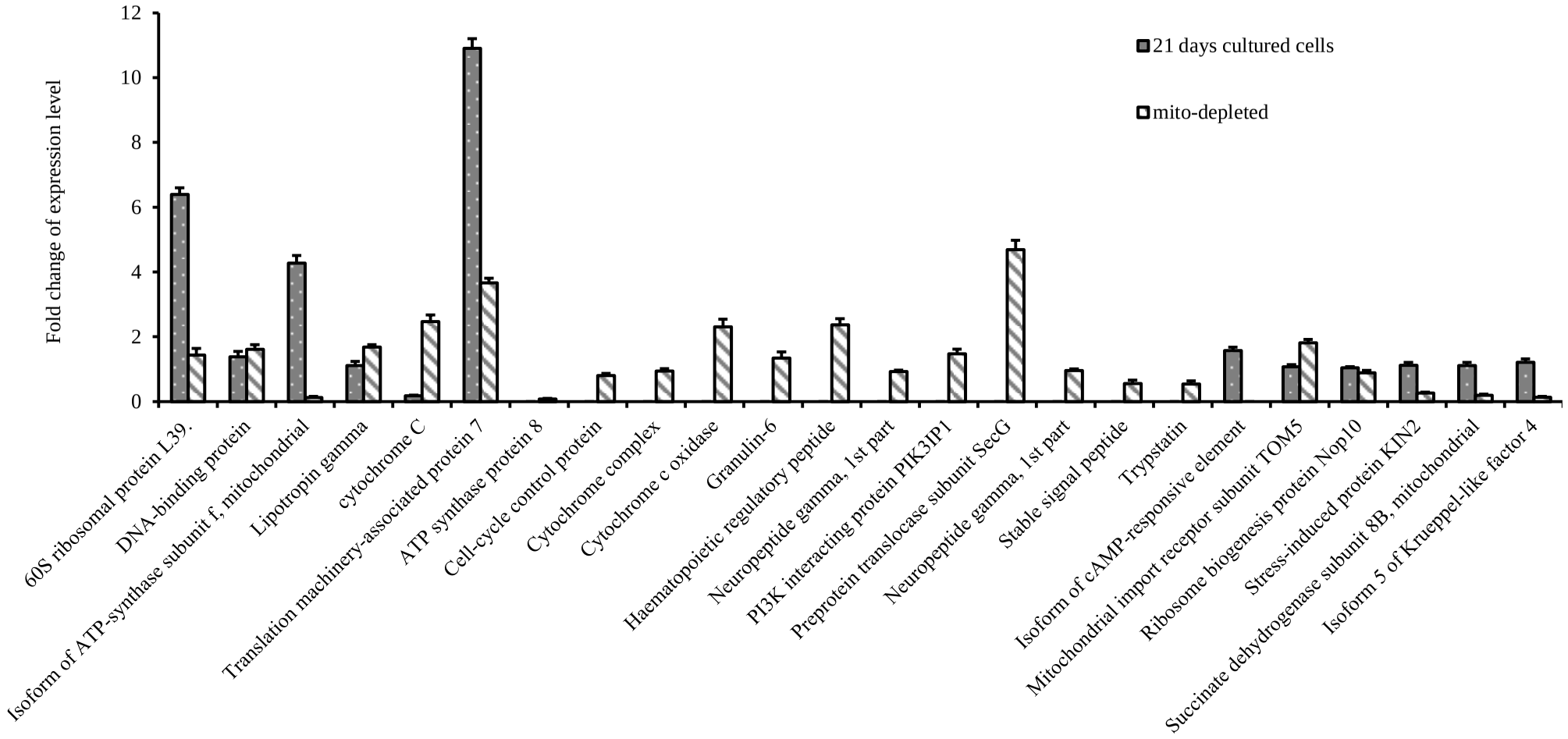

Figure 5.*17* *shows protein levels in exosomes isolated from different conditions using mass spectrometry. Results show that there are 24 different proteins contained in the cargo of exosomes isolated from VSMCs cultured for 21 days and Rho cells. Results also show that some proteins were found to be carried only in exosomes isolated from one condition but not the other and there are proteins found in both conditions but expressed at different levels (n=3)*

Some of the proteins identified were common in exosomes isolated from more than one condition. 18% of the proteins were uniquely found in exosomes isolated from 0.1% FCS cultured cells, 32% were uniquely found in exosomes isolated from 21 days cultured cells and 25% were uniquely found in exosomes isolated from Rho cells. Only 7% of the proteins identified were seen to be present in exosomes isolated from all three conditions (Figure 5.18).

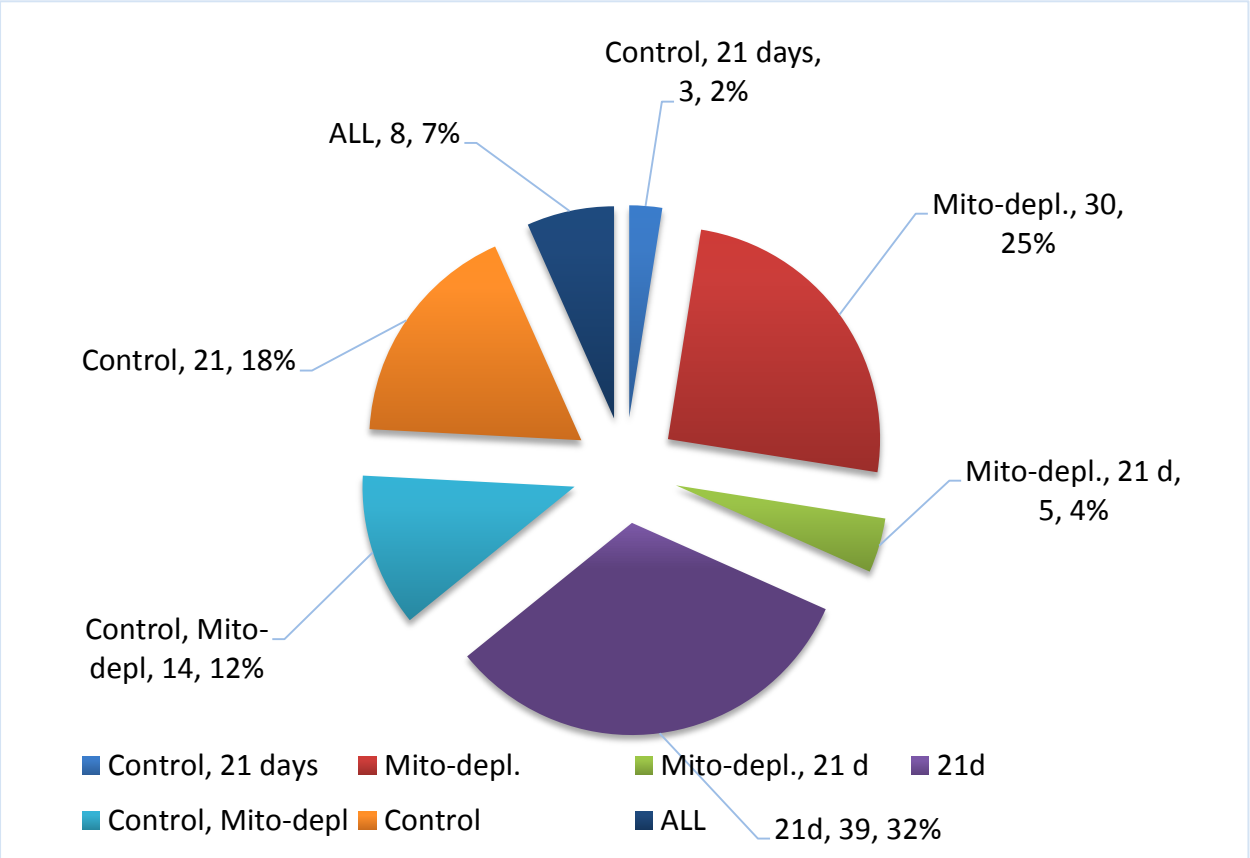

Figure 5.*18* *shows the percentage of protein content in each group and the ratio of proteins isolated from different treatments.*

In addition to RNA, miRNA we were able to detect a high variation in the protein cargo within exosome isolates. There were 46 proteins measured in exosomes isolated from 0.1% FCS not measured in the cultured VSM cells or Rho cells. Likewise 55 different proteins in the 21 day cultured VSM cells and 57 in the Rho cells (Figure 5.19).

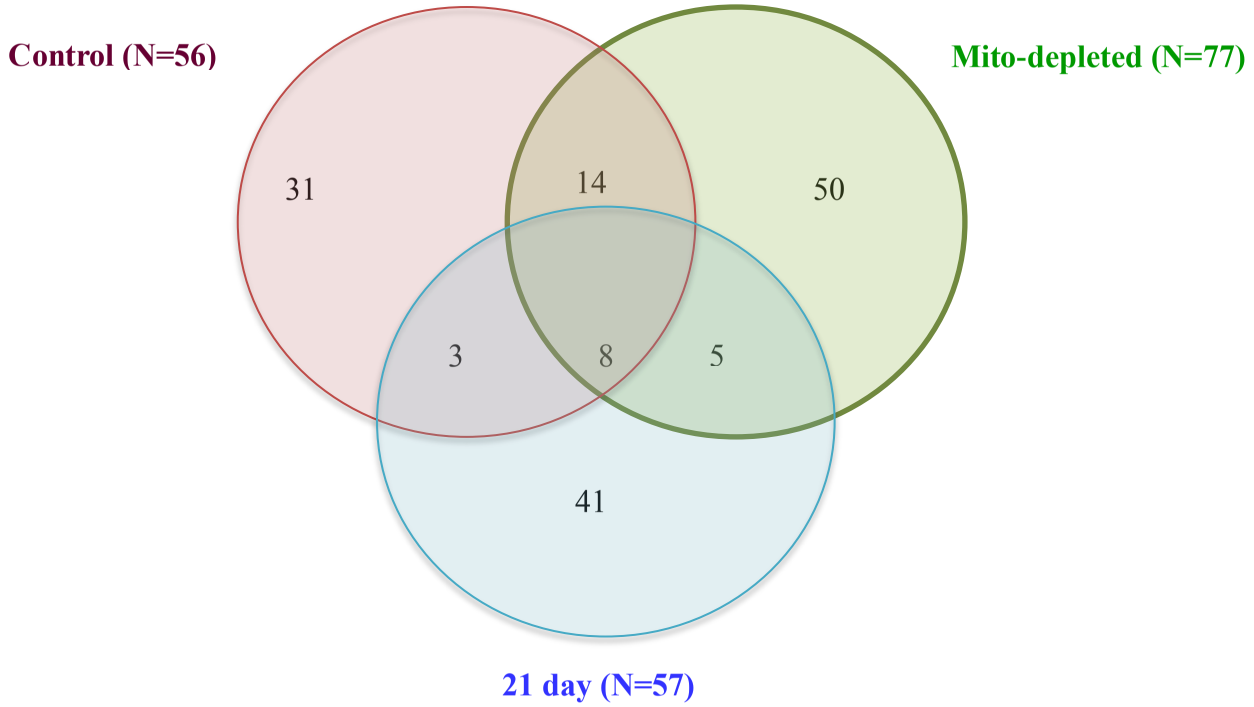

Figure 5.*19* *shows the number of different proteins isolated from each group and the common proteins found in different treatments.*

control 0.1% FCS	21 days cultured	Rho cells
50S ribosomal protein L32	40S ribosomal protein S29	40S ribosomal protein S29
50S ribosomal protein L34	50S ribosomal protein L34	50S ribosomal protein L33
50S ribosomal protein L36	60S ribosomal protein L39.	60S ribosomal protein L39.
50S ribosomal protein L39e	60S ribosomal protein L40-1	Acid shock protein.
60S ribosomal protein L40	Acid shock protein	Albumin-1 chain a.
ATP synthase protein 8.	Angiotensin 1-5	Arginine decarboxylase alpha chain
Beta-defensin 15.	ATP synthase subunit c	Aspartate 1-decarboxylase beta chain
Beta-defensin 40	ATP synthase subunit J, mitochondrial	ATP synthase protein 8
Biogenesis of lysosome-related organelles complex 1 subun	Beta-defensin 135	Aurein-1.1.
Bradykinin-potentiating peptide NDBP12	Bioactive peptide 1	Benzylsuccinate synthase gamma subunit
CAPA-Pyrokinin	Carbon storage regulator homolog	Beta-defensin 123
Capsid protein G8P	Cardioactive peptide	Beta-defensin 135
Carbon storage regulator homolog	Cathepsin B light	Beta-defensin 136
Cell cycle control protein 50C	Contraction-inhibiting peptide 1	Brevinin-2HSa
Cholecystokinin-58	DNA-binding protein	CAPA-Pyrokinin
Cytochrome b6-f complex subunit 6	DNA-directed RNA polymerase subunit omega	Carbon storage regulator homolog
Cytochrome b-c1 complex subunit 6-like, mitochondrial	Essential MCU regulator, mitochondrial	Cell cycle control protein 50C
cytochrome c	Growth-regulated protein homolog gamma	Conjugal transfer protein TrbK.
Cytochrome c oxidase subunit 6, mitochondrial	Hematopoietic cell signal transducer	Cytochrome b6-f complex subunit 8
Defensin-like protein 85.	Insulin A	Cytochrome b-c1 complex subunit 6-like, mitochondrial
DNA-binding protein	Insulin-like peptide INSL6 A	cytochrome c
DNA-directed RNA polymerase subunit K	Intracellular domain 2	Cytochrome c oxidase subunit 7
Ferredoxin-3	Isoform 2 of Actin-related protein 3C	Cytochrome c oxidase subunit 7e
Glucagon-like peptide 2	Isoform 2 of Bcl-2-like protein	DNA-binding protein
Glycoprotein N	Isoform 2 of cAMP-responsive element-binding protein-like	Galanin message-associated peptide
Granulin-6	Isoform 2 of Clathrin coat assembly protein	Granulin-6

Hematopoietic system regulatory peptide	Isoform 2 of Melanoma-derived growth regulatory protein	H/ACA ribonucleoprotein complex subunit 3
Interferon alpha-inducible protein 27- like protein 2A	Isoform 3 of ATP synthase subunit f, mitochondrial	Hematopoietic system regulatory peptide
Isoform 21 of cAMP-responsive element modulator	Isoform 3 of ATP-binding cassette sub-family C member 8	His operon leader peptide.
Isoform 3 of ATP synthase subunit f, mitochondrial	Isoform 3 of Mediator of RNA polymerase II transcription	His3-(33-44)-peptide
Isoform 3 of Tumor necrosis factor receptor superfamily m	Isoform 4 of Vascular endothelial growth factor	Isoform 3 of ATP synthase subunit f, mitochondrial
Isoform 3 of Vesicle-associated membrane protein	Isoform 5 of Krueppel-like factor 4	Isoform C of Protein C' OS=Vesicular stomatitis Indiana v
Isoform 4 of Caspase-5	Kunitz-type U15-theraphotoxin-Hhn1l	Kunitz-type serine protease inhibitor 18
Isoform 5 of CKLF-like MARVEL transmembrane domain-contai	Lipotropin gamma	Kunitz-type serine protease inhibitor NACI
Kunitz-type serine protease inhibitor microlepidin-1	Major outer membrane protein 1	Kunitz-type serine protease inhibitor stephenin-2.
Kunitz-type U15-theraphotoxin-Hhn1l	Metallothionein-1A	Kunitz-type serine protease inhibitor vestiginin-7
Lipotropin gamma	Metallothionein-like protein 3A	Kunitz-type U15-theraphotoxin-Hhn1d
Major outer membrane lipoprotein 1.	Minor histocompatibility protein HMSD variant form	Kunitz-type U15-theraphotoxin-Hhn1l
Metallothionein-1A	Mitochondrial import receptor subunit TOM5	Light-harvesting protein B-880 beta chain
Metallothionein-2A.	Mitochondrial import receptor subunit TOM7 homolog	lipoprotein YvzJ
Metallothionein-4.	NADH dehydrogenase [ubiquinone] 1 alpha subcomplex subunit	Lipotropin gamma
Neuropeptide gamma, 1st part	Non-specific lipid-transfer protein 2	Major outer membrane lipoprotein 3.
Nucleocapsid protein p7	Photosystem I reaction center subunit XII.	mercuric resistance protein MerC
Photosystem I reaction center subunit XII.	Platelet factor 4, short form	Metallocarboxypeptidase inhibitor
PI3K interacting protein PIK3IP1	Probable insulin-like peptide beta-type 1	Metallothionein
Preprotein translocase subunit SecG	Protein translocase subunit SecE	Metallothionein-1A
Putative defensin-like protein 184	Replication factor C small subunit	Metallothionein-1H
Putative uncharacterized protein DDB_G0293430	Ribosome biogenesis protein Nop10	Mitochondrial import receptor subunit TOM5
Relaxin-like protein AGF B chain	Secretin	Mitochondrial import receptor subunit TOM5 homolog
Ribosome modulation factor 1	Signal transducer CD24	Myeloma-overexpressed gene 2 protein homolog
S-adenosylmethionine decarboxylase beta chain	Small, acid-soluble spore protein 1	Neuropeptide gamma, 1st part
Small, acid-soluble spore protein 1	Sodium/potassium-transporting ATPase subunit gamma	Non-structural protein 4A.
Stable signal peptide	Stress-induced protein KIN2.	Penaeidin-3a

Tegument protein UL11 homolog	Succinate dehydrogenase subunit 8B, mitochondrial	Phorbol-12-myristate-13-acetate-induced protein 1
Translation machinery-associated protein 7	Transcriptional regulator Brz	Phosphatidylserine decarboxylase alpha chain
Trypstatin.	Translation machinery-associated protein	Phosvitin
	UPF0391 membrane protein A1S_3910	Photosystem I reaction center subunit XII.
		PI3K interacting protein PIK3IP1
		Preprotein translocase subunit SecG
		Preprotein translocase subunit SecG
		Prolactin-releasing peptide PrRP20
		Protein RALF-like 32.
		Protein translocase subunit SecE
		Ribosome biogenesis protein Nop10.
		Ribosome modulation factor
		S-adenosylmethionine decarboxylase beta chain
		Sec-independent protein translocase protein TatA.
		Serine protease inhibitor Kazal-type 1
		Small, acid-soluble spore protein 1
		sNPF peptide 4.
		SPBc2 prophage-derived uncharacterized protein YopL
		Stable signal peptide
		Stress-induced protein KIN2.
		Succinate dehydrogenase subunit 8B, mitochondrial.
		Translation machinery-associated protein 7
		Trypstatin
		Turripeptide OL172 conotoxin-like

Table 5.3 *Lists the different proteins extracted from exosomes isolated from VSMC cultured under different conditions (n=3)*

5.22 Discussion

5.23 Characterisation of exosomes:

There is increasing evidence highlighting secreted vesicles such as microvesicles and exosomes as important paracrine/ endocrine factors in cell-cell communication (Salomon et al., 2013). Their biological role is being increasingly associated with regulation of biological functions such as growth, differentiation and apoptosis (Huang et al., 2015). Likewise, a clear association with the pathobiology of cancer and cardiovascular disease is established. In fact, such is the change of microvesicles and exosomal secretion they are now used as biomarkers, predictors of disease (Hu et al., 2012). In this experiment chapter, we were able to characterise VSM cell yield of microvesicles by size distribution, imaging and immunoblotting. Based on size characterisation of secreted vesicles, the size of the vesicles that was obtained from the ultracentrifugation method we used was between 37-120 nm. This range of size is the known range for exosomes (Comelli et al., 2014). Images obtained by confocal microscopy also confirmed that the size of the vesicles in the samples were within the expected range for exosomes; between 20-120 nm. The shape of the vesicles seen by confocal microscope resembled clathrin coated pit, a characteristic of the receptor-mediated endocytosis that facilitates exosomes entering cells (Kadiu et al., 2012).

Furthermore, western blotting for exosome markers revealed the presence of CD9 and CD81 in the exosomes samples isolated from different conditions. These markers have been widely used to characterise exosomes isolated from VSM cell samples (Deng et al., 2015).

Interestingly, the RNA yield isolated from exosomes was higher in exosomes isolated from 21 days cultured VSM cell compared to exosomes isolated from 0.1% FCS cultured VSM cell or Rho cells. Protein concentration also varied with the 0.1% FCS cultured cell and Rho cells having the lowest concentration and the 21 days cultured cells having higher protein concentration. This is perhaps unsurprising, highly bioactive proliferating VSM cells secreting large amounts of exosomes. What is remarkable when mitochondrial dynamics are inhibited (MDivi-1) or mitochondrial function inhibited (Rho cells) the yield of exosomal quantity, size and

RNA content is significantly reduced. Thus there is a potential link between mitochondrial activity and exosomal trafficking. The exact mechanism are not defined and this merits further investigation.

5.24 Effect of mitochondrial inhibition on exosomal mRNA cargo in VSM cells:

PI3K/ Akt/ mTOR signalling pathway is an important pathway that is involved in the initiation and progression of VSM cell proliferation and migration and the progression of atherosclerosis (Goncharova et al., 2002). PDGF-induced VSM cell proliferation and migration was seen to be mediated by PI3K/ Akt/ mTOR signalling pathway. Treating VSM cells with PI3K inhibitor negated the proliferative and migratory effect induced by PDGF. mTOR inhibitors such as rapamycin are currently used in drug eluting stents in the percutaneous coronary intervention (Feldman and Shokat, 2010). Thus, we aimed to identify if related mRNA specific to PI3K/ Akt/ mTOR signalling pathway were carried within exosomal cargo. PI3k mRNA was detected in exosomes isolated from different conditions (wildtype vs. 21 day cultured vs. Rho 21 day cultured). PI3K activates Akt and consequently mTOR signalling pathway which initiates VSM cell proliferation when phosphorylated. When compared to unstimulated VSM cells the level of PI3K mRNA was 10 fold higher in exosomes isolated form 72 hour PDGF stimulated cells and 8 fold higher in exosomes isolated from phenotypically switched cells cultured for 21 days. This increase in PI3K mRNA found within exosomes reduced when the PDGF stimulated cells were treated with mitochondrial fission inhibitor MDivi-1. The level of PI3K mRNA in exosomes isolated from mitochondrial-depleted Rho cells was almost similar to the level in unstimulated cells. A previous study has reported that PI3K/Akt signalling pathway was activated following the co-culture of tumour-derived exosomes with SGC7901 cells (Qu et al., 2009). This study also showed that inhibiting PI3K/Akt resulted in a reduction in exosome dependent proliferation. This observation taken together with the data presented here further highlights the importance of the PI3K signalling pathway in cell proliferation. Furthermore, PI3K mRNA measured within exosomes was positively correlated with both proliferative state and mitochondrial fission reaction.

Akt mRNA was also detected in all samples including exosomes isolated from quiescent contractile VSMCs. The level of Akt mRNA, however, contained in exosomes isolated from PDGF stimulated cells was 143 fold higher than that contained in exosomes isolated from quiescent cells. This increase was reduced to 16 fold when the mitochondrial dynamics were inhibited using MDivi-1. Although the exosomes isolated from cells cultured for 21 days showed a lower increase in the level of Akt in comparison to the exosomes isolated from PDGF stimulated cells (4.5 fold), the increase was still significant when compared to the exosomes isolated from fresh contractile cells. This increase was reduced to 2.2 fold in the exosomes isolated from mitochondrial-depleted Rho cells. The low level of Akt mRNA measured after 21 days in comparison to the high level seen following 72 hours gives some insight into the cell-stimulated expression of Akt mRNA. Akt has been previously reported to be present, along with other kinases, in exosomes isolated from cancer cells (van der Mijn et al., 2014, He et al., 2015). It was found that the level of phosphorylation of Akt in the exosomes reflect their level of phosphorylation in cancer cells (van der Mijn et al., 2014). Mian He et al (2015) reported that hepatocellular carcinoma-derived exosomes caused mobilisation of normal hepatocyte leading to metastasis (He et al., 2015). They demonstrated that this was triggered by the activation of PI3K/Akt signalling pathway. We are reporting for the first time that Akt mRNA level of expression in the exosomes is associated with mitochondrial bioactivity and reflect their level of expression in their parent VSM cells.

Another mRNA detected in the exosomes isolated from VSM cells was 4EBP1 which is an mTOR downstream translation inhibitor. 4EBP1 interacts with the translation initiation factor 4E (eIF4E). Upon phosphorylation, 4EBP1 dissociates from eIF4E and results in mRNA translation and protein synthesis which drives cellular proliferation (Shveygert et al., 2010). We saw a small increase in the 4EBP1 mRNA in exosomes isolated from cells stimulated with PDGF for 72 hours and a decrease in their level following mitochondrial inhibition using MDivi-1 in comparison to its level in exosomes isolated from contractile VSM cells. What was significant was the increase in 4EBP1 mRNA level in the synthetic phenotype following 21 days in culture to ~ 7 fold. 4EBP1 mRNA found in exosomes was almost abolished when the mitochondrial activity was inhibited in Rho cells. This

finding could suggest that the level of 4EBP1 is increased upon long term activation regardless of their status whether they are in an active phosphorylated state or inactive non-phosphorylated state. They are then transported to the target cell and in the presence of other stimulants, they are phosphorylated and result in the activation of mTOR signalling pathway. Their higher level of expression in exosomes isolated from 21 day cultured cells means that target cells become more vulnerable to any growth stimulant that would activate the phosphorylation of higher level of 4EBP1 than normal cells. The presence of EIF3A gene was previously reported in hepatocellular carcinoma-derived exosomes (He et al., 2015). The study found that the mRNA content of exosomes derived from hepatocellular carcinoma cells triggered PI3K/Akt signalling pathways and increased secretion of MMP-2 and MMP-9. This has led to the increase of mobility of normal hepatocytes and resulted in metastasis. The increase levels of PI3K, Akt and 4EBP1 in exosomes isolated from PDGF stimulated cells and 21 day phenotypically switched cells could be the trigger that promote the proliferation and migration of the recipient VSM cells. The transport of these genes in neighbouring VSM cell through exosomes could lead to the activation of PI3k/Akt/mTOR signalling pathway which induces VSM cell proliferation and migration.

Varying levels of the cell cycle inhibitor gene cdkn2a was also detected in exosomes. This gene codes for proteins that act as tumour suppressors and initiates apoptosis (Bai et al., 2016). Cdkn2a is an important gene that was found to be decreased in level in cancer (Bai et al., 2016). Overexpressing Cdkn2a in human melanoma cells resulted in a suppression of proliferation and migration of these cells. The level of pro-apoptotic genes in exosomes were previously seen to vary in tumour cells (Galluzzi et al., 2012). Exosomes released by tumour cells have been shown to protect tumours from cell death and enhance cell proliferation signalling pathway (Galluzzi et al., 2012). Thus we aimed to identify if cdkn2a was present in exosomes isolated from VSM cells cultured under different conditions. The level of cdkn2a measured in exosomes isolated from PDGF stimulated cells was reduced by half and was almost abolished in exosomes isolated from 21 days cultured cells. However, exosomes isolated from mitochondrial-depleted Rho cells contained double the level of cdkn2a in comparison to exosomes isolated from contractile cells. Decreased level

of this gene in the stimulated VSM cell released exosomes could contribute in part to the loss of cell cycle inhibition and results in an unregulated cell cycle progression and proliferative state. A previous study has highlighted that exosomes isolated from bladder cancer cells contained higher levels of Bcl-2 and cyclin D1 compared to normal cells (Yang et al., 2013). In this study the authors concluded the increase of anti-apoptotic genes and cell cycle regulatory genes promoted a cellular proliferative state conducive to tumour cell growth. In our experiments, the increased level of cdkn2a contained in Rho cells could theoretically contribute to the inhibition of cell cycle progression in the recipient cells. Again this highlights the selectivity and functionality of the mRNAs enclosed in exosomes isolated from VSM cells (Braicu et al., 2015).

When the mitochondrial activity was inhibited pharmacologically by using MDivi-1 or non-pharmacologically by generating Rho cells, the content within the exosomes favours cell cycle inhibition which may go some way to explaining the reduction in proliferation measured. These findings infer that the mRNA content of exosomes is related to mitochondrial bioactivity.

5.25 Effect of mitochondrial inhibition on exosomal miRNA cargo in VSM cells:

A significant number of exosomal miRNAs involved in cellular proliferation have been identified in cancer which helped in understanding the molecular mechanism of cancer development including miR-21 and miR-96 (Katsuda et al., 2014, Wu et al., 2016). To date assessment of exosomal miRNA in a model of vascular injury/ VSM cell proliferation has not been undertaken. Thus, we identify miRNA cargo in the exosomes isolated from our experimental culture conditions and assessed any correlation with our previous results. We also wanted to see if mitochondrial bioactivity has an effect on the exosomal miRNA cargo. Results highlight that both miR-21 and miR-145 were present in exosomes isolated from all culture conditions. The level of miR-21 was almost 9 fold higher in exosomes isolated from 21 days cultured cells when compared to its level in exosomes isolated from contractile VSM cells. However, the level of miR-21 in exosomes isolated from Rho cells is almost similar to the background level. The presence of miR-21 was previously reported to be higher in level in circulating exosomes of lung cancer patients compared to

control subjects (Rabinowits et al., 2009). The study also reported that the total level of miR-21 isolated from the tumour was subsequently found to be derived from exosomes. The increase in miR-21 we measured in exosomes isolated from PDGF stimulated cells and 21 days cultured phenotypically switched cells correlates, in terms of total miR-21, with what we measured in VSM cell lysates. The expression of miR-21 increased in response to stimulation with PDGF and FCS. What was surprising was that the level of miR-21 expression returned to near baseline levels when mitochondrial dynamics were inhibited with MDivi-1 or culture of Rho (mitochondrial incompetent) cells. These observations again clearly link mitochondria in miR-21 synthesis and exosomal trafficking. Upon arrival in recipient cells, exosomes transfer their cargo of miRNA where they exert their biological effect. miRNAs carried in exosomes were previously reported to be functional in the recipient cell (Pegtel et al., 2010). miRNAs isolated from T-cell exosomes were seen to inhibit the expression of their target genes in dendritic cells (Mittelbrunn et al., 2011). However, when exosomes were inhibited by targeting sphingomyelinase-2, the transfer and functionality of miRNA was lost.

Level of exosomal miR-145 was also seen to be altered by mitochondrial dynamics and bioactivity. Level of expression in exosomes isolated from PDGF stimulated and 21 days cultured cells were both decreased by almost half in comparison to exosomes isolated from freshly isolated wild type cells. The level of miR-145 was significantly increased to almost 3 fold in both PDGF stimulated with MDivi-1 treatment as well as mitochondrial-incompetent Rho cells. This again correlates well with our previous observation that miR-145 expression within the cell is influenced by mitochondrial activity. The presence of miR-143 in exosomes isolated from pulmonary artery smooth muscle cells (PASMCs) has previously been reported by Deng et al (2015). They found that transfecting PASMCs with miR-143 resulted in an enrichment of miR-143 in the secreted exosomes. Functional analysis also showed that co-incubating miR-143 enriched exosomes with PASMC cells resulted in an increase in cell proliferation and migration (Deng et al., 2015).

These findings along with mRNA findings suggest that exosome-mediated transfer of mRNAs and miRNAs are significant mechanism of genetic exchange between

cells (Valadi et al., 2007). The exosomal content and level of expression of mRNA and miRNA is clearly regulated by mitochondrial bioactivity as described by our results.

5.26 Effect of mitochondrial inhibition on exosomal protein cargo in VSM cells:

Different exosomal protein cargo has been reported previously in VSM cells. Proteins involved in growth signalling pathway, extracellular matrix formation, focal adhesion and cell growth have been reported to be increased in expression within exosomes isolated from activated VSMCs when compared to quiescent cells (Comelli et al., 2014).

In this aspect of the project, exosomal protein content was studied. As predicted, depending on culture conditions there was a broad difference in exosomal protein cargo. From freshly isolated (wild type/control) cells 46 proteins were detected in exosomes isolated from contractile cells out of which 21 proteins were only found in contractile cells but not the other treatments. 55 different proteins were detected in exosomes isolated from 21 days cultured cells out of which 39 proteins were unique for this condition. 57 different proteins were detected in exosomes isolated from mitochondrial-depleted Rho cells out of which 30 proteins were uniquely contained in this treatment but not the other treatments. Only 8 proteins were seen to be commonly present in all the three treatments. Previous studies have identified differences in exosomal protein, miRNA and mRNA cargos between different treatment conditions. Protein cargo of exosomes isolated from melanoma tumour cells was found to be different than the protein content in normal melanocytes (Xiao et al., 2012). The proteins carried in melanoma-derived exosomes including HAPLN1 and annexin were associated with melanoma progression and metastasis. In our work, the level of proteins was seen to be different in each treatment. Isoform of ATP-synthase subunit F, which is a mitochondrial protein, and translation machinery-associated protein 7 were seen to be almost 5 fold and 11 fold respectively higher in 21 days in comparison to mitochondrial-depleted Rho cells. This is due to the increased demand for energy in hyper proliferative cells (Yoshida et al., 2005). Inhibiting mitochondria limits ATP supply to cells which is partly responsible for the reduction in proliferation seen after mitochondrial inhibition. This

is seen in the reduced level of ATP-synthase protein in exosomes isolated from mitochondrial inhibited VSM cells.

An interesting protein associated with VSMCs phenotypic switch is Krupple like factor (Kawai-Kowase and Owens, 2007) which is seen to be contained in exosomes isolated from 21 days and almost not present in exosomes isolated from mitochondrial-depleted Rho cells. Krupple like factor 4 suppresses the expression of VSM cell specific marker genes including smooth muscle α-actin and smooth muscle myosin heavy chain. Our finding supports that exosomes contribute to the phenotypic switch of VSM cells from contractile to synthetic partly through the transportation of proteins that promote this shift. Proteins that promote cellular phenotypic switch and induce migration were also found in exosomes isolated from pancreatic adenocarcinoma cells (Mu et al., 2013). The study found that exosomes isolated from pancreatic adenocarcinoma cells contained MMP2 and MMP9 which promoted cellular motility and invasiveness. Exosomes modulated the extracellular matrix by binding to individual components of the extracellular matrix resulting in its degradation.

Cytochrome c is a mitochondrial protein that is important in the initiation of the apoptotic signalling pathway (Scorrano, 2009). This protein was previously associated with inhibition of VSM cell proliferation through the activation of caspase 3/7 and modulation of the apoptotic proteins including Bax/ Bcl-2 (Guo et al., 2007). In our study, cytochrome c was seen to be 3 fold higher in mitochondrial-depleted Rho cells compared to 21 days cultured cells. This is consistent with our previous western blot finding on the effect seen on cytochrome c expression following mitochondrial inhibition with MDivi-1 (Chapter 3). Interestingly, proteins involved in cell-cycle inhibition and apoptosis were found to be transported by exosomes isolated from mitochondrial-depleted cells including cytochrome c oxidase, cell-cycle control protein and PI3K interacting protein. The presence of PI3K interacting protein in exosomes isolated from Rho cells could be responsible in part for the downregulation of PI3K signalling pathway. This reduction then results in inhibition of VSM cell proliferation (Goncharova et al., 2002). This suggests that the exosomal protein cargo isolated from mitochondrial-depleted Rho cells contributes to the

inhibition of VSM cells by working on different pathways including cell-cycle inhibition, promotion of apoptosis and inhibition of PI3k/ mTOR signalling pathway. This is in keeping with our previous findings that mitochondrial bioactivity promotes VSM cell through the regulation of cell-cycle inhibition/ apoptosis signalling pathways. This is strong evidence that exosomal cargo of proteins changes depending upon VSM cell culture conditions which reflects mitochondrial biogenesis. This in turn has a consequent effect on the recipient cells to either change its phenotype from contractile to synthetic and drives the growth of VSM cells or vice versa.

All exosomal data support that mitochondrial bioactivity plays a major role in determining exosomal cargo including mRNAs, miRNAs and proteins. Mitochondria determine the level of expression of genes and proteins involved in the initiation and progression of VSM cell proliferation and migration. These proteins, mRNAs and miRNAs are then transported to other cells where they exert their proliferative effect by stimulating signalling pathways including PI3K/ mTOR and cell-cycle pathway or inhibiting apoptotic intrinsic signalling pathway. Inhibiting mitochondrial bioactivity could then result in less expression of mRNAs and proteins involved in the progression of cell-cycle and PI3k/ mTOR signalling pathway. It also results in alteration of miRNA profile which regulates apoptotic signalling cascade therefore reduce VSM cell proliferation. These data are in keeping with our previous results that inhibiting mitochondria results in an inhibition of VSM cell proliferation and migration through PI3K/Akt/mTOR signalling pathway by initiating apoptosis and inhibiting cell cycle progression. This was found to be regulated by miR-21 and miR-145 expression within the cell which is also found to be transported from one VSM cell to another via exosomes.

The functionality of exosomal cargo has been investigated by many research groups mainly in cancer models. Many reports revealed evidence of cellular function modulations in cancer cells by secreted exosomes (Katsuda et al., 2014). We are demonstrating for the first time that the content of the exosomes isolated from VSM cell is tightly regulated by mitochondrial function.

Summary of the primary experimental findings reported in this chapter:

- Mitochondrial bioactivity influences exosomal release, protein concentration and RNA yield in exosomes.
- Exosomes isolated from mitochondrial incompetent Rho VSM cells contain high level of miR-145 which correlate with the anti-proliferative effect on VSM cells reported.
- Exosomes isolated from 21-day phenotypically switched cells contain high level of miR-21 which correlates with VSM cell proliferation reported
- Exosomes isolated from mitochondrial incompetent Rho VSM cells contain higher levels of genes that induce apoptosis and cell cycle arrest.
- Exosomes isolated from 21-day phenotypically switched cells contain high levels of genes that are involved in the initiation of mTOR signalling pathway including PI3K, Akt and 4EBP1.
- Proteins required for energy supply and phenotype switching of VSM cells including ATP Synthase and KLF4 were found in exosomes isolated from 21-day phenotypically switched cells.
- Proteins involved in the inhibition of PI3K including PI3K interacting protein were found in exosomes isolated from mitochondrial incompetent Rho VSM cells

Chapter 6

General Discussion

Three different layers of the blood vessel including the intima, the media and the adventitia are involved in the initiation and activation of cardiovascular diseases at different degrees. The cells contained in these three layers adapt to different stimulus including growth factors and high blood pressure. This adaptation results in a change in the cellular phenotype and functions of the endothelium, VSM and adventitia. Dysfunctional layers result in an increase in the release of endothelial adhesion molecules, reduction in eNOS and increase in the production of adventitial ROS which negates the effect of the endothelial derived NO and inhibits vessel relaxation. Furthermore, dysfunctional VSM cells become hyper-proliferative and migratory. These changes in the phenotypes can result in the development of vascular atherogenesis and re-stenosis.

Different pharmacological and non-pharmacological approaches have been adapted in an attempt to reduce the incidence of atherosclerosis development and re-stenosis following PCI intervention. This includes gene therapy using antisense oligonucleotides to achieve cytostatic effect of specific transcription factors involved in cell cycle progression (Kutryk et al., 2002). Drug eluting stents is the preferable method for treating atherosclerosis and re-stenosis following PCI. Different drugs have been used to coat these stents including rapamycin and paclitaxel. Despite advances in technology and drug development, stenting remains problematic because of the side effects associated with rapamycin and paclitaxel including de-endothelialisation and thrombosis. Therefore, the aim of this study was to define mitochondrial role in the VSM cell proliferative and migratory phenotype and its relationship to atherogenesis which could provide a novel therapeutic strategy for atherosclerosis and re-stenosis through targeting mitochondrial bioenergetics and bioactivity needed for the proliferative and migratory VSM cell without affecting wild type normal cells.

Different signalling pathways are involved in the initiation and progression of atherosclerosis and re-stenosis. Activation of MAPK, mTOR, NFκβ and AMPK have all been implicated in VSM cell proliferation and migration. It has been previously demonstrated that inhibiting these signalling pathways can lead to a reduction in the proliferative and migratory capacity of VSM cells that ultimately slow the

progression of atherosclerosis and restenosis (Omura et al., 2005). However, due to the unwanted effect that these inhibitors have on healthy cells, there is a need to study the involvement of other potential signalling pathways that could offer new therapeutic targets with fewer off-target effects.

In this work, we have demonstrated that inhibiting mitochondrial fission results in an inhibition of VSM cell proliferation and migration in an in-vitro setting which was closely associated with the change in mitochondrial morphology from fragmented mitochondria to fused mitochondrial network. We have also demonstrated that inhibiting mitochondrial fission resulted in a reduction in the wall thickness of the blood vessel seen following balloon injury. The decrease in wall thickness and the maintenance of the lumen size resulting from mitochondrial division inhibition could potentially be another option for more targeted drug eluting stent that is safer to use and has better success rate. These results were also verified by generating mitochondrial-depleted Rho cells which showed less proliferative and migratory capacities when compared to VSM cells cultured for 21 days. This approach has helped understand the role of mitochondrial bioactivity in the process of VSM cell proliferation and migration since mitochondria respond to the increased demand for cellular energy required for proliferation and migration by changing their morphology and dividing into smaller fragmented mitochondria (Lackner, 2014). Mitochondria form their network to enable them to maintain their DNA, distribute ATP and calcium evenly in the cell. The same effect of inhibiting neo-intima formation following balloon angioplasty was seen when the aorta was cultured with the fission inhibitor MDivi-1 and in culture conditions with ethidium bromide, uridine and sodium pyruvate to inactivate ATP production. These observations support the hypothesis that mitochondrial fission in response to increased mitochondrial bioactivity is an essential step in the progression and development of atherosclerosis and restenosis.

To understand the molecular mechanism behind the reduction in VSM cell proliferation and migration seen in response to mitochondrial inhibition, the expression of proteins that regulate MAPK and mTOR signalling pathways showed that the reduction in VSM cell proliferation and migration following mitochondrial

inhibition is independent of ERK1/2. However, the deactivation of mTOR effector proteins including Akt and 4EBP1 following mitochondrial inhibition suggests the mTOR signalling pathway is likely involved. This is in keeping with known mTOR function of regulating protein synthesis and activation of cell cycle following stimulation (Efeyan and Sabatini, 2010). This in turn activates mitochondrial bioactivity to produce more energy required for protein synthesis. Inhibiting mitochondrial fission using DRP1 inhibitor MDivi-1 locked the cell cycle at G2/M phase. Division of mitochondria during VSM cell proliferation and migration requires the activation of DRP1 by mitosis regulators cyclin B1/ cyclin dependent kinase1 (CDK1). Activation of mTOR cascade is important for the progression of the cell cycle and the disruption caused by mTOR deactivation following DRP1 inhibition is the result of cyclin B1/ CDK1 dysregulation. This further supports that the reduction in VSM cell proliferation and migration following mitochondrial inhibition is due to the prevention of mitotic fission and cell cycle arrest.

To further investigate potential mitochondrial genes involved in the phenotypic switch of VSM cells, we conducted gene profiling study on contractile VSM cells and compare it with mitochondrial genes expressed in synthetic VSM cells and mitochondrial-depleted Rho cells. Results indicated that there is a change in the gene expression of mTOR signalling, cell cycle genes, apoptotic genes, mitochondrial transporter genes and ROS scavenging genes. The increase in Akt gene following stimulation and the decrease following mitochondrial inhibition agrees with our previous finding of the involvement of mTOR signalling pathway. The inhibition of cell cycle inhibitor genes cdkn2a and TP53 in the stimulated cells and the increase in their expression following mitochondrial inhibition is in keeping with cell proliferation data presented in Chapter 3. This was also accompanied with an increase in the expression of apoptotic genes Bnip3 and Pmaip1 suggesting an activation of the apoptotic signalling pathway which we also demonstrated. Other genes involved in the transportation of molecules across mitochondrial membrane between the cytosol and mitochondria showed an increase in their expression in the synthetic cells and a decrease in the Rho cells including Hsp90aa1, Hspd1, Mtx2, sh3glb1 and slc25a16. This might explain the restriction in the movement of important molecules needed for the activation of proliferation cascade from the

mitochondria which contributes to the effect seen on proliferation following mitochondrial inhibition. Moreover, ROS scavenging genes SOD1 and SOD2 were reduced in the 21days cultured cells and increased in the Rho cells. Collectively, these findings strongly suggest that mitochondrial bioactivity is important for the synthesis of genes involved in the progression of VSM cell proliferation and migration. These findings also suggest that the inhibition of mitochondrial bioactivity contributes to the reduction in the synthesis of these genes which leads to inhibition of VSM cell proliferation and migration.

We also demonstrated for the first time that inhibition of mitochondria results in a change in the miRNA profile of the VSM cells which is directly linked to the proliferation and migration process. miR-21 and miR-145 were previously reported to be associated with VSM cell proliferation and migration (Albinsson and Sessa, 2011). Our gene profiling revealed that the expression of miR-21 increased following stimulation of VSM cell proliferation and was decreased to normal level following mitochondrial inhibition. Results also highlight a decrease in the expression of miR-145 following stimulation and an increase back to normal level following mitochondrial inhibition. These findings link mitochondrial bioactivity with the expression of miRNAs involved in VSM cell proliferation and migration. And because miRNAs are negative regulators of gene synthesis, we investigated the potential targets for miR-21 and miR-145 based on the gene profiling results obtained earlier from the phenotypically switched VSM cells cultured for 21 days and compared to the gene expression from mitochondrial-depleted Rho cells.

miRNA transfection with miR-21 and miR-145 inhibitors and mimics revealed that there is a decrease in the cell cycle regulatory genes cdkn2a and P53 with miR-21 mimic and an increase in their expression following transfection with miR-21 inhibitor. This suggests that miR-21 could potentially target cell cycle inhibitory genes resulting in a progression of the cell cycle and proliferation. MiR-21 was also found to target SOD1 which is a gene responsible for ROS scavenging and when its absence could lead to ROS-driven proliferation. On the other hand, transfecting the cells with miR-145 mimic resulted in a decrease in Akt, PI3k, 4EBP1 and mTOR and an increase in their expression following transfection with miR-145 inhibitor. This

suggests that miR-145 potentially targets mTOR signalling genes and that's why when the mitochondria are inhibited we see an increase in miR-145 expression which correlates with the decrease in mTOR activity and the reduction in proliferation and migration. To further validate this finding, we silenced mTOR using siRNA and transfected VSM cells with miR-145 inhibitor which previously showed an increase in VSM cell proliferation and migration. The results showed that there is no increase in VSM cell proliferation and migration seen following transfection with miR-145 inhibitor when mTOR was silenced which demonstrates for the first time that miR-145 targets mTOR and results in inhibition of VSM cell proliferation. This is closely regulated by mitochondrial bioactivity and any disruption to the mitochondria results in a change in miRNA profile which leads to a change in the expression of certain genes involved in the activation of proliferative signalling pathways including mTOR signalling pathway.

We also demonstrated for the first time that mitochondrial bioactivity plays a very important role in transporting mRNA, miRNAs and proteins involved in proliferation and migration through exosomes. Total RNA and protein contained in exosomes was also influenced by the mitochondrial bioactivity suggesting a role for mitochondria in exosomes biogenesis as well as RNA and protein sorting in exosomes. Both RNA yield and protein concentration was reduced in exosomes isolated from Rho cells in comparison to exosomes isolated from contractile and synthetic VSM cells. Inhibiting mitochondrial bioactivity resulted in a change in exosomes content of mRNA, miRNA and protein in comparison to the stimulated cells. This change correlated with the results we obtained from gene profiling experiments for both mRNAs and miRNAs.

Genes involved in the activation of mTOR signalling pathway including Akt, PI3K and 4EBP1 were all seen to be higher in level in exosomes isolated from synthetic VSM cell compared to exosomes isolated from contractile VSM cells. However, exosomes isolated from Rho cells contained lower level of mTOR signalling genes. Although the exact sorting mechanism is not fully understood, it is clear that the active status of mitochondria contributes in the process of exosomal cargo inclusion. The lower level of these genes in exosomes isolated from mitochondrial-depleted

Rho cells is a reflection of the low level of expression of these genes seen earlier following mitochondrial inhibition. This could also be a result of lower number of exosomes being released from mitochondrial-depleted Rho cells in comparison to the number of exosomes released by synthetic VSM cells.

Interestingly, the level of cell cycle inhibitor gene cdkn2a in exosomes isolated from mitochondrial-depleted Rho cells is higher than its level in exosomes isolated from synthetic VSM cells. This again reflects the level of cdkn2a expression in Rho cells which is higher than the level of expression seen in synthetic VSM cells.

Similarly, the level of miRNA enclosed in exosomes was influenced by mitochondrial activity in the same way the expression within the cell was influenced. The level of miR-21 in exosomes isolated from mitochondrial-depleted Rho cells was lower than the level in exosomes isolated from synthetic VSM cells. This is an indication that not only that miR-21 act on the parent cell, but they are also transported to other cells through exosomes where they exert the same effect on their targets and initiate VSM cell proliferation cascade. The low abundance of miR-21 in exosomes isolated from Rho cells suggest that inactive mitochondria influence the transportation of miR-21 to other cells and therefore their effect in activating VSM cell proliferation is limited if not completely abolished.

Conversely, the level of miR-145 is higher in exosomes isolated from mitochondrial-depleted Rho cells compared to exosomes isolated from synthetic VSM cells. This ties on with our previous finding that the expression of miR-145 in stimulated VSM cells is lower than the expression in VSM cells with inactive mitochondria. This suggest that during normal mitochondrial bioactivity, mitochondria responds to the growth stimulants by selectively including genes in exosomes that promote VSM cell proliferation and selectively exclude genes that inhibit proliferation.

The proteins transported in exosomes were also affected by mitochondrial bioactivity in a similar way to the effect on nucleic acids. Exosomal proteins isolated from mitochondrial-depleted Rho cells were slightly different than proteins enclosed in exosomes isolated from synthetic proliferative VSM cells. The level of proteins involved in supplying cells with energy including isoform of ATP-synthase subunit

F, which is a mitochondrial protein, and translation machinery-associated protein 7 were higher in exosomes isolated from synthetic VSM cells than exosomes isolated from Rho cells. This can be explained by the need for higher energy in cells undergoing proliferation and the role played by mitochondria in facilitating the transportation of exosomes and their contents from one cell to another.

Inhibiting mitochondria clearly affects the transportation of these proteins which then leads to lack of energy in other cells inhibits proliferation. Krupple like factor 4 (KLF4) which is a protein required for VSM cells phenotypic switch measured in exosomes isolated from synthetic VSM cells and not present in exosomes isolated from mitochondrial-depleted Rho cells. This novel observation supports the need for mitochondrial activity and ATP production to transport and supply other cells with the proteins associated with transformation from a contractile to a synthetic phenotype via exosomes. Finally, proteins needed for the deactivation of PI3K and cell cycle inhibition were highly expressed in exosomes isolated from mitochondrial-depleted Rho cells. However, by comparison their abundance in exosomes isolated from synthetic VSM cells was significantly less.

In conclusion, we can clearly see the effect of bioactive mitochondria in driving VSM cell proliferation and migration. Figure 6.1 summarises the main finding of the work described in this thesis. Looking at the molecular details, mitochondrial bioactivity is required for the synthesis of miRNAs that can target specific genes involved in the proliferation and migration. Mitochondrial function is a major determinant of the distribution factors that change VSM cells from a contractile to a synthetic phenotype through selectively choosing exosomal cargo of mRNA, miRNA and proteins. Therefore, inhibiting mitochondria in cells of a synthetic phenotype could be a potential cell focused therapeutic target that is specific as a consequence of phenotype, mitochondrial bioenergetics, exosomal transport and consequential effector mechanism inhibition in recipient cells.

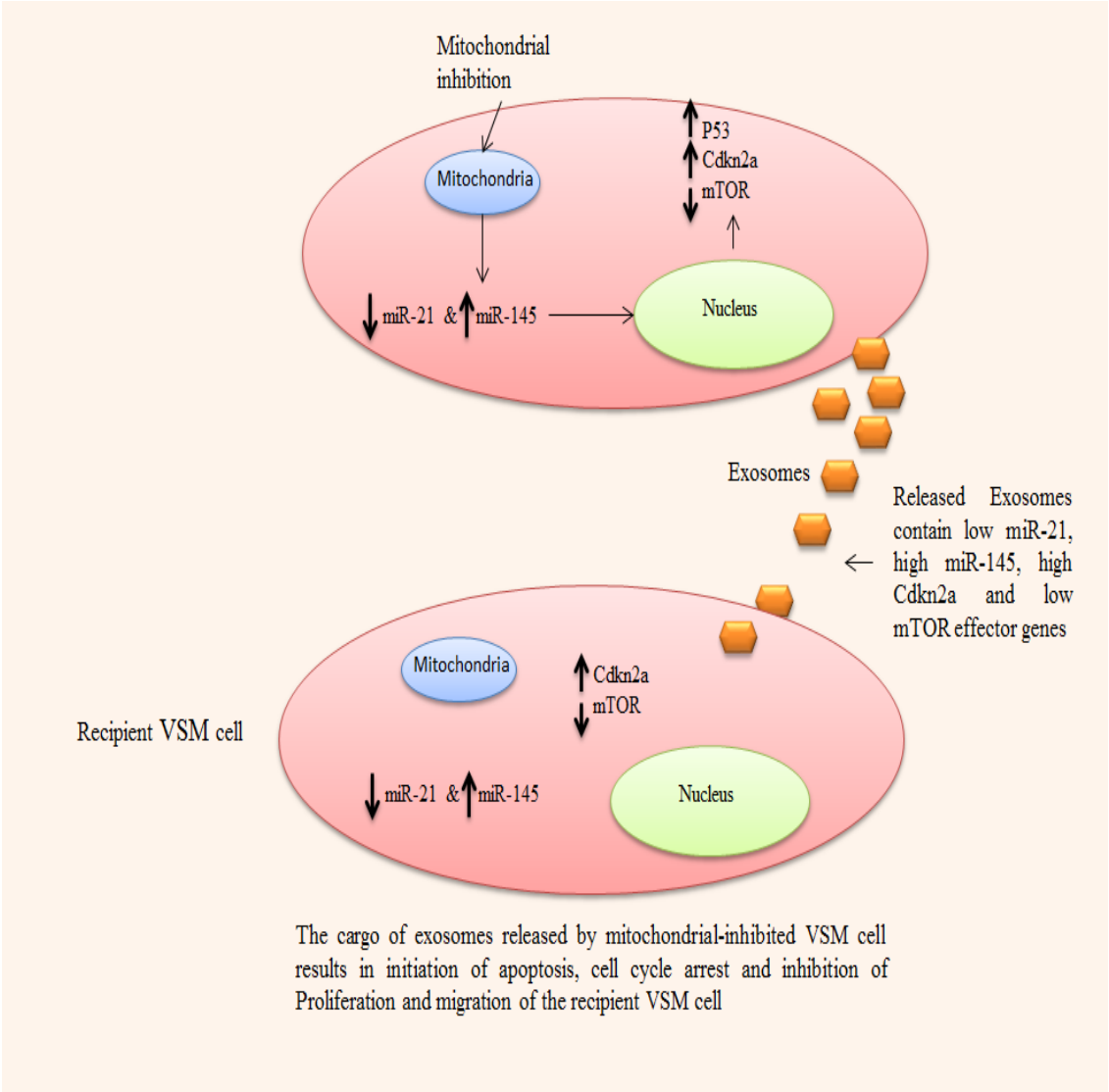

Figure 6.1 *shows a schematic diagram showing summary of the main findings of the project*

Study Limitations and Future Work:

Although the results show an important role for mitochondria in regulating VSM cell proliferation and migration following stimulation, these findings are the results of cell based work and whole artery culture. This does not take into account the response initiated by the immune system in the body which is essential in atherosclerosis or re-stenosis following PCI injury. Therefore, the response we

reported in an in-vitro setting might differ from the response in an in-vivo setting. Thus, there is a need to move this work to a whole animal model. In a study conducted to assess the efficacy of stent based delivery of succinobucol which was previously seen to inhibit SMC proliferation through antioxidant and anti-inflammatory properties, results showed that succinobucol coated stents increased neointimal formation and inflammation compared to bare metal stents and rapamycin coated stents (Watt et al., 2013).

This work is taken further by undertaking next generation sequencing (NGS) of the three main conditions; freshly isolated VSM cells, 21 day cultured VSM cells and Rho cells. The results will give a better understanding of the genotype changes associated with the change in VSM cell phenotype. This might offer known and potentially unknown therapeutic targets. Another work which is currently in the process is next generation sequencing (miRnome) of the exosomal miRNA content for exosomes isolated from freshly isolated VSM cells, 21 day cultured VSM cells and Rho cells. This will also offer a better insight on the effect of the exosomal miRNA content in the recipient VSM cells and can provide a wider picture of the genes targeted by these miRNAs. Both cellular NGS genotyping and exosomal NGS for miRNA will provide potentially novel therapeutic targets for atherosclerosis and re-stenosis.

This work can also be taken in the future into animal model to deliver exosomes locally using infusion catheter to the stenotic region of the blood vessel. This study can also be taken further by using drug eluting stent in an animal model to deliver anti-miRNAs which will be identified from the current NGS study.

References

ADRAIN, C. & MARTIN, S. 2001. The mitochondrial apoptosome: a killer unleashed by cytochrome seas. Trends Biochem Sci, 26, 390–397.

ALBINSSON, S. & SESSA, W. 2011. Can microRNAs control vascular smooth muscle phenotypic modulation and the response to injury? Physiol Genomics, 43, 529-533.

ALBINSSON, S., SUAREZ Y, SKOURA A, OFFERMANNS S, MIANO JM & WC., S. 2010. MicroRNAs are necessary for vascular smooth muscle growth, differentiation, and function. Arterioscler Thromb Vasc Biol, 30, 1118–1126.

ALEXANDER, M. & OWENS, G. 2012. Epigenetic control of smooth muscle cell differentiation and phenotypic switching in vascular development and disease. Annu Rev Physiol, 74, 1–28.

ANTONSSON, B. 2001. Bax and other pro-apoptotic Bcl-2 family ‘‘killer-proteins’’ and their victim, the mitochondrion. Cell Tissue Res, 306, 347–361.

ANTONSSON, B., MONTESSUIT, S., SANCHEZ, B. & MARTINOU, J. C. 2001. Bax is present as a high molecular weight oligomer/complex in the mitochondrial membrane of apoptotic cells. J. Biol. Chem, 276, 11615–11623.

AOI, W., NAITO Y, MIZUSHIMA K, TAKANAMI Y, KAWAI Y, ICHIKAWA H & T., Y. 2010. The microRNA miR-696 regulates PGC-1a in mouse skeletal muscle in response to physical activity. Am J Physiol Endocrinol Metab, 298, E799–E806.

ARCHER, S. 2010. The mitochondrion as a swiss army knife: implications for cardiovascular disease. J Mol Med, 88, 963-965.

ARCHER, S., GLENN MARSBOOM, GENE H. KIM, HANNAH J. ZHANG, PETER T. TOTH, ERIC C. SVENSSON, JASON R.B. DYCK, MARDI GOMBERG-MAITLAND, BERNARD THÉBAUD, ALIYA N. HUSAIN, NICOLE CIPRIANI & REHMAN., J. 2010. Epigenetic Attenuation of Mitochondrial Superoxide Dismutase 2 (SOD2) in Pulmonary Arterial Hypertension: a basis for excessive cell proliferation and a new therapeutic target. Circulation, 24, 2661–2671.

ARCIUCH, V. G. A., ELGUERO, M. E., PODEROSO, J. J. & CARRERAS, M. C. 2012. Mitochondrial regulation of cell cycle and proliferation. Antioxid. Redox Signal, doi:

ARSHAM, A., HOWELL, J. J. & SIMON, M. C. 2003. A novel hypoxia-inducible factor-independent hypoxic response regulating mammalian target of rapamycin and its targets. J. Biol. Chem., 278, 29655-29660.

ASCHRAFI, A., SCHWECHTER AD, MAMEZA MG, NATERA-NARANJO O, GIOIO AE & BB., K. 2008. MicroRNA-338 regulates local cytochrome c oxidase IV mRNA levels and oxidative phosphorylation in the axons of sympathetic neurons. J Neurosci, 28, 12581–12590.

ASHRAFIAN, H., DOCHERTY, L., LEO, V., TOWLSON, C., NEILAN, M., STEEPLES, V., LYGATE, C. A., HOUGH, T., TOWNSEND, S. & WILLIAMS, D., ET AL. 2010. A mutation in the mitochondrial fission gene Dnm1l leads to cardiomyopathy. PLoS Genet., 6, e1001000.

AURELIO, M., FRANCESCO PALLOTTI, ANTONI BARRIENTOS, CARL GAJEWSKI, JENNIFER KWONG, CLAUDIO BRUNO, M. FLINT BEAL & MANFREDI., G. 2001. In Vivo Regulation of Oxidative Phosphorylation in Cells Harboring a Stop-codon Mutation in Mitochondrial DNA-encoded Cytochrome c Oxidase Subunit I. The Journal of biological chemistry, 276, 46925-46932.

BAEK, D., VILLEN J, SHIN C, CAMARGO FD, GYGI SP & DP., B. 2008. The impact of microRNAs on protein output. Nature, 455, 64–71.

BAI, M., NAN-ZE YU, FEI LONG, CHENG FENG & WANG., X.-J. 2016. Effects of CDKN2A (p16INK4A/p14ARF) Over-Expression on Proliferation and Migration of Human Melanoma A375 Cells. cellular physiology and biochemistry, 40, 1367-1376.

BARREY, E., SAINT-AURET G, BONNAMY B, DAMAS D, BOYER O & X., G. 2011. Pre-microRNA and mature microRNA in human mitochondria. PLoS ONE, 6, e20220.

BARTEL, D. 2004. MicroRNAs: genomics, biogenesis, mechanism, and function. Cell 116, 281–297.

BECKER, T., BOTTINGER, L. & PFANNER, N. 2012. Mitochondrial protein import: from trans- port pathways to an integrated network. Trends Biochem. Sci, 37, 85–91.

BELTING, M. & WITTRUP, A. 2008. Nanotubes, exosomes, and nucleic acid – binding peptides provide novel mechanisms of intercellular communication in eukaryotic cells: implications in health and disease. The Journal of cell biology, 183, 1187-1191.

BERAUD, N., PELLOUX S, USSON Y, KUZNETSOV AV, RONOT X, TOURNEUR Y & V., S. 2009. Mitochondrial dynamics in heart cells: very low amplitude high frequency fluctuations in adult cardiomyocytes and flow motion in non beating Hl-1 cells. J Bioenerg Biomembr, 41, 195–214.

BIBERTHALER, P., STEGMAIER J, MAYER V, KIRCHHOFF C, NETH P, MUSSACK T, MUTSCHLER W & M, J. 2004. Initial post-traumatic translocation of NF-kappa B and TNF-alpha mRNA expression in peripheral blood monocytes of trauma patients with multiple injuries: a pilot study. shock, 22, 527-532.

BIUCKIANS, A., ERIC SCOTT, GEORGE MEIER, JEAN PANNETON & GLICKMAN., M. 2008. The natural history of autologous fistulas as first-time dialysis access in the KDOQI era. Journal of vascular surgery, 47, 415-21; discussion 420-1.

BOETTGER, T., BEETZ N, KOSTIN S, SCHNEIDER J, KRUGER M, HEIN L & T., B. 2009. Acquisition of the contractile phenotype by murine arterial smooth muscle cells depends on the miR143/145 gene cluster. J Clin Invest, 119, 2634 – 2647.

BOGER, R., BODE-BOGER SM, TSAO PS, LIN PS, CHAN JR & JP, C. 2000. An endogenous inhibitor of nitric oxide synthase regulates endothelial adhesiveness for monocytes. J Am Coll Cardiol, 36, 2287–2295.

BOLSTER, D., S. J. CROZIER, S. R. KIMBALL & JEFFERSON., L. S. 2002. AMP-activated protein kinase suppresses protein synthesis in rat skeletal muscle through down-regulated mammalian target of rapamycin (mTOR) signaling. J. Biol. Chem., 277, 23977–23980.

BONCI, D. 2010. MicroRNA-21 as therapeutic target in cancer and cardiovascular disease. Recent Pat Cardiovasc Drug Discov, 5, 156–161.

BOOTH, N. & BENNETT, B. 1994. Fibrinolysis and thrombosis. BaillieÁre's Clin Haematol, 7, 559 - 572.

BRAICU, C., C TOMULEASA, P MONROIG, A CUCUIANU, I BERINDAN-NEAGOE & CALIN., G. A. 2015. Exosomes as divine messengers: are they the Hermes of modern molecular oncology? cell death and differentiation, 22, 34-45.

BRAND, K., PAGE S, WALLI AK, NEUMEIER D & PA, B. 1997. Role of nuclear factor-kappa B in atherogenesis. Exp physiol, 82, 297-304.

BRESCIA, M., CIMINO JE, APPEL K & BJ., H. 1966. Chronic hemodialysis using venipuncture and a surgically created arteriovenous fistula. NEngl J Med 275, 1089-92.

BURGERING, B. & COFFER, P. 1995. Protein kinase B (c-Akt) in phosphatidylinositol-3-OH kinase signal transduction. Nature, 376, 599–602.

CADENA, D. & GILL, G. 1992. Receptor tyrosine kinases. FASEB J, 6, 2332–7.

CAMPBELL, S., R. KHOSRAVI-FAR, K. L. ROSSMAN, G. J. CLARK & DER, C. J. 1998. Increasing complexity of Ras signaling. Oncogene, 17, 1395–1413.

CANNINO, G., DI LIEGRO C & A., R. 2007. Nuclear-mitochondrial interaction. Mitochondrion, 7, 359–366.

CAPLICE, N., WANG S & AL., T. M. E. 2007. Neoangiogenesis and the presence of progenitor cells in the venous limb of an arteriovenous fistula in the rat. Am J Physiol Renal Physiol, 293, F470–F475.

CARLING, D., MAYER, F. V., SANDERS, M. J. & GAMBLIN, S. J. 2011. AMP-activated protein kinase: nature's energy sensor. Nat. Chem. Biol., 7, 512–518.

CARRILLO-SEPULVEDA & BARRETO-CHAVES. 2010. Phenotypic modulation of cultured vascular smooth muscle cells: a functional analysis focusing on MLC and ERK1/2 phosphorylation. Mol Cell Biochem, 341, 279–289.

CARTER, T. & PEARSON , J. 1992. Regulation of prostacyclin synthesis in endothelial cells. News Physiol Sci, 7, 64 - 69.

CASSIDY-STONE, A., CHIPUK J., INGERMAN, E., SONG, C., YOO, C., KUWANA, T., KURTH,M., SHAW, J., HINSHAW, J., GREEN, D., & NUNNARI., J. 2008. Chemical Inhibition of the Mitochondrial Division Dynamin Reveals Its Role in Bax/Bak-Dependent Mitochondrial OuterMembrane Permeabilization. Developmental Cell, 14, 193–204.

CHALMERS, S., SAUNTER, C., WILSON, C., COATS, P., GIRKIN, J. & MCCARRON, J. G. 2012. Mitochondrial Motility and Vascular Smooth Muscle Proliferation. Arterioscler Thromb Vasc Biol, 32, 3000-3011.

CHANDEL, N. 2010. Mitochondrial regulation of oxygen sensing. Adv. Exp. Med. Biol., 661, 339-354.

CHANG, C.-J., KO PJ, HSU LA, KO YS, KO YL, CHEN CF, HUANG CC, HSU TS, LEE YS & JH., P. 2004. Highly increased cell prolif-eration activity in the restenotic hemodialysis vascular access after percutaneous transluminal angioplasty : implication in prevention of restenosis. Am J Kidney Dis, 43, 74-84.

CHANG, C.-R. & BLACKSTONE, C. 2007. Cyclic amp-dependent protein kinase phosphorylation of drp1 regulates its gtpase activity and mitochondrial morphology. J Biol Chem, 282, 21583–21587.

CHANG, J.-C., KOU, S., LIN, W., & LIU., C.-S. 2010. Regulatory role of mitochondria in oxidative stress and atherosclerosis. World J Cardiol 2, 150-159.

CHARRON, T., NILI, N., & STRAUSS., B. 2006. The cell cycle: a critical therapeutic target to prevent vascular proliferative disease. Can J Cardiol, 41B-55B.

CHAUDHURY, R., L.M SPERGEL, A. BESARAB, A. ASIF & RAVANI, P. 2007. Biology of arteriovenous fistula failure. J. Nephrol, 20, 150-163.

CHEN, G. & NUNEZ, G. 2010. Sterile inflammation: sensing and reacting to damage. Nat. Rev. Immunol, 10, 826-837.

CHEN, K.-H., K.-H., GUO, X., MA, D., GUO, Y., LI, O., YANG, D., LI, P., QIU, X., WEN, S., XIAO, R.-P. & TANG, J. 2004. Dysregulation of HSG triggers vascular proliferative disorders. Nat. Cell Biol, 6, 872–883.

CHEN, X. & FUJISE, K. 2005. Restenosis: Emerging molecular targets. Going beyond drug-eluting stents. Drug Discovery Today: Disease Mechanisms, 2, 1-9.

CHEN, Y.-R. & ZWEIER, J. 2014. CARDIAC MITOCHONDRIA AND ROS GENERATION. circulation research, 114, 524-537.

CHENG, Y., LIU X, YANG J, LIN Y, XU DZ, LU Q, DEITCH EA, HUO Y, DELPHIN ES & C., Z. 2009. MicroRNA-145, a novel smooth muscle cell phenotypic marker and modulator, controls vascular neointimal lesion formation. Circ Res, 105, 158–166.

CHIEN, K. & OLSON, E. 2002. Converging pathways and principles in heart development and disease Cell, 153–162.

CHIPUK, J., MOLDOVEANU, T., LLAMBI, F., PARSONS, M. J. & GREEN, D. R. 2010. The BCL-2 family reunion. Mol. Cell, 37, 299-310.

CHONG, H., H. G. VIKIS & GUAN, K. L. 2003. Mechanisms of regulating the Raf kinase family. Cell Signal, 15, 463–469.

COBB, M. 1999. MAP kinase pathways. Prog. Biophys. Mol. Biol, 71, 479–500.

COCUCCI, E., RACCHETTI, G., & MELDOLESI., J. 2009. Shedding microvesicles: artefacts no more. trends in cell biology, 19, 43-51.

COLLINS, V., HAJIZADEH, S., HOLME, E., JONSSON, I. M. & TARKOWSKI, A. 2004. Endogenously oxidized mitochondrial DNA induces in vivo and in vitro inflammatory responses. J. Leukoc. Biol, 75, 995-1000.

COMELLI, L., ROCCHICCIOLI, S., SMIRNI, S., SALVETTI, A., SIGNORE, G., CITTI, L., GIOVANNA TRIVELLA, M., & CECCHETTINI., A. 2014. Characterization of secreted vesicles from vascular smooth muscle cells. Mol. BioSyst., 10, 1146-1152.

CONDE-VANCELLS, J., RODRIGUEZ-SUAREZ E, EMBADE N, GIL D, MATTHIESEN R, VALLE M, ELORTZA F, LU SC, MATO JM & JM., F.-P. 2008. Characterization and comprehensive proteome profiling of exosomes secreted by hepatocytes. J Proteome Res, 7, 5157-5166.

CONSIGNY, P. 1995. Pathogenesis of atherosclerosis. AJR, 164, 553-558.

COOK, C., WEISER MCM, SCHWARTZ PE, JONES CL & RA, M. 1994. Developmentally timed expression of an embryonic growth phenotype in vascular smooth muscle cells. Circ Res, 79, 189 –196.

CORDES, K., SHEEHY NT, WHITE MP, BERRY EC, MORTON SU, MUTH AN, LEE TH, MIANO JM, IVEY KN & D., S. 2009. miR-145 and miR-143 regulate smooth muscle cell fate and plasticity. Nature, 460, 705–710.

CORTESE, J., VOGLINO, A. L. & HACKENBROCK, C. R. 1998. Multiple conformations of physiological membrane-bound cytochrome c. Bio-chemistry, 37, 6402–6409.

CROWTHER, M. 2005. Pathogenesis of atherosclerosis. American Society of Hematology, 436-441.

CUNNINGHAM, J., RODGERS, J. T., ARLOW, D. H., VAZQUEZ, F., MOOTHA, V. K. & PUIGSERVER, P. 2007. mTOR controls mitochondrial oxidative function through a YY1-PGC-1alpha transcriptional complex. Nature, 450, 736-740

DAVIES, M. & HAGEN, P.-O. 1994. Pathobiology of intimal hyperplasia. Br. J. Surg, 81, 1254–69.

DAVIES, M. & HAGEN, P.-O. 1995. Pathophysiology of vein graft failure: a review. Eur. J. Vasc. Endovasc. Surg, 9, 7–18.

DAVIES, M., WOOLF N, ROWLES PM & J., P. 1988. Morphology of the endothelium over atherosclerotic plaques in human coronary arteries. Br Heart J, 60, 459–64.

DECHERT, M., HOLDER JM & WT., G. 2001. p21-activated kinase 1 par- ticipates in tracheal smooth muscle cell migration by signaling to p38 Mapk. Am J Physiol Cell Physiol, 281, C123–C132.

DENG, L., BLANCO, F., STEVENS, H., LU, R., CAUDRILLIER, A., MCBRIDE, M., MCCLURE, J., GRANT, J., THOMAS, M., FRID, M., STENMARK, K., WHITE, K., SETO, A., MORRELL, N., BRADSHAW, A., MACLEAN, M., & BAKER, A. H. 2015. MicroRNA-143 Activation Regulates Smooth Muscle and Endothelial Cell Crosstalk in Pulmonary Arterial Hypertension. Circulation Research, 117, 870- 883.

DEYOUNG, M., HORAK, P., SOFER, A., SGROI, D. & ELLISEN, L. W. 2008. Hypoxia regulates TSC1/2-mTOR signaling and tumor suppression through REDD1-mediated 14-3-3 shuttling. Genes Dev., 22, 239-251.

DIACOVO, T., DEFOUGEROLLES AR, BAINTON DF & TA, S. 1994. A functional integrin ligand on the surface of platelets: intercellular adhesion molecule-2. J. Clin. Invest, 94, 1243–51.

DIAZ, F., KOTARSKY, H., FELLMAN, V. & MORAES, C. T. 2011. Mitochondrial disorders caused by mutations in respiratory chain assembly factors. Semin. Fetal Neonatal Med, 16, 197–204.

DICKEY, A. & STRACK, S. 2011. PKA/AKAP1 and PP2A/Bb2 regulate neuronal morphogenesis via Drp1 phosphorylation and mitochondrial bioenergetics. J. Neurosci., 31, 15716–15726.

DINARELLO, C. 2000. Proinflammatory Cytokines. CHEST, 118, 503-508.

DOLLERY, C., HUMPHRIES, S., MCCLELLAND, A., LATCHMAN, D., & MCEWAN., J. 1999. Expression of tissue inhibitor of matrix metalloproteinases 1 by use of an adenoviral vector inhibits smooth muscle cellmigration and reduces neointimal hyperplasia in the rat model of vascular balloon injury. Circulation, 99, 3199–3205.

DROMPARIS, P., SUTENDRA G & E, M. 2010. The role of mitochondria in pulmonary vascular remodeling. Journal of molecular medicine, 88, 1003-1010.

DUBBELHUIS, P. & MEIJER, A. 2002. Hepatic amino aciddependent signaling is under the control of AMP-dependent protein kinase. FEBS Lett, 521, 39–42.

DUCHENE, A.-M., PUJOL, C. & MARECHAL-DROUARD, L. 2009. Import of tRNAs and aminoacyl- tRNA synthetases into mitochondria. Curr. Genet., 55, 1–18.

DZAU, V., BRAUN-DULLAEUS, R., & SEDDING., D. 2002. Vascular Proliferation and Atherosclerosis: New Perspectives and Therapeutic Strategies. Nat Med, 8, 1249-1256.

EAPEN, C., MADESH, M., BALASUBRAMANIAN A., PULIMOOD A., MATHAN M. 1998. Mucosal mitochondrial function and antioxidant defences in patients with gastric carcinoma. Scand. J. Gastroenterol., 33, 975-981.

EDGINGTON, T., MACKMAN N, BRAND K & W, R. 1991. The structural biology of expression and function of tissue factor. Thromb. Haemost, 66, 67–79.

EFEYAN, A. & SABATINI, D. 2010. mTOR and cancer: many loops in one pathway. Current Opinion in Cell Biology, 22, 169-176.

ELIA, L., QUINTAVALLE M, ZHANG J, CONTU R, COSSU L, LATRONICO MV, PETERSON KL, INDOLFI C, CATALUCCI D, CHEN J, COURTNEIDGE SA & G., C. 2009. The knockout of miR-143 and −145 alters smooth muscle cell maintenance and vascular homeostasis in mice: correlates with human disease. Cell Death Differ, 16, 1590–1598.

ESCREVENTE, C., KELLER S, ALTEVOGT P & J., C. 2011. Interaction and uptake of exosomes by ovarian cancer cells. BMC Cancer, 11, 108.

ESMON, C. 1995. Thrombomodulin as model of molecular mechanisms that modulate protease specificity and function at the vessel surface. FASEB J, 9, 946 - 955.

ESTAQUIER, J. & ARNOULT, D. 2007. Inhibiting Drp1-mediated mitochondrial fission selectively prevents the release of cytochrome c during apoptosis. cell death and differentiation, 14, 1086-1094.

FABBRI, M., PAONE, A., CALORE, F., GALLI, R., GAUDIO, E., & SANTHANAM, A. 2012. MicroRNAs bind to Toll-like receptors to induce prometastatic inflammatory response. Proc Natl Acad Sci U S A, 109, E2110–2116.

FADER, C., SANCHEZ, D. G., MESTRE, M. B. & COLOMBO, M. I. 2009. TI-VAMP/VAMP7 and VAMP3/cellubrevin: two v-SNARE proteins involved in specific steps of the autophagy/multivesicular body pathways. Biochim. Biophys Acta, 1793, 1901-1916.

FADINI, G., LOSORDO D & S., D. 2012. Critical Reevaluation of Endothelial Progenitor Cell Phenotypes for Therapeutic and Diagnostic Use. CIRC RES, 110, 624-637.

FALK, E. 2006. Pathogenesis of atherosclerosis. J Am Coll Cardiol 47, C7–12.

FARB, A., WEBER DK, KOLODGIE FD, BURKE AP & R., V. 2002. Morphological predictors of restenosis after coronary stenting in humans. Circulation, 105, 2974–2980.

FELDMAN, M. & SHOKAT, K. 2010. New Inhibitors of the PI3K-Akt-mTOR Pathway: Insights into mTOR Signaling from a New Generation of Tor Kinase Domain Inhibitors (TORKinibs). current topics in microbiology and immunology, 347, 241-262.

FILIPOWICZ, W., BHATTACHARYYA, S., & SONENBERG., N. 2008. Mechanisms of post- transcriptional regulation by microRNAs: are the answers in sight? . Nat. Rev. Genet., 9 102–114.

FINGAR, D. & BLENIS, J. 2004. Target of rapamycin (TOR): an integrator of nutrient and growth factor signals and coordinator of cell growth and cell cycle progression. Oncogene, 23, 3151–3171.

FINKEL, T. 2011. Signal transduction by reactive oxygen species. The Journal of cell biology, 194, 7-15.

FLEISSNER, F., JAZBUTYTE, V., FIEDLER, J., GUPTA, S. K., YIN, X., XU, Q., GALUPPO, P., KNEITZ, S., MAYR, M., ERTL, G. & AL., E. 2010. Short communication: Asymmetric dimethylarginine impairs angiogenic progenitor cell function in patients with coronary artery disease through a microRNA-21-dependent mechanism. Circ. Res, 107, 138–143.

FLEMING, R. 1999. The pathogenesis of vascular disease. Textbook of Angiology. New York: Springer-Verlag, 787-798.

FOLKMAN, J. & SHING, Y. 1992. Angiogenesis. J Biol Chem, 267, 10931 - 10934.

FRANK, F., SONENBERG, N. 2010. Structural basis for 5'-nucleotide base-specific recognition of guide RNA by human AGO2. Nature, 465, 818–822.

FRANK, S., GAUME, B., BERGMANN-LEITNER, E., LEITNER, W., ROBERT, E., & CATEZ, F. 2001. The role of dynamin-related protein 1, a mediator of mitochondrial fission, in apoptosis. Dev Cell 1, 515–525.

FREEDMAN, J., SAUTER R & AL., B. E. E. 1999. Deficient platelet-derived nitric oxide and enhanced hemostasis in mice lacking the NOSIII gene. Circ Res, 84, 1416 - 1421.

FROHMAN, M. 2010. Mitochondria as integrators of signal transduction and energy production in cardiac physiology and disease. J Mol Med, 88, 967-970.

FUKUDA, R., MCNEW, J. A., WEBER, T., PARLATI, F., ENGEL, T., NICKEL, W., ROTHMAN, J. E. & SOLLNER, T. H. 2000. Functional architecture of an intracellular membrane t-SNARE. Nature, 407, 198–202.

FULTON, D., GRATTON J-P & AL., M. T. E. 1999. Regulation of endotheliumderived nitric oxide production by the protein kinase Akt. Nature, 399, 597 - 601.

FURCHGOTT, R. & VANHOUTTE, P. 1989. Endothelium-derived relaxing and contracting factors. FASEB J, 3, 2007-2018.

GALLUZZI, L., VITALE, I., ABRAMS, J., ALNEMRI, E., BAEHRECKE, E., BLAGOSKLONNY, M., DAWSON, T., DAWSON, V., EL-DEIRY, W., FULDA, S., GOTTLIEB, E., GREEN, R., HENGARTNER, M., KEPP, O., KNIGHT, R.

KUMAR, S., LIPTON, S., LU, X., MADEO, F., MALORNI, W., MEHLEN, P., NUÑEZ, G., PETER, M., PIACENTINI, M., RUBINSZTEIN, D., SHI, Y., SIMON, H-U., VANDENABEELE, P., WHITE, E., YUAN, J., ZHIVOTOVSKY, B., MELINO, G., & KROEMER., G. 2012. Molecular definitions of cell death subroutines: recommendations of the Nomenclature Committee on Cell Death 2012. cell death and differentiation, 19, 107-120.

GAO, P., TCHERNYSHYOV, I., CHANG, T., LEE, Y., KITA, K., OCHI, T., ZELLER, K., DE MARZO, A., VAN EYK, J., MENDELL, J. 2009. c-Myc suppression of miR-23a/ b enhances mitochondrial glutaminase and glutamine metabolism. Nature, 458, 762–765.

GAO, S.-M., CHEN, C., WU, J., TAN, Y., YU, K., XING, C., YE, A., YIN, L. 2010. Synergistic apoptosis induction in leukemic cells by miR-15a/16-1 and arsenic trioxide. Biochem Biophys Res Commun, 403, 203–208.

GEYER, M. & WITTINGHOFER, A. 1997. GEFs, GAPs, GDIs and effectors: taking a closer (3D) look at the regulation of Ras-related GTP-binding proteins. Curr. Opin. Struct. Biol, 7, 786–792.

GHOSH, S., MAY, M. 1998. NF-kappa B and Rel proteins: evolutionarily conserved mediators of immune response. Annu Rev immunol, 16, 225-260.

GILMORE, J. 2006. KDOQI clinical practice guidelines and clinical practice recommendations. Nephrology Nursing Journal, 33, 487–488.

GINGRAS, A.-C., KENNEDY, S., O'LEARY, M., SONENBERG, N., & HAY, N. 1998. 4E-BP1, a repressor of mRNA translation, is phosphorylated and inactivated by the Akt(PKB) signaling pathway. Genes & Dev, 12, 502–513.

GLASS, C. & WITZTUM, J. 2001. Atherosclerosis. The road ahead. Cell, 104, 503–16.

GOLDIE, B., DUN, M., LIN, M., SMITH, N., VERRILLS, N. 2014. Activity-associated miRNA are packaged in Map1b-enriched exosomes released from depolarized neurons. Nucleic Acids Res., 42, 9195–9208.

GONCHAROVA, E., AMMIT, A., IRANI, C., CARROLL, R., ESZTERHAS, A., PANETTIERI, R., & KRYMSKAYA., V. 2002. PI3K is required for proliferation and migration of human pulmonary vascular smooth muscle cells. Lung Cellular and Molecular Physiology 283, L354-L363.

GONZALES, P., PISITKUN, T., HOFFERT, J., TCHAPYJNIKOV, D., STAR, R., KLETA, R., WANG, N. 2009. Large-scale proteomics and phosphoproteomics of urinary exosomes. J Am Soc Nephrol 20, 363-379.

GUERTIN, D. & SABATINI, D. 2007. Defining the Role of mTOR in Cancer. Cancer Cell, 12, 9-22.

GUESCINI, M., GUIDOLIN, D., VALLORANI, L., CASADEI, L., GIOACCHINI, A. M., TIBOLLO, P., BATTISTELLI, M., FALCIERI, E., BATTISTIN, L., AGNATI, L. F. & STOCCHI, V. 2010. C2C12 myoblasts release micro-vesicles containing mtDNA and proteins involved in signal transduction. Exp. Cell. Res., 316, 1977-1984.

GUO, X., CHEN, K-H., GUO, Y., LIAO, H., TANG, J., & XIAO., R.-P. 2007. Mitofusin 2 Triggers Vascular Smooth Muscle Cell Apoptosis via Mitochondrial Death Pathway. circulation research, 101, 1113-1122.

HALES, K. & FULLER, M. 1997. Developmentally regulated mitochondrial fusion mediated by a conserved, novel, predicted GTPase. cell, 90, 121-129.

HAMANAKA, R. & CHANDEL, N. 2010. Mitochondrial reactive oxygen species regulate cellular signaling and dictate biological outcomes. Trends Biochem. Sci, 35, 505–513.

HANSSON, G. 2005. Inflammation, atherosclerosis, and coronary artery disease. N Engl J Med, 352, 1685–95.

HARDIE, G., CARLING, D. & GAMBLIN, S. 2011. AMP-activated protein kinase: also regulated by ADP. Trends Biochem. Sci., 36, 470–477.

HARRIS, T., YAMAKUCHI, M., FERLITO, M., MENDELL, J. 2008. MicroRNA-126 regulates endothelial expression of vascular cell adhesion molecule 1. Proc Natl Acad Sci USA, 105, 1516–1521.

HAYNES, W. & WEBB, D. 1998. Endothelin as a regulator of cardiovascular function in health and disease. J Hypertens, 16, 1081 - 1098.

HE, M., QIN, H., POON, T., SZE, S-C., DING, X., NA CO, N., NGAI, S-M., CHAN, T-F., & WONG., N. 2015. Hepatocellular carcinoma-derived exosomes promote motility of immortalized hepatocyte through transfer of oncogenic proteins and RNAs. Carcinogenesis, 36, 1008-1018.

HENN, V., SLUPSKY J & AL, G. M. E. 1998. CD40 ligand on activated platelets triggers an inflammatory reaction of endothelial cells. Nature, 391, 591–4.

HITCHLER, M., OBERLEY L & FE., D. 2008. Epigenetic silencing of SOD2 by histone modifications in human breast cancer cells. Free Radic Biol Med, 45, 1573–1580.

HOCH, R. & SORIANO, P. 2003. Roles of PDGF in animal development. Development, 130, 4769–4784.

HOFFMAN, B., GRASHOFF, C. & MA., S. 2011. Dynamic molecular processes mediate cellular mechanotransduction. Nature, 475, 316–323.

HONDA, H., HSIAI, T., WORTHAM, C., CHEN, M., LIN, H., NAVAB, M. 2001. A complex flow pattern of low shear stress and flow reversal promotes monocyte binding to endothelial cells. Atherosclerosis 158, 385-90.

HSU, C., MOROHASHI, Y., YOSHIMURA, S., MANRIQUE-HOYOS, N., JUNG, S., LAUTERBACH, M. A., BAKHTI, M., GRONBORG, M., MOBIUS, W., RHEE, J., BARR, F. A. & SIMONS, M. 2010. Regulation of exosome secretion by Rab35 and its GTPase-activating proteins TBC1D10A-C. J. Cell Biol. , 189, 223–232.

HU, G., DRESCHER K., & XM., C. 2012. Exosomal miRNAs: biological properties and therapeutic potential. Front Genet, 3, 56.

HUANG, L., WENYA, M., YIDI, M., FENG, D., CHEN, H. 2015. Exosomes in Mesenchymal Stem Cells, a New Therapeutic Strategy for Cardiovascular Diseases. Int. J. Biol. Sci., 11, 238-245.

HUANG, P., HUANG, Z. 1995. Hypertension in mice lacking the gene for endothelial nitric oxide synthase. Nature, 377, 239 - 242.

HUNGERFORD, J. & LITTLE, C. 1999. Developmental biology of the vascular smooth muscle cell: building a multilayered vessel wall. J Vasc Res, 36, 2–27.

HYDEN, M. & GHOSH, S. 2004. Signaling to NF-kappa B. Genes Dev., 18, 2195-2224.

INGERMAN, E., PERKINS, E. M., MARINO, M., MEARS, J. A., MCCAFFERY, J. M., HIN- SHAW, J. E. & NUNNARI, J. 2005. Dnm1 forms spirals that are structurally tailored to fit mitochondria. J. Cell Biol., 170, 1021–1027.

INOKI, K., LI, Y., ZHU, T., WU, J. & GUAN, K. L. 2002. TSC2 is phosphorylated and inhibited by Akt and suppresses mTOR signalling. Nat. Cell Biol., 4, 648-657.

INOUE, T., SOHMA, R., MIYAZAKI, T., IWASAKI, Y., YAGUCHI, I. 2000. Comparison of activation process of platelets and neutrophils after coronary stent implantation versus balloon angioplasty for stable angina pectoris. Am. J. Cardiol, 86, 1057–62.

ISHIWATA, S., TUKADA, T., NAKANISHI, S., NISHIYAMA, S. 1997. Postangioplasty restenosis: platelet activation and the coagulationfibrinolysis system as possible factors in the pathogenesis of restenosis. Am. Heart J., 133, 387–92.

ITO, K., HIRAO, A., ARAI, F., MATSUOKA, S., TAKUBO, K., HAMAGUCHI, I., NOMIYAMA, K., HOSOKAWA, K., SAKURADA, K. & NAKAGATA, N., ET AL. 2004. Regulation of oxidative stress by ATM is required for self-renewal of haematopoietic stem cells. Nature, 431, 997–1002.

JANOWSKA-WIECZOREK, A., WYSOCZYNSKI, M., KIJOWSKI, J., MARQUEZ-CURTIS, L., MACHALINSKI, B., RATAJCZAK, J. 2005. Microvesicles derived from activated platelets induce metastasis and angiogenesis in lung cancer. Int J Cancer 113, 752–760.

JEFFREY, S., SHELBY, H., ELAINE, D., ROBERT, M., RUSS, K., DEAN, L., ROBERT, G., JAMES, R., ERIC, O., & HIROMI., Y. 2005. Altered vascular remodeling infibulin-5-deficient mice reveals a role of fibulin-5 in smooth muscle cell proliferation and migration. Proc. Natl. Acad. Sci. USA, 102, 2946–2951.

JI, R., CHENG, Y., YUE, J., YANG, J., LIU, X., CHEN, H., DEAN, D. 2007a. MicroRNA expression signature and antisense-mediated depletion reveal an essential role of microRNA in vascular neointimal lesion formation. Circ Res, 100, 1579 – 1588.

JOHNSON, G. & LAPADAT, R. 2002. Mitogen-activated protein kinase pathways mediated by ERK, JNK, and p38 protein kinases. Science (New York, N.Y.), 298, 1911-1912.

JONER, M., FINN, A., FARB, A., MONT, E., KOLODGIE, F., LADICH, E., KUTYS, R., SKORIJA, K., & GOLD., H. 2006. Pathology of Drug-Eluting Stents in Humans : Delayed Healing and Late Thrombotic Risk. Journal of the American College of Cardiology, 48, 193-202.

K/DOQI 2006. National Kidney Foundation Kidney Disease Outcomes and Quality Initiative (K/DOQI). Accessed at www.kidney.org.

KADIU, I., NARAYANASAMY, P., DASH, P., ZHANG, W., & GENDELMAN, H. 2012. Exosomes and Microvesicles as Facilitators of Biochemical and Biologic Characterization of HIV-1 Infection in Macrophages. j immunol, 1102244.

KANG, B., TAVECCHIO, M., GOEL, H., HSIEH, C., GARLICK, D., RASKETT, C., LIAN, J., STEIN, G., LANGUINO, L., & ALTIERI., D. C. 2011. Targeted inhibition of mitochondrial Hsp90 suppresses localised and metastatic prostate cancer growth in a genetic mouse model of disease. Br. J. Cancer, 104, 629–634.

KAPUSTIN, A., CHATROU, M., DROZDOV, I., ZHENG, Y., DAVIDSON, S., SOONG, D., FURMANIK, M., SANCHIS, P., DE ROSALES, R., ALVAREZ-HERNANDEZ, D., SHROFF, R., YIN, X., & MULLER, K. 2015. Vascular Smooth

Muscle Cell Calcification Is Mediated by Regulated Exosome Secretion. CIRC RES, 116, 1312-1323.

KARBOWSKI, M., NORRIS, K., CLELAND, M., JEONG, S. & YOULE, R. 2006. Role of Bax and Bak in mitochondrial morphogenesis. Nature, 443, 658–662.

KARBOWSKI, M., JEONG, S., & YOULE., R. 2004. Endophilin B1 is required for the maintenance of mitochondrial morphology. J. Cell Biol., 166, 1027–1039.

KATSUDA, T., KOSAKA, N. & OCHIYA., T. 2014. The roles of extracellular vesicles in cancer biology: Toward the development of novel cancer biomarkers. Proteomics, 14, 412-425.

KATZMANN, D., ODORIZZI, G. & EMR, S. 2002. Receptor downregulation and multivesicular-body sorting. Nat. Rev. Mol. Cell. Biol., 3, 893-905.

KAWAI-KOWASE, K. & OWENS, G. 2007. Multiple repressor pathways contribute to phenotypic switching of vascular smooth muscle cells. American Journal of Physiology - Cell Physiology, 292, C59-C69.

KEREN, G. 1997. Compensatory enlargement, remodeling, and restenosis. Adv Exp Med Biol, 430, 187-96.

KIM, N., HAN, J. 2009. Biogenesis of small RNAs in animals. Nat Rev Mol Cell Biol, 10, 126–39.

KONNER, K., NONNAST-DANIEL, B. 2003. The arteriovenous fistula. J Am Soc Nephrol, 14, 1669-80.

KOPPERS-LALIC, D., HACKENBERG, M., BIJNSDORP, I., VAN EIJNDHOVEN, M., SADEK, P. & SIE, D. 2014. Non templated nucleotide additions distinguish the small RNA composition in cells from exosomes. Cell Rep, 8, 1649–1658.

KOSAKA, N., IGUCHI, H., HAGIWARA, K., YOSHIOKA, Y., TAKESHITA, F. 2013. Neutral sphingomyelinase 2 (nSMase2)-dependent exosomal transfer of angiogenic microRNAs regulate cancer cell etastasis. J Biol Chem, 288, 10849–10859.

KOUMANGOYE, R., SAKWE, A., GOODWIN, J., PATEL, T. 2011. Detachment of breast tumor cells induces rapid secretion of exosomes which subsequently mediate cellular adhesion and spreading. PLoS One, 6:e24234.

KREN, B., WONG, P., SARVER, A., ZHANG, X., ZENG, Y., & STEER, C. 2009. MicroRNAs iden- tified in highly purified liver-derived mitochondria may play a role in apoptosis. RNA Biol., 6, 65–72.

KUEHBACHER, A., URBICH, C., ZEIHER, A., & DIMMELER., S. 2007. Role of Dicer and Drosha for endothelial microRNA expression and angiogenesis. Circ Res, 101, 59–68.

KUTRYK, M., FOLEY, D., VAN DEN BRAND, M., HAMBURGER, J., VAN DER GIESSEN, W., DEFEYTER, P., BRUINING, N., SABATE, M. & SERRUYS, P. 2002. Local intracoronary administration of antisense oligonucleotide against c-myc for the prevention of in-stent restenosis: results of the randomized investigation by the Thoraxcenter of antisense DNA using local delivery and IVUS after coronary stenting (ITALICS) trial. J Am Coll Cardiol. , 39, 281-287.

LACKNER, L. & NUNNARI, J. 2010. Small Molecule Inhibitors of Mitochondrial Division: Tools that Translate Basic Biological Research into Medicine. Chemistry & Biology, 17, 578-583.

LACKNER, L. 2014. Shaping the dynamic mitochondrial network. BMC Biology, 12, 35.

LACOLLEY, P., REGNAULT, V., NICOLETTI, A., LI, Z., & MICHEL., J.-B. 2012. The vascular smooth muscle cell in arterial pathology: a cell that can take on multiple roles. Cardiovascular Research, 95, 194–204.

LAKKARAJU, A. & RODRIGUEZ-BOULAN, E. 2008. Itinerant exosomes: emerging roles in cell and tissue polarity. Trends in cell biology, 18, 199-209.

LAPLANTE, M. & SABATINI, D. 2009. mTOR signaling at a glance. Journal of Cell Science, 122, 3589-3594.

LEDUC, L., LEVY, E., BOUITY-VOUBOU, M., & DELVIN., E. 2010. Fetal programming of atherosclerosis: Possible role of the mitochondria. European Journal of Obstetrics & Gynecology and Reproductive Biology, 149, 127-130.

LEE, D.-F., KUO, H., CHEN, C., WEI, Y., CHOU, C., HUNG, J., YEN, C. & HUNG, M. 2008. IKKbeta suppression of TSC1 function links the mTOR pathway with insulin resistance. Int. J. Mol. Med., 22, 633-638.

LEE, M., DAVID, E., MAKKAR R. 2004. Molecular and cellular basis of restenosis after percutaneous coronary intervention: the intertwining roles of platelets, eucocytes, and the coagulation-fibrinolysis system. J. Pathol, 203, 861–70.

LEE, R., FEINBAUM, R. 1993. The C. elegans heterochronic gene lin-4 encodes small RNAs with antisense complementarity to lin-14. Cell, 75, 843–854.

LEE, S., JEONG, S., LIM, W., KIM, S., PARK, Y., SUN, X., YOULE, R., & CHO., H. 2007. Mitochondrial fission and fusion mediators, hFis1 and OPA1, modulate cellular senescence. J. Biol. Chem., 282, 22977–22983.

LEE, Y., JEON, K., LEE, J., KIM, S. 2002. MicroRNA maturation: stepwise processing and subcellular localization. EMBO J, 21, 4663–70.

LEHOUX, S., CASTIER, Y. 2006. Molecular mechanisms of the vascular responses to haemodynamic forces. J Intern

LEWIS, B., BURGE, C. 2005. Conserved seed pairing, often flanked by adenosines, indicates that thousands of human genes are microRNA targets. Cell, 120, 15–20.

LI, J., DONATH, S., LI, Y., QIN, D., PRABHAKAR, B. 2010a. miR-30 regulates mitochondrial fission through targeting p53 and the dynamin-related protein-1 pathway. PLoS Genet, 6, e1000795.

LI, P.-F., DIETZ, R. & HARSDORF, V. 1997. Differential effect of hydrogen peroxide and super- oxide anion on apoptosis and proliferation of vascular smooth muscle cells. . Circulation 96, 3602–3609.

LI, Z., WANG, C., PRENDERGAST, G. 2006. Cyclin D1 functions in cell migration. Cell Cycle, 5, 2440–2.

LIBBY, P. 2002. Inflammation in atherosclerosis. Nature, 420, 868 –74.

LIGHTELL, D. & WOODS, T. 2015. Increased Atherosclerotic Plaque Formation in Response to Exosomes Derived from VSMCs of Diabetic Origin. DIABETES, 641, A136-A137.

LIN, Y., LIU, X., CHENG, Y., YANG, J., HUO, Y. 2009. Involvement of MicroRNAs in hydrogen peroxide-mediated gene regulation and cellular injury response in vascular smooth muscle cells. J Biol Chem, 284, 7903–7913.

LIU, X., CHENG, Y., ZHANG, S., LIN, Y., YANG, J. 2009. A necessary role of miR- 221 and miR-222 in vascular smooth muscle cell proliferation and neointimal hyperplasia. Circ Res 104, 476–487.

LOPEZ, M., KRISTAL, B., CHERNOKALSKAYA, E., LAZAREV, A., SHESTOPALOV, A., BOGDANOVA, A. & ROBINSON, M. 2000. High-throughput profiling of the mitochondrial proteome using affinity fractionation and automation. Electrophoresis, 21, 3427–3440.

LOVREN, F., PAN, Y., QUAN, A., SINGH, K., SHUKLA, P., GUPTA, N., STEER, B., INGRAM, A., GUPTA, M., AL-OMRAN, M., TEOH, H., MARSDEN, P., & VERMA, S., 2012. MicroRNA-145 Targeted Therapy Reduces Atherosclerosis. Circulation, 126, S81–S90.

LUND, E., GUTTINGER, S., CALADO, A., DAHLBERG, J. 2004. Nuclear export of microRNA precursors. Science, 303, 95–8.

MA, L., CHEN, Z., ERDJUMENT-BROMAGE, H., TEMPST, P. & PANDOLFI, P. 2005. Phosphorylation and functional inactivation of TSC2 by Erk implications for tuberous sclerosis and cancer pathogenesis. Cell, 121, 179-193.

MADAMANCHI, N. & RUNGE, M. 2007. Mitochondrial dysfunction in atherosclerosis. Circ Res, 100, 460–473.

MALLIKA, V., GOSWAMI, B., & RAJAPPA, M. 2007. Atherosclerosis Pathophysiology and the Role of Novel Risk Factors: A Clinicobiochemical Perspective. Angiology, 58, 513-522.

MALUMBRES, M. & BARBACID, M. 2003. RAS oncogenes: the first 30 years. Nat. Rev. Cancer, 3, 459–465.

MANIATAKI, E. & MOURELATOS, Z. 2005. Human mitochondrial tRNAMet is exported to the cytoplasm and associates with the Argonaute 2 protein. RNA, 11, 849–852.

MARCUM, J., KENNY J. 1984. Acceleration of thrombinantithrombin complex formation in rat hindquarters via heparin-like molecules bound to the endothelium. J Clin Invest, 74, 341 - 350.

MARSBOOM, G., TOTH, RYAN, J., HONG, Z., WU, X., FANG, Y-H., THENAPPAN, PIAO, L., ZHANG, H., POGORILER, J., CHEN, Y., MORROW, E., WEIR, K., REHMAN, J., & ARCHER., S. 2012. Dynamin-Related Protein 1 (DRP1)-Mediated Mitochondrial Mitotic Fission Permits Hyperproliferation of Vascular Smooth Muscle Cells and Offers a Novel Therapeutic Target in Pulmonary Hypertension. *Circ Res*, 110(11), 1484-1497.

MARUI, N., OFFERMAN, N. 1993. VCAM-1 gene transcription and expression is regulated through an antioxidant sensitive mechanism in human vascular endothelial cells. J Clin Invest 92, 1866 - 1874.

MATHIVANAN, S. & SIMPSON, R. 2009. ExoCarta: A compendium of exosomal proteins and RNA. Proteomics, 9, 4997-5000.

MAZURE, N. & POUYSSÉGUR, J. 2010. Hypoxia-induced autophagy: cell death or cell survival? Curr Opin. Cell Biol. , 22, 177–180.

MCCARRON, J., WILSON, C., SANDISON, M., OLSON, M., GIRKIN, J., SAUNTER, C., & CHALMERS., S. 2013. From Structure to Function: Mitochondrial Morphology, Motion and Shaping in Vascular Smooth Muscle. J Vasc Res 50, 357–371.

MCEVER, R. & CUMMINGS, R. 1997. Role of PSGL-1 binding to selectins in leucocyte recruitment. J. Clin. Invest, 100, S97–103.

MCNAMARA, C., SAREMBOCK, I. 1996. Thrombin and vascular smooth muscle cell proliferation: implications for atherosclerosis and restenosis. Semin. Thromb. Hemost, 22, 139–44.

MEDZHITOV, R. 2007. Recognition of microorganisms and activation of the immune response. Nature, 449, 819-826.

MENDEZ, R., MYERS, M., WHITE, M., & RHOADS, R. 1996. Stimulation of protein synthesis, eukaryotic transla- tion initiation factor 4E phosphorylation, and PHAS-I phos- phorylation by insulin requires insulin receptor substrate 1 and phosphatidylinositol 3-kinase. Mol. Cell. Biol. , 16, 2857– 2864.

MENG, Q.-H., JAMAL, W. 2006. Application to vascular adventitia of a nonviral vector for TIMP-1 gene therapy to prevent intimal hyperplasia. Hum Gene Ther, 17, 717–727.

MENNES, P., GILULA, L. & ANDERSON, C. 1978. Complications associated with arteriovenous fistulas in patients undergoing chronic hemodialysis. Archives of InternalMedicine, 138, 1117–1121.

MERCER, T., NEPH, S., DINGER, M., CRAWFORD, J., SMITH, M., SHEARWOOD, A., HAUGEN, E., BRACKEN, C., RACKHAM, O., STAMATOYANNOPOULOS, J., FILIPOVSKA, A. & MATTICK, J. 2011. The human mitochondrial transcriptome. Cell, 146, 645–658.

MEYERSON, S., SKELLY, C., CURI, M., SHAKUR, U., VOSICKY, J., GLAGOV, S., SCHWARTZ, L., CHRISTEN, T. 2001. The effects of extremely low shear stress on cellular proliferation and neointimal thickening in the failing bypass graft. J Vasc Surg, 34, 90-97.

MIANO, J., VLASIC, N., TOTA, R. 1993. Localization of Fos and Jun proteins in rat aortic smooth muscle cells after vascular injury. Am J Pathol 142, 715–724.

MICHEL, J.-B., ZHENLIN, L. & LACOLLEY., P. 2012. Smooth muscle cells and vascular diseases. Cardiovascular Research, 95, 135-137.

MILEWICZ, D., KWARTLER, C., PAPKE, C., REGALADO, E., CAO, J. & REID., A. 2010. Genetic variants promoting smooth muscle cell proliferation can result in diffuse and diverse vascular diseases: Evidence for a hyperplastic vasculomyopathy. Genetics in Medicine 12, 196-203.

MILLIMAGGI, D., MARI, M., D'ASCENZO, S., CAROSA, E., JANNINI, E., ZUCKER, S. 2007. Tumour vesicle-associated CD147 modulates the angiogenic capability of endothelial cells. . Neoplasia, 9, 349–357.

MITRA, A., GANGAHAR, D., & AGRAWAL, D. 2005. Cellular, molecular and immunological mechanisms in the pathophysiology of vein graft intimal hyperplasia. Immunology and Cell Biology, 84, 115-124.

MITTELBRUNN, M., GUTIÉRREZ-VÁZQUEZ, C., VILLARROYA-BELTRI, C., GONZÁLEZ, S., SÁNCHEZ-CABO, F., ÁNGEL GONZÁLEZ, M., BERNAD, A., & SÁNCHEZ-MADRID., F. 2011. Unidirectional transfer of microRNA-loaded exosomes from T cells to antigen-presenting cells. Nature Communications, 2, 282.

MNJOYAN, Z., DUTTA, R., ZHANG, D., TENG, B-B. & FUJISE, K. 2003. Paradoxical upregulation of tumor suppressor protein p53 in serum-stimulated vascular smooth muscle cells: a novel negative-feedback regulatory mechanism. Circulation, 108, 464–471.

MU, W., RANA, S., & ZÖLLER, M. 2013. Host Matrix Modulation by Tumor Exosomes Promotes Motility and Invasiveness. Neoplasia, 15, 875-887.

MULCAHY, L., PINK R. 2014. Routes and mechanisms of extracellular vesicle uptake. J Extracell Vesicles, doi: 10.3402/jev.v3.24641.

MUNICH, S., SOBO-VUJANOVIC, A., BUCHSER, W., BEER-STOLZ, D. 2012. Dendritic cell exosomes directly kill tumor cells and activate natural killer cells via TNF superfamily ligands. Oncoimmunology, 1, 1074–1083.

MURPHY, G., SAUNDERS, R., METCALFE, M. 2002. Elbow fistulas using autogeneous vein: patency rates and results of revision. Postgrad Med J, 78, 483–486.

MURPHY, M. 2009. How mitochondria produce reactive oxygen species. Biochem. J., 417, 1–13.

NAKAGAWA, Y., IINUMA, M., NAOE, T., NOZAWA, Y. 2007. Characterized mechanism of a-mangostin-induced cell death: Caspase-independent apoptosis with release of endonuclease-G from mitochondria and increased miR-143 expression in human colorectal cancer DLD-1cells. Bioorg Med Chem, 15, 5620–5628.

ARAKAKI, N., NISHIHAMA, T., OWAKI, H., KURAMOTO, Y., SUENAGA, M., MIYOSHI, E., EMOTO, Y., SHIBATA, H., SHONO, M. & HIGUTI, T. 2006. Dynamics of Mitochondria during the Cell Cycle. Biol. Pharm. Bull, 29(9), 1962—1965.

NARUKO, T., UEDA, M., HAZE, K., VAN DER WAL, A., VAN DER LOOS, C., ITOH, A., KOMATSU, R., IKURA, Y., OGAMI, M., SHIMADA, Y., EHARA, S., YOSHIYAMA, M., TAKEUCHI, K., YOSHIKAWA, J., & BECKER, A. 2002. Neutrophil infiltration of culprit lesions in acute coronary syndromes. Circulation, 106, 2894 –900.

NEUPERT, W. & HERRMANN, J. 2007. Translocation of proteins into mitochondria. Annu. Rev. Biochem, 76, 723–749.

NEUSPIEL, M., ZUNINO, R., GANGARAJU, S., RIPPSTEIN, P. & MCBRIDE, H. 2005. Activated mitofusin 2 signals mitochondrial fusion, interferes with Bax activation, and reduces susceptibility to radical induced depolarization. J. Biol. Chem., 280, 25060–25070.

NEWBY, A. & GEORGE, S. 1993. Proposed roles for growth factors in mediating smooth muscle proliferation in vascular pathologies. Cardiovasc. Res., 27, 1173–1183.

NI, C.-W., QIU, H. 2011. MicroRNA-663 upregulated by oscillatory shear stress plays a role in inflammatory response of endothelial cells. Am J Physiol Heart Circ Physiol, 300, H1762–H1769.

NUNNARI, J. & SUOMALAINEN, A. 2012. Mitochondria: in sickness and in health. Cell, 148, 1145-59.

O'NEILL, L. 1995. Towards an understanding of the signal transduction pathways of interleukin 1. Biochim. Biophys. Acta, 1266, 31–44.

OBERST, A., BENDER, C. & GREEN, D. R. 2008. Living with death: the evolution of the mitochondrial pathway of apoptosis in animals. Cell Death Differ, 15, 1139-1146.

OKUNO, D., IINO, R. & NOJI, H. 2011. Rotation and structure of FoF1-ATP synthase. J. Biochem, 149, 655–664.

OMURA, T., YOSHIYAMA, M., IZUMI, Y., KIM, S., MATSUMOTO, R., ENOMOTO, S., KUSUYAMA, T., NISHIYA, D., NAKAMURA, Y., AKIOKA, K., IWAO, H., TAKEUCHI, K., & YOSHIKA,W. 2005. Involvement of c-JunNH2 Terminal Kinase and p38MAPK in Rapamycin-Mediated Inhibition of Neointimal Formation in Rat Carotid Arteries. J Cardiovasc Pharmacol , 46, 519-525.

ONG, S.-B., SUBRAYAN, S., LIM, S., YELLON, D., DAVIDSON, S. 2010. Inhibiting mitochondrial fission pro- tects the heart against ischemia/reperfusion injury. Circulation, 121, 2012-2022.

ORFORD, J., SELWYN, A., GANZ, P., POPMA, J. & ROGERS, C. 2000. The Comparative Pathobiology of Atherosclerosis and Restenosis. The American Journal of Cardiology, 86, 6H-11H.

ORRENIUS, S. 2004. Mitochondrial regulation of apoptotic cell death. Toxicol. Lett., 149, 19–23.

ORRENIUS, S. 2007. Reactive oxygen species in mitochondria-mediated cell death. Drug Metabolism Reviews, 39, 443–455.

OSTROWSKI, M., CARMO, N., KRUME- ICH, S., FANGET, I., RAPOSO, G., SAVINA, A., MOITA, C., SCHAUER, K., HUME, A., FREITAS, R., GOUD, B., BENAROCH, P., HACOHEN, N., FUKUDA, M., DESNOS, C., SEABRA, M., DARCHEN, F., AMIGORENA, S., MOITA, L. & THERY, C. 2010. Rab27a and Rab27b control different steps of the exosomesecretion pathway. Nat.Cell Biol., 12, 19–30.

OWENS, G., KUMAR, M. 2004. Molecular regulation of vascular smooth muscle cell differentiation in development and disease. Physiol Rev, 84, 767– 801.

PAKALA, R., WILLERSON, J. 1997. Effect of serotonin, thromboxane A2, and specific receptor antagonists on vascular smooth muscle cell proliferation. Circulation, 96, 2280–2286.

PANT, S., HILTON, H. & BURCZYNSKI., M. 2012. The multifaceted exosome: Biogenesis, role in normal and aberrant cellular function, and frontiers for pharmacological and biomarker opportunities. Biochemical Pharmacology, 83, 1484-1494.

PARONE, P., DA CRUZ, S., TONDERA, D., MATTENBERGER, Y., JAMES, D., MAECHLER, P., BARJA, F. & MARTINOU, J. 2008. Preventing mitochondrial fission impairs mitochon- drial function and leads to loss of mitochondrial DNA. PLoS ONE, 3, e3257.

PARRA, V., VERDEJO, H., IGLEWSKI, M., DEL CAMPO, A., TRONCOSO, R., JONES, D., ZHU, Y., KUZMICIC, J., PENNANEN, C., LOPEZ CRISOSTO, C., JAÑA, F., FERREIRA, J., NOGUERA, E., CHIONG, M., BERNLOHR, D., KLIP, A., HILL, J., ROTHERMEL, B., DALE ABEL, E., ZORZANO, A. & LAVANDERO, S. 2014. Insulin Stimulates Mitochondrial Fusion and Function in Cardiomyocytes via the Akt- mTOR-NFkB-Opa-1 Signaling Pathway. diabetes, 63, 75-88.

PASZKOWIAK, J. & DARDIK, A. 2003. Arterial wall shear stress: observations from the bench to the bedside. Vasc Endovascular Surg, 37, 47-57.

PEARSON, J. 2000. Normal endothelial cell function. Lupus, 9, 183-188.

PEGTEL, M., COSMOPOULOS, K., THORLEY-LAWSON, D., VAN EIJNDHOVEN, M., HOPMANS, E., LINDENBERG, J., DE GRUIJL, T., WÜRDINGER, T., & MIDDELDORP, J. 2010. Functional delivery of viral miRNAs via exosomes. PNAS, 107, 6328-6333.

PIEK, J., DER WAL, V. 2000. Plaque inflammation in restenotic coronary lesions of patients withstable or unstable angina. J. Am. Coll. Cardiol, 35, 963–7.

QIN, X., WANG, X., WANG, Y., TANG, Z., CUI, Q., XI, J., LI, Y., CHIEN, S. 2010. MicroRNA-19a mediates the suppressive effect of laminar flow on cyclin D1 expression in human umbilical vein endothelial cells. Proc Natl Acad Sci USA, 107, 3240–3244.

QIU, J., ZHENG, Y., HU, J., LIAO, D., GREGERSEN, H., DENG, X., FAN, Y. & WANG, G. 2014. Biomechanical regulation of vascular smooth muscle cell functions: from in vitro to in vivo understanding. J. R. Soc. Interface, 11, 20130852.

QU, J., QU, X., ZHAO, M., TENG, Y., ZHANG, Y., HOU, K. 2009. Gastric cancer exosomes promote tumour cell proliferation through PI3K/Akt and MAPK/ERK activation. Dig Liver Dis, 41, 875–880.

RABINOWITS, G., GERÇEL-TAYLOR, C., DAY, J., TAYLOR, D. & KLOECKER, G. 2009. Exosomal MicroRNA: A Diagnostic Marker for Lung Cancer. clinical lung cancer, 10, 42-46.

RAIBORG, C., RUSTEN, T. & STENMARK, H. 2003. Protein sorting into multivesicular endosomes. Curr. Opin. Cell Biol, 15, 446-455.

RAITOHARJU, E., LYYTIKAINEN, L., LEVULA, M., OKSALA, N., MENNANDER, A., TARKKA, M., KLOPP, N., ILLIG, T., KAHONEN, M., KARHUNEN, P., LAAKSONEN, R. 2011. miR-21, miR-210, miR-34a, and miR-146a/b are up-regulated in human atherosclerotic plaques in the Tampere Vascular Study. Atherosclerosis, 219, 211–217.

RAKESH, K. & AGRAWAL, D. 2005. Cytokines and growth factors involved in control and proliferation of apoptotic smooth muscle cells. Int. Immunopharmacol, 5, 1487–506.

REHMAN, J., ZHANG, H., TOTH, P., ZHANG, Y., MARSBOOM, G., HONG, Z., SALGIA, R., HUSAIN, A., WIETHOLT, C. & ARCHER, S. 2012. Inhibition of mitochondrial fission prevents cell cycle progression in lung cancer. The FASEB journal: official publication of the Federation of American Societies for Experimental Biology.

RELIGA, P., BOJAKOWSKI, K., MAKSYMOWICZ, M., BOJAKOWSKA, M., SIRSJÖ, A., GACIONG, Z., OLSZEWSKI, W., HEDIN, U. 2002. Smooth-muscle progenitor cells of bone marrow origin contribute to the development of neointimal thickenings in rat aortic allografts and injured rat carotid arteries. Transplantation, 74, 1310– 1315.

REN, J., PULAKAT, L., WHALEY-CONNELL, A., & SOWERS, J. 2010. Mitochondrial biogenesis in the metabolic syndrome and cardiovascular disease. Journal of molecular medicine, 88, 993-1001.

REY, F. & PAGANO, P. 2002. The Reactive Adventitia Fibroblast Oxidase in Vascular Function. Arterioscler Thromb Vasc Biol., 22, 1962-1971.

RICHTER, J. & SONENBERG, N. 2005. Regulation of cap-dependent translation by eIF4E inhibitory proteins. Nature, 433, 477-480.

ROSS, R. 1993. The pathogenesis of atherosclerosis: a perspective for the 1990s. Nature, 362, 801-809.

ROSS, R. 1999. Atherosclerosis. An inflammatory disease. N Engl J Med, 340, 115-126.

ROUX, P., BALLIF, B., ANJUM, R., GYGI, S. & BLENIS, J. 2004. Tumor-promoting phorbol esters and activated Ras inactivate the tuberous sclerosis tumor suppressor complex via p90 ribosomal S6 kinase. Proc. Natl. Acad. Sci. USA, 101, 13489-13494.

ROY-CHAUDHURY, P., ZHANG, J., KRISHNAMOORTHY, M., WANG, Y., BANERJEE, R., TEVAR, A., HEFFELFINGER, S. 2006. Cellular phe- notypes in dialysis access stenosis: myofibroblasts, fibrob- lasts and contractile smooth muscle cells. J Am Soc Nephrol, 17.

ROY-CHAUDHURY, P., WANG, Y., KRISHNAMOORTHY, M., ZHANG, J., BANERJEE, R., MUNDA, R., HEFFELFINGER, S. & AREND, L. 2009. Cellular phenotypes in human stenotic lesions from haemodialysis vascular access. Nephrol dial Transplant, 24, 2786-2791.

RUBIO, M., RINEHART, J., KRETT, B., DUVEZIN-CAUBET, S., REICHERT, A. S., SOLL, D. & ALFONZO, J. 2008. Mammalian mitochondria have the innate ability to import tRNAs by a mechanism distinct from protein import. Proc. Natl. Acad. Sci. U. S. A., 105, 9186–9191.

RZUCIDLO, E., MARTIN, K. & POWELL, R. 2007. Regulation of vascular smooth muscle cell differentiation. J Vasc Surg, 45 Suppl A, A25–A32.

SABATEL, C., MALVAUX, L., BOVY, N., DEROANNE, C., LAMBERT, V., GONZALEZ, M., COLIGE, A., RAKIC, J., NOEL, A., MARTIAL, J. 2011. MicroRNA-21 exhibits antiangiogenic function by targeting RhoB expression in endothelial cells. PLoS One, 6, e16979.

ABDULRAHMAN, S., AL-MUEILO, S., BOKHARY, H., LADIPO, G. & AL-RUBAISH, A. 2002. A prospective study of hemodialysis access-related bacterial infections. Journal of Infection and Chemotherapy, 8, 242–246.

SALOMON, C., RYAN, J., SOBREVIA, L., KOBAYASHI, M,. ASHMAN, K., MITCHELL, M. & RICE, G. 2013. Exosomal Signaling during Hypoxia Mediates Microvascular Endothelial Cell Migration and Vasculogenesis. PloS one, 8, e68451.

SARKAR, J., GOU, D., TURAKA, P., VIKTOROVA, E., RAMCHANDRAN, R. & JU, R. 2010. MicroRNA-21 plays a role in hypoxia-mediated pulmonary artery smooth muscle cell proliferation and migration. Am J Physiol Lung Cell Mol Physiol, 299, L861–L871.

SARKAR, R., MEINBERG, E., STANLEY, J., GORDON, D. 1996. Nitric oxide reversibly inhibits the migration of cultured vascular smooth muscle cells. Circ Res, 78, 225–230.

SASAGURI, Y., MURAHASHI, N., SUGAMA, K., KATO, S., HIRAOKA, K., SATOH, T., ISOMOTO, H. 1994. Development-related changes in matrix metalloproteinase expression in human aortic smooth muscle cells. Lab

SATA, M. & NAGAI, R. 2002. Circulating recipient cells contribute to graft coronary arteriolosclerosis. J Cardiol, 39, 48–49.

SCHEINMAN, M., ASCHER, E., LEVI, G., HINGORANI, A., SHIRAZIAN, D. & SETH, P. 1999. p53 gene transfer to the injured rat carotid artery decreases neointimal formation. J. Vasc. Surg., 29, 360–369.

SCHIEKE, S., PHILLIPS, D., MCCOY, J., APONTE, A., SHEN, R., BALABAN, R. & FINKEL, T. 2006. The mammalian target of rapamycin (mTOR) pathway regulates mitochondrial oxygen consumption and oxidative capacity. J. Biol. Chem., 281, 27643-27652.

SCHOREY, J. & BHATNAGAR, S. 2008. Exosome function: from tumor immunology to pathogen biology. Traffic, 9, 871-881.

SCHWARTZ, S., DEBLOIS, D. & O'BRIEN, E. 1995. The Intima.Soil for Atherosclerosis and Restenosis. circulation research, 77, 445-465.

SCHWARTZ, S., VIRMANI, R. 2000. The good smooth muscle cells in atherosclerosis. Curr Atheroscler Rep, 2, 422–9.

SCORRANO, L. 2009. Opening the doors to cytochrome c: Changes in mitochondrial shape and apoptosis. The International Journal of Biochemistry & Cell Biology, 41, 1875–1883.

SCRIBNER, B., BURI, R., CANER, J., HEGSTROM, R. 1960. The treatment of chronic uremia by means of intermittent hemodialysis: a preliminary report. Trans Am Soc Artif Intern Organs, 6, 114-122.

SHELAT, H., LIU, T., HICKMAN-BICK, D., BARNHART, M., VIDA, T., DILLARD, P., WILLERSON, J. & ZOLDHELYI, P. 2001. Growth suppression of human coronary vascular smooth muscle cells by gene transfer of the transcription factor E2F-1. Circulation 103, 407–414.

SHI, Y., O'BRIEN, J. 1996a. Adventitial myofibroblasts contribute to neointimal formation in injured porcine coronary arteries. Circulation, 94, 1655–1664.

SHI, Y., PIENIEK, M., FARD, A., O'BRIEN, J., MANNION, J. & ZALEWSKI, A. 1996b. Adventitial remodeling after coronary arterial injury. Circulation, 93, 340–348.

SHIOGAI, Y., STEFANOVSKA, A. & MCCLINTOCKA, P. 2010. Nonlinear dynamics of cardiovascular ageing. Phys Rep. , 488, 51–110.

SHVEYGERT, M., KAISER, C., BRADRICK, S. & GROMEIER, M. 2010. Regulation of Eukaryotic Initiation Factor 4E (eIF4E) Phosphorylation by Mitogen-Activated Protein Kinase Occurs through Modulation of Mnk1-eIF4G Interaction. mol cell biol, 30, 5160-5167.

SIMONS, M. & RAPOSO, G. 2009. Exosomes: vesicular carriers for intercellular communication. Curr. Opin Cell. Biol., 21, 575-581.

SIMPSON, R., JENSEN, S. 2008. Proteomic profiling of exosomes: current perspectives. Proteomics, 8, 4083–99.

SKULACHEV, V. 2001. Mitochondrial filaments and clusters as intracellular power-transmitting cables. Trends Biochem. Sci., 26, 23–29.

SOMLYO, A. & SOMLYO, A. 2003. Ca2 sensitivity of smooth muscle and nonmuscle myosin II: modulated by G proteins, kinases, and myosin phosphatase. Physiol Rev, 83, 1325–1358.

SPENCER, G. 2010. A matter of balance between life and death: targeting reactive oxygen species (ROS)-induced autophagy for cancer therapy. Autophagy, 6 835–837.

SPRAGUE, A. & KHALIL, R. 2009. Inflammatory cytokines in vascular dysfunction and vascular disease. Biochemical Pharmacology, 78, 539–552.

SPRINGER, T. 1995. Traffic signals on endothelium for lymphocyte recirculation and leukocyte emigration. Annu Rev Physiol 57, 857 887.

SRIPADA, L., TOMAR, D., PRAJAPATI, P., SINGH, R., SINGH, A. & SINGH, R. 2012. Systematic analysis of small RNAs associated with human mitochondria by Deep Sequencing: Detailed analysis of mitochondrial associated miRNA. PLoS One, 7, e44873.

STARY, H. 1990. The sequence of cell and matrix changes in atherosclerotic lesions of coronary arteries in the first forty years of life. Eur. Heart J, 11(Suppl. E), 3–19.

STRACKE, S., KONNER, K., KOSTLIN, I., FRIEDL, R., JEHLE, P., HOMBACH, V., KELLER, F. 2002. Increased expression of TGF-beta1 and IGF-I in inflammatory stenotic lesions of hemodialysis fistulas. Kidney international, 61, 1011-1019.

SU, S.-A., XIE, Y. FU, Z., WANG, Y., WANG, J. & XIANG, M. 2017. Emerging role of exosome-mediated intercellular communication in vascular remodeling. oncotarget, 1-13.

SUAREZ, Y., FERNANDEZ-HERNANDO, C., POBER, J. 2007. Dicer dependent microRNAs regulate gene expression and functions in human endothelial cells. Circ Res, 100, 1164–1173.

SUBRA, C., LAULAGNIER, K., PERRET, B. 2007. Exosome lipidomics unravels lipid sorting at the level of multivesicular bodies. Biochimie, 89, 205-212.

SUDHOF, T. & ROTHMAN, J. 2009. Membrane fusion: grappling with SNARE and SM proteins. Science, 323, 474–477.

SUEN, D.-F., NORRIS, K. & YOULE, R. 2008. Mitochondrial dynamics and apoptosis. Genes Dev., 22, 1577-1590.

SUGIOKA, R., SHIMIZU, S. & TSUJIMOTO, Y. 2004. Fzo1, a Protein Involved in Mitochondrial Fusion, Inhibits Apoptosis. J. Biol. Chem., 279, 52726–52734.

YOUNG AHN, S., CHOI, KOO, H-J., HOON JEONG, J., HA PARK, W., KIM, M., PIAO, Y. & PAK, Y. 2010. Mitochondrial dysfunction enhances the migration of vascular smooth muscles cells via suppression of Akt phosphorylation. Biochimica et Biophysica Acta 1800, 275–281.

SUOMALAINEN, A. 2011. Therapy for mitochondrial disorders: little proof, high research activity, some promise. Semin. Fetal Neonatal Med, 16, 236–240.

SZABADKAI, G., SIMONI, A., CHAMI, M., WIECKOWSKI, M., YOULE, R. 2004. Drp-1-dependent division of the mitochondrial network blocks intraorganellar Ca 2+ waves and protects against Ca2+-mediated apoptosis. Mol Cell, 16, 59–68.

TAIT, S. & GREEN, D. 2010. Mitochondria and cell death: outer membrane permeabilization and beyond. Nat. Rev. Mol. Cell Biol., 11, 621-632.

TAKAHASHI, Y., COPPOLA, D., MATSUSHITA, N., CUALING, H., SUN, M., SATO, Y., LIANG, C., JUNG, J., CHENG, J., MUL, J., PLEDGER, W., & WANG, H. 2007. Bif-1 interacts with Beclin 1 through UVRAG and regulates autophagy and tumorigenesis. Nat. Cell Biol, 9, 1142–1151.

TAKAHASHI, Y., KARBOWSKI, M., YAMAGUCHI, H., KAZI, A., WU, J., SEBTI, S., YOULE, R. & WANG, H. 2005. Loss of Bif-1 suppresses Bax/Bak conformational change and mitochondrial apoptosis. Mol. Cell Biol. , 25, 9369–9382.

TAYLOR, D. & TAYLOR, C. 2008. MicroRNA signatures of tumor-derived exosomes as diagnostic biomarkers of ovarian cancer. Gynecologic Oncology, 110, 13-21.

TCHAKARSKA, G., ROUSSEL, M., TROUSSARD, X. & SOLA, B. 2011. Cyclin D1 Inhibits Mitochondrial Activity in B Cells. 71, 1690-9.

THERY, C., AMIGORENA, S., RAPOSO, G. 2006. Isolation and characterization of exosomes from cell culture supernatants and biological fluids. Curr Protoc Cell Biol (Chapter 3: Unit 3, 22).

THIBODEAU, G. & PATTON, K. 2003. Anatomy & Physiology. 5, St. Louis, Mosby, 566-568.

TIAN, T., ZHU, Y., HU, F., WANG, Y., HUANG, N. 2013. Dynamics of exosome internalization and trafficking. J Cell Physiol 228, 1487–1495.

TIMPL, R. 1996. Macromolecular organization of basement membranes. Curr. Opin. Cell Biol, 8, 618–24.

TORDOIR, J., CANAUD, B., HAAGE, P., KONNER, K., BASCI, A., FOUQUE, D., KOOMAN, J., MARTIN-MALO, A., PEDRINI, L., PIZZARELLI, F., TATTERSALL, J., VENNEGOOR, M., WANNER, C., TER WEE, P. & VANHOLDER, R. 2007. EBPG on vascular access. Nephrol *Dial Transplant* 22(Suppl 2)**,** ii88–ii117.

TWIG, G., ELORZA, A., MOLINA, A., MOHAMED, H., WIKSTROM, J., WALZER, G., STILES, L., HAIGH, S., KATZ, S., LAS, G., ALROY, J., WU, M., PY, B., YUAN, J., DEENEY, J., CORKEY, B. & SHIRIHAI, O. 2008. Fission and selective fusion govern mitochondrial segregation and elimination by autophagy. Embo J., 27, 433–446.

TYYNISMAA, H., CARROLL, C., RAIMUNDO, N., AHOLA-ERKKILA, S., WENZ, T., RUHA- NEN, H., GUSE, K., HEMMINKI, A., PELTOLA-MJØSUND, K. & TULKKI, V., ET AL. 2010. Mitochondrial myopathy induces a starvation-like response. Hum. Mol. Genet, 19, 3948–3958.

URBANELLI, L., MAGINI, A., BURATTA, S., BROZZI, A., SAGINI, K., POLCHI, A., TANCINI, B., & EMILIANI, C. 2013. Signaling Pathways in Exosomes Biogenesis, Secretion and Fate. genes, 4, 152-170.

VALADI, H., EKSTROM, K., BOSSIOS, A., SJOSTRAND, M., LEE, J. & LOTVALL, J. 2007. Exosome-mediated transfer of mRNAs and microRNAs is a novel mechanism of genetic exchange between cells. Nat. Cell. Biol. , 9, 654-659.

VAN DER MIJN, J., SOL, N., MELLEMA, W., JIMENEZ, C., PIERSMA, S., DEKKER, H., SCHUTTE, L., SMIT, E., BROXTERMAN, H., SKOG, J., TANNOUS, B., WURDINGER, T., & VERHEUL, H. 2014. Analysis of AKT and ERK1/2 protein kinases in extracellular vesicles isolated from blood of patients with cancer. Journal of Extracellular Vesicles, 3, 25657.

VASUDEVAN, S., TONG, Y. & STEITZ, J. 2007. Switching from repression to activation: microRNAs can up-regulate translation. Science, 318 1931–1934.

VILLARROYA-BELTRI, C., GUTIERREZ-VAZQUEZ, C., SANCHEZ-CABO, F., PEREZ-HERNANDEZ, D., VAZQUEZ, J. & MARTIN-COFRECES, N. 2013. Sumoylated hnRNPA2B1 controls the sorting of miRNAs into exosomes through binding to specific motifs. Nat Commun, 4, 2980.

WAGNER, D. 1990. Cell biology of von Willebrand factor. Annu Rev Cell Biol, 6, 217 - 246.

WAKABAYASHI, J., ZHANG, Z., WAKABAYASHI, N., TAMURA, Y., FUKAYA, M., KENSLER, T., LIJIMA, M. 2009. The dynamin-related GTPase Drp1 is required for embryonic and brain development in mice. J cell Biol, 186, 805-816.

WANG, G., SHIMADA, E., KOEHLER, C. & TEITELL, M. 2012a. PNPASE and RNA trafficking into mitochondria. Biochim Biophys Acta, 1819, 998–1007.

WANG, J.-X., JIAO, J., LI, Q., LONG, B., WANG, K., LIU, J., LI, Y. 2011. miR-499 regulates mitochondrial dynamics by targeting calcineurin and dynaminrelated protein-1. Nat Med, 17, 71–78.

WANG, L., YU, T., LEE, H., O'BRIEN, D., SESAKI, H., & YOON, Y. 2015. Decreasing mitochondrialfissiondiminishes vascular smoothmuscle cellmigration and ameliorates intimal hyperplasia. Cardiovascular Research, 106, 272–283.

WANG, M., LI, W., CHANG, G-Q., YE, C-S., OU, J-S., LI, X-X., LIU, Y., CHEANG, T-Y., HUANG, X-L. 2011. MicroRNA-21 regulates vascular smooth muscle cell function via targeting tropomyosin 1 in arteriosclerosis obliterans of lower extremities. Arterioscler Thromb Vasc Biol, 31, 2044–2053.

WATT, J., KENNEDY, S., MCCORMICK, C., AGBANI, E., MCPHADEN, A., MULLEN, A., CZUDAJ, P., BEHNISCH, B., WADSWORTH, R. & OLDROYD, K. 2013. Succinobucol-Eluting Stents Increase Neointimal Thickening and Peri-Strut Inflammation in a Porcine Coronary Model. Catheter Cardiovasc Interv., 81, 698-708.

WEAKLEY, B. 1976. Variations in mitochondrial size and ultrastructure during germ cell development. Cell Tissue Res, 169, 531—550.

WEBBER, J., STEADMAN, R., MASON, M., TABI, Z. 2010. Cancer exosomes trigger fibroblast to myofibroblast differentiation. . Cancer Res 70, 9621–9630.

WEBER, C., SCHOBER, A. 2010. MicroRNAs in arterial remodelling, inflammation and atherosclerosis. Curr Drug Targets, 11, 950–956.

WEBER, J., BAXTER, D., ZHANG, S., HUANG, D., HUANG, K. 2010. The microRNA spectrum in 12 body fluids. Clin Chem, 56, 1733–41.

WEI, M., ZONG, W., CHENG, E., LINDSTEN, T., PANOUTSAKOPOULOU, V., ROSS, A., ROTH, K., MACGREGOR, G., THOMPSON, C. & KORS-MEYER, S. 2001. Proapoptotic BAX and BAK: a requisite gateway to mitochondrial dysfunction and death. Science (New York, N.Y.), 292, 727–730.

WEIL, R. & ISRAEL, A. 2004. T-cell-Receptor-and B-cell-Receptor-mediated activation of NF-kappaB in lmphocytes. Curr Opin Immunol, 16, 374-381.

WESTERMANN, B. 2010. Mitochondrial fusion and fission in cell life and death. Nat. Rev. Cancer Mol. Cell Biol. , 11, 872-884.

WU, C.-C., WEN, S., YANG, C., PU, S., TSAI, K. & CHEN, J. 2009. Plasma ADMA Predicts Restenosis of Arteriovenous Fistula. J Am Soc Nephrol, 20, 213-222.

WU, H., ZHOU, J., MEI, S., WU, D., MU, Z., CHEN, B., XIE, Y., YE, Y. & LIU, J. 2016. Circulating exosomal microRNA-96 promotes cell proliferation, migration and drug resistance by targeting LMO7. journal of cellular and molecular medicine, 1-9.

WU, H., XIAO, Z., WANG, K., LIU, W. 2013. MiR-145 is downregulated in human ovarian cancer and modulates cell growth and invasion by targeting p70S6K1 and MUC1. Biochem Biophys Res Commun, 441, 693-700.

WU, W., XIAO, H., LAGUNA-FERNANDEZ, A., VILLARREAL, G., WANG, C., GEARY, G., ZHANG, Y., WANG, W., HUANG, H., ZHOU, J., LI, Y., CHIEN, S., GARCIA-CARDENA, G. 2011. Flow-Dependent Regulation of Kruppel-Like Factor 2 Is Mediated by MicroRNA-92a. Circulation, 124, 633–641.

WUBBOLTS, R., LECKIE, R., VEENHUIZEN, P., SCHWARZMANN, G., MOBIUS, W., HOERNSCHEMEYER, J., SLOT, J., GEUZE, H. 2003. Proteomic and biochemical analyses of human B cell-derived exosomes. Potential implications for their function and multivesicular body formation. J Biol Chem, 278, 10963-10972.

WYMANN, M. & PIROLA, L. 1998. Structure and function of phosphoinositide 3-kinases. Biochim. Biophys. Acta, 1436, 127–150.

XIAO, D., OHLENDORF, J., CHEN, Y., TAYLOR, D., RAI, S., WAIGEL, S., ZACHARIAS, W., HAO, H. & MCMASTERS, K. 2012. Identifying mRNA, MicroRNA and Protein Profiles of Melanoma Exosomes. plos one, 7, e46874.

GUO, X., CHEN, K-H., GUO, Y., LIAO, H., TANG, J. & XIAO, R.-P. 2007. Mitofusin 2 Triggers Vascular Smooth Muscle Cell Apoptosis via Mitochondrial Death Pathway. Circ Res, 101, 1113-1122.

XIN, M., SMALL, E., SUTHERLAND, L., QI, X., MCANALLY, J., PLATO, C., RICHARDSON, J., BASSEL-DUBY, R. 2009. MicroRNAs miR-143 and miR-145 modulate cytoskeletal dynamics and responsiveness of smooth muscle cells to injury. Genes Dev., 23, 2166–2178.

YAMBOLIEV, L. & GERTHOFFER, W. 2001. Modulatory role of ERK MAPK-caldesmon pathway in PDGF-stimulated migration of cultured pulmonary artery SMCs. Am J Physiol Cell Physiol, 280, C1680–C1688.

YAMBOLIEV, L., CHEN, J. 2001. PI 3-kinases and Src kinases regulate spreading and migration of cultured VSMCs. Am J Physiol Cell Physiol, 281, C709–C718.

YANG, L., XIAO-HOU, WU., DAN, WANG., CHUN-LI, LUO. & CHEN, L.-X. 2013. Bladder cancer cell-derived exosomes inhibit tumor cell apoptosis and induce cell proliferation in vitro. molecular medicine reports, 8, 1272-1278.

YOSHIDA, T., AZUMA, H., AIHARA, K-I., FUJIMURA, M., AKAIKE, TAKAO MITSUI, M. & MATSUMOTO, T. 2005. Vascular smooth muscle cell proliferation

is dependent upon upregulation of mitochondrial transcription factor A (mtTFA) expression in injured rat carotid artery. Atherosclerosis, 178, 39-47.

YOULE, R. & KARBOWSKI, M. 2005. Mitochondrial fission in apoptosis. Nat Rev Mol Cell Biol 6, 657–663.

YU, X., HARRIS, S. 2006. The regulation of exosome secretion: a novel function of the p53 protein. Cancer Res, 66, 4795–4801.

ZAMPETAKI, A., ZHANG, Z., HU, Y. 2005. Biomechanical stress induces IL-6 expression in smooth muscle cells via Ras/Rac1-p38 MAPK-NF-kB signaling pathways. Am. J. Physiol. Heart Circ. Physiol., 288, H2946–H2954.

ZAMZAMI, N. & KROEMER, G. 2001. The mitochondrion in apoptosis: how Pandora's box opens. Nat. Rev. Mol. Cell Biol., 2, 67–71.

ZHANG, C. 2008. MicroRNomics: a newly emerging approach for disease biology. Physiol Genomics, 33, 139–147.

ZHANG, J., GUO, H., QIAN, G., GE, S., JI, H., HU, X. & CHEN, W. 2010. MiR-145, a new regulator of the DNA Fragmentation Factor-45 (DFF45)-mediated apoptotic network. molecular cancer, 9, 211.

ZHANG, J., LI, S., LI, L., LI, M., GUO, C., YAO, J. 2015. Exosome and Exosomal MicroRNA: Trafficking, Sorting, and Function. Genomics Proteomics Bioinformatics, 13, 17-24.

ZHANG, Q., RAOOF, M., CHEN, Y., SUMI, Y., SURSAL, T., JUNGER, W., BROHI, K., ITAGAKI, K. & HAUSER, C. J. 2010. Circulating mitochondrial DAMPs cause inflammatory responses to injury. Nature, 464, 104-107.

ZHAO, Y., BISWAS, S., MCNULTY, P., KOZAK, M., JUN, J. & SEGAR, L. 2011. PDGF-induced vascular smooth muscle cell proliferation is associated with dysregulation of insulin receptor substrates. Am J Physiol Cell Physiol., 300, C1375–C1385.

ZHENG, J., XUE, H., WANG, T., JIANG, Y., LIU, B., LI, J., LIU, Y., WANG, W., ZHANG, B. & SUN, M. 2011. miR-21 Downregulates the Tumor Suppressor P12 CDK2AP1 and Stimulates Cell Proliferation and Invasion. Journal of Cellular Biochemistry, 112, 872-880.

ZHENG, M. & XIAO, R.-P. 2010. Role of mitofusin 2 in cardiovascular oxidative injury. J Mol Med, 88, 987-991.

ZHOU, J., WANG, K., WU, W., SUBRAMANIAM, S., SHYY, J., CHIU, J., LI, J. 2011. MicroRNA-21 targets peroxisome proliferators-activated receptor-alpha in an

autoregulatory loop to modulate flow-induced endothelial inflammation. Proc Natl Acad Sci USA 108, 10355–10360.